TOLL RECEPTORS REGULATE BRAIN STRUCTURAL PLASTICITY *VS.* NEURODEGENERATION

by

GUIYI LI

A thesis submitted to

University of Birmingham

for the degree of

DOCTOR OF PHILOSOPHY

School of Biosciences
College of Life and Environmental Sciences
University of Birmingham
October 2018

UNIVERSITY OF
BIRMINGHAM

University of Birmingham Research Archive

e-theses repository

This unpublished thesis/dissertation is copyright of the author and/or third parties. The intellectual property rights of the author or third parties in respect of this work are as defined by The Copyright Designs and Patents Act 1988 or as modified by any successor legislation.

Any use made of information contained in this thesis/dissertation must be in accordance with that legislation and must be properly acknowledged. Further distribution or reproduction in any format is prohibited without the permission of the copyright holder.

Abstract

Structural plasticity and homeostasis enable the brain to adapt to environmental changes and learning. However, the underlying molecular mechanisms are poorly understood. In humans, these processes depend on neurotrophins functioning through Trk and $p75^{NTR}$ receptors. *Drosophila* neurotrophins bind *Toll* receptors instead. Thus, understanding how *Tolls* operate is important to understand the brain. Here, I investigated the function of *Toll-2* in the *Drosophila* brain. Using CRISPR/Cas9, I generated mutant and knock-in *Toll-2* alleles and showed that *Toll-2* is expressed in neurons, and loss of *Toll-2* function impaired behaviour, longevity, connectivity and cell survival during development. In the central brain, Toll-2 knock-down reduced cell number, whereas *Toll-2* over-expression increased cell number. Interference with *Toll-2* function, neuronal activity or downstream signalling effectors at the adult critical period only, also altered cell number in the central brain and medulla. However, these manipulations did not affect Kenyon cell number. Multiple *Tolls* are expressed in the brain, and together they regulate brain size and shape. Loss of multiple *Tolls* affected Kenyon cell clusters, meaning that *Tolls* redundantly provide robustness to mushroom body cells. To conclude, *Tolls* regulate brain development, and structural plasticity in the adult brain involves changes in neuronal number regulated via cell signalling.

For Mum and Dad

致我最爱的父母

Acknowledgement

First of all, the person I would like to thank is my supervisor, Dr Alicia Hidalgo. Thank you for all the patience, encouragement, inspiration, knowledge and skills. This project would have not been possible without you and your excellent supervision. Also, thank you for making the amazing paella and tortilla.

I would like to thank my parents for all the support in all the ways, from the minute when I decided to do a PhD until now. Your love and support are always the source of my determination and courage.

I would like to thank my boyfriend, Dr Tong Yin. Thank you for being with me at all the up and down moments, and for always having faith in me more than I do.

I would like to thank our collaborators Professor Martin Heisenberg and Dr Reinhard Wolf for welcoming me to your lab and sharing all the techniques and gadgets on optogenetics. Thank to Dr Manuel Forero for developing the *Dead-Easy* Plug-in making the cell counting “dead easy”.

I would like to thank my sunshines: Suzana, Marta and Lizzie, and all the past and present lab members from our lab: Neale, Niki, Maria, Karthik, Mei-Ann, Maria-Doleres, and Jun. I would also like to thank people from Brogna, Fan, Soller and Rezaval lab: Marija, Jianming, Mingli, Jake, Shiyao, and Sherry. Thank you for all the suggestions, help, support and friendship over the years. You make this lab such a wonderful place to work.

Table of Contents

Chapter 1 INTRODUCTION 1

1.1 Structural brain plasticity in vertebrates 3
1.1.1 Neuronal number plasticity in vertebrate adult brain 3
1.1.2 Plasticity in adult brain circuitry 5
1.1.3 Diseases related to lack of brain plasticity 6

1.2 Structural brain plasticity in *Drosophila* 7
1.2.1 Structural plasticity in neural circuitry in the *Drosophila* brain 7
1.2.2 Cell number plasticity in the *Drosophila* adult brain 9

1.3 Neurotrophins in mammals 11
1.3.1 *Trk* receptor-mediated signaling pathways 12
1.3.2 *p75* neurotrophin receptor-mediated signalling pathways 14

1.4 Neurotrophins in *Drosophila* 16
1.4.1 Discovery of *Drosophila* neurotrophins 16
1.4.2 Neuronal functions of *DNTs* 18
1.4.3 Neuronal functions of other *Spz* family members 19

***1.5 Toll* receptors in *Drosophila* 20**
1.5.1 Structure of *Toll* receptors 20
1.5.2 Functions of *Toll* receptors in development 21
1.5.3 Functions of *Toll* receptors in immunity 22
1.5.4 Function of *Toll* receptors in the central nervous system 23

1.6 Downstream signalling of *Toll* receptors 24
1.6.1 *Toll* signalling pathway in dorsal-ventral pattern establishment 25
1.6.2 *Toll* signaling pathways in immune system 26
1.6.3 *Toll* signaling pathways in nervous system 28

1.7 Mammalian *Toll*-like receptors 29
1.7.1 Functions of *TLRs* in immunity 30
1.7.2 Functions of *TLRs* in nervous system 31

1.8 1.8 *Drosophila* as a working model 32
1.8.1 Structure of *Drosophila* larval CNS 33
1.8.2 Structure of *Drosophila* pupal and adult brain 33

1.9 Aims 36

Chapter 2 Materials and Methodology 38

2.1 Genetics 38
2.1.1 Fly maintenance 38
2.1.2 Genetic protocols 38
2.1.3 Temperature shifting regimes 38

2.2 Cloning of pTV^{mCherry}-Toll-2 47
2.2.1 Genomic DNA extraction 47
2.2.2 Polymerase Chain Reaction (PCR) 47
2.2.3 Gel electrophoresis and gel purification 48
2.2.4 Restriction enzyme digestion, ligation 48
2.2.5 Transformation and colony selection 49

2.2.6 Plasmid amplification through mini-prep and diagnostic digestion test 50
2.2.7 Sequencing and PCR checking 51

2.3 *gRNA* designing and ligation with vector U6.3 54
2.3.1 Defining the sequence of *gRNA* 54
2.3.2 Produce Polynucleotide kinase (PNK) treated double-stranded *gRNA* 55
2.3.3 Preparation of *U6:3* plasmid for ligation 55
2.3.4 Ligation, transformation, plasmid selection and amplification 55

2.4 Generation of *pUAS-Toll-2 CDS* via Gateway Cloning 56

2.5 Reverse Transcription (RT)-PCR 57

2.6 Confocal microscopy and imaging 57
2.6.1 Confocal microscopy 57
2.6.2 Cell number quantification using *DeadEasy* 58

2.7 Adult behaviour tests 58
2.7.1 Longevity test 58
2.7.2 Survival index 59
2.7.3 Climbing assay 60
2.7.4 Buridan Arena test 60

2.8 Dissection and immunostaining of larval, pupal and adult brains 61

2.9 Data analysis 62

Chapter 3 Toll-2 is expressed in the CNS and Toll-2 mutants have altered behaviour and brain circuits 63

3.1 Introduction 63

3.2 Results 64
3.2.1 Generation of *pU6.3 Toll-2 gRNA* construct 64
3.2.2 Generation of *Toll-2 pTV^{mCherry}* construct 65
3.2.3 Generation and verification of transgenic *Toll-2^{pTV}* 66
3.2.4 Generation of *Toll-2^{pTV} Gal4* lines 69
3.2.5 Visualization of *Toll-2* expression in the CNS in Toll-2^{pTV} transgenic flies 70
3.2.6 Loss of *Toll-2* function causes defects in survival 71
3.2.7 Loss of *Toll-2* function causes defects in longevity of adult flies 73
3.2.8 Loss of *Toll-2* function causes defects in adult fly locomotion 73
3.2.9 Loss of Toll-2 function causes defects in visual system of adult flies 74
3.2.10 Test *Toll-2* functions in brain circuitry by using *UAS Flybow* 76
3.2.11 *Toll-2* mutant clone causes mistargeting in neurons in pupae 77

3.3 Discussion 78

Chapter 4 Function of Toll-2 in regulating cell number in the brain during development 81

4.1 Introduction 81

4.2 Result 82
4.2.1 *Toll-2* and *MyD88* are expressed in overlapping sets of neurons throughout the brain 82
4.2.2 Loss of *Toll-2* function during development decreased cell number in the pupal central brain 83

4.2.3 A pulse of *Toll-2* function specifically in pupa stage increased cell number in pupal brain 84
4.2.4 *Toll-2* function did not change the number of MB KCs during development 85
4.2.5 Pulse of *Toll-2* function specifically in pupal stages did not significantly change MB cell number 86

4.3 Discussion 87

Chapter 5 Regulation of cell number by Toll-2 in adult brain: brain structural plasticity 90

5.1 Introduction 90

5.2 Results 91
5.2.1 *Toll-2* is involved in regulating cell number in the central brain in adult flies 91
5.2.2 Gain or loss of *Toll-2* function during development did not affect MB Kenyon cell number in the adult brain 92
5.2.3 Conditional gain of *Toll-2* function during the adult critical period increased cell number in the medulla 93
5.2.4 Conditional gain and loss of *Toll-2* function during the critical period increased cell number in the adult central brain 94
5.2.5 Conditional alteration of *Toll-2* function during the adult critical period did not affect MB cell number 95
5.2.6 Cell number in the brain decreased during ageing 96
5.2.7 Loss of *Toll-2* function caused neurodegeneration in ageing fly brains 97

5.3 Discussion 98

Chapter 6 Neuronal activity influences neuronal number 100

6.1 Introduction 100

6.2 Results 101
6.2.1 Blocking neuronal activity during the adult critical period reduced cell number in the optic lobe medulla 101
6.2.2 Activating neurons caused cell number increase in adult optic lobe medulla 102
6.2.3 Blocking neuronal activity causes two different phenotypes in cell number in the adult central brain 103

6.3 Discussion 103

Chapter 7 Function of Toll signalling pathways and other Toll receptors in regulating cell number in the adult brain 106

7.1 Introduction 106

7.2 Results 107
7.2.1 Both cell pro-survival and pro-apoptotic pathways are active in the pupal brain 107
7.2.2 Both cell pro-survival and pro-apoptotic pathways are present in adult brain 109
7.2.3 Changing the activity of downstream molecules changed cell number in the adult brain. 110
7.2.4 *Toll-2* expressing cells in the mushroom body are able to proliferate 111
7.2.5 Other *Toll* receptors are expressed in the adult brain 112
7.2.6 Knocking down multiple *Toll* receptors causes lethality and affects brain structure in late pupae 113

7.3 Discussion 116

Chapter 8 Discussion 119

8.1 Summary of findings 119

8.2 *Toll-2* is required throughout development and in the adult Drosophila 121

8.3 *Toll-2* functions in the brain of Drosophila 123

8.4 *Toll-2* is required to maintain cell survival via MyD88-NFκB pathway during development 124

8.5 Cell number is plastic in the adult brain during critical period 126

8.6 Neuronal activity is linked with the cell number plasticity in the adult brain 128

8.7 Multiple *Tolls* play redundant roles in mushroom body 129

8.8 Cell proliferation via non-canonical signalling pathways downstream of *Toll-2* in adult brain 130

8.9 Future work 131

8.10 Conclusion and implications 132

References 134

List of Figures

Figure 1.1 *Trk* signalling pathways

Figure 1.2 *p75* signalling pathways

Figure 1.3 Structure of *Toll* and *TLR* receptors

Figure 1.4 *Toll* signalling pathways

Figure 1.5 Structure of *Drosophila* CNS

Figure 2.1 Genetics protocol for generating Toll-2^{pTV} transgenic flies

Figure 2.2 Genetics protocol for generating Toll-2^{pTV} Gal4 transgenic flies

Figure 2.3 Genetics protocol for generating Toll-3^{MiMIC} Gal4 transgenic flies

Figure 2.4 Genetics protocol for generating UAS Toll-2^{attP2}

Figure 2.5 Genetics protocol for MARCM clone

Figure 2.6 Experimental regimes of MARCM clone

Figure 2.7 Genetics protocol for combination of 2nd and 3rd chromosome

Figure 2.8 Genetics protocol for changing eye colour background and balancer on 2nd chromosome

Figure 2.9 Genetics protocol for generating recombinants of Gal4 lines with UAS histone YFP on the 2nd chromosome

Figure 2.10 Molecular basis of Gateway Cloning

Figure 2.11 PCR amplification of *Toll-2* CDS

Figure 2.12 Generation of pDonor-Toll-2 CDS

Figure 2.13 Generation of pUAS-Toll-2 CDS attB

Figure 2.14 Cell number is quantified using *DeadEasy*

Figure 3.1 pU6.3 *Toll-2* gRNA cloning and sequencing

Figure 3.2 Design of the Toll-2^{pTV} vector and generation of the 5' and 3'HA

Figure 3.3 Virtual clone of Toll-2^{pTV} and generation of the Toll-2^{pTV} plasmid

Figure 3.4 Midi-prep of Toll-2^{pTV} and diagnostic digestion with BsaI

Figure 3.5 PCR tests to check the locus of Toll-2^{pTV} insertion

Figure 3.6 PCR tests to check whether the pTV cassette is intact

Figure 3.7 PCRs to test whether Toll-2^{pTV} was a null mutant

Figure 3.8 Sequencing of *Toll-2* CDS in Toll-2^{pTV} transgenic flies

Figure 3.9 RT-PCR to test whether Toll-2^{pTV} is a null mutant

Figure 3.10 RT-PCR to test whether Toll-2^{pTV} is a null mutant

Figure 3.11 Generation of Toll-2^{pTV} Gal4 line

Figure 3.12 *Toll-2* is expressed in the CNS throughout development

Figure 3.13 *Toll-2* is expressed in the CNS and throughout brain in multiple brain domains

Figure 3.14 The effect of loss of *Toll-2* function on survival of pupae and adult

Figure 3.15 Loss of *Toll-2* function shortened life span of adult flies

Figure 3.16 Effect of loss of *Toll-2* function on adult climbing behaviour

Figure 3.17 Effect of *Toll-2* loss of function on visual system using Buridan Arena test

Figure 3.18 Knocking down *Toll-2* caused defects in visual system

Figure 3.19 Comparison of brain circuitry between control and *Toll-2* loss of function using UAS Flybow

Figure 3.20 *Toll-2* mutant clones caused cell loss and disrupted connectivity

Figure 4.1 Comparison of *Toll-2* and *MyD88* expression patter in the brain

Figure 4.2 Loss of *Toll-2* function during development causes cell number decrease in D4 pupal central brain

Figure 4.3 A pulse of *Toll-2* function in pupa stage increased cell number in the pupal central brain

Figure 4.4 Gain and loss of *Toll-2* function in regulating *Toll-2* cells in MB during development

Figure 4.5 Gain of *Toll-2* function during development did not change the MB cell number significantly in D4 pupal brain

Figure 4.6 Gain and loss of *Toll-2* function specifically in pupae did not change *Toll-2* cell number in D3 pupal MB

Figure 5.1 Loss of *Toll-2* function causes cell loss in D3 adult central brain

Figure 5.2 Gain or loss of *Toll-2* function did not affect MB Kenyon cell number in D3 adult brain

Figure 5.3 Gain of *Toll-2* function during development causes no effect on MB cell number in D3 adult brain

Figure 5.4 Gain of *Toll-2* function at the adult critical period only increased cell number in adult medulla

Figure 5.5 Alteration of *Toll-2* function at the critical period only changes cell number in the adult central brain

Figure 5.6 Alteration of *Toll-2* function at the critical period only did not affect cell number change in adult MB

Figure 5.7 Cell number in the central brain decreases during development and ageing

Figure 5.8 Kenyon cell number does not change significantly during development and ageing

Figure 5.9 Loss of *Toll-2* function causes cell loss in central brain in D30 old flies

Figure 5.10 Alteration of *Toll-2* function does not cause significant effect on cell number in D30 adult MB

Figure 6.1 Blocking neuronal activity decreases cell number in adult medulla

Figure 6.2 Activating neurons increases cell number in adult medulla

Figure 6.3 Blocking neuronal activity increased cell number in D6 adult central brain

Figure 7.1 Signalling pathways for both cell survival and cell death are active in pupa brain

Figure 7.2 Downstream *Toll*-signalling effectors are present in the adult brain

Figure 7.3 Altering Toll-receptor signalling in the adult central brain increases cell number

Figure 7.4 Altering Toll-receptor signalling in the adult brain does not affect Kenyon cell number significantly

Figure 7.5 *Toll-2* cells undergo proliferation during development

Figure 7.6 *Toll-3*, 6, 7, 8 are expressed in the adult brain

Figure 7.7 Simultaneous RNAi knock-down for multiple *Tolls* reduces brain size

Figure 7.8 Simultaneous RNAi knock-down for multiple *Tolls* alters brain structure

List of Tables **Page No.**

Table 2.1 Stock list 40-43

Table 2.2 Primer list 44-45

Table 2.3 List of plasmid and vectors 46

Table 2.4-Table 2.9 PCR reactions 51-54

Table 2.10 List of antibodies 62

List of abbreviations

BDNF:	Brain derived neurotrophic factor
CRISPR:	Clustered Regularly Interspaced Short Palindromic Repeats
CRC:	Cystine-rich clusters
DAG:	diacylglycerol
DAMPs:	Damage Associated Molecular Patterns
Dif :	Dorsal-related immune factor
FRS2:	factor receptor substrate 2
GAB1:	GRB-associated binder-1
GMC:	Ganglia Mother Cell
Grass:	Gram-positive-specific serine protease
GRB2:	growth factor receptor-bound protein 2
Ins(1,4,5)P3:	inositol-1,4,5-trisphosphate
IRS1:	insulin-receptor substrate 1
IRS2:	insulin-receptor substrate 1
KC:	Kenyon cell
Kek	kekkon
LPS:	Lipopolysaccharide
LRR:	Leucine rich repeat
MARCM:	mosaic analysis with a repressible cell marker
MB:	mushroom body
MBNB:	mushroom body neuroblast
MiMIC:	*Minos* mediated integration cassette
MMPs:	matrix metalloproteases
ModSP:	modular serine protease
MWZ:	Morris water maze
NB:	neuroblast

NFκB: nuclear factor kappa-light-chain-enhancer of activated B cells

NGF: nerve growth factor

NMDA: N-methyl-D-aspartate

NT: Neurotrophins

PtdIns(4,5)P_2: phopphatidylinositol-4,5-biphosphate

PDPK1: 3-phophoinisitde-dependent protein kinase 1

PH3: phospo-Histone-H3

Rbf: *Retinoblastoma-family protein*

SPE: Spz processing enzyme

SOS: son of sevenless

Spz: Spätzle

TLR: Toll-like receptor

Trk: Tropomyosin-Receptor-Kinase

tPA: tissue plasminogen activator

TrpA1: Transient receptor potential cation channel, subfamily A, member 1

TNT: Tetanus neurotoxin light chain

Wts: Warts

Yki: Yorkie

Chapter 1 INTRODUCTION

The brain changes though out life as neurons, glia, axons, dendrites, and synapses are formed during growth and as the brain adapts to the environment. They are also eliminated to maintain homeostasis. The balance between plasticity and homeostasis enables the brain to deliver appropriate behaviour. However, the molecular mechanisms underlying brain plasticity and homeostasis remain largely unknown.

Levi-Montalcini and her colleagues proposed the neurotrophic theory, by which neurons are generated in excess, and only the cells that form contact with the target will survive and the ones do not will be eliminated through apoptosis (Levi-Montalcini, 1987). Neurotrophins (NTs) are secreted by the target to maintain neuronal survival.

Neurotrophins can function either as pro-proteins or cleaved mature proteins to activate either cell death or cell survival, respectively (Lu et al., 2005). Pro-neurotrophins bind to $p75^{NTR}$ to promote cell apoptosis and mature neurotrophins bind 75^{NTR} and *Trk* receptors to promote cell survival (Minichiello, 2009, Reichardt, 2006). Genome sequencing analysis has revealed that there are also neurotrophins in *Drosophila* encoded by *Spz*, *DNT1* and *DNT2* (Zhu et al., 2008). The structure of *Drosophila* neurotrophins is highly conserved compared with mammalian neurotrophins (Foldi et al., 2017). However, in *Drosophila*, neurotrophins bind to *Toll* receptors instead. *Spz* is the well-known ligand of *Toll-1* in both embryonic dorsal-ventral axis determination and innate-immunity (Moussian and Roth, 2005, Anderson, 2000). *DNT1* and *DNT2* are the known ligands of *Toll-7* and *Toll-6*, respectively, although their binding is promiscuous (McIlroy et al 2013, Foldi et al 2017). *Toll-6* promotes cell survival in the larval and pupal CNS via the canonical *MyD88-NFkB*

pathway, and it promotes cell death via the *Wek-Sarm-JNK* signalling pathway (Foldi et al., 2017). Pro-*DNT1* was shown to promote cell death, and mature *DNTs* cell survival, but whether this involves only activation of *Toll-6* and *-7* receptors is unknown (Zhu et al., 2008, Foldi et al., 2017).

Reminiscent of the mammalian brain, the *Drosophila* brain is also plastic both during development and in adulthood. Evidence shows that brain size, cell morphology, neuronal projections, synaptic structures and cell number are all plastic. However, the mechanisms underlying brain structural plasticity are poorly understood, and cell number plasticity in the brain has been little explored.

In this context, the aim of my PhD project is to investigate the mechanisms regulating brain structural plasticity using *Drosophila* as a model organism. Focusing on *Toll-2*, I asked whether cell number is plastic in the brain and whether *Toll-2* is involved in its regulation. In this thesis, I showed that *Toll-2* is expressed in the central nervous system (CNS) from larvae to adult. I also showed that *Toll-2* is required to maintain survival and normal behaviour including locomotion and vision. I produced evidence that loss of *Toll-2* function in development caused cell number loss and disrupted connectivity. I showed that *Toll-2* is required to maintain cell survival in the central brain during development and at critical period in adulthood. Moreover, I provided evidence that neuronal activity is linked with cell number plasticity. Furthermore, I showed that *Toll* signalling pathways are active in pupal and adult brain and that interference with the *Toll* signalling pathway can alter cell number in the adult critical period. Remarkably, my data show that mushroom body Kenyon cells are more robust than the central brain, are not affected by interference with *Toll-2* function and

only loss of multiple *Tolls* affects them. I showed that multiple *Tolls* are active in the brain and knocking down multiple *Tolls* during development could change the structure of the brain.

I hope that this project will contribute to a better understanding on how cell number plasticity is regulated in the brain, and the non-immune functions of *Toll* receptors in the brain. My findings on the neuronal functions of *Toll* receptors and their nuclear signalling pathways in *Drosophila* could help the exploration of the neuronal functions of *TLRs* in the mammalian brain.

1.1 Structural brain plasticity in vertebrates

Before the 1960s, the adult brain was believed to lack plasticity and it was thought that it could not repair after injury (Gage, 2004). It was firstly proposed in 1969 that plasticity occurs in adult rat brain, as damaged axons could be regenerated under specific conditions (Gage, 2004; Raisman, 1969). It was later found that the adult human brain is also plastic, as neurogenesis was detected in adult dentate gyrus by BrdU staining which labels the DNA during S phase during mitosis (Eriksson et al., 1998). It was also revealed that neurogenesis occurs constitutively throughout life (Eriksson et al., 1998). This finding shed the light on the studies on structural brain plasticity.

1.1.1 Neuronal number plasticity in vertebrate adult brain

Structural plasticity underlies brain function. Neurogenesis in the mammalian adult hippocampus occurs throughout life and it has been reported that around 2000 cells are generated every day in the adult brain (Deng et al., 2010). Importantly,

neurogenesis in the adult brain reflects an adaption to the environment. For example, it has been found that the number of neurons increased significantly after moving a mouse bred in a sterile environment to a cage with more complexity and diversity. Exercise is also found to promote neurogenesis in adult brain as more proliferating cells were observed in mice on a running wheel (Gage, 2004). Neurogenesis is also important for brain functions like learning and memory. Mice that have been trained in the Morris Water Maze (MWZ) showed a significant increase of neurons in the hippocampus via both maintaining the survival of early-born neurons and increasing cell proliferation (Dupret et al., 2007). Importantly, newly generated neurons are integrated into functional circuits, which is necessary for the encoding of new memories. This allow events that occur at the same time to be stored in memory without interference with older memories (Deng et al., 2010).

In adult human brains, neurogenesis occurs constitutively. It has been found that approximate 700 hundred neurons were generated every day in adult hippocampus (Spalding et al., 2013). However, recently, a study revealed that the level of neurogenesis decreases significantly compared between early postnatal and middle-aged brain by detecting dividing or progenitor cells in dentate gyrus (Sorrells et al., 2018). Moreover, it has also been found that young neurons could be rarely detected in dentate gyrus of adult epilepsy patients (Sorrells at al., 2018). Therefore, it is suggested that the neurogenesis is required for brain function and is tightly related with ageing or brain diseases.

When neurogenesis happens during learning and memory, cell apoptosis is also observed. Intriguingly, whilst 13-day old cells were kept alive, younger cells like 7-9-

day old cells were eliminated instead (Dupret et al., 2007). It was later found that it normally took two weeks for a new-born cell to mature and start to form synaptic contact with other cells (Deng et al., 2010). It has also been found that the selective cell survival and death of new-born cells depends on the activity of *NMDA*-type glutamate receptor, which is responsible for receiving signals from other cells. Only cells with activated *NMDA* receptors are selected to survive (Tashiro et al., 2006). These findings further support the neurotrophic theory: only cells that already integrates into the brain network are able to survive while the immature cells would be eliminated to make place for the appropriately connected new-born cells. Moreover, blocking cell apoptosis during the MWZ training was also found to inhibit cell proliferation and interfere with learning and memory formation (Dupret et al., 2007). Collectively, both neurogenesis and cell apoptosis are required during brain development and adaptation, and the balance between both is vital for the brain to deliver appropriate behaviour.

1.1.2 Plasticity in adult brain circuitry

Changes to brain circuits including changes to synaptic, axonal and dendritic structure are also responsible for adaptation to the environment (Holtmaat and Svoboda, 2009). For instance, when one eye of a cat was closed after birth, the light-evoked response of the neurons that are responsible for the deprived eye were weakened when the eye was re-opened (Wiesel and Hubel, 1965). It was concluded that the synaptic activity of those neurons was reduced. Moreover, the cortical ocular dominance columns for the deprived eye were much narrower, while the ones for the open eye became wider (Wiesel and Hubel, 1965). This suggests that not only the

neurons responsible for deprived eye were changed, but also that the activity of ones behind the open eyes was also adjusted to compensate the weakened visual activity. Similar experiment found that when one eye of a mouse was light-deprived, the spine density on the apical dendrites of cortical neurons responsible of the non-deprived eye were increased in the binocular region on the visual cortex (Hofer et al., 2009). This further indicates that dendrites and synapses are plastic and are able to adjust their structure to neuronal activity, thus adapting to the environment. However, when recovering binocular vision, the spine dynamics were restored to the original level when the size of the spines decreased but the newly formed spines were not retracted. And when the eye was deprived again, no new spines was formed but the size of the spines of non-deprived eyes increased again (Hofer et al., 2009). These experiments show that neuronal activity causes structural changes. They further show that structural changes might also store information from the past, helping the brain to respond faster when facing similar conditions.

1.1.3 Diseases related to lack of brain plasticity

Alteration in structural brain plasticity also underlies multiple brain diseases. Continuous activation of microglia with increasing level of inflammatory cytokines caused by psychological stress can eliminate synapses and neurons, which induces depressive disorders (Wohleb et al., 2016). There are two main regions where neurogenesis happens in the healthy rodent adult brain, the dentate gyrus and the olfactory bulb; however, auto-immune responses causing cell loss in other parts of the brain will induce stroke, which is difficult to repair due to the lack of neurogenesis (Gage, 2004, Yagita et al., 2001). Alzheimer's, Parkinson's and Huntington's Disease

correlate with the loss of specific types of neurons such as hippocampal, dopaminergic and small spine neurons, respectively (Gage, 2004). Therefore, understanding the mechanisms regulating structural brain plasticity can help understand better the brain both in health and disease.

1.2 Structural brain plasticity in *Drosophila*

Whether the *Drosophila* brain is plastic has been discussed for many years. Over the last two decades, evidence has accumulated to unveil plasticity in the fly brain. In 1995, Martin Heisenberg and colleagues found that the size of multiple brain domains can change when flies lived in different population densities in their early adulthood (Heisenberg et al., 1995). For instance, lobula, medulla and calyx all showed smaller sizes when flies were kept in 40-flies population vials compared to flies being kept in vials alone. It was also discovered that keeping flies in constant darkness decreased and in constant light increased the volume of the optic lobes (Heisenberg et al., 1995, Barth et al., 1997). These findings showed that plasticity occurs in the *Drosophila* brain. As plasticity occurs just as much in the fly as in the mammalian brain, this suggests that plasticity underlies fundamental aspects of how brains are formed and work.

1.2.1 Structural plasticity in neural circuitry in the *Drosophila* brain

When observing the change of calyx size with different population densities, it was noticed that the number of mushroom body fibres in the peduncle also changed (Heisenberg et al., 1995). This suggests that the number of axonal fibres in the brain is adjustable depending on the environment. Thereafter, more studies investigated

on the detailed mechanisms of how the brain circuitry could be changed. Inhibiting action potential firing in olfactory projection neurons increases the fraction and size of the microglomeruli in the mushroom body, which are the sites of synaptic contact between projection neurons and mushroom body neurons (Kremer et al., 2010). Moreover, the pre-synaptic active zone density was also increased when silencing the neurons (Kremer et al., 2010). Therefore, it suggests that the synaptic organization and function in the adult brain is activity-dependent. Not only the synaptic structure, cell morphology was also found to change following the change of the environment. It has been found that the size of L2 neurons nuclei in the lamina can be changed following the circadian rhythm, in which the size of nuclei is biggest at the beginning of the day while smallest in the middle of the night (Gorska-Andrzejak et al., 2005). A similar pattern was also observed in L2 neurons dendrites when the dendritic trees are biggest at the beginning of the day and smallest in the middle of the night (Weber et al., 2009). Moreover, the size of both neurons and glia can also change following the circadian rhythm, as neuron size is biggest at the beginning of the day and smallest at the beginning of the night, whilst glial cells present an opposite rhythm. It was also found that the circadian rhythm of glia is responsible for regulating the rhythm of neurons, because blocking glia induces the loss of rhythm of neurons (Pyza and Gorska-Andrzejak, 2004). All these data suggest that both neurons and glia can respond to changes in the environment. Remarkably, they suggest that changes in cell morphology are responsible for the activity state of the flies, as flies are more active during early morning and are resting during the night.

1.2.2 Cell number plasticity in the *Drosophila* adult brain

Although structural plasticity of circuits including axons, dendrites, and synapses in the brain has received more attention, cell number plasticity remains little explored. When proposing that MB calyx fibre number changed with different population densities, Heisenberg and colleagues proposed this could be due to alterations in cell number although, although no evidence was provided (Heisenberg et al., 1995). For a long time, it was thought that cells in the adult brain are not plastic. However, evidence has shown that there is some cell apoptosis in day 2 adult brain around the antennal lobes, but apoptosis has not been observed in older flies (Kato et al., 2009). On the other hand, Fernandez-Hernandez et al. (2013) proposed that new neurons could be generated during adult stages. Using MARCM clones, they showed that cell proliferation could be visualised in the medulla cortex (Fernandez-Hernandez et al., 2013). These data suggest that cell number in the adult brain can change. It has also been shown that injury in the medulla could increase the number of neurons visualised by MARCM clones (Fernandez-Hernandez et al., 2013). This indicates that even if cell number may not normally vary, it is plastic when the brain faces a challenge from the environment.

Neuroblasts should be required to induce neurogenesis in the adult brain. Typically, type I neuroblasts is divide asymmetrically to generate a new neuroblast and a Ganglia Mother Cell (GMC), which further generate neurons or/and glia, and type II neuroblasts go through an intermediate stage first that expands the progenitor pool before producing GMCs. All of the neuroblasts are thought to finish proliferation after making the adult CNS, disappearing at the end of the pupal stages (Homem and

Knoblich, 2012, Gallaud et al., 2017). However, when changing specific conditions, the activity of neuroblasts could persist into the adult stage. For example, it was found that when preventing cell apoptosis by mutating the transcription factor *foxo* and the proapoptotic gene *reaper* together could prolong the survival of mushroom body neuroblasts (MBNBs), sustaining neurogenesis into the adult stage (Siegrist et al., 2010). Similarly, overexpression of the transcription factor *retinal homeobox* (*Rx*) promotes the survival of MBNB and increases their mitotic activity (Kraft et al., 2016). These studies suggest that changing conditions in the brain, such as following injury or variations in gene expression, can activate neuroblasts or other progenitor cells in the adult brain.

Like neuronal number, glial cell number is also plastic in the adult brain. It has been found that injury in the adult brain induced proliferation of glial cells (Kato et al., 2009). Furthermore, mutated microRNA miR-31a induced apoptosis of glia in young adult flies, which was followed by compensatory proliferation (Foo et al., 2017).

Interestingly, the plasticity of different cell lineages is unequal based on their different functions in different brain domains. MB neuroblasts have been found to be highly plastic during development. When flies are bred in a protein-starved condition, pupation is delayed. As a result, the neuroblasts generating α'β' neurons in late larval stages keep proliferating resulting in bigger α'β' lobes (Lin et al., 2013). By contrast, upon starvation, in the visual system cell diversity is more protected than cell number thus preserving neural circuit architecture in the optic lobes (Lanet et al., 2013, Lin et al., 2013). Therefore, these results suggest that when confronting a change of

environment, like injury, lack of food, or changes in gene expression, plasticity allows molecular and cellular changes in the brain.

1.3 Neurotrophins in mammals

It has been found in mammalian brains that neurons are generated in excess, and cells that fail to contact the targets are eliminated through apoptosis (Levi-Montalcini, 1987). Neurotrophins are the key molecules that are secreted by the targets to maintain cell survival. The firstly discovered neurotrophic molecule was nerve growth factor (*NGF*), purified from snake venom. It was firstly found to promote cell survival and axonal growth (Levi-Montalcini, 1987). There are four neurotrophins in the mammalian neurotrophin family: *NGF*, Brain-Derived Neurotrophic Factor (*BDNF*), neurotrophin 3 (*NT3*), and neurotrophin 4 (*NT4*) (Lu et al., 2005). Neurotrophins are composed of a signal peptide, an N-terminal pro-domain and a C-terminal Cystine-knot (Bibel and Barde, 2000). The pro-domain has important functions in the folding, intracellular trafficking and processing of the *NTs* (Mowla et al., 1999). The intracellular processing pathway differs between pro-*NGF* and pro-*BDNF*. *NGF* is cleaved intracellularly by serine protease furin and secreted through the constitutive pathway as a mature Cystine-knot (Seidah et al., 1996). *BDNF* is secreted via the regulated secretory pathway as a pro-protein and cleaved extracellularly by matrix metalloproteases (*MMPs*) or by the serine protease plasmin. The cleavage of *BDNF* is activity-dependent, as it relies on active plasminogen. *Plasminogen* is located extracellularly at the synaptic cleft and its activity depends on the secretion of tissue plasminogen activator (*tPA*) by the presynaptic terminal when neuronal activity is

increased. Secreted *tPA* cleaves plasminogen into plasmin which cleaves *BDNF* (Mowla et al., 1999).

Importantly, neurotrophins can function as pro-proteins or mature proteins regulating different cellular processes. To fulfil different functions, pro-neurotrophins and mature neurotrophins have different preferences of binding receptors. Neurotrophins bind to two different classes of receptors: $p75^{Trk}$ receptors and Tropomyosin-Receptor-Kinase (*Trk*) family including *TrkA*, *TrkB*, and *TrkC*. It has been shown that pro-neurotrophins, like pro-*NGF* and pro-*BDNF*, have higher affinity for $p75^{Trk}$ receptors whilst mature neurotrophins have higher affinity for *Trk* receptors (Lee et al., 2001). Moreover, among different *Trk* receptors, *NGF* shows higher affinity binding to *TrkA*, *BDNF* and *NT4* preferentially bind *TrkB*, and *NT3* prefers to bind *TrkC*, although there is some promiscuity (Reichardt, 2006).

1.3.1 *Trk* receptor-mediated signalling pathways

In *Trk* receptors, the extracellular domain is formed of three LRRs flanked by Cystine-rich clusters on both N- and C-terminals, followed by two immunoglobulin C2 domains. The intracellular domain is a tyrosine-kinase domain that can phosphorylate downstream proteins (Martin-Zanca et al., 1989, Treanor et al., 1995) (Figure 1.1).

The activation of *Trk* receptor leads to the phosphorylation of the tyrosine residues in the juxtamembrane domain, which then become the docking sites for adaptor proteins to bind. One of the well-known adaptors is Shc, which binds with *Trk* at Y515 docking site. Another adaptor is fibroblast growth factor receptor substrate 2 (*FRS2*), which also binds at Y515 site. *Shc* and *FRS2* compete with each other to activate

Figure 1.1 *Trk* signalling pathways

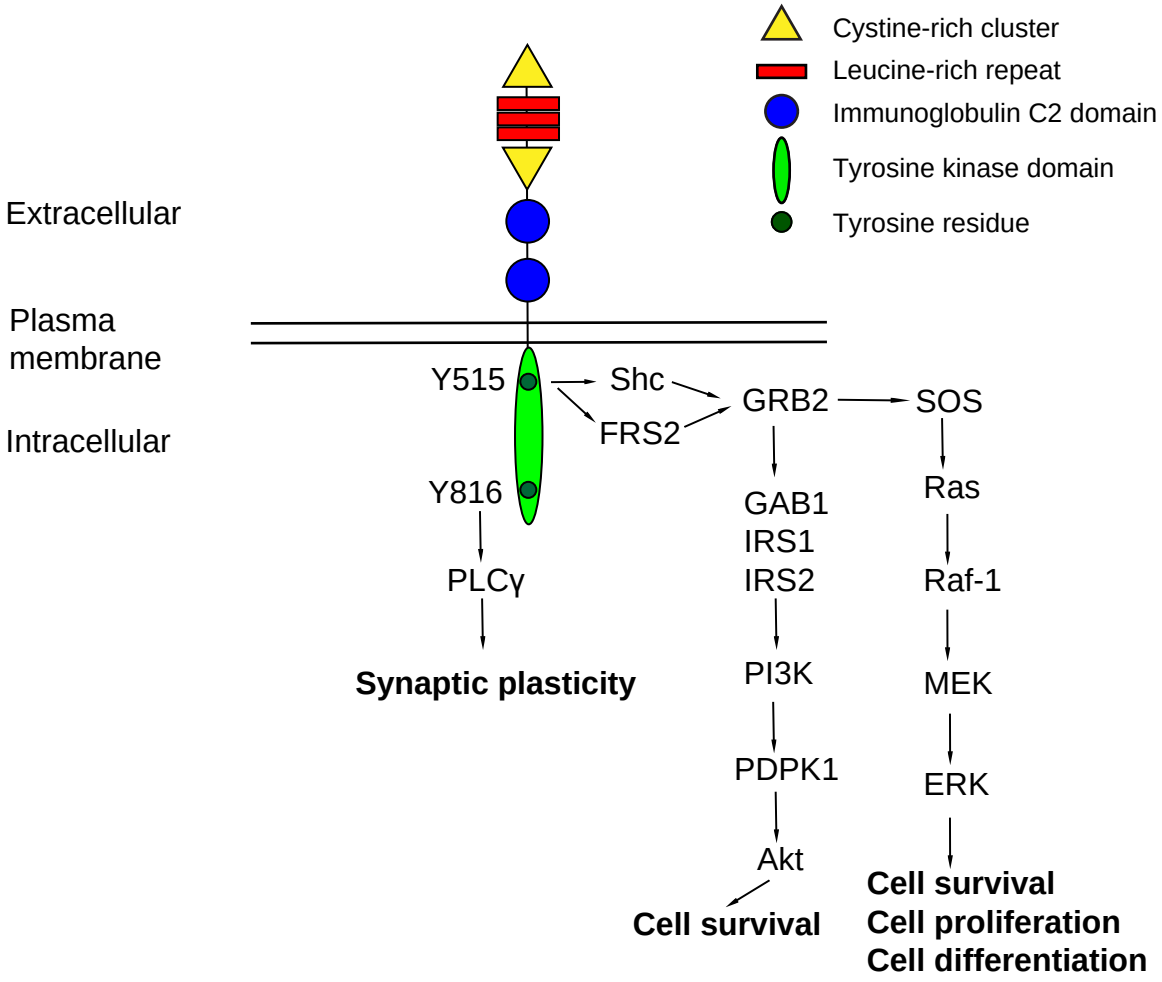


Figure 1.1 *Trk* signalling pathways

Trk receptors function mainly via three pathways. Ectodomain is composed of Cystine-Rich clusters (yellow triangle), Leucine-Rich repeats (Red rectangle) and immunoglobulin C2 domain (blue circle). Intracellular domain is the tyrosine kinase domain (light green ellipse) with tyrosine residues (dark green circles).

downstream pathways (Minichiello, 2009). Activation of *Shc* adaptors leads to the recruitment of growth factor receptor-bound protein 2 (*GRB2*) and son of sevenless (*SOS*), which then activate the *Ras-ERK* pathway. At the same time, another adaptor *FRS2* also competes to bind with *GRB2* to activate *Ras* via a *Shc*-independent pathway (Kouhara et al., 1997). Activation of this pathway will then activate the expression of genes that are involved in promoting cell survival, proliferation and differentiation (Huang and Reichardt, 2003).

Another pathway that Trk receptors activate is phosphatidylinositol 3-kinase PI3K-Akt pathway. *PI3K* interacts with Trks indirectly by binding to adaptor complexes including GRB-associated binder-1 (*GAB1*), and insulin-receptor substrate 1 and 2 (*IRS1* and *IRS2*), which binds *GRB2* (Holgado-Madruga et al., 1997, Yamada et al., 1997). Activated *PI3K* then generates 3-phosphoinositides and activate 3-phophoinisitde-dependent protein kinase 1 (*PDPK1*). *PDPK1* then activates protein kinase *Akt* that promotes the downstream proteins that are involved in regulating the cell cycle (Franke et al., 1997, Crowder and Freeman, 1998).

Activation of *Trk* receptors also induces the activation of the PLCγ-Ca^{2+} pathway. Phosphorylation of the *TrkB* receptor at Y816 causes the recruitment and activation of *PLCγ1*, which then hydrolyzes phopphatidylinositol-4,5-biphosphate (*PtdIns(4,5)P_2*) to generate inositol-1,4,5-trisphosphate (*Ins(1,4,5)P_3*) and diacylglycerol (*DAG*) (Kaplan and Miller, 2000). As a result, *Ins(1,4,5)P_3* can promote release of Ca^{2+} from the internal stores and activation of downstream proteins like Ca^{2+}/calmodulin-dependent protein kinases such as *CaMKII*, *CaMKK*, and *CaMKIV*. This pathway is

important to regulate synaptic plasticity and LTP which is important for learning and memory (Gartner et al., 2006).

1.3.2 *p75* neurotrophin receptor-mediated signalling pathways

p75^{NTR} is composed of 4 Cystine-rich domains extracellularly and a death domain intracellularly (Chao, 2003) (Figure 1.2). Since *p75^{NTR}* does not have a tyrosine kinase domain intracellularly, it requires adaptor proteins to activate the downstream signalling pathway. After the activation of the receptors, recruitment of tumour necrosis factor receptor associated factor 6 (*TRAF6*), neurotrophin receptor-interacting factor (*NRIF*), and neurotrophin receptor-interacting MAGE homologue (*NRAGE*) can activate the Jun kinase-signalling cascade which further activates *p53* and induced the expression of pro-apoptotic gene leading to apoptosis (Reichardt, 2006).

Activation of *p75^{NTR}* has also been shown to activate acidic sphingomyelinase, which then activates the generation of ceramide (Dobrowsky et al., 1994). Ceramide then interacts with and inhibits the activity of *Ras*, which inhibits the *ERK* pathway to inhibit cell survival (Muller et al., 1998).

p75^{NTR} can also activate downstream signalling to promote cell survival. *TRAF6* binding with *p75^{NTR}* can also recruit interleukin-1 receptor associated kinase (*IRAK*), atypical protein kinase C-ι (*aPKC-ι*), and aPKS-interacting protein *p62* (Wooten et al., 2001, Vandenplas et al., 2002). The complex then activates *IκB kinase-β* to phosphorylate *IκB* factors and release the *NFκB* factors, which then translocate to

Figure 1.2 ***p75*** **signalling pathways**

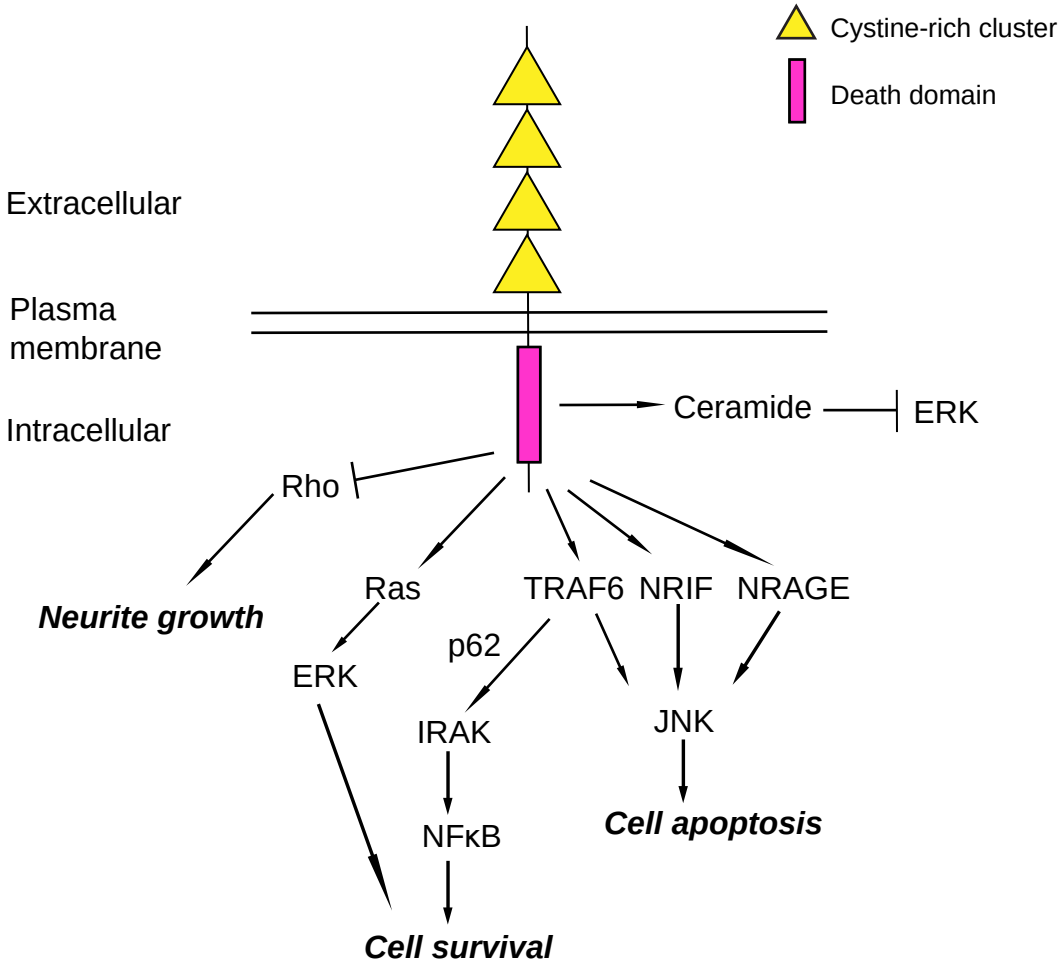


Figure 1.2 *p75* signaling pathways

p75 can activate pathways involved in regulating cell survival, cell apoptosis and axonal growth. Ectodomain of *p75* is composed of 4 Cystine-Rich clusters (yellow triangle) and intracellular domain is a death domain (magenta rectangle).

the nucleus and activate the expression of genes that promote cell survival. Furthermore, *NFkB* is also a regulator of synaptic plasticity.

p75^{NTR} is also shown to activate *Ras*, a small G-protein which is also known as a downstream factor of *Trk* receptor. Activation of *Ras* can further active the *MAP* kinase *ERK* to promote cell survival (Blochl et al., 2004).

p75^{NTR} is also involved in regulating axonal outgrowth by interacting with *Rho* family-GTPase (Yamashita et al, 1999). Unbound *p75^{NTR}* has been found to release and activate *RhoA* to inhibit axonal elongation. However, when neurotrophins including *NGF*, *BDNF* and *NT3* bind with *p35^{NTR}*, the activation of *RhoA* would be eliminated, thus allowing axonal outgrowth (Yamashita et al., 1999).

Apart from activating the signalling pathway by itself, *p75^{NTR}* can also interact with other receptors to bind ligand. *P75^{NTR}* can bind *Trk* receptors forming a 2:2 complex with the dimerised ligands. The interaction of p75^{NTR} with *Trks* increases the affinity of ligand binding to the *Trk* receptors (Roux and Barker, 2002). Moreover, *p75^{NTR}* could also interact with *Sortilin* receptor, a Vps 10-domain containing protein (Chen et al., 2005). Both receptors interact directly with the neurotrophins and it has been found that the interaction with *Sortilin* receptor increases significantly the affinity of the pro-neurotrophins for *p75^{NTR}* (Nykjaer et al., 2004).

Collectively, *p75^{NTR}* is involved in promoting both cell apoptosis and cell survival, and regulating neurite growth. By interacting with *Trk* receptors, it can also regulate cell proliferation, differentiation and synaptic plasticity. The different functions of the same receptor not only depend on the binding of different types of neurotrophins, but also

depend on the different protein adaptors downstream of the receptor, and the interacting receptors.

1.4 Neurotrophins in *Drosophila*

Neurotropism is a mechanism that is conserved between flies and vertebrates. For example, the development and survival of adult photoreceptor cells require retrograde signals from the optic ganglia in *Drosophila* (Campos et al., 1992). Neuronal survival in the optic lobe also needs input signals from retinal neurons and glia (Dearborn and Kunes, 2004; Xiong and Montell, 1995). Therefore, the discovery and study of the neurotrophins in *Drosophila* is important to understand the neurotrophic mechanisms in the central nervous system.

1.4.1 Discovery of *Drosophila* neurotrophins

The existence of neurotrophins in *Drosophila* had long been sought and found to be controversial. However, sequence and modelling analysis, as well as biochemical properties, revealed that Spätzle (Spz), which is an important element for dorsal-ventral determination, had high similarity to nerve growth factor in vertebrates; however, it was also similar to coagulogen in horseshoe crab, which does not dimerise to function (DeLotto and DeLotto, 1998) (Mizuguchi et al., 1998). However, the sequencing of the human and *Drosophila* genomes in the year 2000 seemed to show that neurotrophins were absent from the Drosophila genome (Adams et al., 2000) These claims, together with the similarity to coagulen, buried Spz in controversy. Nevertheless, subsequent structural analysis suggested that Spz belongs to the neurotrophin superfamily (Weber et al., 2007), which was later

confirmed. Thereafter, the study of neurotrophic functions of Spz further confirm the existence of neurotrophins in *Drosophila* (Zhu et al., 2008).

Using TBLASTN and PSI-BLASTN with FUGUE to search for DNA sequence similarity to mammalian neurotrophin sequences, the gene CG18318 was detected from the *Drosophila* genome and was identified as the homologue of vertebrate BDNF (Zhu et al. 2008). The study of the predicted protein sequence using FUGUE, and reverse BLAST to mammalian NTs, further confirmed gene CG18318 as the Drosophila neurotrophin homologue. Moreover, PSI-BLASTN also identified this gene as a distant paralogue of *spz*, *spz2*. The gene CG18318 was renamed as *Drosophila* neurotrophin 1 (DNT1) (Zhu et al., 2008).

There are six spz paralogues. Within the *Spz* family, *Spz1* to *Spz6*, the protein structure-based study FUGUE revealed that *Spz5* and *Spz2* are very close to each other and more closely related to BDNF, followed by *Spz*, whereas other *Spzs* such as *spz 3* and *4* are less related, and spz6 is only very distantly related. *Spz5* was therefore renamed *DNT2* (Zhu et al., 2008).

Although sequence identity is low across the Drosophila and mammalian NTs, 3D structural modelling of the proteins revealed that the cysteine-knot domains of of Spz, *DNT1* and *DNT2* are highly conserved vs. mammalian neurotrophins at the structural level. There is also conservation in protein processing between the mammalian and Drosophila NTs. *Spz* is cleaved extracellularly by serine proteases, whose processing pathway is similar to that of pro-BDNF by plasmin. It has been discovered recently that, contrary to *Spz*, *DNT1* and *DNT2* are cleaved by Furin proteases intracellularly instead, which is similar to pro-NGF (Foldi et al., 2017). This further

demonstrates the conserved cleavage procedure between mammalian and *Drosophila* NTs. Still, structural differences of receptor-binding sites between *Drosophila* and mammalian NTs, and between *Spz* and *DNTs*, suggest distinct receptor affinities and functions (Foldi et al., 2017).

Finally, there is also functional conservation between *Drosophila* and mammalian NTs, as explained below.

1.4.2 Neuronal functions of DNTs

Spz was firstly known as the ligand of the Toll receptor, functioning in establishment of dorsal-ventral axis (Morisato and Anderson, 1994). The Spz-Toll signalling pathways were then subsequently rediscovered for their vital roles in immunity as anti-microbial and anti-fungal functions in larvae and adult flies (Lemaitre et al., 1996; Lewis et al., 2013; Shia et al., 2009). Importantly, the neuronal functions of neurotrophins are being more explored. When neurotrophins were discovered in flies, it was found that mutant of *Spz*, *DNT1*, or *DNT2* caused an increase in cell death in the embryonic CNS (Zhu et al., 2008). Conserved with mammalian neurotrophins, *Drosophila* neurotrophins also form a matured cystine-knot structure (Mizuguchi et al., 1998; Zhu et al., 2008). It has been revealed that overexpression of the Cys-knot of *Spz*, *DNT1* or *DNT2* rescued cell death, promoting cell survival in the embryonic CNS (Zhu et al., 2008). Moreover, knocking down *DNT1* in muscles caused the mistargeting of motoraxons in embryos (Zhu et al., 2018).

DNTs also have functions in the larval CNS. In situ hybridization has revealed that *Spz*, *DNT1* and *DNT2* are expressed in the L3 larval body wall muscle (Sutcliffe et al., 2013). *Spz* mutant and double mutant of *DNT1* and *DNT2* was found to cause semi-

lethality, which could be rescued by overexpression of *Spz* CK, DNT1 CK, DNT2 CK and apoptosis inhibitor *p35* in neurons (Sutcliffe et al., 2013). These results indicate that Spz and *DNTs* function in the larval CNS. It was also found that alteration of the expression of *DNTs* affect neuronal axonal length, number of active zones , and causes an increase in the number of ghost boutons which are lack of postsynaptic scaffold and synaptic debris, at the neuromuscular junction (NMJ) (Sutcliffe et al., 2013; Ulian-Benitez et al., 2017). As the increase in ghost boutons and synaptic debris indicates an increase in neuronal activity, these data suggested that *DNTs* are involved in structural plasticity in response to neuronal activity (Davis and Goodman, 1998). Recently, a new mechanism of the interaction between *DNT2* and a group of kinase-less Trk-like receptors encoded by *kekkons* have been discovered in *Drosophila* to regulate structural synaptic plasticity (Ulian-Benitez et al., 2017). Furthermore, full-length or Cystine-knot *DNTs* were also discovered to regulate cell number via Toll receptors through canonical *MyD88-NFkB* or non-canonical *JNK* signalling pathways in the larval CNS (Foldi et al., 2017). Therefore, studies of *Drosophila* neurotrophins in both structure and functions indicate that neurotrophins in *Drosophila* and mammals are highly conserved.

1.4.3 Neuronal functions of other Spz family members

There are 6 *Spz* ligands in the *Spz* family. Apart from the *Spzs* mentioned above, other ligands from this family, such as *Spz3* also functions in the nervous system. Genetic inference suggested that *Spz3* could be a potential candidate ligand for Toll-8 to regulate the synaptogenesis in larvae, although no evidence was provided (Ballard et a., 2014). *Spz3* homozygous mutants were found to die as L1 larvae.

Knocking down of *Spz3* in cortex glia was also found to cause changes in morphology and function of glia cells, which further induced neuronal loss in L3 larvae VNC (Coutinho-Budd et al., 2017). Based on the sequence alignment, *Spz3* and *4* are closely related and more distant from NTs and DNTs, and *Spz6* is very distant from NTs and DNTs (Zhu et al., 2008). So far, there has not been clear evidence showing that *Spz4* or *Spz6* ligands are involved in the nervous system.

1.5 Toll receptors in *Drosophila*

1.5.1 Structure of *Toll* receptors

Toll receptors are type I transmembrane proteins. *Toll* (Toll-1) was firstly identified in *Drosophila* embryo for dorsal-ventral axis determination (Belvin and Anderson, 1996). Genome sequencing identified Toll receptors in other species including vertebrates like human and mouse, and invertebrates like mosquitos. There are nine paralogues of *Toll* in *Drosophila*, *Toll* to *Toll-9* (Tauszig et al., 2000, Ooi et al., 2002, Luo and Zheng, 2000). The structure of *Drosophila Toll* receptor is characterised by the intracellular Toll/Interleukin-1 Receptor (TIR) domain which is a 150-amino-acid intracellular domain (Imler and Zheng, 2004) (Figure 1.3). The TIR domain does not have catalytic function but plays an important role for binding with the downstream adaptors (Imler and Zheng, 2004). The hallmark of the extracellular domain of the Toll receptor is the amino-terminal leucine-rich repeats (LRR). LRR is composed of two clusters of LRR flanked by cystine-rich clusters. The first cluster is composed of 15 LRR with a cystine-rich cluster at the C-terminal end. The second cluster is composed of three LRR flanked by cystine-rich cluster on both N- and C-terminal ends (Imler and Zheng, 2004). Other Toll receptors in *Drosophila* share similar

Figure 1.3 Structure of *Toll* and *TLR* receptors

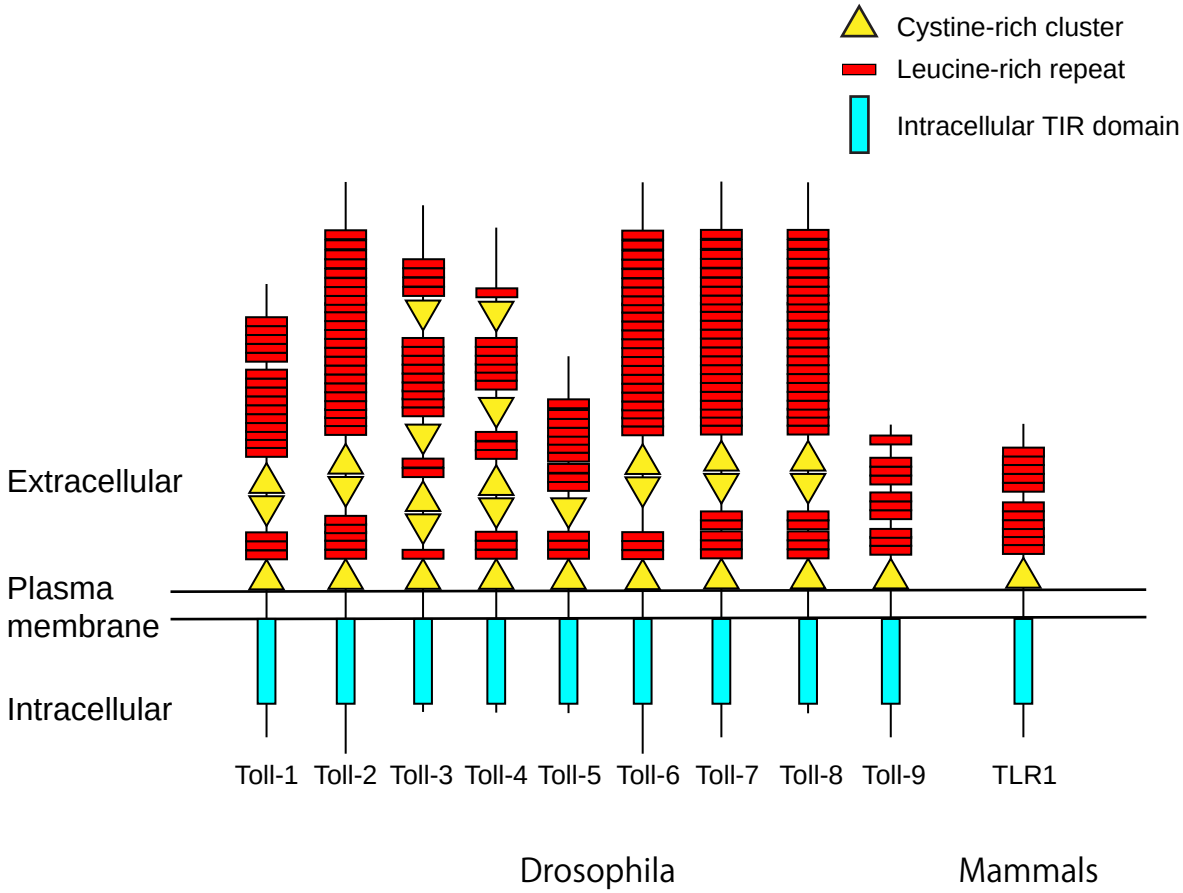


Figure 1.3 Structure of Toll and *TLR* receptors

Toll receptor and *TLR* receptors are composed of ectodomain including Cystine-rich clusters (yellow triangles) and Leucine-rich repeats (red rectangles) and intracellular TIR domain (blue rectangle). This figure is redrawn refering to Tauszig et al., 2000 and Anthoney et al., 2018.

structures to *Toll* with 18-31 extracellular LRR repeats and similar intracellular TIR domain (Tauszig et al., 2000, Eldon et al., 1994). However, the sequence and structure showed that Toll-9 is the most distant from other *Drosophila Toll* paralogues and closest to the mammalian Toll-like receptor (TLR) subfamily (Imler and Zheng, 2004).

1.5.2 Functions of *Toll* receptors in development

As mentioned above, *Toll* has important function in embryogenesis and the detailed signalling pathway will be explained in Chapter 1.7. As the result of the *Toll* signalling pathway, the nuclear form of *NFκB* factor *Dorsal* forms a gradient along the ventral half of the embryo (Stathopoulos and Levine, 2002). The concentration of the nuclear form of *Dorsal* is the highest at the ventral side, which promotes the expression of *snail* and *twist* that drive the formation of mesoderm. Above the ventral-most side, the lower level of *Dorsal* promotes the expression of snail alone, which further specifies the mesectoderm. Nuclear dorsal further above promotes the expression of Rhomboid that specifies the formation of neuroectoderm. In later development, mesoderm forms the muscle, mesectoderm forms the ventral midline, and neuroectoderm forms the central nervous system (Stathopoulos and Levine, 2002). All this suggest that *Toll* and *Toll* pathway play key roles in defining cell fate during embryogenesis.

Multiple *Tolls* also have functions to mediate cell-cell contact via cross talking during embryogenesis. *Toll-2* and *Toll-8* can work as cell adhesion molecules interacting with each other to regulate cell migration (Keith and Gay, 1990, Eldon et al., 1994).

Deficiency for *Toll-2, 6*, and *Toll-8* was found to cause defects in planar polarity, convergent extension, and cell intercalation in embryos (Pare et al., 2014).

Toll receptors also have functions in cell competition. During embryogenesis, multiple *Toll* receptors are involved in removing the "loser" cells via apoptosis through different pathways (Meyer et al., 2014). For example, *Toll-3* and *Toll-9* could induce cell apoptosis via Dorsal and Dif, when *Toll-2*, *4*, *8*, and *9* could induce apoptosis via *Sarm*, *Rel*, and *Hid* (Meyer et al., 2014).

1.5.3 Functions of *Toll* receptors in immunity

Toll is also well-known for its functions in innate immunity. Lemaitre et al. firstly found that knocking down *Toll* in adult flies induced the decrease of the expression level of *Drosomycin* that is an anti-fungal peptide (Fehlbaum et al., 1994, Lemaitre et al., 1996). This was the first study that links the *Toll* receptor with innate immunity. They also found that *Toll* mutant flies are more susceptible to *E. coli* and infected flies have significantly shortened life span (Lemaitre et al., 1996).

In order to investigate whether other *Toll* receptors have immune functions, Tauszig et al. transfected cells with chimeric proteins, in which the truncated ectodomain of *Toll* was combined with transmembrane and intracellular domain of *Toll-2* to *Toll-8* so that the proteins were constitutively activated in the cells. Among all the proteins, only *Toll-5* was found to increase the level of Drosomycin promotor (Tauszig et al., 2000). Interestingly, the sequence study has suggested that *Toll-5* is the closest paralogue of *Toll* receptor indicating that *Toll-5* may share overlapping functions with *Toll* (Luo and Zheng, 2000). Moreover, a later study also found that expression of *Toll-5* in S2 cells induced the increase mRNA level of anti-fungal peptides

Drocomycin and *Metchnikowin*, which further suggests that *Toll-5* might be involved in anti-fungal responses (Luo et al., 2001). Moreover, it was also found that expression of *Toll-5* in S2 cells also increase the level of cecropin and defensin suggesting the function of *Toll-5* in anti-bacterial response (Ooi et al., 2002). Although *Toll-5* was found to promote the expression of *Dorsal*, and physically interact with *Pelle*, which are downstream signalling molecules of *Toll* receptor, more direct evidence is needed to explain the detailed mechanisms of how *Toll-5* activates the downstream cascade (Luo et al., 2001).

Toll-3, another *Toll* paralogue, was also found to increase the expression level of anti-bacterial peptides indicating its potential function in immunity (Ooi et al., 2002).

Another *Toll* receptor that shows significant functions in immunity is *Toll-9*. It has been found that expression of *Toll-9* in S2 cells increases the level of cecropin and defensin up to 20-fold, and it also increase the level of Drosomycin significantly (Ooi et al., 2002). This suggests that *Toll-9* may have functions in anti-fungal and -bacterial response. Similar to *Toll-5*, *Toll-9* was found to induce the expression of *Pelle* suggesting a potential pathway shared among *Toll*, *Toll-5* and *Toll-9* (Ooi et al., 2002). However, it was later found that *Toll-9* mutant flies did not show immunity deficiency (Narbonne-Reveau et al., 2011). To conclude, so far there is only in vivo evidence that *Toll-1* is involved in immunity, as cell culture evidence that *Toll-3*, *Toll-5* and *Toll-9* could be too has not been validated in vivo.

1.5.4 Function of *Toll* receptors in the central nervous system

Toll receptors have important functions regulating the development of the central nervous system. *Toll* regulates CNS development in late embryogenesis (Rose et al.,

1997, Halfon et al., 1995). *Toll* mutations caused loss of motoneurons in late embryonic CNS, which further affects neural circuits innervating the muscle and leading to the deficiency in muscle patterning (Halfon et al., 1995). *Toll* mutations also cause incorrect innervation of motor neuron growth cones into muscle and deficiency in synaptogenesis between neurons and muscle cells (Rose et al., 1997). During metamorphosis in pupae, *Toll-6* and *Toll-7* are involved in mediating the specificity of neuronal wiring between dendrites of projection neurons and axons of olfactory receptor neurons in the forming adult brain (Ward et al., 2015). However, this function does not require the canonical, intracellular *Toll* signalling pathway, and relies on cell-cell contact instead.

Toll receptors are also involved in regulating structural plasticity in the CNS. Loss of *Toll-6* or *Toll-7* function causes the mistargeting of motor axons as well as defects in larval crawling behaviour (McIlroy et al., 2013). Moreover, *Toll-6* is involved in regulating cell number in larval and early pupal CNS, where it could promote both cell survival or cell death via either *MyD88-NFκB* or *wek-Sarm-JNK* pathway, respectively (Foldi et al., 2017). Toll receptors are also involved in structural synaptic plasticity. *Toll-6* and *Toll-8* mutant has been found to cause reduced volume of neuromuscular junctions (NMJs) (Foldi et al., 2017, Ballard et al., 2014), and Toll-6 mutants have smaller NMJs (Ulian-Benitez et al., 2017). At the NMJ, *Toll-6* has been shown to function forming a presynaptic complex with Kek-6, the alternative kinase-less *Trk* receptor for *DNT2*.

1.6 Downstream signalling of *Toll* receptors

1.6.1 *Toll* signalling pathway in dorsal-ventral pattern establishment

In the embryonic dorsal-ventral axis establishment, *Toll* functions as the receptor of *Spz* that is produced by the female fly and secreted into the perivitelline space of the embryo (Stathopoulos and Levine, 2002). Spz is cleaved by *Easter*, a serine protease, resulting in the active and dimerized form of the *Spz* (DeLotto and DeLotto, 1998; Chasan and Anderson, 1989). The active *Spz* dimer binds with one *Toll* receptor at the N-terminus and induces the dimerization of *Toll* receptors and the formation of a 2:2 complex (Gangloff et al., 2008; Morisato and Anderson, 1994). The activated *Toll* receptor then allows the downstream adaptor *MyD88* to bind at the intracellular Toll/IL-1 receptor (TIR) domain (Kambris et al., 2003; Medzhitov et al., 1998) (Figure 1.4). *MyD88* then recruits the downstream molecules *Tube* and *Pelle* to the plasma membrane, which bind at its death domains (Hecht and Anderson, 1993; Medzhitov et al., 1998). *Tube* and *Pelle* then interact with each other at their death domains and induce the activation of *Pelle* (Xiao et al., 1999). The activated *Pelle* functions as a protein kinase that then phosphorylates and causes the degradation of *Cactus* and releases the transcription factor *Dorsal* to translocate to the nucleus to activate the expression of different genes to generate different cell types along dorsal-ventral axis (Moussian and Roth, 2005).

Before the *Toll* receptor is activated by *Spz*, the *Rel* family *NFκB* factor *Dorsal* is bound with *IκB* family protein *Cactus* in the cytoplasm (Edwards et al., 1997). When the *Toll* pathway is activated, the active *Pelle* phosphorylates both *Cactus* and *Dorsal*, which leads to the degradation of *Cactus* and the released *Dorsal* then move to the nucleus (Edwards et al., 1997; Moussian and Roth, 2005; Whalen and Steward,

Figure 1.4 *Toll* signalling pathways

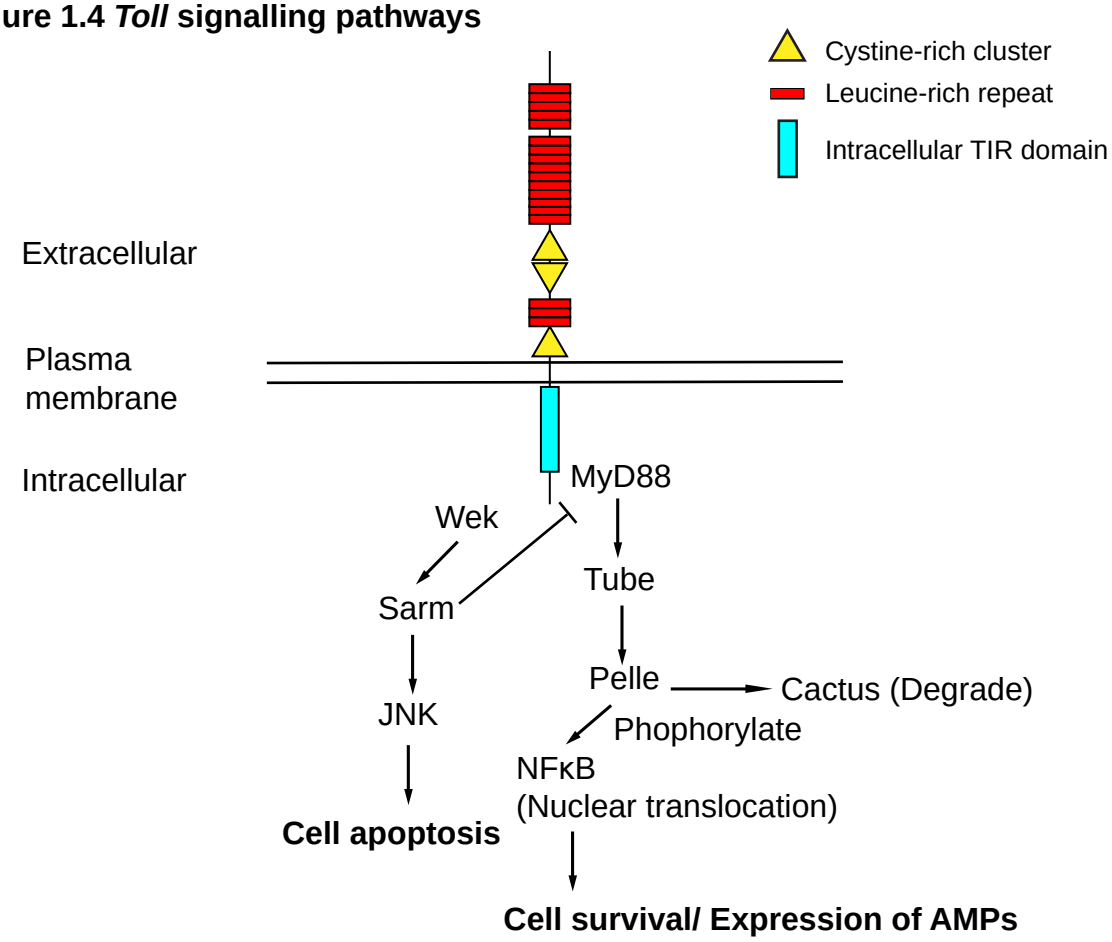


Figure 1.4 *Toll* signalling pathways

This figure illustrates the main pathways of *Toll* signalling. *Toll* promotes cell survival or innate immunity *MyD88-NFκB* pathway, while *Toll* can also function via *wek-Sarm-JNK* pathway to promote cell death.

1993). Moreover, the concentration of the nuclear isoform *Dorsal* varies along the dorsal-ventral axis, which regulates the development of different parts of embryos. Thus, in this way, *Toll* signalling pathway is involved in the establishment of the dorsal-ventral axis.

1.6.2 *Toll* signalling pathways in immune system

Apart from the function in embryonic dorsal-ventral axis determination, the *Toll* pathway also plays key roles in the immune system in larvae and adult flies (Lemaitre et al., 1996; Manfruelli et al., 1999). Instead of being cleaved by *Easter*, *Spz* in the immune system is cleaved by *Spz* processing enzyme (*SPE*) that is activated by different protease cascades (Mulinari et al., 2006) . Antigens like β-glucan or peptidoglycan from fungi or Gram-positive bacteria firstly activate a modular serine protease (*ModSP*), which then activates the Gram-positive-specific serine protease (*Grass*) that further activates the *SPE* (Buchon et al., 2009, El Chamy et al., 2008). In parallel, different types of antigens such as virulence factors from fungi and Gram-positive bacteria induce the activation of *Persephone* (*PSH*) instead, which then directly activate *SPE* to cleave *Spz* (Gottar et al., 2006).

The Toll pathway is highly conserved in both embryo and antimicrobial reaction in larvae and adult. Similarly, the activated *Toll* further activates the *MyD88-Tube-Pelle* multicomplex to promote the nuclear translocation of *NF-κB* transcription factors. Meanwhile, a conserved molecule, *Pellino*, from *Toll* pathway was also identified as a positive regulator of *Pelle* to promote the immune response to Gram-positive bacteria (Haghayeghi et al., 2010). Apart from *Dorsal*, a *dorsal*-related immune factor (*Dif*) was also identified as the *NF-κB* factor that plays key roles in immune system (Ip et

al., 1993). The activated *Dorsal* and *Dif* then translocated to the nucleus to bind to the promotor of anti-microbial peptides (*AMPs*) coding genes and promote the expression of *AMPs* such as *Drosomycin* (Fehlbaum et al., 1994, Hetru et al., 2003) (Figure 1.4).

A cross-link has been found between the *Toll* and *Hippo* signalling pathways. The *Hippo* pathway is best known for its function in regulating cell proliferation, which plays key roles in keeping homeostasis of tissue growth and suppressing tumour formation (Johnson and Halder, 2014; Pan, 2010). *Hippo* is activated by various extracellular signalling peptides, such as Crumbs homolog (CRB) complex for specifying cell polarity and E-cadherins for cell-cell interaction (Bazellieres et al., 2009, Genevet et al., 2009). As a protein kinase, activated Hippo together with the adaptor protein Sav phosphorylates and activates the downstream kinase Warts (*Wts*) and the cofactor *Mats*, which in turn phosphorylate the transcription co-activator Yorkie (Yki) (Huang et al., 2005; Tapon et al., 2002; Wei et al., 2007). The phosphorylated *Yki* then export from the nucleus and gets degraded by the proteasome in in the cytoplasm (Dong et al., 2007; Oh and Irvine, 2008). Without the activation of *Yki*, the transcription factor *Scalloped* (*Sd*) is then bound and suppressed by tondu domain-containing growth inhibitor (*Tgi*) and the expression of target genes is therefore inhibited (Guo et al., 2013). On the other hand, when the *Hippo* pathway is not activated, the target genes such as cell death inhibitor *diap1* and cell-cycle regulator *cyclin E* will are expressed to promote the cell proliferation (Huang et al., 2005; Wu et al., 2003).

The signalling molecules and function in regulating cell proliferation of *Hippo* pathway is highly conserved in mammals. Importantly, *Hippo* signalling pathway recently was also identified to have functions in the immunity downstream of *Toll* receptor (Liu et al, 2016). It has been noticed that knocking down key elements of *Hippo* pathway in fat bodies made the adult flies more susceptible to Gram-positive bacteria. It was also found that *Toll* mutants lost the cytoplasmic translocation of *Yki* caused by bacterial infection, which suggests that the *Hippo* pathway may work downstream of the *Toll* receptor (Liu et al., 2016). Moreover, it was found that the protein kinase *Pelle* could negatively regulate the expression of *Cka*, one of the upstream inhibitors of *Hippo*. Furthermore, knocking down *Cka* decreased mRNA levels of *Cactus*, the inhibitor of *NFκB* factors, which indicates that *Cactus* is a target gene of *Hippo* pathway in fat bodies. Therefore, these findings unveiled the novel function of *Hippo* pathway in the immune system downstream of *Toll* receptors (Liu et al., 2016).

1.6.3 *Toll* signalling pathways in nervous system

Recent studies started to unveil the functions of *Toll* signalling pathways in the CNS. In immunity, *Toll-1* activates the *JNK* pathway causing cell apoptosis in larvae (Liu et al., 2015). Similarly, in the larval CNS it was also found that loss of *Toll* function caused the increase of Eve+ neurons, whereas conversely, gain of *Toll* function reduced neuronal number (Foldi et al., 2017). This indicates that *Toll-JNK* pathway functions to regulate cell apoptosis in CNS (Figure 1.4).

As *Toll-6* and *Toll-7* has been discovered to have functions in the central nervous system (CNS), it was then studied whether their neuronal function was via *Toll* signalling pathways (McIlroy et al., 2013). It was firstly found that *Toll-6* could

promote cell survival via canonical *MyD88-NFκB* signalling pathway in larval CNS, in which both overexpression of *Toll-6* and *MyD88* could increase the number of Eve+ neurons when *Toll-6* could also bind with *MyD88* physically (Foldi et al., 2017). Meanwhile, in contrast to larvae, it was also noticed that overexpression of *Toll-6* and *MyD88* induced the increase of neuronal death in early pupae. The epistasis tests also revealed that the apoptosis function of *Toll-6* is via a *wek-Sarm-JNK* pathway (Figure 1.4). Moreover, the apoptosis caused by gain of *Sarm* function was more significant in *MyD88* mutant background, which indicates that *Sarm* functions as the antagonist of *MyD88* (Foldi et al., 2017). Collectively, *Toll-6* could promote both cell survival and apoptosis in CNS via either *MyD88* or *JNK* pathway, respectively. The question was therefore addressed whether other *Toll* receptors also function via these signalling pathways and whether they are active in other stages like adult brain.

1.7 Mammalian *Toll*-like receptors

Mammalian *Toll*-like receptors were identified and named as homologues of *Drosophila Toll*. There have been 12 *TLRs* identified in mice and 10 identified in human. The structure of *TLRs* is similar to *Drosophila Toll* family with an ectodomain composed of LRRs and Cystine rich clusters and an intracellular tail with a TIR domain. The main difference in the ectodomain is that mammalian *TLRs* only have one cystine cluster flanking the C-terminal end of LRR domain, when *Drosophila Tolls* have two or more cystine cluster flanking both C- and N- terminus of LRR domain (Luo and Zheng, 2000, Gay and Gangloff, 2008) (Figure 1.3). Furthermore, whereas *Drosophila Tolls* bind NT-family *Spz* ligands and do not directly bind

pathogens, mammalian *TLRs* are pattern recognition receptors that directly bind products in pathogens' cell walls.

The canonical signalling pathway downstream of *TLRs* is conserved vs. that of *Drosophila Tolls*. *MyD88* or *Sarm*, the antagonist of *MyD88*, binds downstream of *TLRs* at the TIR domain. Downstream of *MyD88* are *IRAK4* and *IRAK1* which are the orthologues of *Tube* and *Pelle* in *Drosophila* (Akira and Takeda, 2004a). *NFκB* factors are then translocated to nucleus and regulate the gene expression which are involved in immunity and development (Leulier and Lemaitre, 2008). TLRs can also function via *MyD88*-indepenent pathways. For example, *TLR4* mediates LPS-dependent maturation of dendritic cells via a My88-independent pathway. *TLR3* also mainly functions via *MyD88*-independent pathways (Akira and Takeda, 2004b).

1.7.1 Functions of *TLRs* in immunity

TLRs are best known for their functions in innate immune responses (Leulier and Lemaitre, 2008). They are expressed in tissues involved in innate immune responses like lung, gastrointestinal tract, peripheral blood leukocyte and spleen (Zarember and Godowski, 2002). Differently from *Drosophila Toll*, mammalian *TLRs* can identify and interact directly with different antigens from bacteria, fungi and virus initiating immune responses through the activation of nuclear factor-kappa B (*NF-κB*) (Leulier and Lemaitre, 2008). Evidences have indicated that different *TLRs* can recognize distinct microbial components. *TLR-4*, for example, can recognize lipopolysaccharide (*LPS*) Gram-negative bacterial cell wall (Akira, 2006). *TLR-2* can detect Gram-positive bacteria through lipoteichoic acid, lipoproteins and peptidoglycan. *TLR-5* can bind to flagellin, the major protein of bacterial flagella, on domain D1 (Akira, 2006). *TLRs*

also have antiviral functions like recognition of single-stranded RNA by *TLR-7* and *8*, double-stranded RNA by *TLR-3*, and DNA by *TLR-9* (Akira et al., 2006, Alexopoulou et al., 2001, Heil et al., 2004, Hemmi et al., 2002). Moreover, *TLR-2* and *4* are also showing functions in fungal recognition (Akira et al., 2006). Besides the innate immune responses, TLRs in immunocytes like T cells, B cells and dendritic cells also bind distinct microbes, which further activate adaptive immune responses through the activation of naïve T cells by accessory signals. This links the function of *TLRs* with adaptive immunity (Muzio and Mantovani, 2001, Pasare and Medzhitov, 2003).

Activation of *TLRs* is also involved in neuroinflammation and neurodegeneration. It has been found that activating microglia with *LPS* causes neuronal death and death of oligodendrocytes, while knocking down *TLR-4* in microglia rescued these phenotypes (Lehnardt et al., 2002, Lehnardt et al., 2003). Similarly, *TLR-2* in microglia exposed to specific antigen also induced toxicity in neurons (Lehnardt et al., 2006). The toxicity induced by *TLRs* have been found to have close relationships with neurodegenerative diseases like Alzheimer's Disease, Multiple Sclerosis and cerebral ischemia (Carpentier et al., 2008, Okun et al., 2009).

1.7.2 Functions of *TLRs* in nervous system

Studies have revealed that *TLRs* are expressed widely in glial cells in the brain (Carpentier et al., 2008). *TLRs* are expressed in glial cells and lymphocytes in the nervous system, which are involved in innate immunity when confronting pathogens or *PAMPs* (Carpentier et al., 2008). TLRs are also thought to bind and mediate the clearance of Damage Associated Molecular Patterns (*DAMPs*) such as cell debris

resulting from cell fragmentation upon brain damage (Piccinini and Midwood, 2010, Medzhitov and Janeway, 2002).

Recently, the neuronal functions of *TLRs* have also been uncovered. It has been found that *TLRs* in neural progenitor cells are involved in regulating neuronal differentiation and proliferation (Rolls et al., 2007). For example, *TLR-2* and *TLR-4* can mediate cell fate determination of neural progenitor cells. Knocking down *TLR-2* in NPC will lead to the generation of astrocytes, while overexpression leads to the generation of neurons (Rolls et al., 2007). Moreover, knocking down *TLR-4* results in the increase of the proliferation of NPCs (Rolls et al., 2007). *TLR-8* has also been found to regulate neurite outgrowth and cell survival, as knocking down *TLR-8* in cortical neurons causes the inhibition of neurite outgrowth and induces the apoptosis. Moreover, it has also been found that this function of *TLR-8* is not via canonical *TLR* signalling pathway (Ma et al., 2006). The above data suggests that *TLRs* may underlie structural brain plasticity. However, the endogenous ligands of mammalian *TLRs* in the CNS are still little explored. Recently, studies in the cell culture revealed that mammalian *NTs*, *BDNF* and *NGF* can bind with *TLRs* and trigger their downstream signalling. For example, both *BDNF* and *NGF* could induce the expression of *NFκB* in the *TLR-4* expressing cells (Foldi et al., 2017). This suggests that mammalian neurotrophins could trigger neuronal functions of *TLRs* regulating structural brain plasticity.

1.8 ***Drosophila* as a working model**

Drosophila has been used as a model organism in neuroscience for decades. High similarity to human genome, small size of organism, large number of progeny flies

and short generation time all make *Drosophila* an ideal experimental system (Lloyd and Taylor, 2010). *Drosophila* also has complex structure of brain and nervous system involved in neuronal development during different stages. Many of the molecular mechanisms are revealing homology to those of humans (Nichols, 2006). Therefore, investigation of developmental processes in the *Drosophila* CNS can help understand the working mechanisms of the nervous system in humans. Moreover, as one of the organisms whose genome has been fully sequenced, genomic manipulation of *Drosophila* will become easier in this project (Adams et al., 2000).

1.8.1 Structure of *Drosophila* larval CNS

The larval CNS is composed of neurons and glial cells derived from postembryonic neuroblasts (Prokop and Technau, 1991). The larval CNS is relatively simple compared with the adult brain as there are around 2000 neurons in the larval CNS while around 135,000 in the adult brain. However, the larval CNS is complex enough to study brain function, as most of the cell classes in adult brain can be traced to larval CNS (Prokop and Technau, 1991, Truman, 1990) (Figure 1.5 a). The larval CNS is formed of thoracic ventral nerve cord and 2 optic lobe hemispheres. Within the optic lobes, the visual system is composed of two classed of cells which are from outer proliferation centre (OPC) and inner proliferation centre (IPC) (Apitz and Salecker, 2015). In the central brain flanked by the optic lobes, there are the larval mushroom body (MB) neuropils that are dorsal lobes (DL) and medial lobes (ML) which are projected from the Kenyon cells (Kurusu et al., 2002).

1.8.2 Structure of *Drosophila* pupal and adult brain

During metamorphosis in pupa, drastic changes occur to in order to form the adult brain (Figure 1.5 b). Neuroblasts remained from the embryo entered a second wave of proliferation to form the neurons and glia for the adult brain (Prokop and Technau, 1991). There are some cells from the larval CNS the remained to form the adult brain. These cells receive signals from their targets and extend axons and dendrites to form the neuropils in the adult brain (Truman, 1990). Meanwhile, cells that are not required for the adult brain are eliminated via apoptosis (Truman, 1990).

The adult optic lobe functions in vision, and is composed of 3 ganglia including medulla, lobula plate and lobula. Outer medulla and lamina are generated from OPC of larval CNS, whereas the inner medulla, lobula and lobula plate are derived from IPC (Apitz and Salecker, 2015). In the visual system, the lamina is required for motion detection. The Medulla is the largest neuropil in the optic lobe, and it receives information from colour photoreceptor for colour detection (Neriec and Desplan, 2016). Lobula plate functions for motion information processing. The function of lobula is more for object features detection such as orientation and texture (Zhu, 2013)

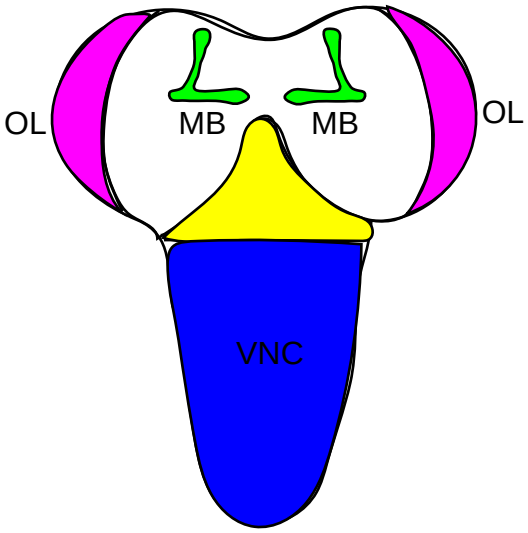
The adult mushroom body is best known for its functions in olfactory learning and memory. It contains two symmetric neuropils in each side of the central brain. Each neuropil consists of a group of Kenyon cells whose dendrites form a cup-shaped calyx and the axons further form the neuropils including α, α', β, β' and γ lobes (Heisenberg, 1998). Previous studies have suggested that $\alpha\beta$ lobes functions in long term memories formation, when γ lobe is functional for short-term memories (van Swinderen, 2009).

The central complex is composed of the ellipsoid body, fan-shaped body, Protocerebral Bridge, and a pair of noduli. The Ellipsoid body is a formed by a group of ring neurons whose axons form a ring-shaped neuropil. It has functions in navigation and locomotion of the adult fly (Pan et al., 2009). The Fan-shaped body is reported to have functions in processing visual information and sleep (Pan et al, 2009, (Xie et al., 2017).

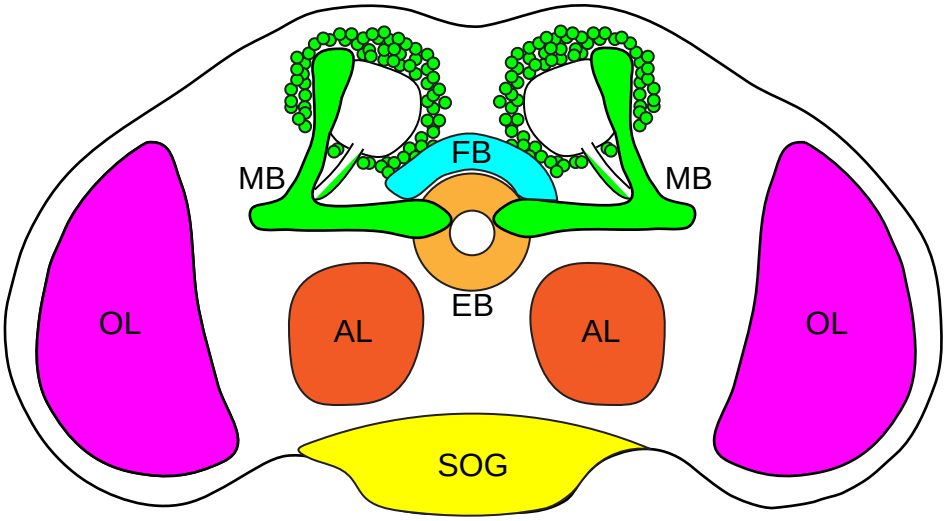
The structure below the central complex is a pair of antennal lobes which play key roles in receiving and processing olfactory information (Silbering et al., 2008). At the ventral side of olfactory lobe is the sub-oesophageal ganglion (SOG) which is derived from the top part of larval VNC (Truman, 1990). Neurons in SOG are connected with proboscis and salivary gland, which are related to behaviour in food taking.

Figure 1.5 Structure of *Drosophila* CNS

a.



b.



a), *Drosophila* larval CNS

b), *Drosophila* adult brain

AL, antennal lobe; EB, ellipsoid body; FB, Fan-shapped body;

MB, mushroom body; OL, optic lobe; SOG, Sub-oesophageal ganglian

1.9 Aims

The overall aim of my PhD project is to investigate the mechanisms involved to regulate brain structural plasticity. Focusing on *Toll-2*, I asked how cell number plasticity is regulated in the brain.

Therefore, the aims of my PhD project are:

1. To test whether *Toll-2* is expressed and required in the brain. This will be achieved by:
    - generating tools with CRISPR/Cas9
    - testing for phenotypes in behaviour and testing neurodegeneration and connectivity using MARCM.
2. To study the function of *Toll-2* in regulating cell number in metamorphosis. This will be achieved by:
    - looking at cell number in the late pupal brain when manipulating *Toll-2* loss and gain of function through development or specifically at pupa.
3. To investigate the function of *Toll-2* in regulating cell number in the adult. This will be achieved by:
    - looking at how *Toll-2* loss or gain of function would affect the adult brain either through development or at a pulse specifically during the adult critical period.

4. To test whether altering neuronal activity specifically at the adult critical period affects cell number. This will provide evidence of experience dependent structural plasticity influencing cell number in the brain.

5. To investigate whether *Toll* signalling pathways and other *Tolls* function in structural plasticity in the adult brain. This will be achieved by:

    - looking at how loss or gain of function of the downstream molecules affect the brain at a pulse specifically during the adult critical period.

    - looking at how manipulating the function of multiple Toll receptors affects brain structure.

Chapter 2 Materials and Methodology

2.1 Genetics

2.1.1 Fly maintenance

All the fruit flies were kept in standard cornmeal agar medium in bottles or vials. All the flies were cultured at 25°C with 12 hours Light/Dark cycle unless indicated (Chapter 2.1.3). All the stocks were kept at 18°C with 12 hours Light/Dark cycle, transferred once in every 5 weeks. Stocks generated and used for this project are listed in Table 2.1.

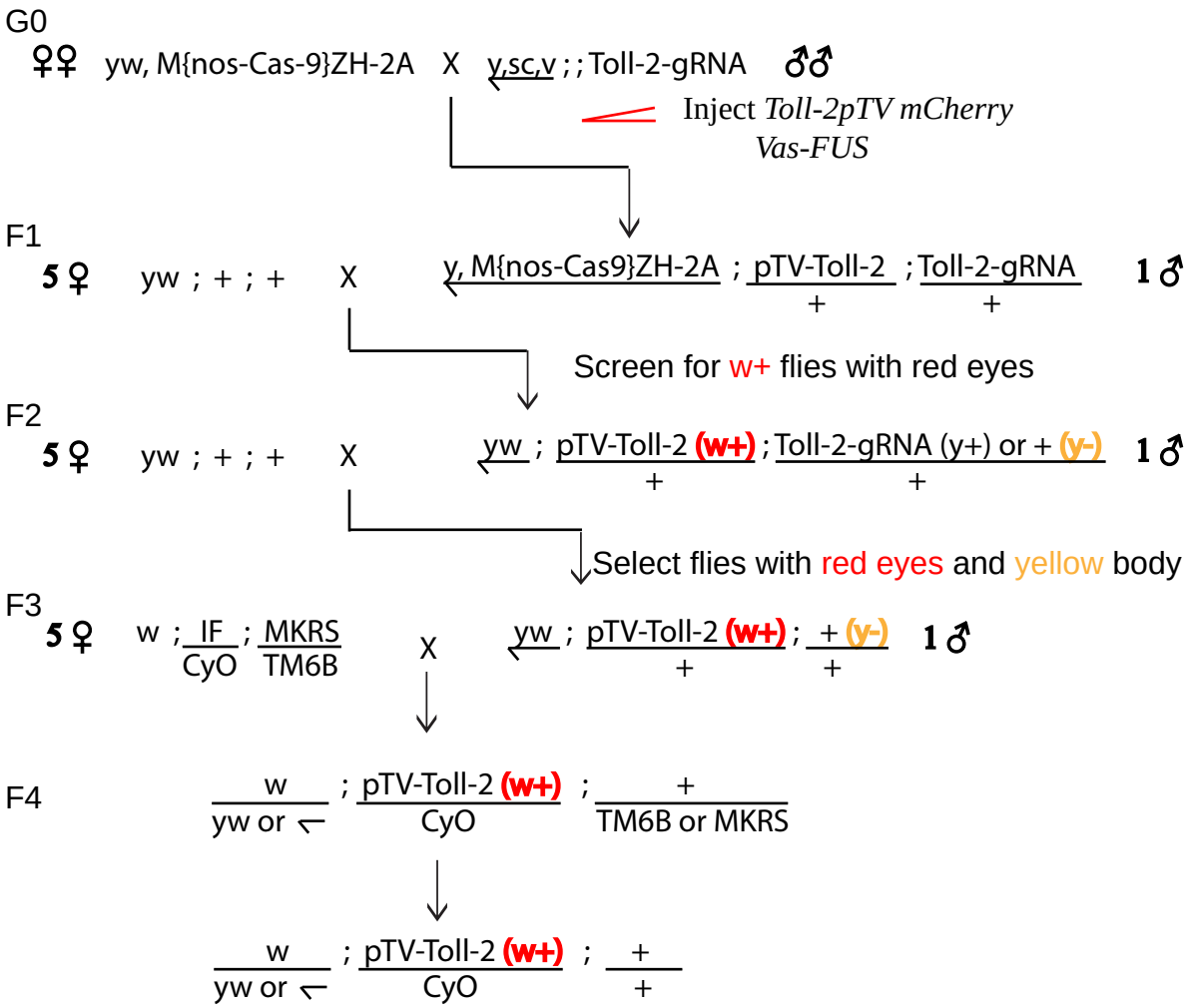
2.1.2 Genetic protocols

Transgenic flies generated from microinjection were balanced to build stable stocks. Transgenic flies generated in this project were *Toll-2*^{pTV} (Figure 2.1), *Toll-2*^{pTV} Gal4, (Figure 2.2) *Toll-3*^{MiMIC} Gal4 (Figure 2.3), and *UAS Toll-2*^{attP2} (Figure 2.4). Recombinant flies were generated for MARCM clone (Figure 2.5 and 2.6). Conventional genetic techniques were applied to combine 2nd and 3rd chromosome, change balancer on the 2nd chromosome and generate recombinant on the 2nd chromosome (Figure 2.7 to 2.9).

2.1.3 Temperature shifting regimes

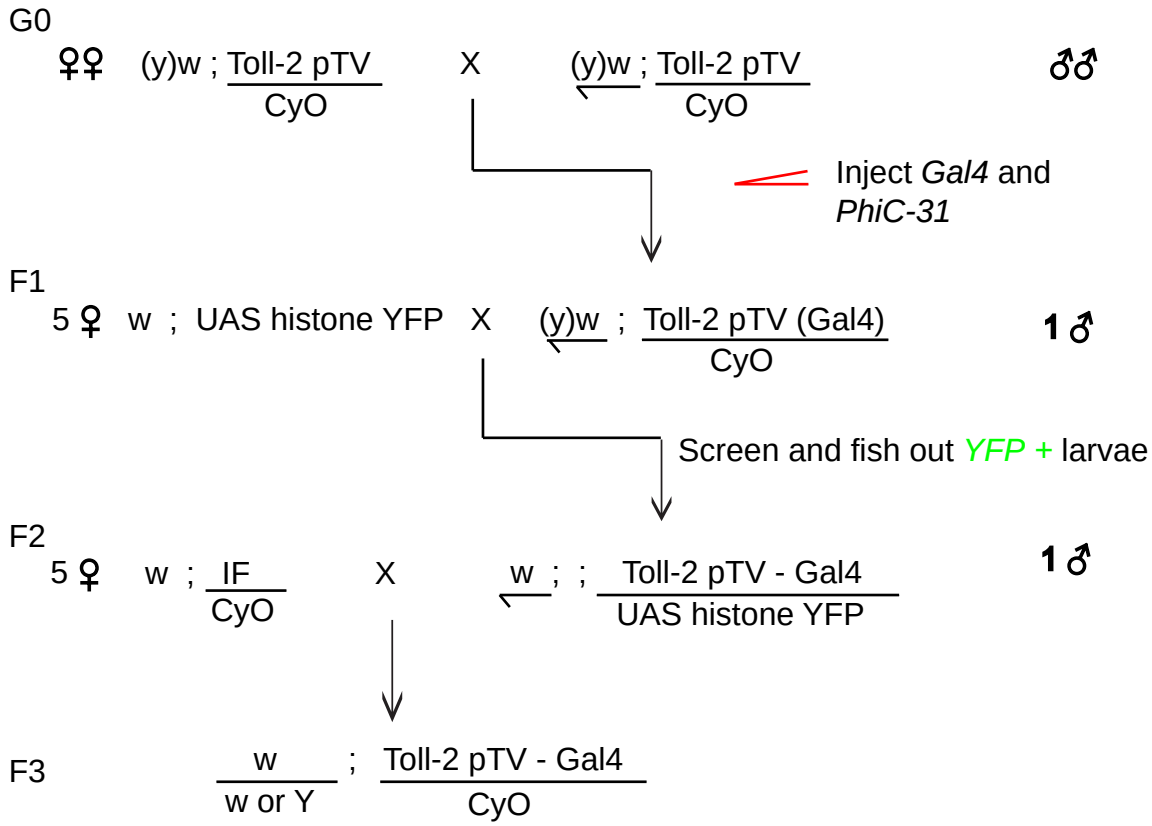
In order to switch the genes on or off at the specific stage of the flies, Gal4/UAS system was applied to control the expression of the genes. Meanwhile, TubulinGal80^{ts}, the inhibitor of Gal4, which is a temperature sensitive gene was used to control the expression of Gal4. To induce the gain and loss of function of *Toll-2*

Figure 2.1 Genetics protocol for generating *Toll-2^{pTV}* transgenic flies



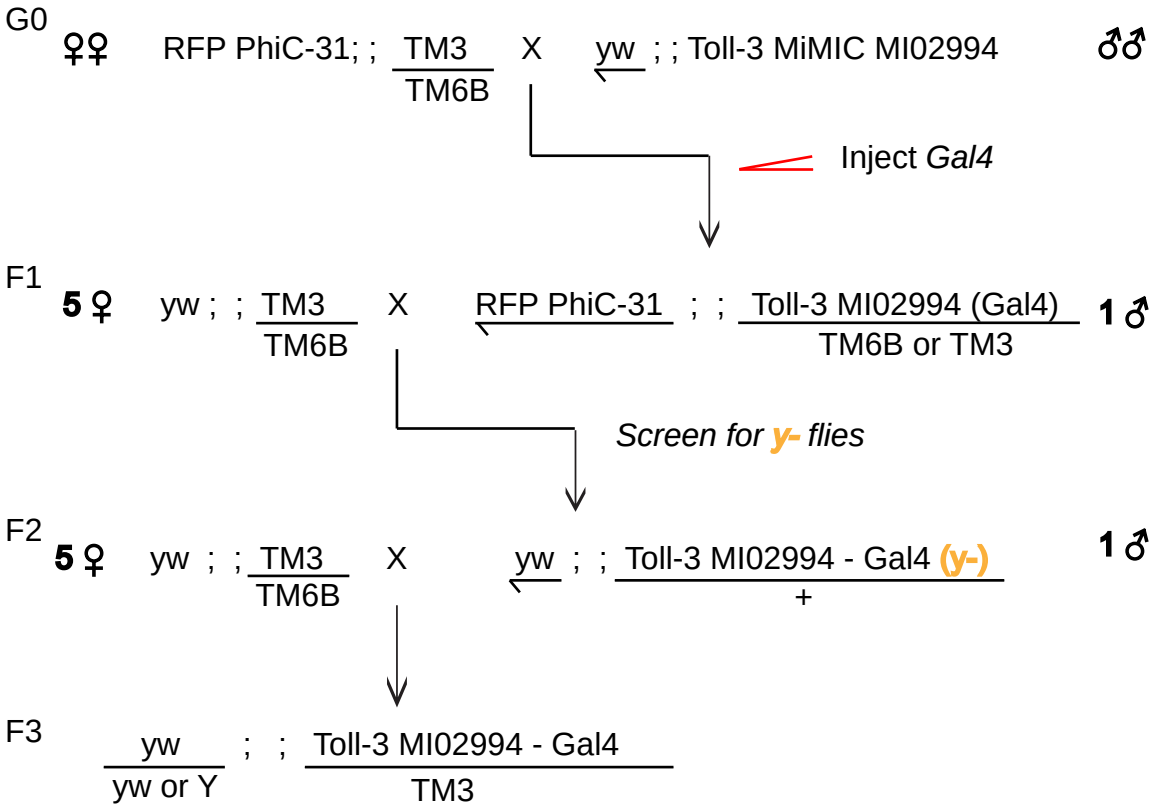
In this protocol, F2 flies with red eyes were screened from flies with orange eyes as transgenic candidates. To remove Toll-2 gRNA, only flies with red eyes and yelllow body were selected in F3 and further balanced.

Figure 2.2 Genetics protocol for generating *Toll-2^{pTV}* Gal4 transgenic flies



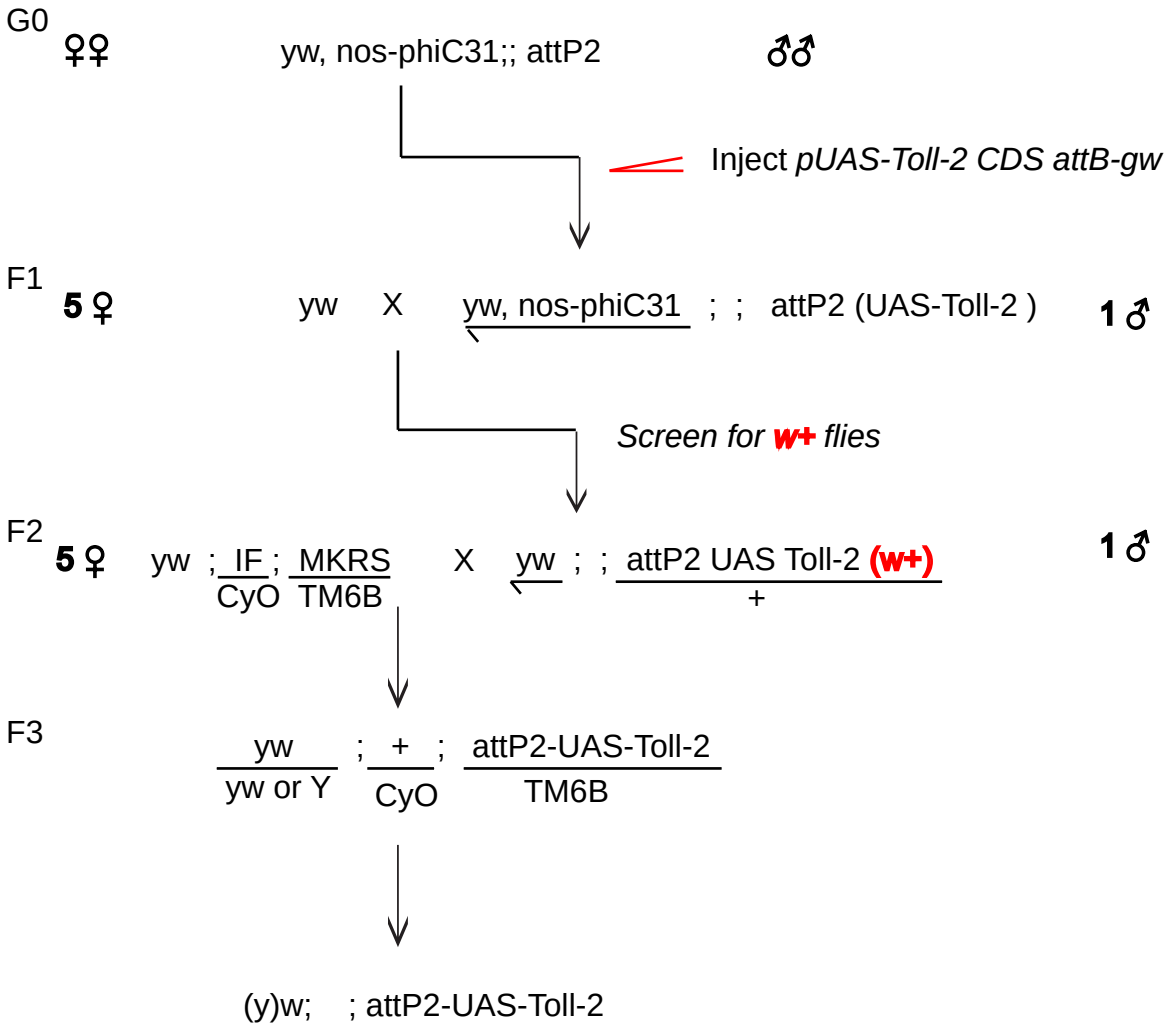
Injected flies were crossed with UAS histoneYFP and the progeny F2 larvae were screened for green fluoroscence,suggesting that the larvae carried Toll-2^{pTV} Gal4. Selected F2 flies were then balanced to build stable stocks.

Figure 2.3 Genetics protocol for generating *Toll-3*^{MiMIC} Gal4 transgenic flies



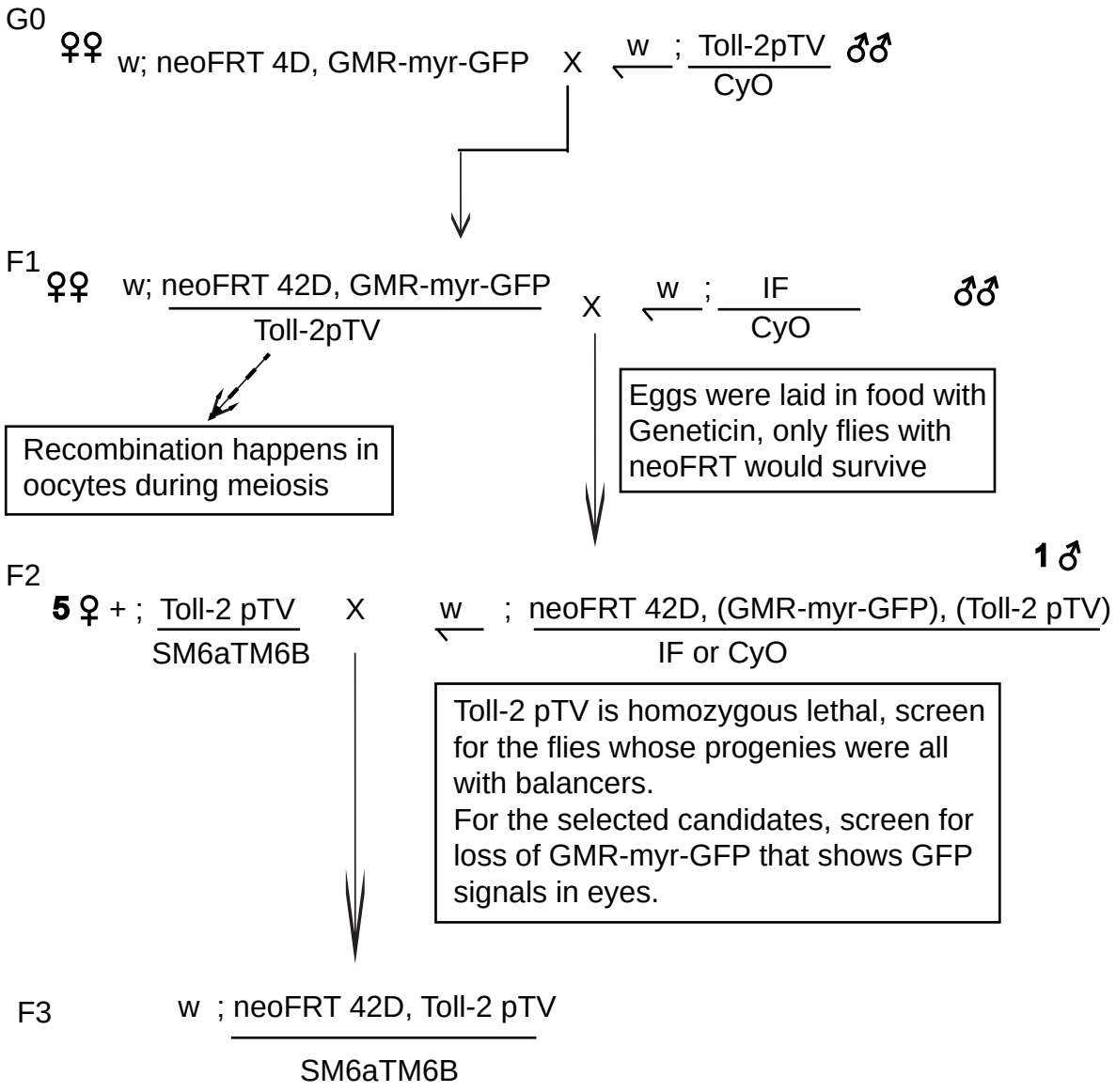
F2 flies were screened for yellow- with yellow body. MiMIC cassette in the genome carried yellow+, when Gal4 was inserted into the genome swapping with MiMIC cassette, yellow+ would be removed. Because the flies carried yellow- on the X chromosome, removing yellow+ would make the body colour of flies yellow. Selected candidates were then balanced and crossed with UAS reporters to further confirm whether Gal4 was functional or not.

Figure 2.4 Genetic protocol for generating UAS *Toll-2*^{attP2}



F1 flies were screened for gain of w+ because plasmid pUAS-Toll-2 CDS attB-gw carries w+ element. Therefore, when the plasmid was inserted into genome, where the genetic background was w-, the transgenic flies would show red eyes.

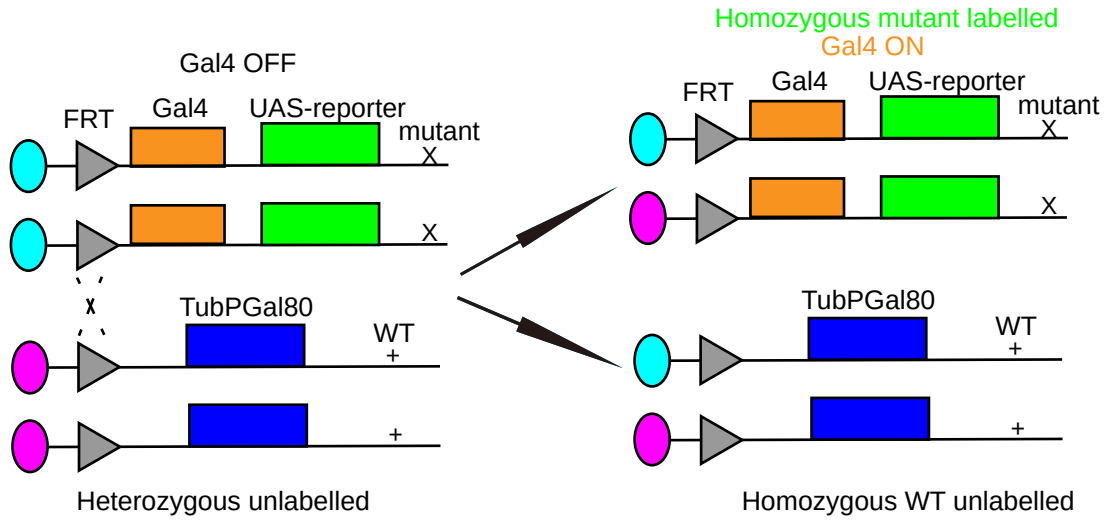
Figure 2.5 Genetics protocol for MARCM clone



To screen for neoFRT site in F2, fly food were made containing 1mg/ml Geneticin, only flieswith neo gene could survive from Geneticin.In F1 oocytes, recombination occurs among neoFRT, GMR-myr-GFP, and Toll-2^{pTV}, GMR-myr-GFP is not related with this experiment and its GFP signals would introduce noise to the result. Therefore, both gain of Toll-2^{pTV} and loss of GMR-myr-GFP was screened.

Figure 2.6 Experimental regimes of MARCM clone

a.



b.

♀♀ w, elav Gal4 UAS mCD8GFP, hs FLP ; neoFRT42D tubPGal80 / SM6a TM6B

X

Mutant: w ; neoFRT 42D, Toll-2 pTV / SM6a TM6B

♂♂

Control: yw, eye-FLP ; neoFRT 42D

↓

Select pupae without balancers and carry out heat-shock, use males only

c.

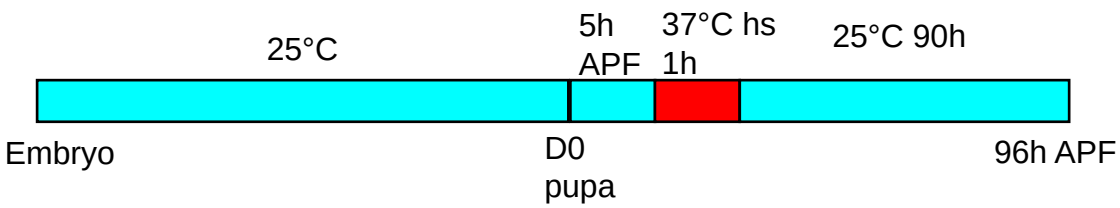
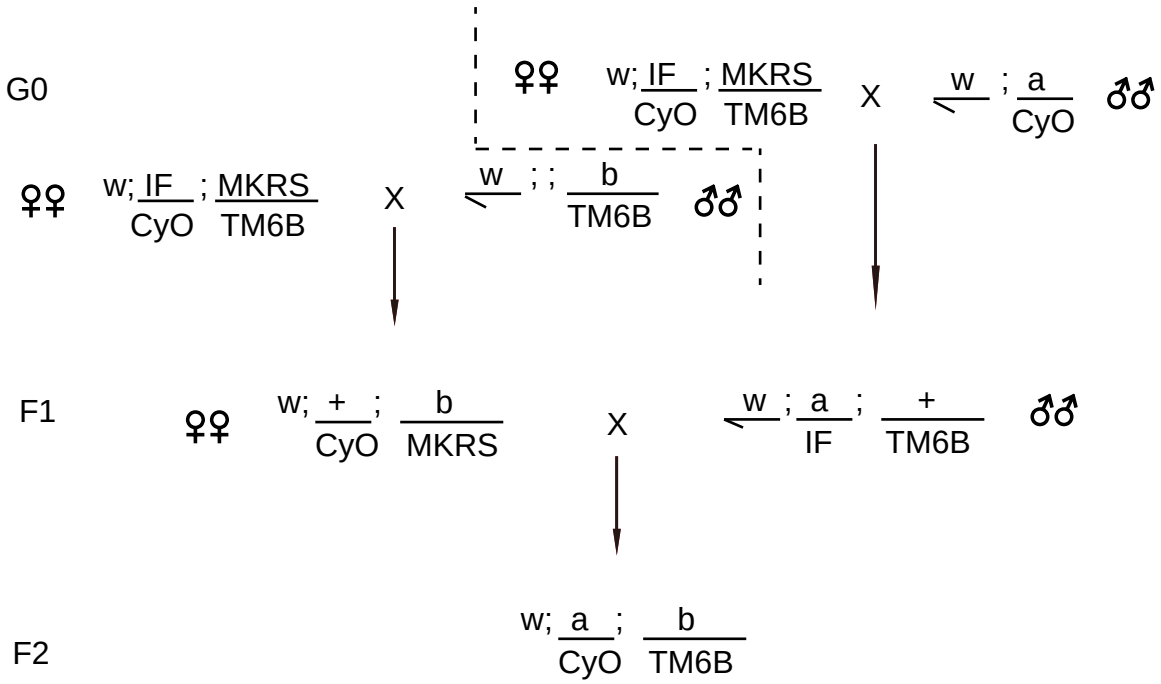
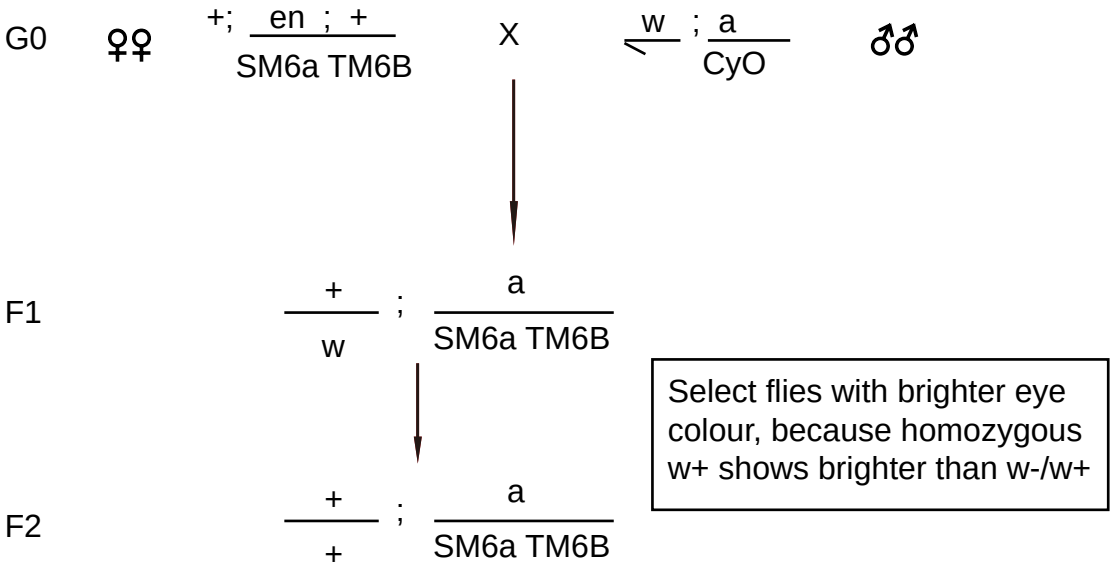


Figure 2.7 Genetics protocol for combination of 2nd and 3rd chromosome



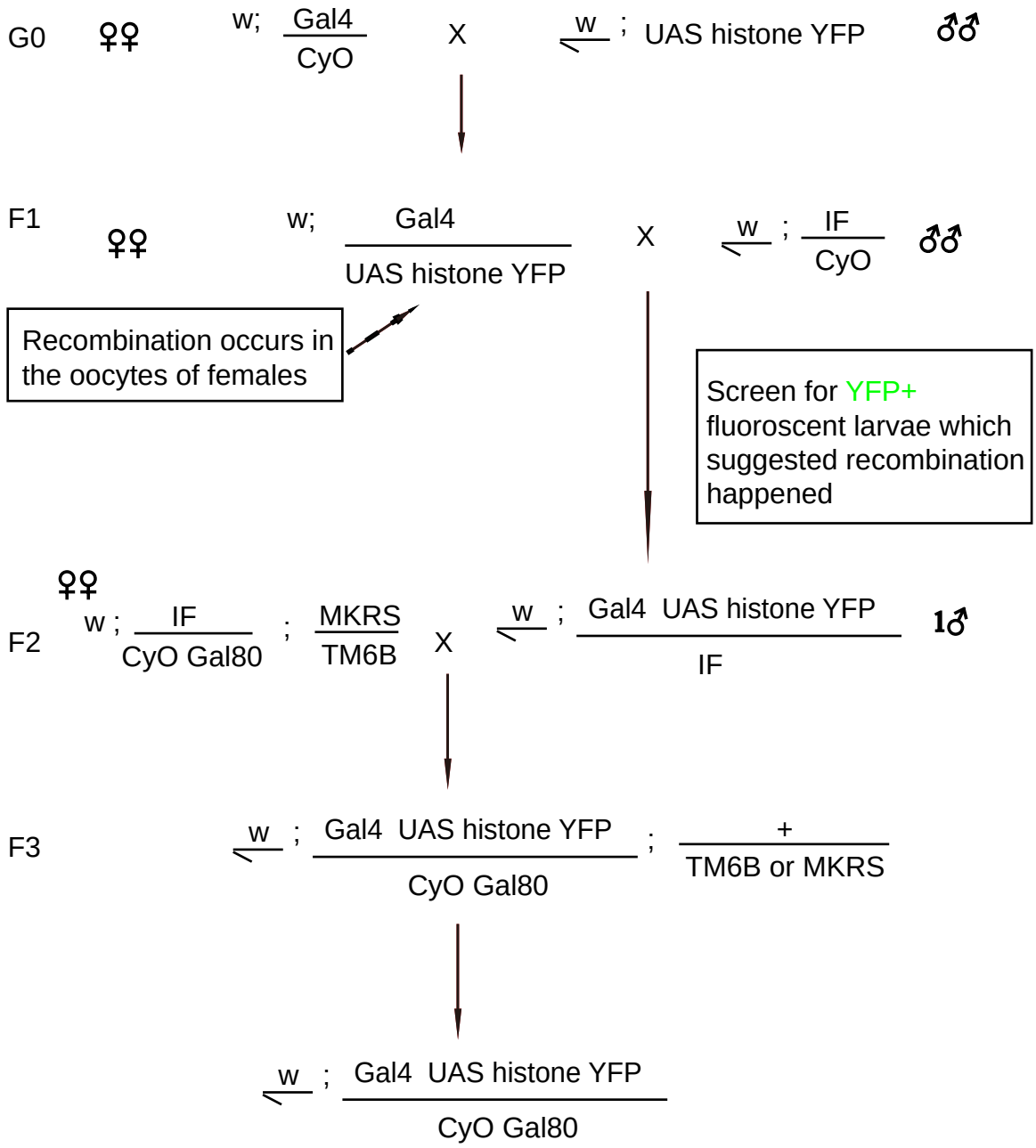
This protocol was used to combine alleles on 2nd and 3rd chromosomes.

Figure 2.8 Genetics protocol for changing eye colour background and balancer on 2nd chromosome



This protocol was used to change the balancer of 2nd chromosome, and to change the eye colour background at the same time.

Figure 2.9 Genetics protocol for generating recombinants of Gal4 lines with UAS histone YFP on the 2nd chromosome



This protocol was used to generate recombinants in which different Gal4 lines on the 2nd chromosome were recombined with UAS histone YFP. In F2, CyO Gal80 was applied as the balancer of the recombinant allele to switch off Gal4 in the stock, so that histone YFP would not be expressed in the stock.

Figure 2.9 Experimental regimes of MARCM clone

(a). Genetic basis of MARCM. In the heteozygous mother cells, tubPGal80 inhibits the expression of Gal4, so that UAS-reporter is not activated. When recombination occurs during mitosis, two homozygous daughter cells were generated. The homozygous mutant cells did not contain tubPGal80, so that the Gal4 was switched on and the mutant cells could be labelled with UAS-reporter.

(b). Genotypes of G0 flies for MARCM.

(c). Temperature shifting regime of MARCM. Flies were kept at 25°C from embryo until 5 hours after puparium formation. Pupae were then heat-shocked at 37°C for one hour and shifted back to 25°C for 90 hours. Finally, pupae at 96h APF was fixed and stained.

specifically at pupal stage, flies were kept at 18°C from embryo until puparium formation. D0 pupae were then transferred to 30°C incubator for another 72 hours (3 days) after which D3 pupae were dissected and analysed. For adult analysis, flies were kept at 18°C from embryo until eclosion. D0 adult flies were transferred to 30°C for another 48 hours (2 days), then D2 adult flies were dissected and analysed.

To carry out MARCM, mitosis is required for mitotic recombination to happen. In order to visualize as many clones as possible, the time for heat shock was selected as 5 hours after puparium formation (APF), which was found to be the peak time for cell proliferation in pupae. The flies were kept at 25°C from the embryo until 5 hours APF, after which pupae were shifted to 37°C water bath for another 1 hour, during which the hs-FLP will be activated and induce the homologous recombination to happen in mitotic cells. Afterwards, the heat shocked pupae were shifted back to 25°C for another 90 hours. Finally, 96hAPF was dissected, stained and analysed (Figure 2.6).

To study the effect of neuronal activity on cell number, TrpA1 was used to activate the neurons and TNT was used to block the activity of neurons. In order to study the effect specifically in adult, flies were kept at 18°C from embryo until 5 days after eclosion. Flies were then transferred to 30°C incubator for 5 hours to switch off the Tubulin Gal80^{ts} and switch on Gal4. Since activating neurons for too long may induce toxicity to cells, flies were then shifted between 30°C water bath and 18°C incubator every 10 minutes for an hour. This way could ensure that TrpA1 and TNT are still functional in the cells but avoiding toxicity caused by TrpA1. For TNT experiment, flies were transferred to 25°C hours to recover and finally dissected and analysed.

Table 2.1 Stock List

Name	Full genotype	Source
Toll-2^{pTV}	(y)w; pTV-Toll-2 $^{1M-b}$/CyO	Guiyi Li
Toll-2pTV/SM6a TM6B	+;Toll-2^{pTV}1M-b/SM6aTM6B	Guiyi Li
UAS Toll-2EP709	UAS Toll-2 P{GSV1}EP709	BDSC #43442
18wΔ7-35	yw;18w$^{\Delta 7-35}$/CyO	BDSC#4372
18wΔ7-35/SM6aTM6B	+;18w$^{\Delta 7-35}$/SM6aTM6B	Guiyi Li
Toll-3 MiMIC	w;Mst Prox MiMIC MI02994	BDSC#35889
Toll-3 MiMIC Gal4	yw; MstProxGal4 MI02994/TM3 Sb-	Guiyi Li
Toll-6 Gal4	yw; Toll-6 MI02127 Gal4/TM3 Line 1-6M	Hidalgo lab collection
Toll-2pTV Gal4	Toll-2^{pTV} Gal4/CyO	Guiyi Li
Toll-2pTV Gal4 UAS histone YFP	w; Toll-2pTV Gal4 UAS histone YFP/CyO GAL80	Guiyi Li
18wΔ7-35 UAS histone YFP	w; 18wΔ7-35 UAS histone YFP/CyO	Guiyi Li
Toll-2 RNAi	yv;;PTRIP HM05241/TM3	BDSC#30498
Toll-2 RNAi	+;;PTRIP HM05241/TM6B	Guiyi Li
MyD88 Gal4	yw;MyD88 NP6394/CyO lacz	DGRC#105-229
MyD88 Gal4 histone YFP	w;MyD88NP6394 Gal4 UAS histone YFP/CyO Gal80	Guiyi Li
MyD88 Gal4 histoneYFP;TubGal80ts	MyD88 Gal4 UAS histone YFP/CyO Gal80;TubGal80ts	Guiyi Li
Toll-8 Gal4	PGawB MD806/TM6B	BDSC #36548
Toll-2 pTV Gal4; TubGal80ts	+;Toll-2pTV Gal4;TubulinGal80ts/SM6aTM6B	Guiyi Li
Toll-2 pTV Gal4	+;Toll-2 pTV Gal4/CyO	Guiyi Li
UAS Toll-2 attP2	w;UAS-Toll-2 attP2	Guiyi

Toll-2 pTV Gal4 UAS histone YFP;TubGal80ts	Toll-2pTV Gal4 UAS histone YFP/CyO Gal80; TubulinGal80ts	Guiyi Li
Toll-2 gRNA	y,sc,v;; U6.3 Toll-2 gRNA	Guiyi Li
UAS FB 18wΔ7-35	w/yw;UAS FB 18wΔ7-35/CyO	Guiyi Li
Oregon	Oregon	Hidalgo lab collection
yw	y-w-	Hidalgo lab collection
CantonS	CantonS	Hidalgo lab collection
WTB	Wild type (Berlin)	Heisenberg lab collection
w; IF/CyO lacZ;MKRS/TM6B		Hidalgo lab collection
w; IF/CyO Gal80;MKRS/ TM6B		Hidalgo lab collection
+; IF/CyO;MKRS/TM6B		Guiyi Li
w; IF/CyO		Guiyi Li
+; IF/CyO		Guiyi Li
w;IF MKRS/SM6a TM6B		Hidalgo lab collection
en/SM6a TM6B	+;Df enE/SM6a TM6B	Hidalgo lab collection
UAS histone YFP; MKRS/TM6B	W; UAS histone YFP;MKRS/TM6B	Guiyi Li
UAS tdtomato	w-; ; 10X UAS myr-Td-tomato	Hidalgo lab collection
UAS DenMark	w;UAS DenMark 2	Hidalgo lab collection
UAS mCD8 GFP	w; UAS mCD8 GFP	Hidalgo lab collection
ElavGal4	+;; ElavGal4	Guiyi Li
ElavGal4	w;;Elav Gal4	Hidalgo lab

		collection
DfBSC 594	W;DfBSC 594/CyO	
DfBSC 594	+;DfBSC 594/SM6a TM6B	Guiyi Li
y,vas-PhiC31;;sb/TM6B		BDSC
UAS TrpA1	w; UAS TrpA1; Tubulin Gal80ts	Hidalgo lab collection
UAS TNT	w; UAS TNT; Tubulin Gal80ts	Hidalgo lab collection
Tubulin Gal80ts	Tubulin Gal80ts	Hidalgo lab collection
Nos-Cas9	y[1] M{w[+mC]=nos-Cas9.P}ZH-2A w[*]	BDSC#54591
Neo FRT, GMR-myr-GFP	w;p{ry+=neoFRT},P{w+, GMR=myrGFP}2R	BDSC#7110
neoFRT42D,tubP=Gal80	yw;p{ry+=neoFRT}42D,p{w+=tubP=Gal80}/CyO	BDSC #9917
Elav Gal4 UAS mCD8GFP, hs-FLP	P{GawB}elav,P{UAS-mCD8=GFP} P{hs-FLP}w/FM7c;+/CyO	BDSC #5146
Elav Gal4, hs-FLP; tubP-Gal80	P{gawB}elav155,P{hs-FLP}w;P{FRT(whs)}GB, P{tubP-Gal80}LL2/CyO	BDSC #5145
Dorsal-GFP	w;PBac}dl-GFP-FPTB}VK0033	BDSC#42677
Elav Gal4 UAS mCD8,hs-FLP;neoFRT42D,tubGa80	w,p{GawB}, p{UAS-mCD8GFP},P{hs-FLP};neoFRT42D, TubgulinGal80/CyO Dfd YFP	Guiyi Li
Toll-2pTV Gal4 UAShisYFP;UAS Toll-2 RNAi	w;Toll-2pTV Gal4 UAShisYFP/CyO Gal80;UAS Toll-2 RNAi/TM6B	Guiyi Li
18wΔ7-35;UAS Toll-2 RNAi	+;18wΔ7-35;UAS Toll-2 RNAi/TM6B	Guiyi Li
UAS Rbf	UAS Rbf280/TM6B	Hidalgo lab collection
UAS p35	UAS p35 3w	Hidalgo lab collection
neoFRT,Toll-2pTV	+/(w);ry+=neoFRT,w+=GMR-myr-GFP, Toll-2pTV/SM6a TM6B	Guiyi Li

UAS Toll-7 RNAi; UAS Toll-6 RNAi	w;UAS Toll-7 RNAi/CyO;UAS Toll-6 RNAi	Guiyi Li
UAS Toll-7 RNAi; UAS Toll-8 RNAi	w;UAS Toll-7 RNAi/CyO;UAS Toll-8 RNAi	Guiyi Li
UAS Toll-7 RNAi; UAS Toll-1 RNAi	w;UAS Toll-7 RNAi/CyO;UAS Toll-1 RNAi	Guiyi Li
UAS histoneYFP; UAS Toll-2 attP2	w;UAS histoneYFP;UAS Toll-2 attP2	Guiyi Li
Toll-7 Gal4	Toll-7 Gal4 MI13963/SM6a	Hidalgo lab collection
Sarm Gal4	yw;P{w+ GawB} Ect4 NP7460/TM6B UAS lacZ	Kyoto #105471
Sarm Gal4	yw;P{ GawB} NP0257/TM6, P{UAS-lacZ.UW23-1}	Kyoto #103571
Wek-GFP	w; PBac,wek GFP-FLAG-FPTB VK00033/TM6c	BDSC #67719
Dif-GFP	w;PBa{Dif-GFP.FPTB}VK00033	BDSC#42673

Table 2.2 Lists of primers

Primer No.	ORIGINAL NAME	GENE/PLASMID	PRIMER SEQUENCE(5'-->3')	DESCRIPTION
1	Toll-2 3'HRF2	Toll-2	ggactagtcc aaactccccctatggccata	Forward primer to amplify Toll-2 3'HR, with SpeI cut site
2	Toll-2 3'HRRN2	Toll-2	ttggcgcgccaa gtgagggttgtacatagccac	Reverse primer to amplify Toll-2 3'HR, with AscI cut site
3	Toll-2 NP 3'HRF	Toll-2	cgagtcggagtacagtgcgtatgatcagc	Forward primer to amplify Toll-2 3'HR outer in Nested-PCR
4	Toll-2 NP 3'HRR	Toll-2	ctgcagacaatagttctcggcagcattgc	Reverse primer to amplify Toll-2 3'HR outer in Nested-PCR
5	Toll-2 5'HRF2	Toll-2	ataagaatgcggccgcggcaattagttaggcctgaa	Forward primer to amplify Toll-2 5'HR, with NotI cut site
6	Toll-2 5'HRR2	Toll-2	cggggtaccccgtttggtgatttgctagttgg	Reverse primer to amplify Toll-2 5'HR, with KpnI cut site
7	Toll-2 3'HRcPCR R	Toll-2	gcatactctcgtctgccgat	Reverse primer for colony PCR to test Toll-2 3'HR insertion in plasmid
8	Toll-2 5'HRcPCR R	Toll-2	cttgccagcatttgaggctct	Reverse primer for colony PCR to test Toll-2 5'HR insertion in plasmid
9	3' polylinker F	pTV^{mCherry}	cagaagcttatcgataccgtc	Forward primer for sequencing the front part of 3'HR insertions
10	3' polylinker R	pTV^{mCherry}	gacagtactccgacctgcactc	Reverse primer for sequencing the latter part of 3'HR insertions
11	5' polylinker F	pTV^{mCherry}	ctgttgccgagcacaattccg	Forward primer for sequencing the front part of 5'HR insertions
12	5' polylinker R	pTV^{mCherry}	cttgatgatggccatgttatc	Reverse primer for sequencing the latter part of 5'HR insertions
13	posR1mCherry	pTV^{mCherry}	cttctagtggatccagacatg	Reverse primer for PCR to test front part of *mCherry*
14	posF2mCherry	pTV^{mCherry}	cactacgacgctgaggtcaag	Forward primer for PCR to test latter part of *mCherry*
15	posR2white	pTV^{mCherry}	gttgcagaatagtccgcgtgtc	Reverse primer for PCR to test front part of *mini-white*
16	posF3whiteS	pTV^{mCherry}	gagcggcttcgcagagctgc	Forward primer for PCR to test *mini-white* from starting
17	posF4whiteE	pTV^{mCherry}	cgcatatctggctctaagac	Forward primer for PCR to test *mini-white* and *Gal4* from ending part of *mini-white*
18	posR4Gal4M	pTV^{mCherry}	gattgcacactgtgataacag	Reverse primer for PCR to test Gal4 at middle part of *Gal4*
19	posR3Gal4S	pTV^{mCherry}	gttcgatagaagacagtagc	Reverse primer for PCR to test *Gal4* and *mini-white* at starting part of *Gal4*
20	posF5Gal4	pTV^{mCherry}	ctgtcgacgatgtgcagcgtac	Forward primer for PCR to test *Gal4* at middle part of *Gal4*
21	U6.3 seqF	pU6.3	acctactcagccaagaggc	Forward primer for inserted gRNA sequencing
22	U6.3 seqR	pU6.3	tgcatacgcattaagcgaac	Reverse primer for inserted gRNA sequencing
23	Toll-2 gRNA SOM	Toll-2	gtcgctcctgcatgccagtgaac	Toll-2 gRNA sense oligonucleotides for U6.3
24	Toll-2 gRNA ASO	Toll-2	aaacgttcactggcatgcaggagc	Toll-2 gRNA anti-sense oligonucleotides for U6

Primer No.	ORIGINAL NAME	GENE/PLASMID	PRIMER SEQUENCE(5'-->3')	DESCRIPTION
25	pTV TL2 null	Toll-2	ctgagtgagatggatatggc	Reverse primer at downstream of the Toll-2 exon to test whether Toll-2 exon is knocked out completely
26	pTV TL2 int 5'F new	Toll-2	agtggtctgcatctgtgttg	Forward primer at upstream of pTV-Toll-2 5'HR to test the inserting locus of pTV-Toll-2, work with 5'polylinker 5'R
27	pTV TL2 int 3'R new	Toll-2	ctagcaatccggctaaaatg	Reverse primer at downstream of pTV-Toll-2 3'R to test the inserting locus of pTV-Toll-2, work with 3' polylinker 3'F
28	pTV TL2 int 5'F Seq	Toll-2	cactatcagagcaccgcactc	Forward primer to sequence the part where 5'HR recombined with genome region
29	ptv TL2 null F2	Toll-2	ggagttgagggaactgcatc	Primer to check whether Toll-2 is fully knocked out
30	ptv TL2 null R2	Toll-2	cactcgcactgttcgtactc	Primer to check whether Toll-2 is fully knocked out
31	ptv TL2 null F3	Toll-2	ccgactttgtgtgcaagtatg	Primer to check whether Toll-2 is fully knocked out
32	TL2 ptv null F4	Toll-2	gctcggtgccagtatacctc	Primer to check whether Toll-2 is fully knocked out
33	TL2 ptv null F5 S	Toll-2	gctgcacatcgtcgaacacc	To sequence the part behind mini-white in Toll-2 pTV flies, for checking whether Toll-2 exon is left and in frame in the genome
34	18w RT PCR F	Toll-2	gcaatatcgtcacagcctc	Forward primer for 18w RT PCR that gives a 462bp fragment
35	18w RT PCR R	Toll-2	cacacaaactcgtagtccttc	Reverse primer for 18w RT that gives a 462bp fragment
36	GAPDH Fw	GAPDH	tcaccaccattgacaaggc	Forward primer of control gene GAPDH for RT-PCR that gives a 434 fragment
37	GAPDH Rev	GAPDH	cggtaagatccacaacggag	Revers primer of control genen GAPDH for RT-PCR that give a 434 fragment
38	Toll-2 CDS attB Fwd	Toll-2	ggggacaagtttgtacaaaaaagcaggctatgccagccacatcttcca	Forward primers for amplification of Toll-2 CDS for gateway cloning
39	Toll-2 CDS attB Rev	Toll-2	ggggaccactttgtacaagaaagctgggtgaccaggaaagcttggccgt	Reverse primers for amplification of Toll-2 CDS for gateway cloning
40	Sam-GAL4F-seq	Gal4	cgaacaagcatgcgatattt	Forward primer hybridizing beginning of Gal4
41	Sam-GAL4R-seq	Gal4	tccattgtagtggtattaaacatcc	Reverse primer hybridizing beginning of Gal4

Table 2.3: List of plasmids and vectors

Constructs	Antibiotic-resistance gene	Inserts	Comments
pTV^{mCherry}-Toll-2 5'HR-3'HR	Ampicillin	~5kb of Toll-2 upstream homologous arm and ~3kb of Toll-2 downstream homologous arm	For CRISPR to generate Toll-2-knocked out flies
U6.3-Toll-2 gRNA	Ampicillin	23bp of Toll-2 guide RNA	Expression of Toll-2 gRNA leading Cas-9 to cut at specific site of the Toll-2 to induce CRISPR with U6.3 promoter
pDonor-Toll-2 CDS	Kanamycin	4.213kb of Toll-2 CDS	Entry clone in gateway cloning for generating pUAS-Toll-2 CDS attB
pUAS-Toll-2 CDS attB	Ampicillin	4.213kb of Toll-2 CDS	Expression clone in gateway cloning carrying Toll-2 coding region with UAS promotor and attB site
Vector			
pTVmCherry	Ampicillin	mCherry, mini-white, Gal4	For cloning of homologous arms of genes in CRISPR
Vas-Cas9	Ampicillin		For CRISPR injection to induce double-strand cut with guidance of gene-specific gRNA
Vas-FUS	Ampicillin		For CRISPR injection, express endonuclease cutting at SceI site to linearize pTVmcherry to help with homologous recombination after CRISPR
pCFD3-dU6-3:gRNA	Ampicillin	pU6-3:gRNA	Express U6.3 promoter to promote the expression of gene-specific gRNA, which is more efficient than U6
Gal4-Hsp-70pA	Ampicillin	attB1-2-GT-SA-GAL4-Hsp70pA	For MiMIC injection to induce Gal4 to promote the expression of UAS-*gene*
pDonor221	Kanamycin		Vector of entry clone in gateway cloning,
pUAS-attB-gw	Ampicillin		Destination vector of gateway cloning, it carries UAS promotor and attB site

For TrpA1 experiment meanwhile, flies were transferred to 23°C instead for another 24hour and dissected. This is because that TrpA1 itself is temperature sensitive and is active at 25°C, which will further lead to toxicity. Finally, the flies were dissected and analysed.

2.2 Cloning of pTV^{mCherry}-Toll-2

2.2.1 Genomic DNA extraction

Genomic DNA of adult flies was made by using PureLink® Genomic DNA Mini Kit (Invitrogen). 20 Oregon R, one of the wild type strains, adult flies were collected and anaesthetized on ice in an Eppendorf tube. 180µl PureLink® Genomic Digestion Buffer was added into Eppendorf tube containing flies to make homogenate with yellow tips. 20µl Proteinase K was then added into homogenate and mixed well. After incubating the homogenate at 55˚C for 3-4 hours until complete lysis, genomic DNA was isolated following the supplied instructions and finally dissolved in 30µl TE buffer (10 mM Tris-HCl, 1 mM disodium EDTA, pH 8.0, Invitrogen).

2.2.2 Polymerase Chain Reaction (PCR)

DNA fragments were amplified from genomic DNA mentioned above or plasmid DNA. To amplify *Toll-2* and *Toll-5* homologous region, high fidelity is required by applying Expand High Fidelity PCR System (Roche) or Phusion High-Fidelity DNA polymerase (Thermo Scientific). For PCR diagnostic test, GoTaq® Flexi G2 DNA polymerase (Promega) was used. Detailed reaction mix of each PCR system and thermo cycle of each PCR programme is explained in Table 2.1 to Table 2.6.

2.2.3 Gel electrophoresis and gel purification

After the PCR reaction, gel electrophoresis and gel purification were carried out to check the size of DNA fragments and obtain pure PCR products. To run the gel, 0.5g agarose was dissolved in 50ml 1xTAE buffer and mixed with 2µl Ethidium Bromide (Sigma) in a mini-gel tank. After 30-minute solidification, PCR sample was mixed with 6x loading buffer that was made of 0.25% bromophenol blue, 0.25% xylene cyanol FF, 30% glycerol (Sigma) in water and then loaded onto the solidified gel. 0.4µg 1kb ladder (NEB) was loaded as molecular weight marker. Gel was run at 70V for 50min to 1h10min until the front dye had run to the end of the gel. Gel was placed under UV in a GeneBox (SYNGENE) to visualize DNA. DNA bands with expected size were cut with razor blade then purified with Gel Extraction Kit (Qiagen) following supplied protocol and finally dissolved in 20µl EB buffer (10mM Tris-HCl, pH 8.5, Qiagen).

2.2.4 Restriction enzyme digestion, ligation

Pure PCR product that amplified with primers with restriction sites (Table 2.8 Primer list) was digested with appropriate restriction enzymes. Vector *pTV*^{Cherry} was digested by the same enzymes at the same time. Restriction digestion was carried out in 20µl volume, which contained 200ng-1µg DNA, 2µl 10x buffer (NEB), 1µl of both enzymes (NEB), and appropriate volume of ddH_2O to compensate the reaction volume. The reaction mixture was incubated at 37°C for 3-4 hours then mixed with 4µl of 6x loading buffer and run on a gel. Both PCR insertion and *pTV*^{Cherry} with sticky restriction sites on both ends were purified from agarose gel by using Gel Extraction Kit following supplied protocol and dissolved in 20µl EB buffer respectively.

The DNA inserts were then ligated into *pTV*^{Cherry} by using T4 DNA ligase (Promega). The reaction was carried out in 15µl volume containing 1µl T4 DNA ligase, 1.5µl 10x buffer and appropriate volume of ddH_2O, in which 100ng vector was ligated with DNA inserts in molar ratio 1:3. The ligation mixture was incubated at 18°C overnight. Another ligation mixture with only vector but DNA inserts was also set up as the negative control to estimate the efficiency of ligation.

2.2.5 Transformation and colony selection

5µl of ligation mixture and negative control was then transformed into 50µl 10-beta competent *E. coli* (NEB) cells. Ligation mixture and cells were mixed gently and incubated on ice for 30 minutes, heat-shocked at 42°C for 30 seconds, and chilled on ice for 5 minutes. Then, 950µl of 37°C pre-warmed SOC medium (NEB) was added and cells were grown in a 37°C shaking incubator at 250rpm for 1 hour. Cells were then spun down at 10,000rpm for 1 minute and resuspended in 250µl medium while the other 750µl of supernatant had been take out and discarded. 50µl and 200µl resuspended cells were plated onto pre-warmed LB+agar plates with 100µg/ml of Carbenicillin. Plates were incubated at 37°C overnight.

To select positive colonies with successful ligation, 8 to 24 colonies from positive plates were selected and tested by mini-prep that will be described in 2.1.6. The number of selected colonies is adjusted based on the ratio of colonies grown on positive and negative plates. GoTaq® Flexi G2 DNA polymerase was used to do colony PCR. Colonies were picked up with white tips and dropped into 15ml centrifuge tubes containing 5ml LB broth with 100µg/ml of Carbenicillin. LB medium with colonies were then incubated in 37°C shaker at 225rpm overnight.

2.2.6 Plasmid amplification through mini-prep and diagnostic digestion test

After the cell culture had been incubated overnight as described above, 3ml (1.5mlx2) of selected cell culture was then put into a 1.5ml microcentrifuge tube and spun down at 10,000 rpm for 1 minute. Supernatant was disgarded and pellet was resuspended in 400µl resuspension buffer containing 25mM Tris-HCl (pH 8.0), 10mM EDTA, and 100µg/ml RNAse A. 200µl of Lysis buffer (1% SDS, 0.2M NaOH) was added into the suspension and mixed thoroughly by inverting tubes 5-6 times. 200µl of iced-cold Precipitation buffer (3M potassium-acetate, pH5.5) was added and mixed thoroughly. Samples were then centrifuged at 13,000 for 20 minutes. Supernatant from the centrifugation was transferred to a new 1.5ml microcentrifuge tube while pellet was discarded. Supernatant was then mixed with 400µl isopropanol and incubated at room temperature for 5 minutes followed by centrifuging at 13,000rpm for 30 minutes. Supernatant from the centrifugation was discarded while pellet was kept and washed with 400µl 70% ethanol by centrifuging at 13,000rpm for 10 minutes. Finally, the supernatant was discarded and pellet after air-drying was dissolved in 30µl TE buffer.

In order to check whether the insertions were ligated into vectors at the right site, appropriate enzymes were chosen to carry out diagnostic digestion tests. 300-500ng of the extracted plasmid was digested in 20µl reaction mixture at proper temperature for at least 1 hour and checked on agarose gels.

Plasmids shown correct bands after restriction digestion were then amplified in large scale. 100µl from the previous mini-prep cell culture was added into 100ml LB broth containing 100µg/ml of Carbenicillin. The culture was incubated in 37°C shaker

overnight and then midi-prepped by using Plasmid Midi Kit (Qiagen) following the supplied protocol.

2.2.7 Sequencing and PCR checking

Plasmids or PCR products were sent for sequencing when necessary. 300ng of plasmid, 3.2pmol of primer (Table 2.8), and appropriate volume of ddH_2O were required to make 10µl sequencing mixture. Samples were sent to DNA sequencing services, School of Biosciences, University of Birmingham for sequencing.

Table 2.4 Components of Expand High Fidelity DNA polymerase PCR System

Component	Volume
10xBuffer with $MgCl_2$	5 µl
10mM dNTP	1 µl
2µM Forward primer	7.5 µl
2µM Reverse primer	7.5 µl
Template DNA	0.1-250ng
Enzyme Mix	0.75 µl
dd H_2O	X µl
TOTAL	50 µl

Table 2.5 Components of Phusion High-Fidelity DNA polymerase PCR System

Component	Volume
5xBuffer with $MgCl_2$	4 µl
10mM dNTP	0.4 µl
2µM Forward primer	5 µl
2µM Reverse primer	5 µl
Template DNA	0.4pg-4ng
Enzyme	0.2 µl
dd H_2O	X µl
TOTAL	20 µl

Table 2.6 Components of GoTaq® Flexi G2 DNA polymerase PCR system

Component	Volume
5x Green Buffer	5 µl
25mM $MgCl_2$	1.5 µl
2mM dNTP	2.5
2µm Forward primer	5 µl
2µm Reverse primer	5 µl
Template DNA	<250ng
Enzyme	0.25 µl
dd H_2O	X µl
TOTAL	25 µl

Table 2.7 PCR program when using Expand High Fidelity DNA polymerase

Temperature	Time	Cycles
94°C	2min	1
94°C	15s	
45°C-65°C	30s	10
68°C	4min	
94°C	15s	
45°C-65°C	30s	25
68°C	45s-4min + 5s for each successive cycle	
68°C	7min	1
4°C	Unlimited	1

Table 2.8 PCR program when using Phusion High-Fidelity DNA polymerase

Temperature	Time	Cycles
98°C	30s	1
98°C	10s	
45°C-65°C	20s	35
72°C	30s/kb	
72°C	5min	1
4°C	Unlimited	1

Table 2.9 PCR program when using GoTaq® Flexi G2 DNA polymerase

Temperature	Time	Cycles
95°C	2min (4min for colony PCR)	1
95°C	30s	
45°C-65°C	30s	25
72°C	1min/kb	
72°C	5min	1
4°C	Unlimited	1

2.3 *gRNA* designing and ligation with vector U6.3

2.3.1 Defining the sequence of *gRNA*

gRNA finder program (http://crispr.mit.edu/) was applied to design the *gRNA*. The first 250bp of the coding DNA sequence (CDS) of *Toll-2* or *Toll-5* was taken and pasted into the program. A list of gRNA candidates, which are all 20nt followed by a 3-nt (NGG) PAM sequence was generated. The best result was then selected from the list and defined as the sense oligo of the *gRNA* because this is the one that can cause the least off-target effect based on the BLAST result. The antisense oligo of *gRNA* was then generated by SeqBuilder (DNAStar®), which is the reverse complimentary sequence of the sense oligo. Since *gRNA* and plasmid *U6:3* were ligated at BbsI site, 3bp of “gtc” was added to the 5’end of sense oligos and 4bp of “aaac” was added to the 5’end of antisense oligo. Then both oligos were ordered from Eurofins.

2.3.2 Produce Polynucleotide kinase (PNK) treated double-stranded *gRNA*

Since the oligos were made without phosphatase group on either side, both oligos were firstly treated with polynucleotide kinase (Promega). In both reactions, 8µl of 100µM oligo stock solution was mixed with 1µl PNK and 1ul T4 ligase buffer, and incubated at 37˚C for 30 minutes followed by 65˚C for 20 minutes to inactivate the kinase. Then both of the 10µl PNK treated oligos were mixed together with 10µl 10x annealing buffer (100mM Tris-HCl, pH7.5, 1MNaCl, 10mM EDTA) and 70µl H_2O to get double-strand *gRNA*. The mixture was incubated at 95˚C in heating block for 5 minutes and left in block to cool down to room temperature, therefore both oligos would get annealed gradually when temperature was decreased.

2.3.3 Preparation of *U6:3* plasmid for ligation

1µg of U6.3 plasmid was cut by BbsI for 2 hours at 37˚C and incubated at 65˚C for 20 minutes to inactive the enzyme. Digested U6.3 plasmid was then treated with 1µl of alkaline phosphatase mixed with 3µl of alkaline phosphatase 10x buffer and 6µl of ddH_2O to remove the phosphatase group at the end of cut plasmid to prevent self-ligation. Phosphatase treated U6.3 plasmid was then loaded on a gel and purified by Gel Extraction Kit (Qiagen).

2.3.4 Ligation, transformation, plasmid selection and amplification

40µg of digested and gel purified U6.3 plasmid were ligated with 6µl PNK treated and annealed oligo in a 20µl reaction mixture containing 2µl 10x ligase buffer and 1µl T4 ligase at 4˚C overnight.

10µl of ligation reaction was then transformed into 10-Beta *E. coli* competent cells and 6-10 colonies were selected and amplified through mini-prep. All samples were sent for sequencing. One of the plasmids with gRNA insertion will be midi-prepped. After getting big amount of plasmids, 50µg of both U6.3-Toll-2 gRNA and U6.3-Toll5 gRNA were then sent to BestGene Inc. to generate gRNA line transgenic flies.

2.4 Generation of *pUAS-Toll-2 CDS* via Gateway Cloning

In order to generate a *Toll-2* gain of function line, the plasmid *pUAS-Toll-2 CDS* was firstly generated via Gateway cloning following the standard protocol of Gateway® Technology with Clonase® II (Thermo Fischer Scientific) (Figure 2.10). For this purpose, *Toll-2* coding sequence was firstly PCR amplified with primer 38 and 39 flanked with *attB* site (Figure 2.11, table 2.2). 50fmol of the gel purified PCR product was then ligated with 150ng pDonor221 together with 2µl BPClonase II (Thermo Fisher Scientific) and TE buffer to make a 10µl mixture at 25˚C for 6 hours. 1µl of Proteinase K was then added to stop the reaction after 6 hours. 2µl of the reaction mixture was then transformed into 50µl DH5α *E.coli* competent cells following the standard protocol (NEB). After the transformation, 6 colonies were selected and grown in the LB broth overnight for mini-preparation. The DNA harvested from mini-preps was then digested using BglII for diagnostic purpose to select the correct cloning (Figure 2.12). The result indicates that all of the 6 colonies were with the correct bands (Figure 2.12 b). Thereafter, DNA from Colony 1 was selected randomly as the entry clone for the LR reaction in the next step. Afterwards, 75ng of the entry clone and 75ng of the destination vector, pUAS-gw-attB, was then mixed together with 2µl LR Clonase II (Thermo Fisher Scientific) and TE buffer as a 10µl mixture

incubating at 25˚C for 6 hours. Similarly, 2μl of the mixture was then transformed into 50μl DH5α *E.coli* competent cells and 6 colonies were selected for mini-preparation. Within 6 colonies, 3 of them showed correct bands after diagnostic digestion with BglII (Figure 2.13 a and b). Colony 4 was then selected to be midi-prepped and diagnostic digested again (Figure 2.13 c). The completed construct was then sent to Cambridge Fly Facility for microinjection. The genetics of the screening for the transgenic flies is shown in Chapter 2.1 (Figure 2.4).

2.5 Reverse Transcription (RT)-PCR

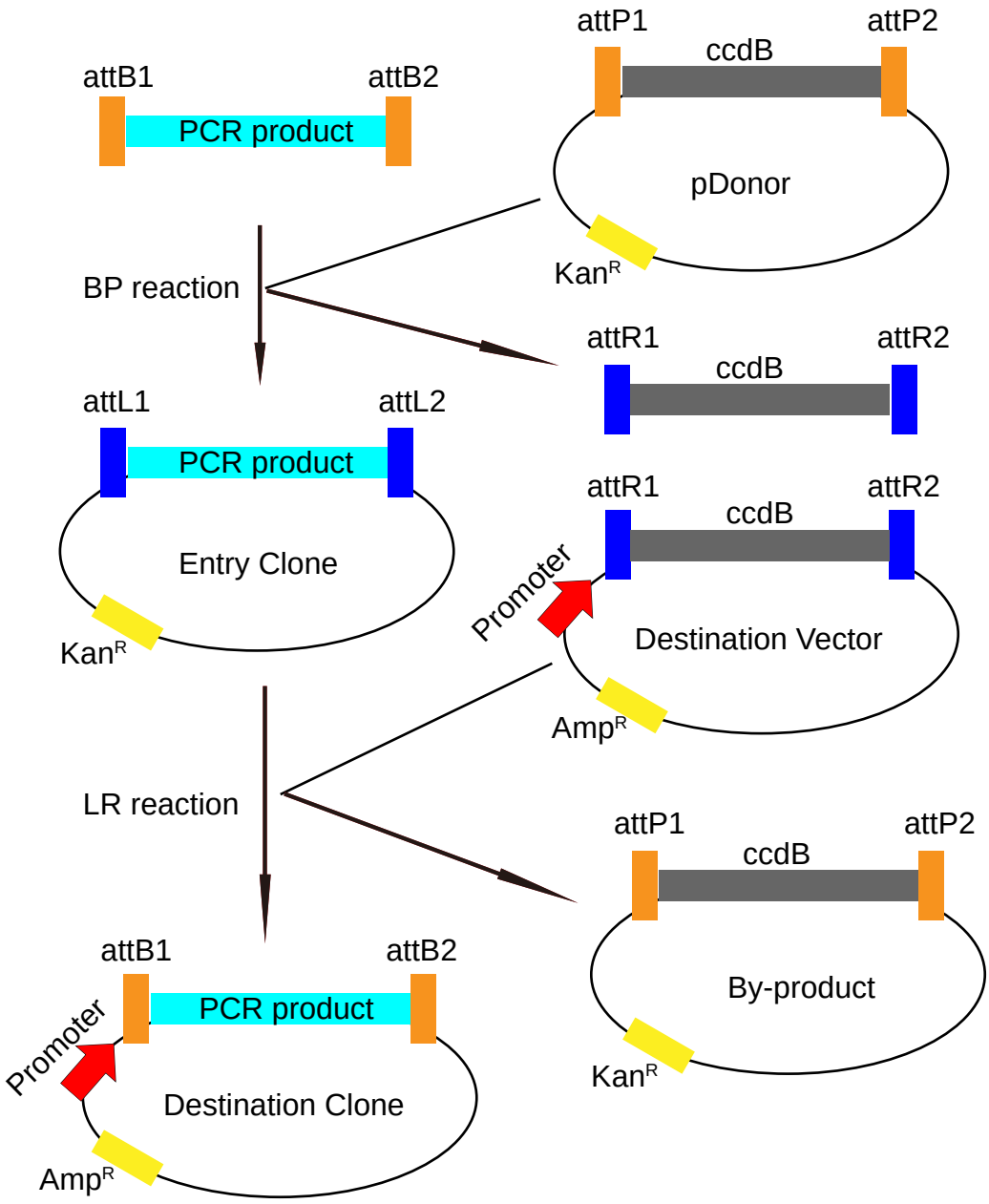
10 adult heads were used in each group to harvest RNA. After chopping the heads off the bodies, they were placed into TRI reagent immediately (Ambion #AM9738) and frozen in -80°C overnight. RNA was then extracted following the manuscript of GoScript™ Reverse Transcription System (Promega #A5001). Then, 300ng of DNase treated RNA was reverse transcribed to cDNA by using random primers following the same manuscript. Finally, cDNA after reverse transcription was diluted 1:3 in nuclease–free water (VWR, #E476-1L) and applied as DNA template for PCR (Table 2.3) in the next step.

2.6 Confocal microscopy and imaging

2.6.1 Confocal microscopy

All the samples for YFP cell counting was scanned by confocal microscope Leica SP8. The resolution of all the images was set at 1024x1024 pixels. The speed for scanning was set at 400Hz. For optic lobes, 40x oil lens was used and the interval for each step was set as 0.96μm. For central brains, 20x oil lens was used with 0.9x

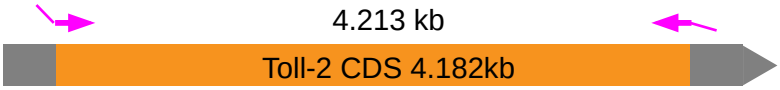
Figure 2.10 Molecular basis of Gateway Cloning



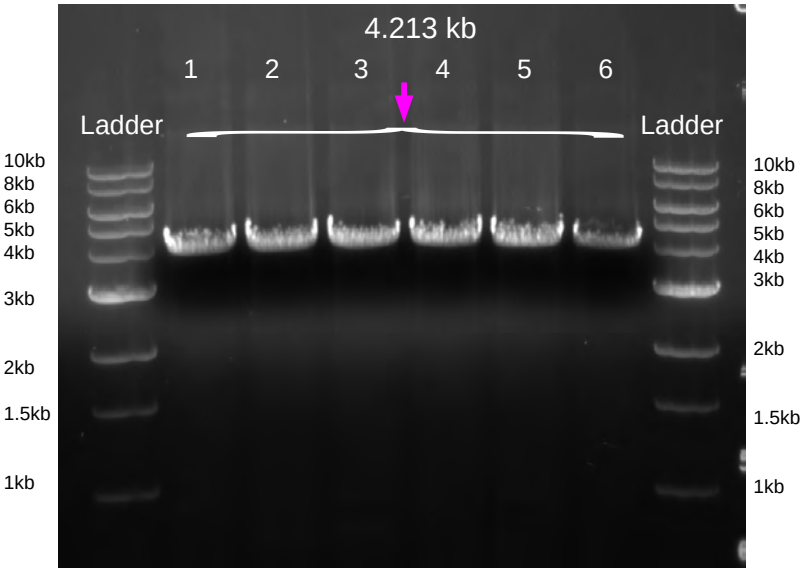
Gateway cloning is divided in mainly two steps, BP reaction and LR reaction. In BP reaction, PCR product is cloned into pDonor via recombination between attB and attP sites, the clones are selected by Kanamycin. In LR reaction, recombination occurs between attL and attR sites from entry clone and destination vector. Thus, the DNA fragment was cloned into destination clone. The clones are selected by Ampicilin. Both pDonor and destination vector carry ccdB which could kill the bacteria if recombination did not occur.

Figure 2.11 PCR amplification of Toll-2 CDS

a.



b.

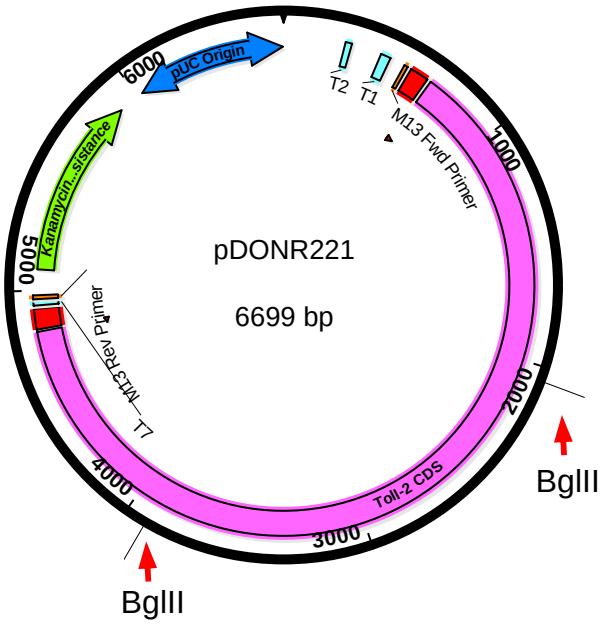


(a). Map of Toll-2 CDS. The PCR product of Toll-2 CDS flanked with attB sites was 4.213kb. Primers were illustrated in with pink arrows.

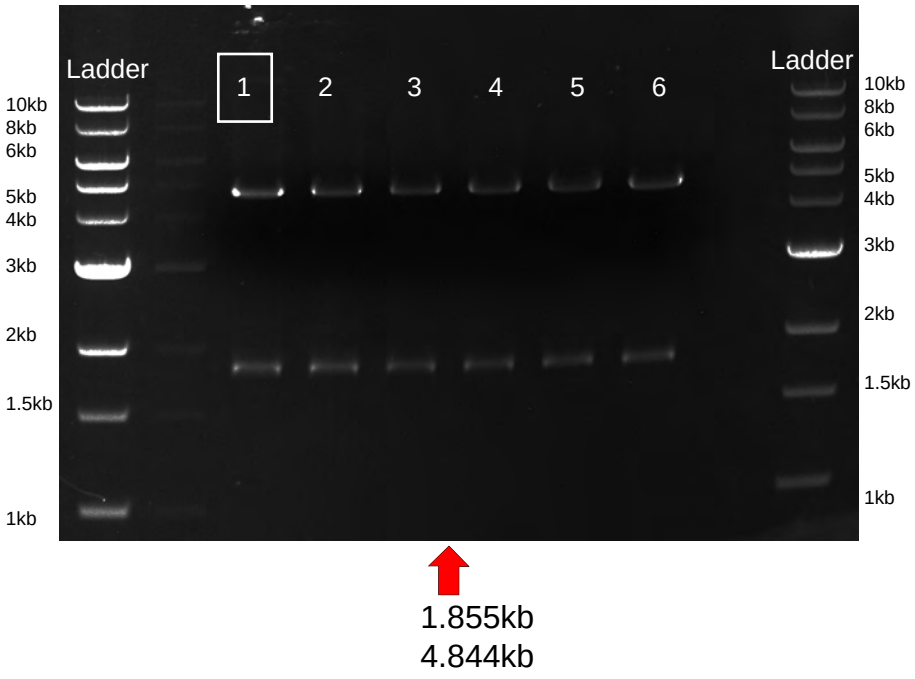
(b). Gel picture of PCR product of Toll-2 CDS. 6 reactions were set to harvest enough DNA and all of the six reactions showed bands with same size at 4.213kb.

Figure 2.12 Generatinon of pDonor-Toll-2 CDS

a.



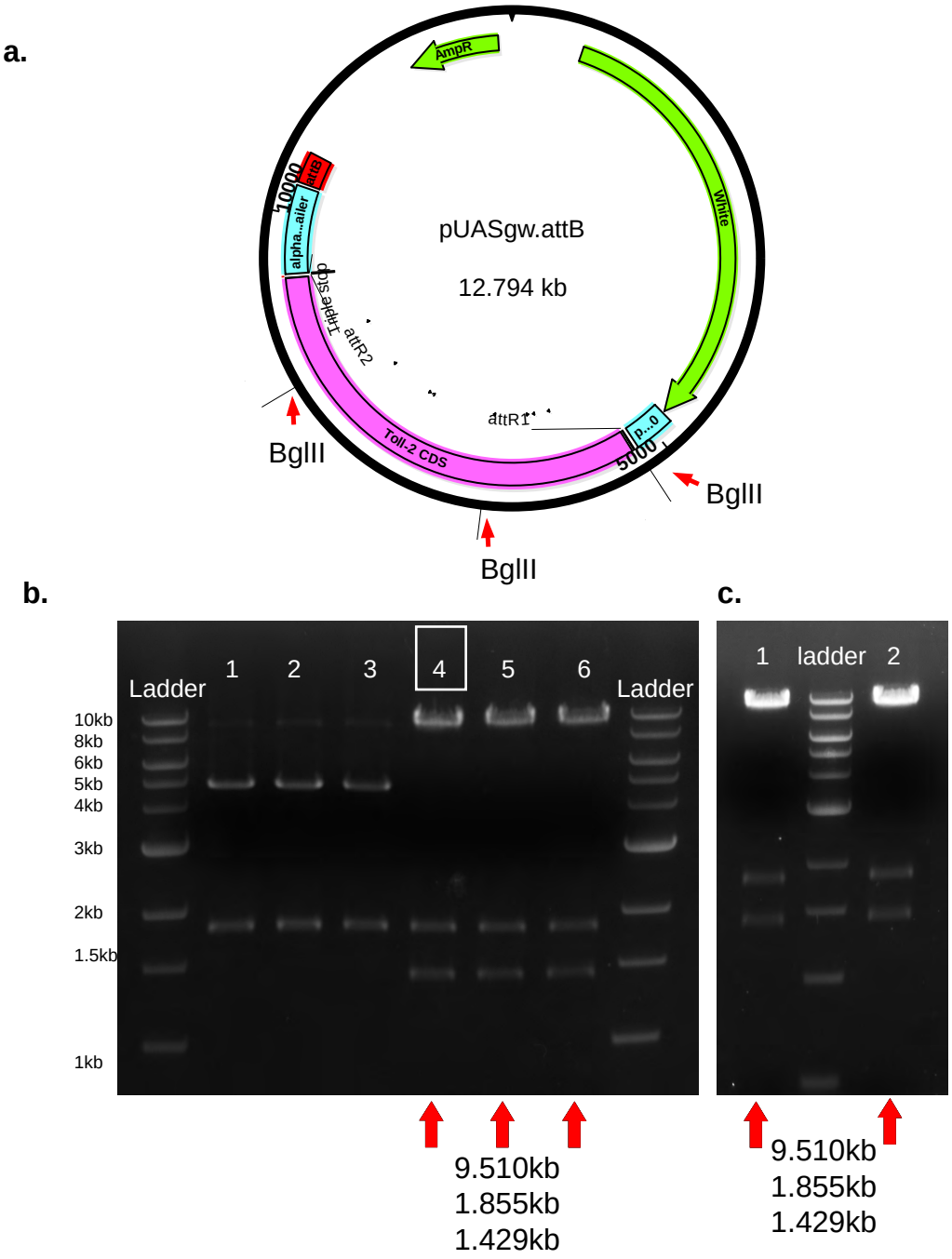
b.



(a). Structure of pDonor-Toll-2 CDS.Digestion sites of BglII were illustrated with red arrows.

(b). Six colonies were selected and mini-prepped, and digested with BglII. All six samples showed bands with expected sizes: 1.855 kb and 4.844kb. Therefore, colony 1 was selected to carry on LR reaction in the next step.

Figure 2.13 Generatinon of pUAS-Toll-2 CDS attB



(a). Structure of pUAS-Toll-2 CDS attB. Digestion sites of BglII were illustrated with red arrows.

(b). Six colonies were selected and mini-prepped, and digested with BglII. Sample 4-6 showed bands with expected sizes. Therefore, colony 4 was selected to be midi-prepped.

(c). Midi-prep of colony 4. Two reactions were set to harvest enough DNA. Both samples were digested with BglII and showed expected bands.

zooming out. The interval for each step was set as 0.96μm. For mushroom bodies, 63x oil lens was used. For adult MB, the interval for each step was set as 0.2μm and the pupal MB was set as 0.25μm.

Samples for expression pattern visualization was scanned by either confocal microscope Leica SP8 or Zeiss (LSM 710). For Leica SP8, the resolution of all the images was set at 1024x1024 pixels using 20x oil lens. The speed of scanning was set at 400Hz, and the interval of each step was 1μm. For Zeiss LSM710, the resolution was also 1024x1024, lens used was 25x oil lens. the speed of scanning was set at 7 with averaging twice, and the interval for each step was set as 1μm. All the images were examined and analysed with *ImageJ*.

2.6.2 Cell number quantification using *DeadEasy*

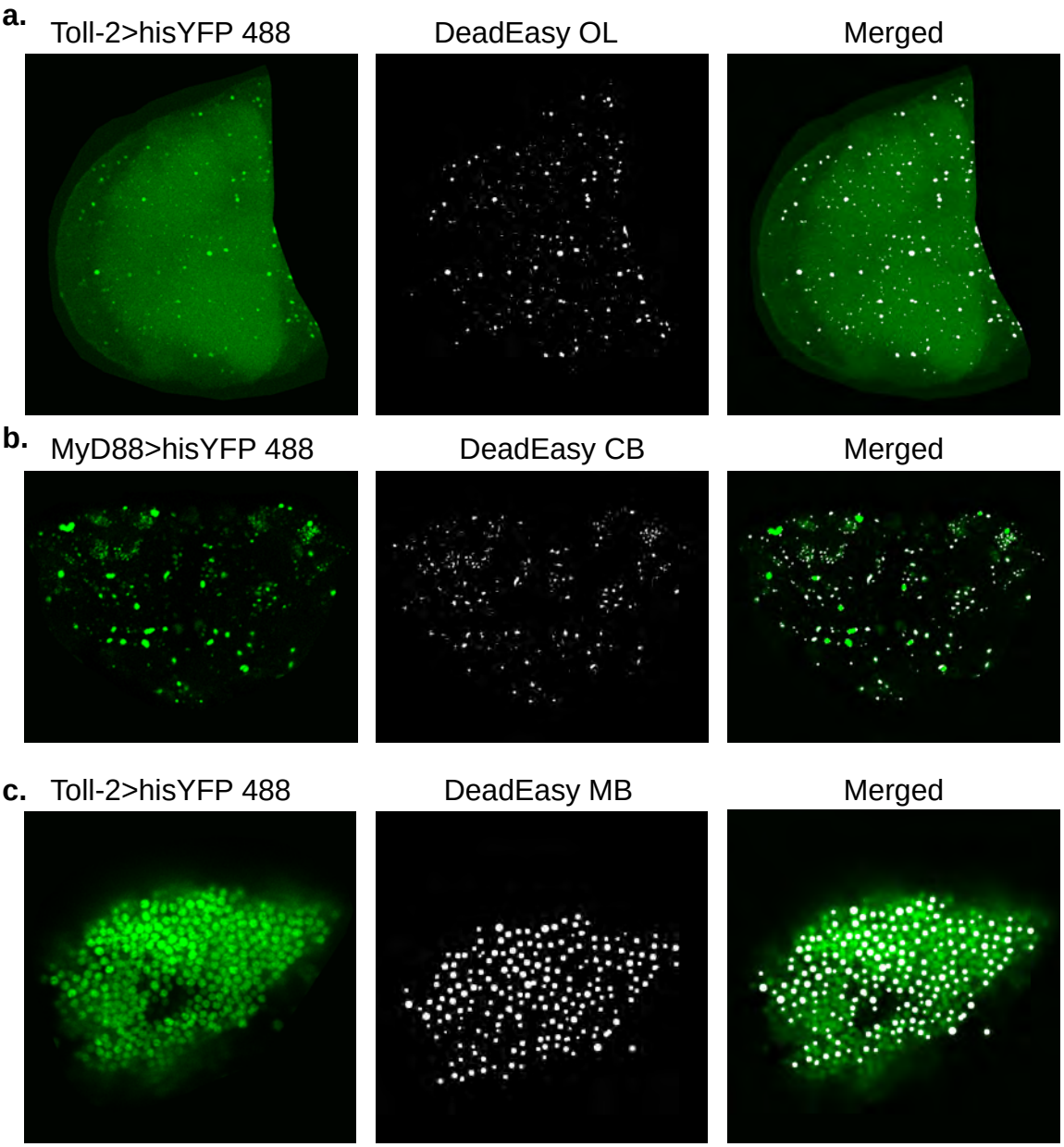
YFP cells were quantified by running an *ImageJ* plug-in *Deadeasy GliaAdult* written by a previous lab member Dr. Manuel Forero. This programme could recognize cells from the stacks in 3D and count the cells automatically (Figure 2.14). Because of the difference in size and shape of the cells, three versions of the *Deadeasy* was used including *GliaAdult OL*, *GliaAdult CB* and *Glia Adult MB*.

2.7 Adult behaviour tests

2.7.1 Longevity test

For longevity analysis, flies with the same genotype eclosing on the same day were collected into the same vials and each vial contained 10-20 flies. The day of eclosion was counted as Day 1. At the end of each day, flies from each vial were anaesthetized on CO_2 pad and counted. All the flies with capability to move were

Figure 2.14 Cell number is quantified using DeadEasy



(a). DeadEasy in adult optic lobe. DeadEasy counted cells in 3D manner and the white signals illustrated cells recoganised by DeadEasy.The merged image showed that DeadEasy could count cells accurately.

(b). DeadEasy in adult central brain.

(c). Deadeasy in adult mushroom body.

counted as surviving ones. Flies were transferred into clean vials with freshly made food once in two days to keep them healthy and clean.

2.7.2 Survival index

All the flies were kept at 25°C. The parents were heterozygous mutants balanced with *SM6aTM6B*. Since the progenies inherited one chromosome from each side of the parents, they were either trans-heterozygous mutant or heterozygous over balancer. In pupae, the balancer was identified as marker *Tb*- showing shorter and rounder puparium than wild type. In adult flies, the balancer was identified as marker *CyO*- showing curly wings instead of straight. In the wild-type, based on the Mendelian segregation, 4 genotypes were equally distributed including 1/4 homozygous, 2/3 heterozygous over balancer, and 1/4 homozygous balancer. Since homozygous balancer is lethal, there will be 1/3 homozygous and 2/3 heterozygous over balancer. Therefore, the survival index of wild type is 1 calculated in the formula shown below:

$$S.I. = 2 \times \frac{\frac{1}{3}\ of\ the\ progeny}{\frac{2}{3}\ of\ the\ progeny} = 1$$

And the survival index of the mutant is calculated as below：

$$S.I. = 2 \times \frac{number\ of\ the\ homozygotes}{number\ of\ the\ heterozygotes\ over\ balancer}$$

2.7.3 Climbing assay

Flies with the same genotypes that eclosed on the same day were collected into the same vials. The day of eclosion was counted as day 1 (D1). D4 to D6 flies were pulled together and every 20 to 30 flies were grouped into each vial. A piece of white A4 paper was used as the background. 2cm above the bottom of the paper was measure and labelled as a landmark. Vials with different genotypes were aligned in front of the background paper and tapped at the same time to make all the flies dropped to the bottom of the vials. At the same time, a timer was set for 10 seconds counting down. A camera was used to record the flies climbing. After 10 seconds, the recording was stopped, and a 30 seconds period was set for the flies to rest. The whole process was repeated for 15 times for each genotype. Finally, the video was analysed and the number of the flies that could climb on or above 2cm was counted. All the experiments were carried out in the fly behaviour room with temperature set at 25°C.

2.7.4 Buridan Arena test

Flies were collected on the day of eclosion counted as day 1. Day 4 to Day 6 flies were used for this experiment. To carry out Buridan test, the wings of the flies were clipped using small scissors the day before the test and then each fly was kept individually in a small cuvette at 25°C overnight with a small amount of sucrose and a piece of filter paper soaked with water. On the day of test, each fly was transferred into the arena. The wall of the area is white with a black stripe on both sides of the wall. A camera was installed on the top of the area to record the behaviour of the fly.

Each fly was recorded for 10 minutes and the trajectory was recorded and then analysed.

2.8 Dissection and immunostaining of larval, pupal and adult brains

All the dissections were carried out in ice-cold 1xPBS, dissected brains were transferred into ice-cold 2% paraformaldehyde (PFA) diluted in 1xPBS immediately After 20min dissection, all the brains dissected within this 20min were transferred into 750µl fresh 2% PFA and blocked for another 45min. Brains were then washed in 750µl 0.5% PBT (0.5% Triton X-100 dissolved in 1xPBS) for 5 times and 15min each. For observing endogenous fluorescent signals, brains were mounted with vectashield (Vector labs) directly after washing. For immunostaining, brains were then blocked in 750µl 10%NGS (#S1000, Vector Labs) dissolved in 0.5% PBT for 1 to 2 hours at room temperature. Then, NGS was removed from Eppendorf replacing with 100µl primary antibody and incubated over 2 nights in 4°C cold room. Afterwards, brains were washed in 750µl 0.5% PBT for 5 times and 15min each, and then incubated in 100µl secondary antibody overnight at 4°C. Finally, stained brains were washed in 750µl 0.5% PBT for 5 times, 750µl 1x PBS for one time and 15min each and then mounted with vectashield (Vector labs).

Table 2.10 Antibodies

Antibody	Donor	Working dilution
Primary		
Anti-GFP	Rabbit	1:250
Anti-DsRED	Rabbit	1:100
Anti-Elav	Rat	1:250
Anti-Repo	Mouse	1:10
Anti-Dpn	Guinea- pig	1:1000
Secondary		
Anti-rabbit 488	Donkey	1:250
Anti-rabbit 546	Goat	1:250
Anti-mouse 647	Goat	1:250
Anti-rat 647	Goat	1:250
Anti-Guinea-pig 633	Goat	1:250

2.9 Data analysis

Data were collected by *Excel* (Microsoft) and analysed by GraphPad Prism®. Data from lethality, climbing assay, and Buridan Arena test were categorical, therefore $\chi 2$ test was carried out. Data from Cell number counting were numerical continuous data. Data that are distributed normally were analysed using One-Way ANOVA and Dunnett's test was performed for multiple comparison. Data that are not distributed normally were analysed using Kruskal-Wallis test and Dunn's test was performed for multiple comparison. Unpaired t-test or Mann-Whitney U test was conducted for sample group equals 2 when data were distributed normally or not normally respectively.

Chapter 3

Toll-2 is expressed in the CNS and *Toll-2* mutants have altered behaviour and brain circuits

3.1 Introduction

Toll and *Toll*-related receptors are best-known for their functions in dorsal-ventral determination in embryo and in innate-immunity. Among 9 *Tolls*, *Toll-2* is one of the receptors that have not been studied. *Toll-2* has been found to have developmental functions during embryogenesis (Eldon et al., 1994, Pare et al., 2014). Other than that, the knowledge about *Toll-2* is very limited. Lacking tools is one of the drawbacks that slow down the study of *Toll-2*. Therefore, the aim of this chapter is to generate tools to firstly visualize the expression pattern of *Toll-2*, and secondly generate *Toll-2* mutant alleles to study the function of *Toll-2*.

The *CRIPR/Cas9* system is a powerful tool to edit genome. Baena-Lopez et al. generated a tool to apply the CRISPR/Cas9 in *Drosophila* genome. The key element of this method is the vector $pTV^{mCherry}$ (Baena-Lopez et al., 2013). $pTV^{mCherry}$ is composed of several key factors: an *attP* site for further insertions, a red fluorescent protein reporter *mCherry*, a *mini-white* for genetic screening, and two homologous arms of the target gene flanking these elements. When homologous recombination happens, the homologous arms of the target gene will bring the cassette inserted at the locus of the target gene. Therefore, the *mCherry* will be expressed under the regulation of the target gene, which will show the expression pattern of the target gene. At the same time, the *attP* site can be inserted by any DNA fragment flanked with *attB* sequence, such as *attB-Gal4*, therefore, a *Gal4* line of the target gene can

also be generated based on the *pTV^{mCherry}* line. Moreover, when the homologous recombination happens between the construct and the genome, the target gene would be replaced by the *pTV^{mCherry}* construct. Therefore, by using this method, the expression pattern of *Toll-2* could be visualized by staining of *mCherry* and a *Toll-2* knock-out allele could be generated at the same time.

3.2 Results

3.2.1 Generation of *pU6.3 Toll-2 gRNA* construct

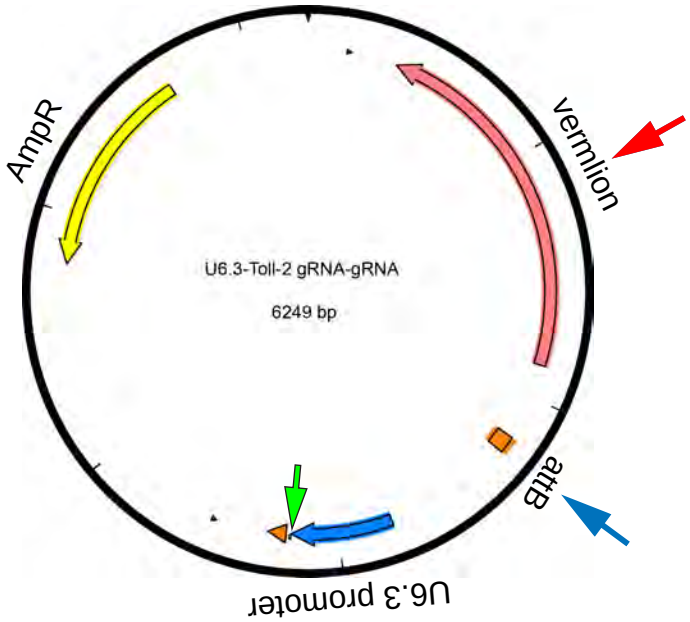
To carry out a *CRISPR* event, *gRNA* is one of the key elements that is gene specific and can bring the *Cas9* to the specific site of the gene. The first experiment I did is to clone Toll-*2* gRNA (see Method 2.3) into plasmid *pU6.3* and generate a fly strain that carries Toll-2 gRNA. The construct of the plasmid *pU6.3* is shown in Figure 3.1a. *pU6.3* carries an *attB* site, so with this, the construct was inserted into *attP* landing site in the genome via homologous recombination. The construct also carries a *vermillion*+ gene, which would be used for screening the transgenic flies after injection. Toll-2 gRNA oligos was designed and generated following steps in Method 2.3, I then cloned Toll-2 gRNA flanked by BbsI sites into *pU6.3* which has already been digested with *BbsI* via conventional cloning strategy. After transformation, I selected 6 colonies to do mini-prep and sent them for sequencing. 4 out of 6 colonies had right sequence of gRNA, therefore, I selected colony 1 to do midi-prep, and then finalised by sequencing again (Figure 3.1b). Midi-prepped plasmid was then sent to *Best gene.Inc* for injection and screening. Two lines of flies that carry *Toll-2* gRNA were sent back to me. 2M was selected for further experiments and named as *Toll-2 gRNA*.

3.2.2 Generation of *Toll-2 pTV^{mCherry}* construct

For homologous recombination to happen, the *Toll-2 pTV^{mCherry}* plasmid bearing *Toll-2* 5' homologous arm (5'HA) and 3'HA was generated (Figure 3.2). Referring to the fly genome sequence downloaded from Flybase (Flybase.org), 4.993kb upstream of Toll-2 coding sequence right before the start codon was taken and designed as 5'HA and 3.419kb downstream if *Toll-2* CDS right after the stop codon was taken as 3'HA (Figure 3.2a). 5'HA was amplified by primer 5 and 6 flanking with *NotI* and *KpnI* restriction site and 3'HA is amplified by primer 1 and 2 flanking with *SpeI* and *AscI* restriction site (Figure 3.2c). 3'HA and 5'HR is then ligated into the *pTV^{mCherry}* sequentially at corresponding locations (Figure 3.2b). To select the right clone, mini-preps and diagnostic digestions were carried out from nine colonies. *BsaI* was used to digest the plasmid DNA extracted from colony 1 to 9 (Figure 3.3 a and b). Afterwards, the correct colony was selected and midi-prepped. In order to obtain enough DNA product, 2 aliquots of midi-prep cell culture were set up. After midi-prep, both aliquots were tested by diagnostic digestion again by *BsaI* (Figure 3.4a). When cut by *BsaI*, 5 bands were expected on the gel, which were 6.865 kb, 4.455kb, 4.266kb, 3.031kb, and 1.664kb (Figure 3.4 b, blue arrows). Apart from the bands with 4.455kb and 4.266kb, all other bands were seen clearly on the gel. This is because these two bands were with similar size and overlapped. DNA product was then sent to *Bestgene Inc.* to be injected and 4 lines of candidates were received to be further tested.

Figure 3.1 *pU6.3 Toll-2 gRNA* cloning and sequencing

a.



b.

Reference

U6.3 Toll-2 gRNA

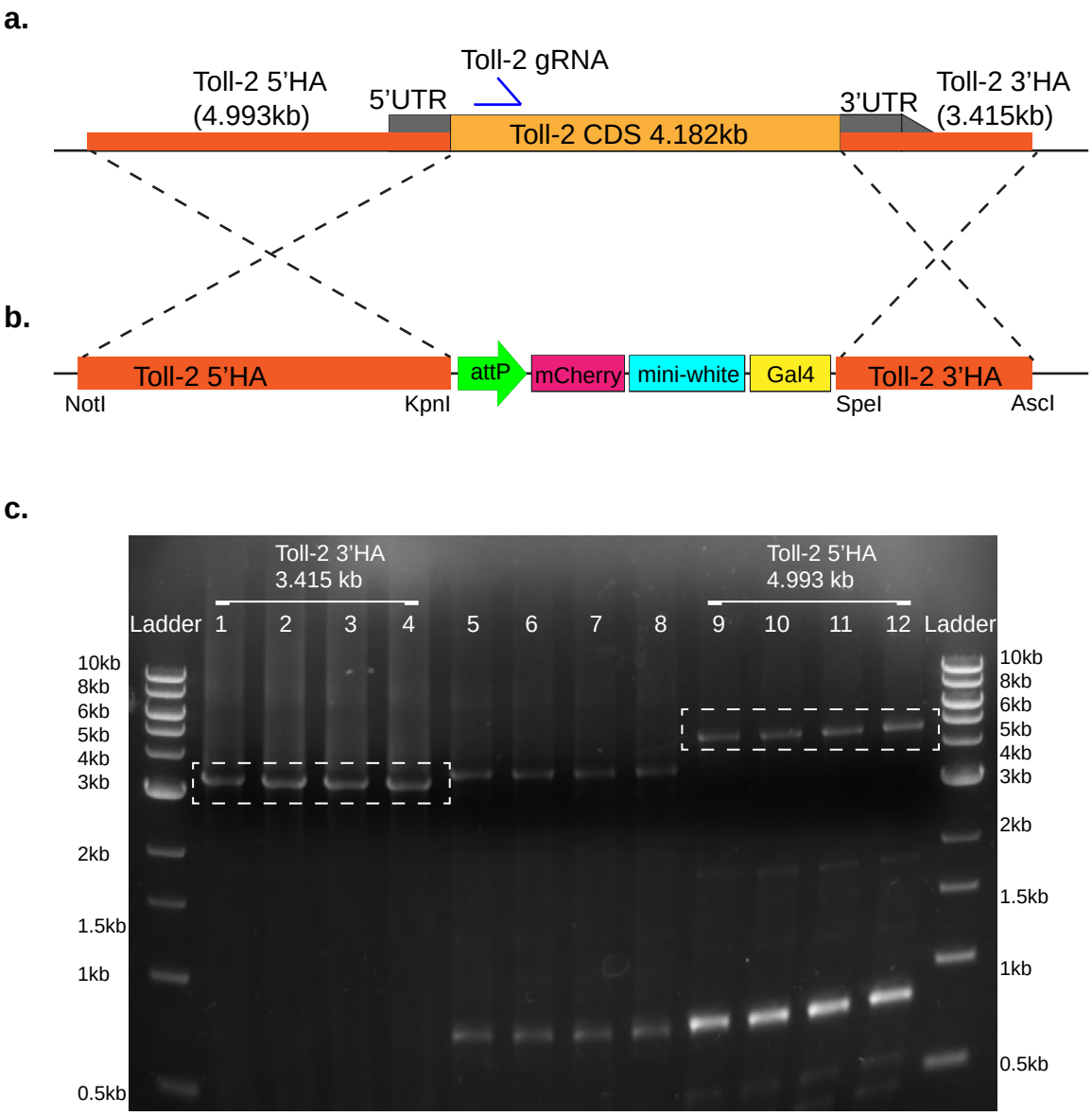
```
                                                
```

Figure 3.1 *pU6.3 Toll-2 gRNA* cloning and sequencing

(a), the U6.3-Toll-2 gRNA construct. The Toll-2 gRNA is pointed in green arrow. The vector carries an attB site (blue arrow) which will help the construct to be inserted into an attP landing site. The plasmid also carries a vermillion+ (red arrow) which issued for screening.

(b), the sequencing result of U6.3-Toll-2 gRNA. The upper line is the reference sequence from the cloning design and the lower line is the experimental sequence from the colony 1. The sequence highlighted in yellow is the gRNA sequence. Perfect alignment shows cloning was successful.

Figure 3.2 Design of the *Toll-2*^{pTV} vector and generation of the 5' and 3'HA



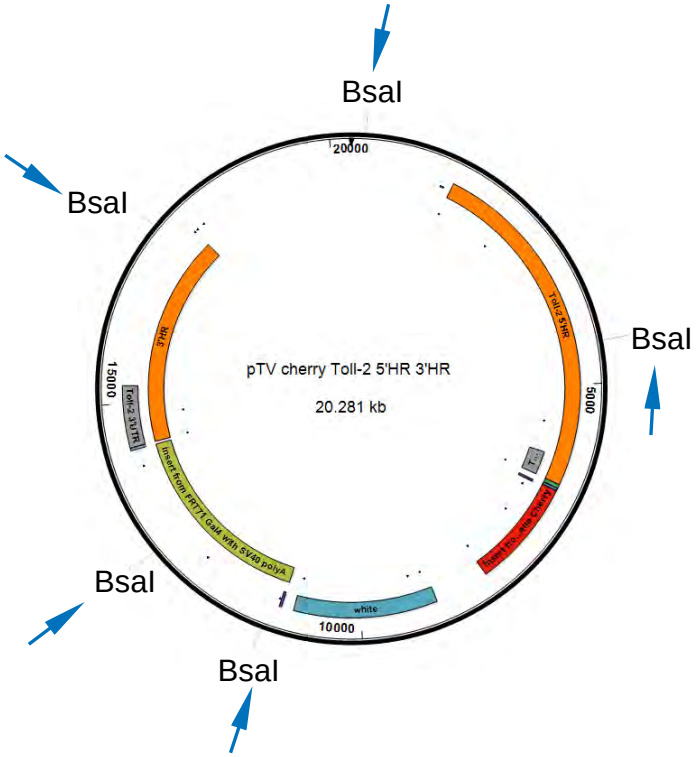
(a), the design of Toll-2 5'HA, 3'HA and gRNA. Toll-2 coding sequence is shown as an orage rectangle flanked by untranslated region (UTR) on both sides shown in grey. the 5'HA and 3'HA are located right before the start codon and right after the stop codon, respectively (dark orage rectangle). The location of Toll-2 gRNA is shown in blue arrow above Toll-2 CDS.

(b), the design of Toll-2 pTV cassette. The pTV cassette is redrawn from Baena-Lopez et al., 2014. Toll-2 3'HA and 5'HA were cloned into the vector flanking the pTV cassette.

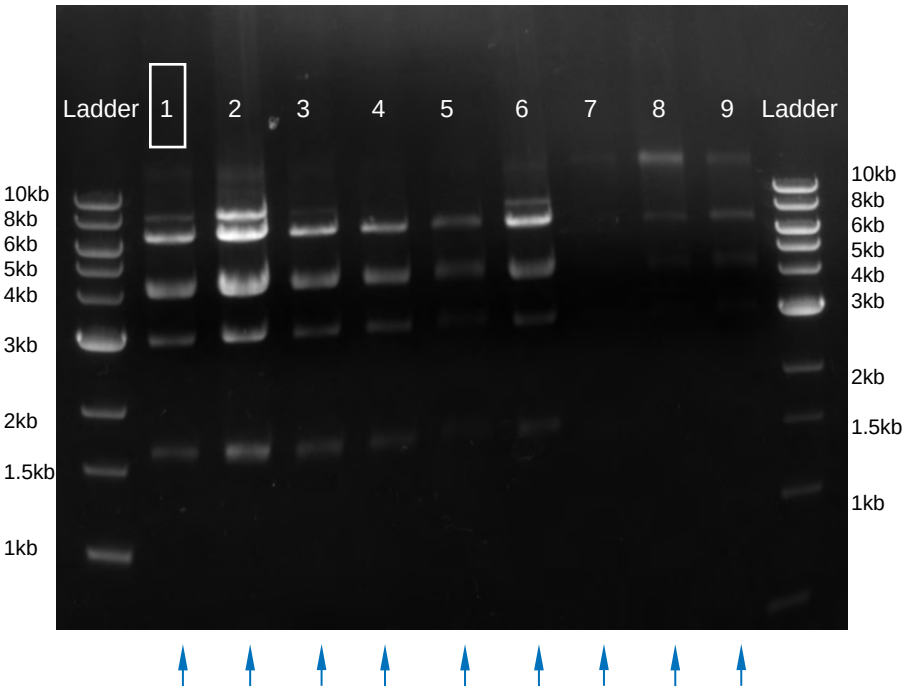
(c), generation of Toll-2 3'HA and 5'HA via PCRs. Lane 1-4 show Toll-2 3'HA and lane 9-12 show Toll-2 5'HA. Each PCR reaction was set in 4 eppendorfs to avoid artifacts and increase the DNA product. Lane 5-8 are reactions that are unrelated.

Figure 3.3 Virtual clone of *Toll-2*^{pTV} and generation of the *Toll-2*^{pTV} plasmid

a.



b.

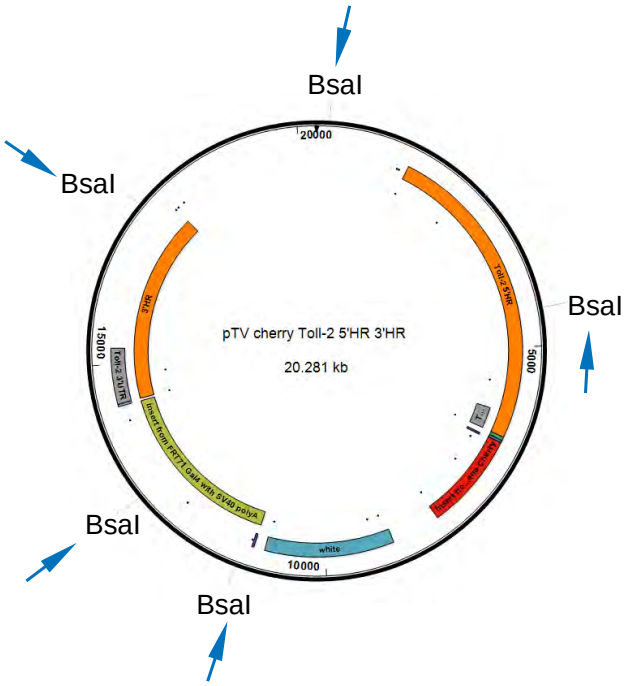


6.865kb
4.455kb
4.266kb
3.031kb
1.664kb

Figure 3.3 Virtual clone of *Toll-2^{pTV}* and generation of the *Toll-2^{pTV}* plasmid
(a). The virtual clone of the plasmid Toll-2 pTV and the digestion sites of BsaI (blue arrows).
(b). The mini-preps screening for the right colony with the correct plasmid (lane 1-9). Lane 1-6 showed correct bands while 7-9 did not. Colony 1 (in square) was selected for further amplification and test. The expected size of the bands were labelled below the gel picture.

Figure 3.4 Midi-prep of *Toll-2*^{pTV} and diagnostic digestion with *BsaI*

a.



b.

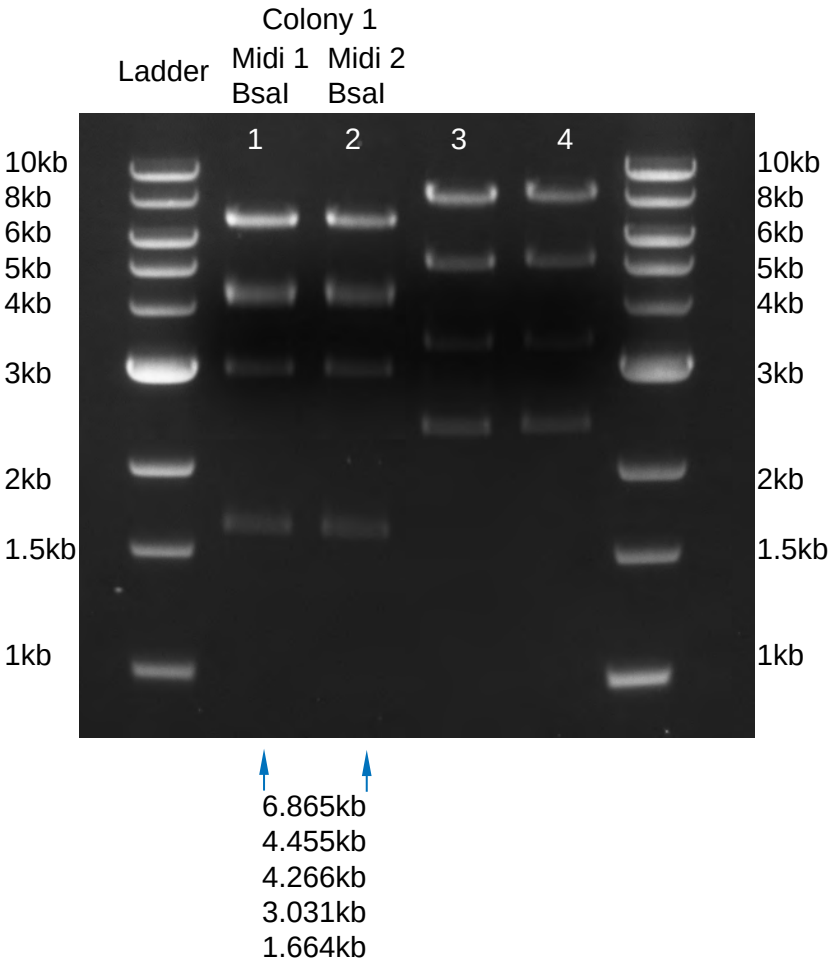


Figure 3.4 Midi-prep of *Toll-2^{pTV}* and diagnostic digestion with *BsaI*

(a). The virtual clone of the plasmid Toll-2^{pTV} with digestion sites of BsaI (blue arrows)

(b). The gel picture of the diagnostic digestion results. Toll-2^{pTV} was digested by BsaI (blue arrows) shown as lane 1 and 2.

Lane 3 and 4 are reactions that are unrelated.

3.2.3 Generation and verification of transgenic *Toll-2^{pTV}*

After the injection and screening by the *Bestgene Inc,* I received 4 lines of Toll-2^{pTV} candidates as four unbalanced stocks. I then balanced the flies to generate 4 stable stocks (Figure 2.1). In order to test whether the *Toll-2 pTV^{mCherry}* has been inserted correctly into the genome at the right locus and whether the pTV^{mCherry} cassette was intact, I then extracted the genomic DNA from all these four lines and carried out PCRs. I first tested whether homologous recombination happened at the Toll-2 locus. Both 5'HA and 3'HA were tested using the primers indicated in Figure 3.5a. To test 5'HA, forward primer F1 was designed to hybridise with sequences located in the genome upstream of the 5'HA and reverse primer R1 hybridised with the sequence at the beginning of *mCherry* (Figure 3.5a, red arrows). Each PCR was carried out in 2 aliquots to test for any artifacts. All 4 lines showed the expected band with right size at 5'HA (Figure 3.5b). At the same time, 3'HA was also tested with two sets of PCRs. Forward primer F3 were designed to hybridise with the sequence at the end of *Gal4*, and reverse primer R3 were designed to hybridise with the sequences in the genome downstream of the 3'HA (Figure 3.5a, orange arrows). However, PCR with F3 R3 did not show any bands (Figure 3.5b). *Gal4* in the cassette might not be working after homologous recombination (Baena-Lopez *et al.*, 2014). Thus, it is possible that *Gal4* is already damaged when inserted into the fly genome. Hence, the primer F3 might not be able to recognize the sequence. To solve this issue, F2 primer was designed upstream of the Gal4 fragment (Figure 3.5a, black arrows). From the result of the new set of PCR at 3'HA (Figure 3.5c), it can be seen that all 4 lines produced the expected band. Both PCR results conclude that homologous recombination

happened successfully, with *pTV^{mcherry}* inserted at the right locus. However, the *Gal4* fragment might be damaged, which needs to be further tested.

To test whether the pTV cassette was still intact including *mCherry*, *mini-white*, and *Gal4*, 3 pairs of primers were designed (Figure 3.6). In all 4 lines tested, PCRs testing *mCherry* and *white* gene showed the right bands with correct sizes (Figure 3.6 b and c, blue and green arrows). This means that *mCherry* is intact and *mCherry* and *white* are in frame. However, when testing whether *Gal4* is intact, the PCR did not work (3.6 b and c, purple arrows), which was consistent with to previous PCR result (Figure 3.5 a and b, orange arrows). Therefore, in the genome of all 4 lines of transgenic flies, the pTV cassette is inserted at *Toll-2* locus correctly and all the elements are in frame and intact apart from Gal4 which might be damaged

I also carried out PCRs to test whether *Toll-2* CDS was truly knocked out (Figure 3.4a and b). The length of the *Toll-2* CDS is 4.182kb with a single exon and without any introns. 3 sets of PCRs were designed to make sure that the whole *Toll-2* CDS was covered (Figure 3.7a). All 4 lines were tested. For Line 1M-a and 2M, the *Toll-2* CDS could be detected with all 3 PCRs, which suggests that in these 2 lines, *Toll-2* CDS was still in the genome (Figure 3.7 b and c). In Line 1M-b and 1M-c, roughly the first 2kb of the *Toll-2* CDS were missing, nevertheless, the last 2kb were still detected by PCR (Figure 3.7 b and c). Therefore, this suggests that in Line 1M-b and -c, the first half of *Toll-2* CDS might have been damaged during homologous recombination, while the second half was still left intact in the genome.

To test whether the first half of *Toll-2* CDS was damaged, I carried out PCRs to amplify the first half of *Toll-2* CDS. When I used a forward primer located in *mini-*

Figure 3.5 PCR tests to check the locus of *Toll-2*^{pTV} insertion

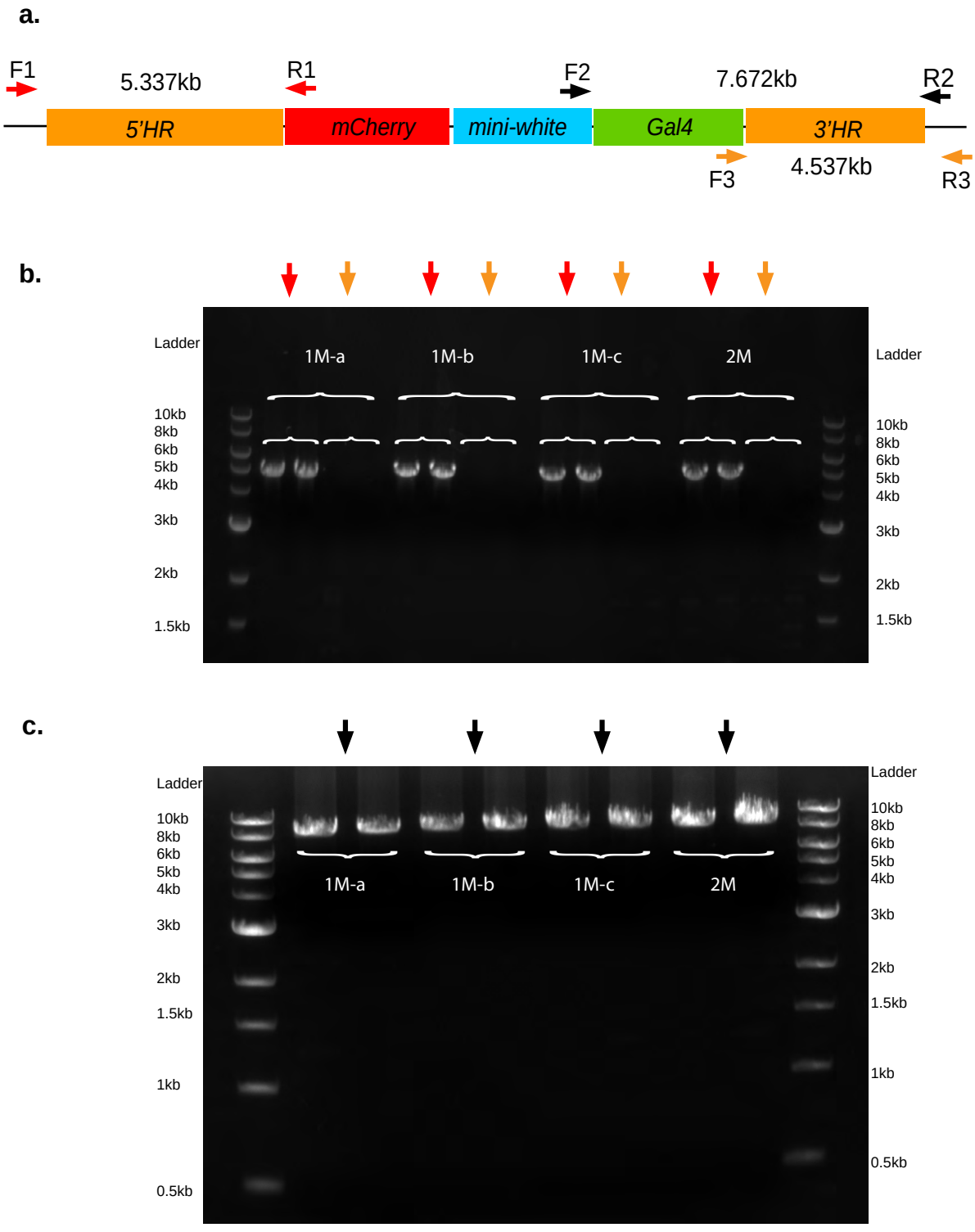


Figure 3.5 PCR tests to check the locus of *Toll-2^{pTV}* insertion

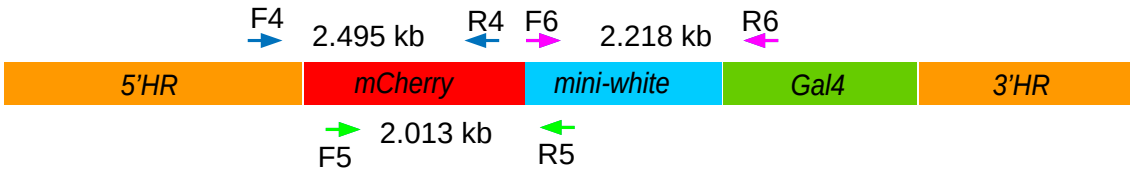
(a). The construct of *Toll-2^{pTV}* cassette inserted in the genome. F1 and R1 (red arrows) are the pair of primers to test whether the 5' of the cassette was inserted at the correct locus. F2, R2 (black arrows) and F3, R3 (yellow arrow) are two pairs of primers to test whether the 3' of the cassette was inserted at the correct locus of the genome.

(b). PCR results to test whether both 5' and 3' of *Toll-2^{pTV}* cassette was inserted into the genome at the right locus, which corresponding to F1R1 and F3R3. 4 transgenic lines including 1M-a, 1M-b, 1M-c, and 2M were tested.

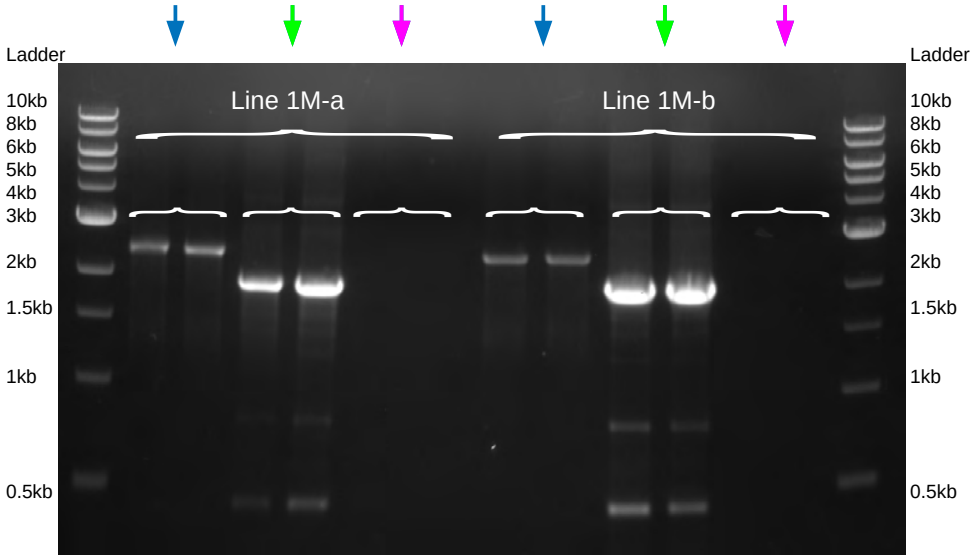
(c). PCR results to test whether 3' of *Toll-2^{pTV}* cassette was inserted into the genome at the right locus, which corresponding to F2R2. 4 transgenic lines including 1M-a, 1M-b, 1M-c, and 2M were tested

Figure 3.6 PCR tests to check whether the pTV cassette is intact

a.



b.



c.

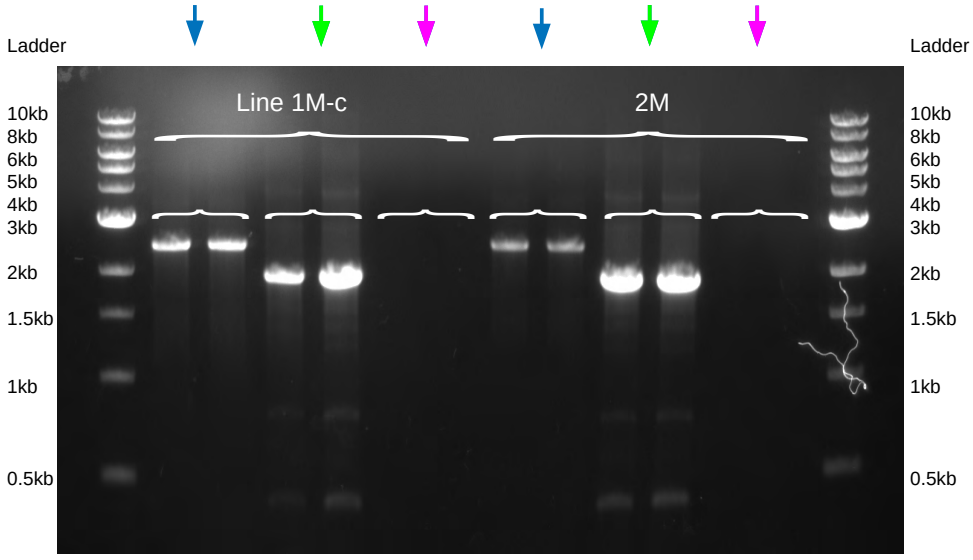


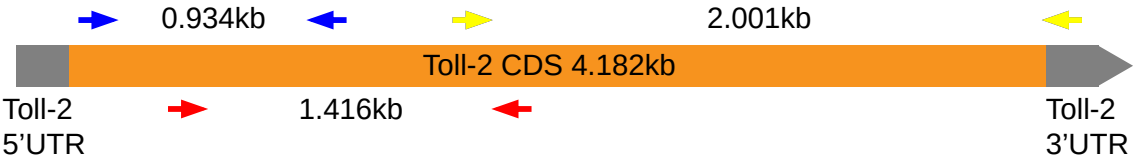
Figure 3.6 PCR tests to check whether the pTV cassette is intact

a). The construct of *Toll-2*^{pTV}cassette inserted in the genome. 3 pairs of primers: F4R4 (blue), F5R5 (green) and F6R6 (purple) are designed to test whether the construct inside of the cassette was intact after homologous recombination.

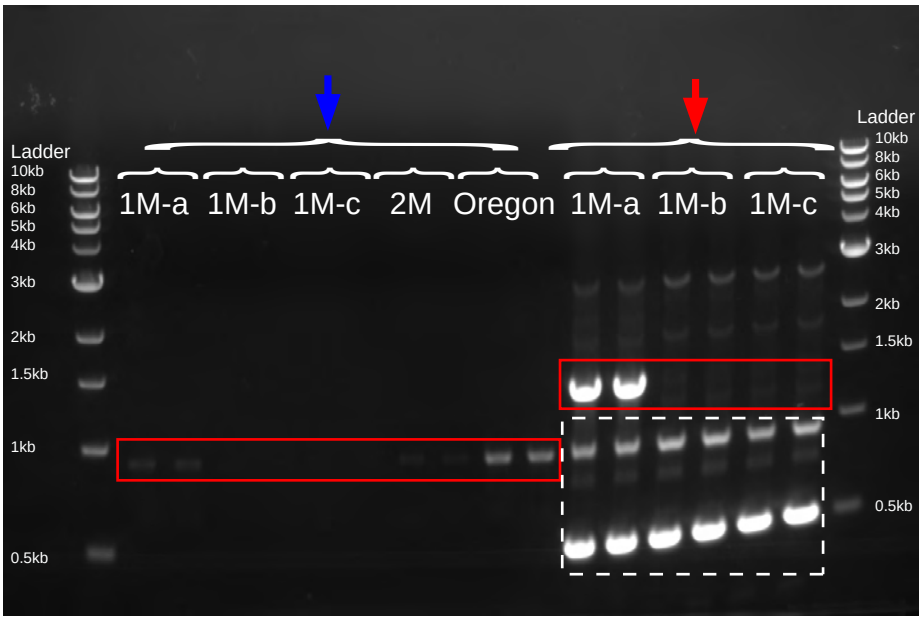
b) and c). PCR results corresponding to the 3 sets of PCR reactions illustrated in (a). Four transgenic lines were all tested: 1M-a, 1M-b, 1M-c, and 2M.

Figure 3.7 PCRs to test whether *Toll-2*^{pTV} was a null mutant

a.



b.



c.

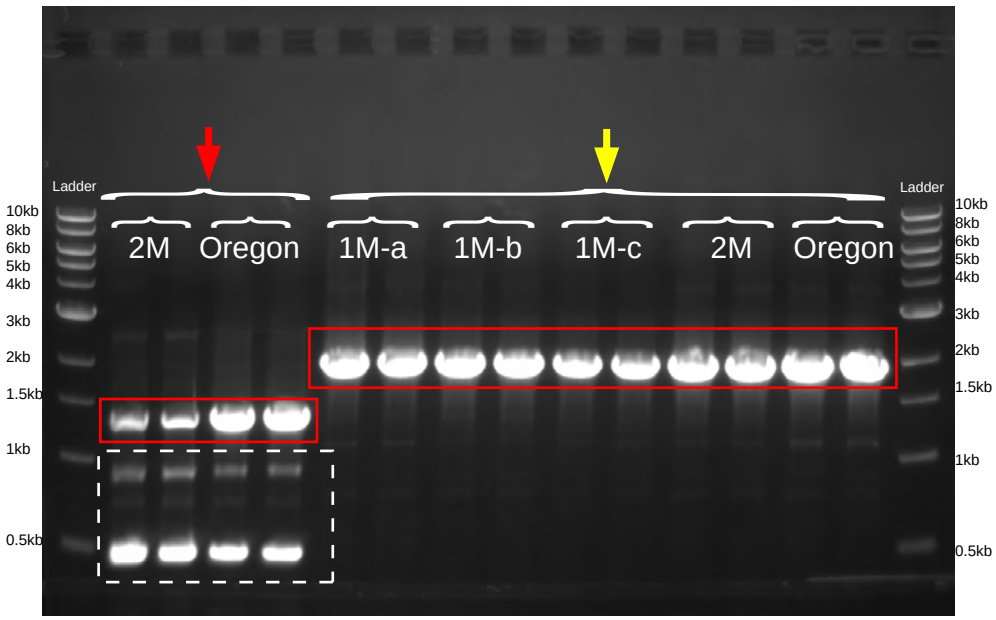


Figure 3.7 PCRs to test whether *Toll-2^{pTV}* was a null mutant

(a), shows the construct of Toll-2 coding sequence. Three pairs of primers were designed to test whether the Toll-2 CDS is fully knocked out in Toll-2^{pTV} transgenic flies. The same pair of primers are labelled in the same colour.

(b) and c), gel pictures of three sets of PCRs using three pairs of primers testing whether different parts of Toll-2 CDS have been knocked out in Toll-2^{pTV} transgenic flies. The colour of three pairs of primers correspond to the ones in (a) shown in blue, red and yellow, respectively. In each PCR, 4 lines of transgenic flies and control (Oregon) were tested. The expected bands were labelled in red squares. Bands labelled in white squares are non-specific bindings or primer-dimers.

white and reverse primer located in *Toll-2* CDS, a fragment with expected size (2.227kb) was produced, which further suggests that *Toll-2* CDS was not knocked out and the pTV cassette (*mCherry* and mini-*white*) was inserted into the locus right before *Toll-2* CDS (Figure 3.8 a and b). All four lines were tested and showed the same result in PCR (Figure 3.8b). In order to test whether the first half of *Toll-2* CDS was intact or not, I sent this fragment to sequencing. It was shown that the sequence of *mini-white* was accurate and clean, however, the sequence of *Toll-2* CDS started to be noisy and no accurate sequence could be read from this sequencing result (Figure 3.8c). The sequencing results of all four lines were similar. Thus, I was not able to tell the sequence of the beginning part of *Toll-2* CDS. However, the noisy sequence indicates that there might be gene duplication at the locus of *Toll-2* CDS in the genome of *Toll-2*^{pTV} flies, which might interfere with the expression of *Toll-2*.

To further test whether *Toll-2* CDS is functional or not, I carried out an RT-PCR to test whether *Toll-2* could be transcribed into mRNA (Figure 3.9). It is shown that both in Line 1M-b and -c, *Toll-2* cDNA could be detected (Figure 3.9b). This suggests that at least part of *Toll-2* CDS could be transcribed. Because of the time restrictions, no further experiment was carried out to test whether *Toll-2* in these transgenic lines is still functional.

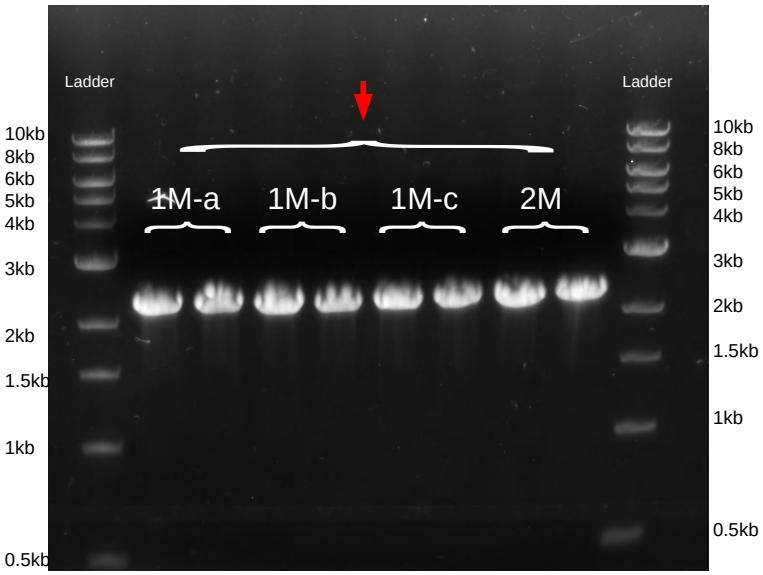
To conclude, via homologous recombination after CRISPR, instead of generating a knock-out mutant (Figure 3.10 a), a *Toll-2* knock-in allele was generated, where the pTV cassette was inserted before *Toll*-2 CDS and Gal4 fragment in the cassette was damaged (Figure 3.10b). Since the *pTV* cassette was inserted at the *Toll-2* locus, *mCherry* in the cassette could be expressed under the regulation of *Toll*-2 promoters

Figure 3.8 Sequencing of Toll-2 CDS in *Toll-2^{pTV}* trangenic flies

a.



b.



c.

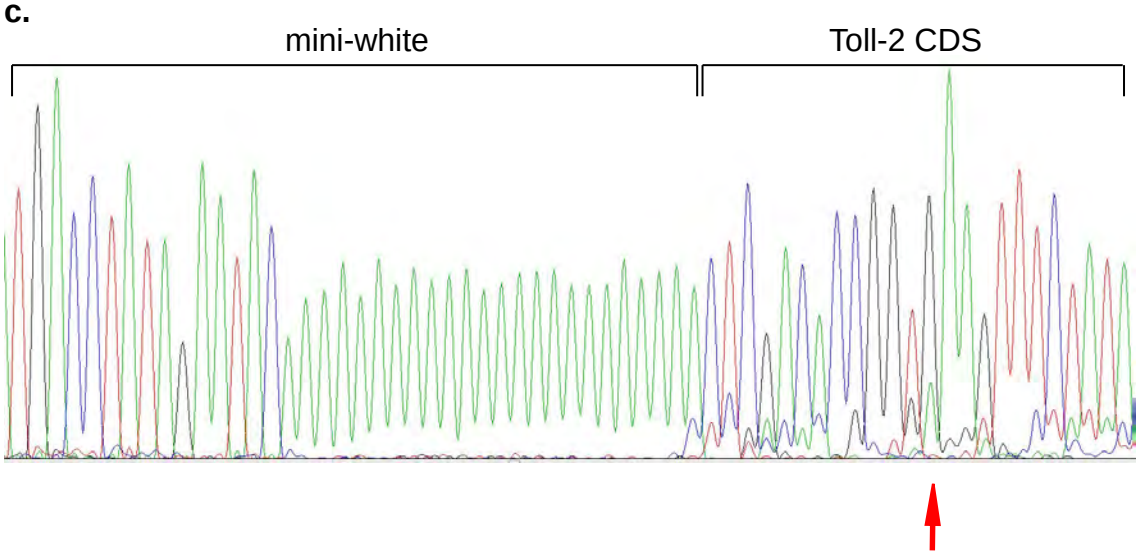


Figure 3.8 Sequencing of Toll-2 CDS in *Toll-2^{pTV}* trangenic flies

(a). PCR reactions revealed how the pTV cassette was inseted into the genome of Toll-2^{pTV}. Instead of knocking out Toll-2 CDS, the pTV cassette was inserted before the locus of Toll-2 CDS. Arrows labelled in red indicates the primers used to amplify the fragment, whose size was 2.722kb.

(b). Gel picture of PCR illustrated in a. All four lines were tested and showed the bands with expected size.

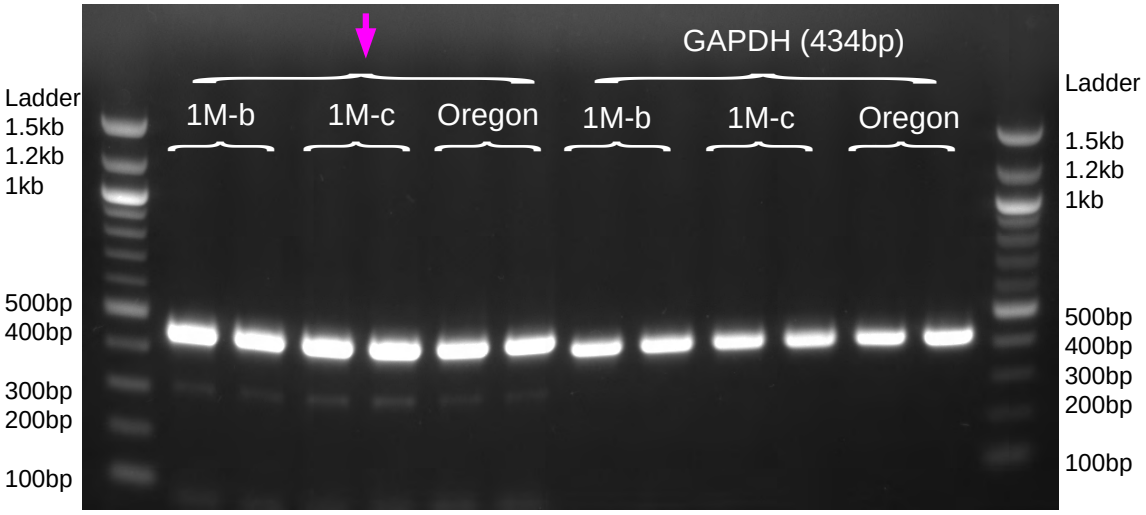
(c). The sequencing result of PCR fragment illustrated in b. The mini-white part showed correct and clean sequence, while the part of Toll-2 CDS started to become noisy (pointed by red arrow) and no accurate sequence could be obtained from this fragment.

Figure 3.9 RT-PCR to test whether *Toll-2^{pTV}* is a null mutant

a.



b.

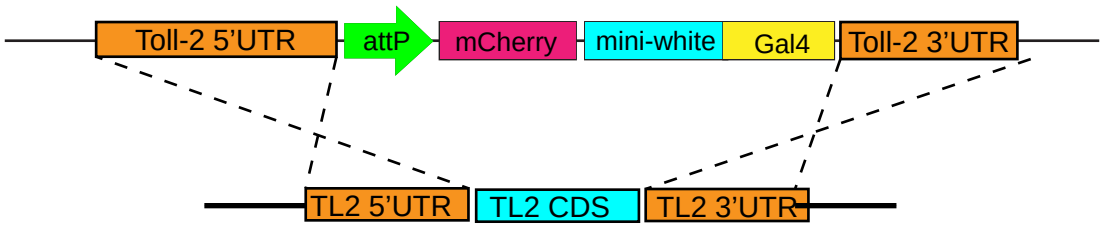


(a), shows the structure of Toll-2 coding sequence and the design of the primers hybridising with the Toll-2 cDNA in RT-PCR.

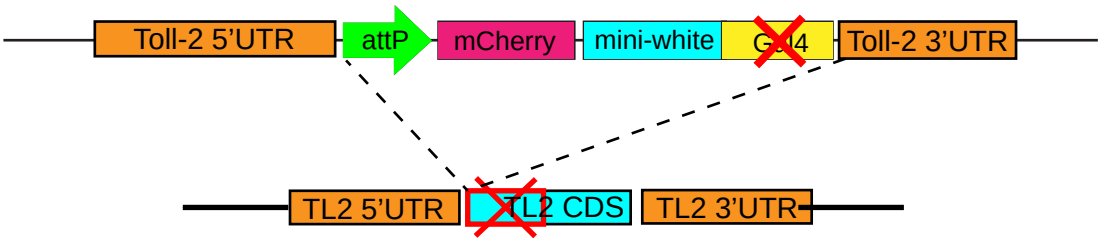
(b), the gel picture of RT-PCR testing using primers illustrated in (a). PCRs were carried out in both line 1M-b and 1M-c. Oregon was tested as control. Positive control was set by using primers hybridising with GAPDH.

Figure 3.10 RT-PCR to test whether *Toll-2^{pTV}* is a null mutant

a.



b.



(a), shows the expected result after Toll-2^{pTV} was inserted into the genome after homologous recombination, where Toll-2 is knocked out and pTV cassette is inserted into Toll-2 locus.

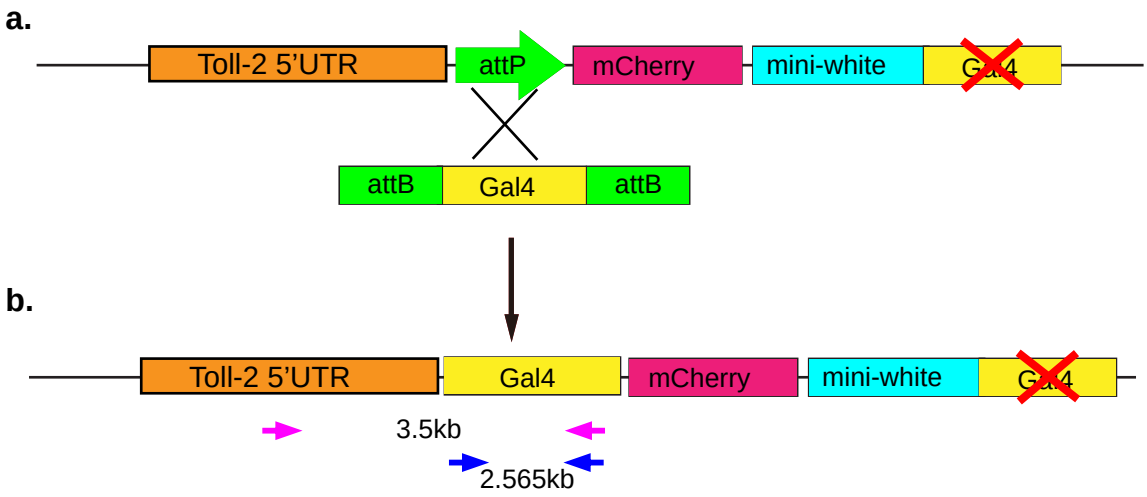
(b), illustrates the actual result in 1M-b and 1Mc transgenic flies. pTV cassette is inserted into Toll-2 locus, however, Gal4 in the cassette is damaged during recombination. Moreover, Toll-2 CDS is not fully knocked out but the beginning of Toll-2 CDS might be damaged.

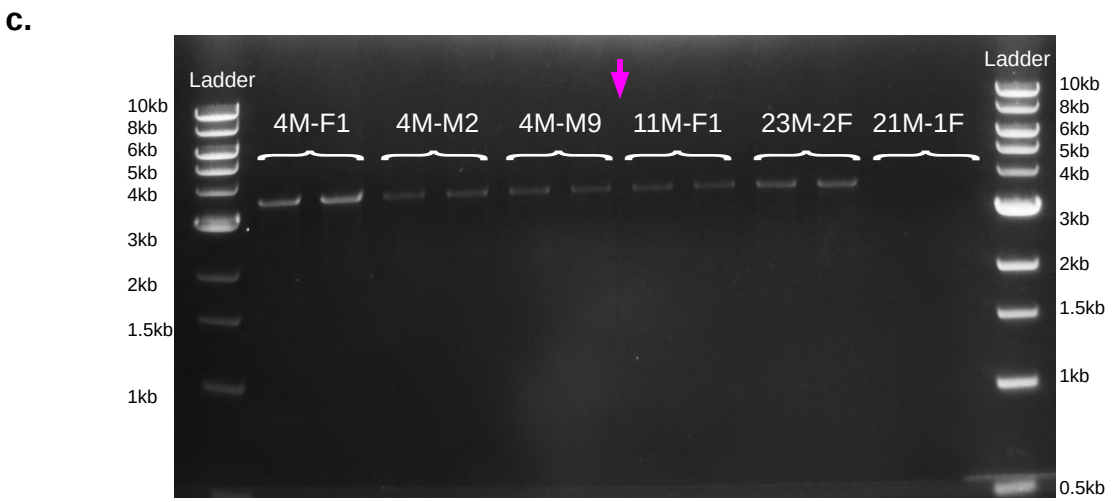
and revealed the expression pattern of *Toll-2*. Although *Toll-2* is not knocked out, the missing first half of the CDS in 1M-b and -c and the messy sequences around the starting codon suggest that the *Toll-2* CDS is highly likely to result in a null allele which would not produce proteins. Moreover, if the protein were made, it is likely that the protein would lack the intact signal peptide, so that the protein would not be inserted into the membrane to function. Therefore, the *Toll-2^{pTV}* knock-in allele could be used both to visualize the expression pattern of Toll-2 and as a mutant allele for the further functional analysis. Finally, 1M-b is selected to carry out all later experiments, named as *Toll-2^{pTV}*.

3.2.4 Generation of *Toll-2^{pTV} Gal4* lines

PCR analysis had revealed that the Gal4 sequence in the original pTV cassette was most likely damaged, as in fact stated in Baena-Lopez et al. This implied that Gal4 in the cassette could not be used as a *Toll-2* reporter. Fortunately, the pTV cassette also carries an attP site that enables the integration of attB-bearing construct. Therefore, by injecting a Gal4-attB construct into *Toll-2^{pTV}* flies, Gal4 could be inserted into the attP landing site at *Toll-2* pTV locus (Figure 3.11a). The *Gal4* construct was ordered from *Addgene* and I did midi-preps to generate enough amount of DNA for microinjection. Gal4-attB and *Toll-2^{pTV}* flies were sent to *BestGene Inc.* to be injected, and I screened for *Toll-2^{pTV}* Gal4 transgenic flies (Figure 2.2). During the screening, six fluorescent larvae were fished out as candidates and stable stocks were built from these six larvae. To test whether *Gal4* is inserted at the right locus, I then carried out two sets of PCRs. Primers were designed to bind the end of *Toll-2* 5'HA and the end of *Gal4* (Figure 3.11b, pink

Figure 3.11 Generation of *Toll-2^{pTV} Gal4 line*





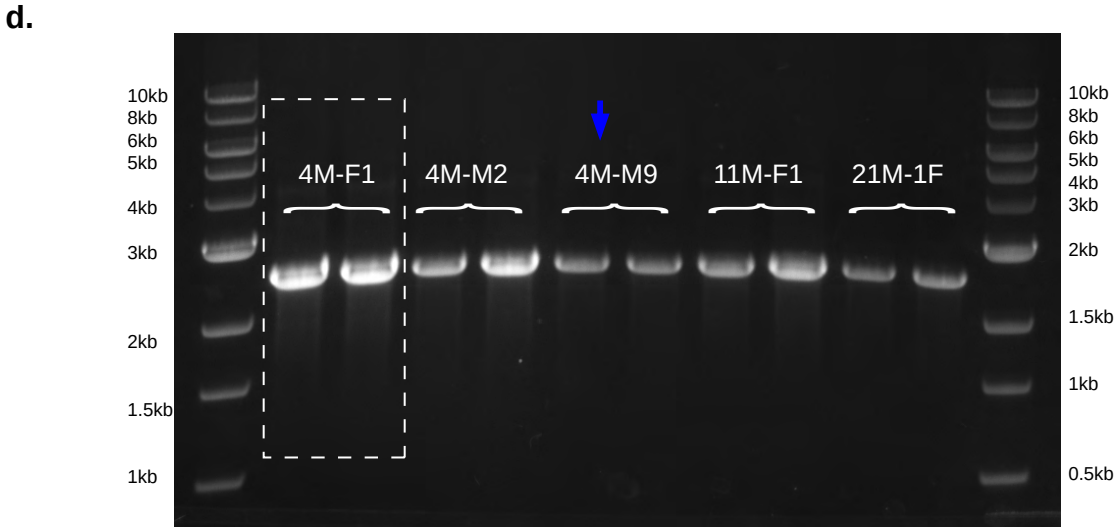


Figure 3.11 Generation of *Toll-2^{pTV} Gal4 line*

(a). Gal4 flanked with attB sequences could be inserted into attP site in Toll-2^{pTV} flies.

(b). Two pairs of primers were designed to test whether Gal4 has been inserted into the right locus (pink arrows) and whether Gal4 was still intact in the genome (blue arrows).

(c).It was tested whether Gal4 was inserted at the right locus in six lines of candidatesusing PCR. Line 21M-1F did not show bands with expected size, while other 5 lines did.

(d). It was tested whether Gal4 insertion was intact in the genome in 5 lines. All the lines showed expected DNA band on the gel. 4M-F1 was seleceted for further experiments.

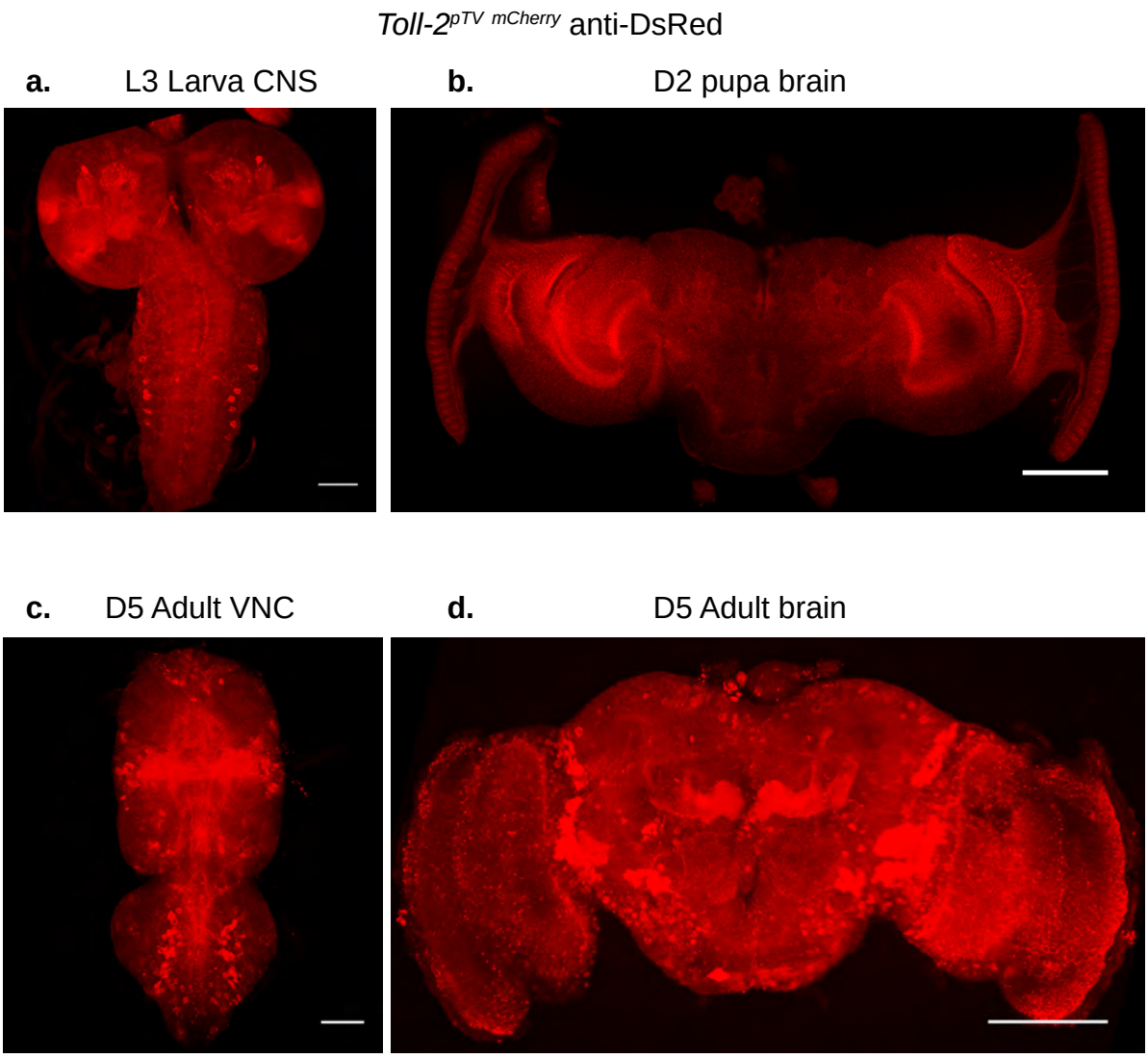
arrows). PCR result indicate that 5 out from 6 lines showed the band with expected size (Figure 3.11c), which indicates that *Gal4* was inserted at the right locus in these 5 lines. I then further tested whether the *Gal4* in these 5 lines was intact using primers located in the *Gal4* sequence (Figure 3.11b, blue arrows). All of the 5 lines showed correct bands of *Gal4*, which suggests that they all carried intact *Gal4* element (Figure 3.11 d). Line 4M-F1 was selected for further experiments and named as *Toll-2^{pTV} Gal4.* Therefore, a *Toll-2* driver line is generated in which *Gal4* is expressed under the regulation of *Toll-2* promotors. At the same time, *Toll-2^{pTV}* Gal4 is also a mutant that could be used later for functional analysis.

3.2.5 Visualization of *Toll-2* expression in the CNS in Toll-2^{pTV} transgenic flies

In *Toll-2^{pTV}* transgenic flies, the expression of all elements within this cassette including *mCherry*, *mini-white* and *Gal4* should be under the regulation of *Toll-2* promotors. Therefore, by staining *mCherry* using anti-DsRed antibody, I could visualize the expression pattern of *Toll-2* (Figure 3.12). I did dissections and immunostainings in 3 stages of fly including L3 wandering larvae, D2 pupae and D5 adult. It could be seen that *Toll-2* was expressed throughout development. In L3 larvae CNS, *Toll-2* was expressed in the optic lobes and cells in the ventral nerve cord (VNC) (Figure 3.12a). In day 2 pupal brain, *Toll-2* was expressed pronouncedly in the optic lobe (Figure 3.12b). In adult brain, *Toll-2* is also pronouncedly expressed in optic lobes and the mushroom bodies, and also in the VNC (Figure 3.12c and d).

I also visualized *Toll-2* expression by crossing *Toll-2^{pTV} Gal4* with *UAS FlyBow* (Figure 3.13). UAS FlyBow is a reporter that encodes multiple membrane-tethered fluorescent proteins (Hadjieconomou *et al.*, 2011), and each protein is flanked with

Figure 3.12 *Toll-2* is expressed in the CNS throughout development



Expression of *Toll-2* in different stages of CNS stained by anti-DsRed antibody. Genotype: *Toll-2*$^{pTV\ mCherry}$*/CyO.*

(a). L3 larval CNS

(b). Day 2 pupal brain

(c). D5 adult ventral nerve cord

(d). Day 5 adult brain

Scale bars: a and c: 50μm; b and d: 100μm

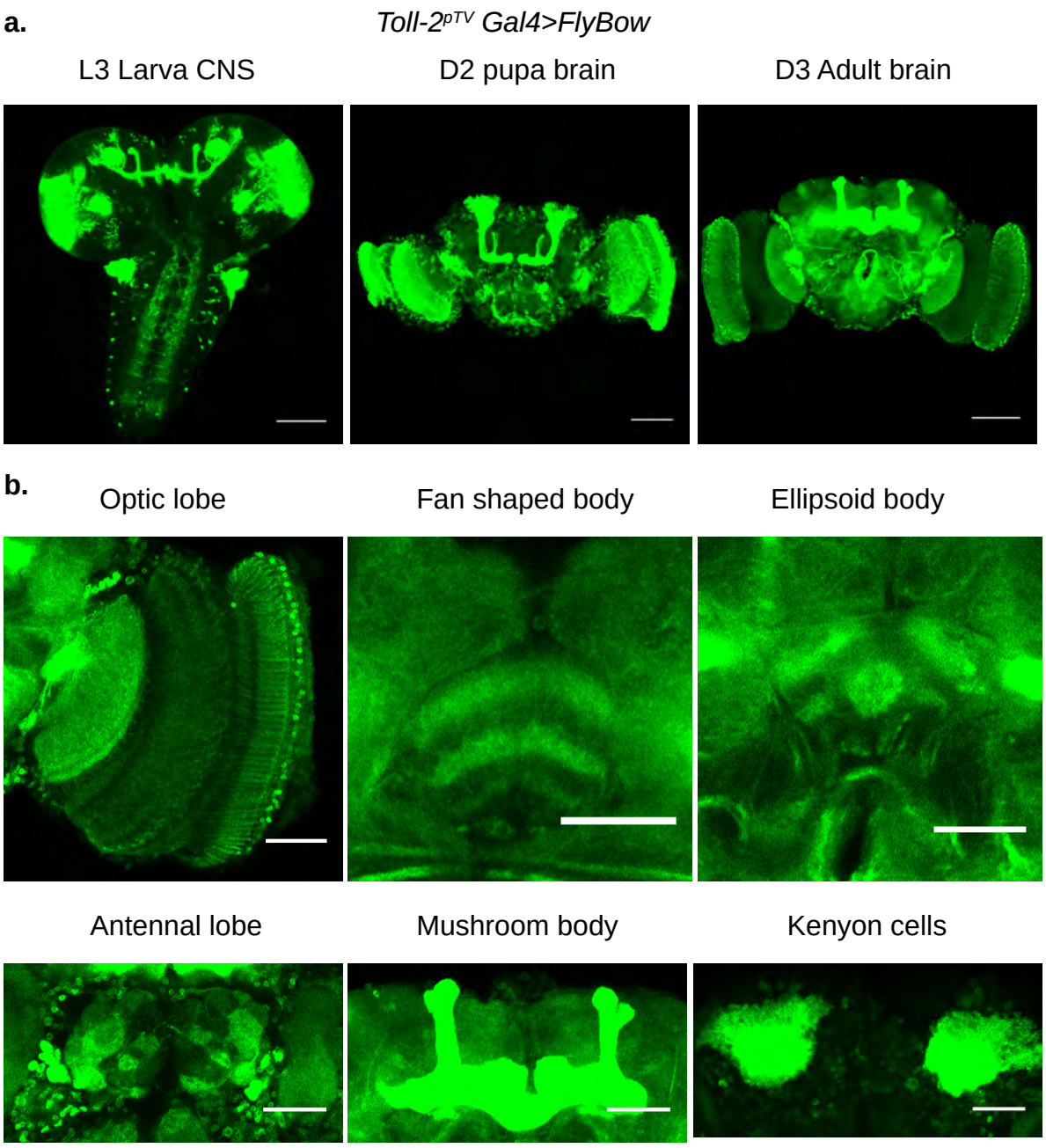
FRT sites which can be flipped out randomly when heat shocked. However, when kept at 25°C, *UAS FlyBow* can be used as an enhanced and high resolution, membrane tethered GFP reporter. Therefore, overexpressing GFP driven by *Toll-2^{pTV} Gal4* might provide stronger signal and resolution than *mCherry*. Three stages including L3 larvae, D2 pupae and D5 adult flies were dissected and scanned (Figure 3.13 a). Endogenous EGFP was strong enough, so antibody staining was not required in this genotype. Toll-2 is highly expressed in L3 larvae, day 2 pupae and day 5 adult, which is consistent with *mCherry* signal shown in Figure 3.12. Moreover, it could be seen that *Toll-2* is highly expressed in multiple brain domains in adult including lamina and medulla and lobula in optic lobes, central complex such as fan shaped body and ellipsoid body, antennal lobes. *Toll-2* was also pronouncedly expressed in adult mushroom bodies (Figure 3.13b).

Together, these data show that *Toll-2* is expressed in the CNS through development to adulthood. It is highly expressed in optic lobes, VNC and the central brain including MB, which suggests that *Toll-2* might have functions in visual system, motor system, and maybe in learning and memory.

3.2.6 Loss of *Toll-2* function causes defects in survival

It has been observed that the appearance and behaviour of the flies that carried one Toll-2^{pTV} allele (Toll-2^{pTV}/+ or Toll-2^{pTV}/ balancer) looked the same as wild type flies. In order to further test whether Toll-2^{pTV} is a mutant allele, I carried out genetic tests. Survival index calculation was the first test I did. No homozygous Toll-2^{pTV} flies have been obtained so far. There are two possibilities causing this effect: firstly, Toll-2^{pTV} is a mutant allele and loss of *Toll-2* function is homozygous lethal; secondly, the genetic

Figure 3.13 *Toll-2* is expressed in the CNS and throughout brain in multiple brain domains



(a). *Toll-2* is expressed throughout development shown in L3 larval CNS, D2 pupal brain and D3 adult brain.

(b). In adult brain, *Toll-2* is expressed throughout brain in multiple domains.

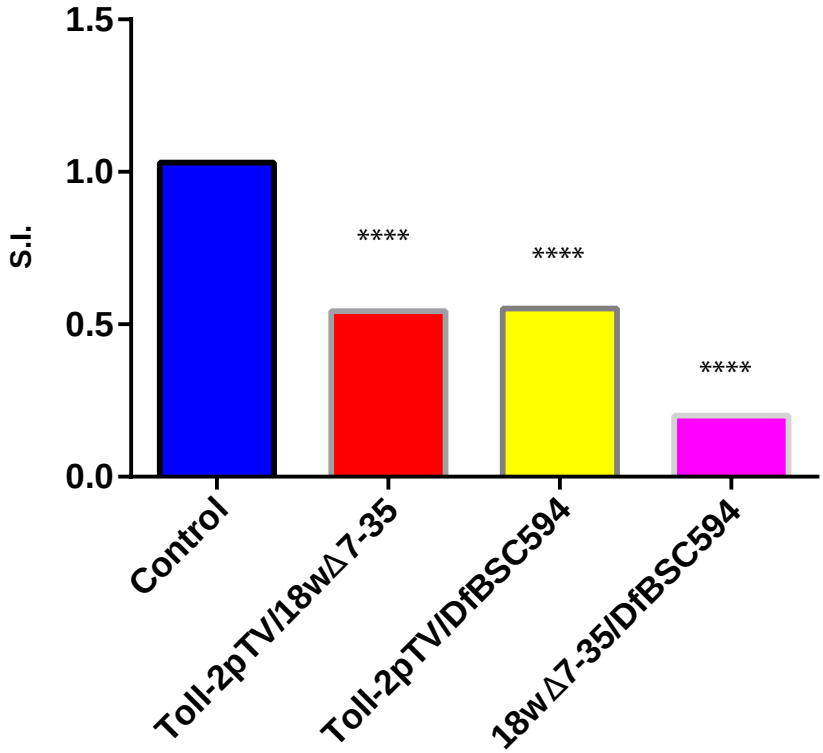
Genotype: *w;Toll-2^{pTV} Gal4/UAS Flybow*
Scale bar: a: 100μm; b: 50μm.

background might cause the homozygous lethality. To avoid the effects from genetic background, I used two other *Toll-2* mutant alleles to cross with Toll-2^{pTV}, which are *18w$^{\Delta 7\text{-}35}$* and *DfBSC594* (BDSC #4372 and #25678). *18w$^{\Delta 7\text{-}35}$* has been published to be a *Toll-2* null mutant, and *DfBSC594* is a deficiency line that *Toll-2* was fully knocked out (Eldon et al., 1994). The survival index of Toll-2^{pTV}/Df(2R)BSC594, Toll-2^{pTV}/18w$^{\Delta 7\text{-}35}$, and 18w$^{\Delta 7\text{-}35}$/Df(2R)BSC594 are all significantly reduced compared to control. Toll-2^{pTV}/Df(2R)BSC594 and Toll-2^{pTV}/18w$^{\Delta 7\text{-}35}$ are reduced at similar level. However, the survival index of 18w$^{\Delta 7\text{-}35}$/Df(2R)BSC594 is the lowest among all mutant groups which is less than half of the other two groups (Figure 3.14a). This suggests that Toll-2^{pTV} might not be a null mutant. However, the decreased survival rate indicates that *Toll-2* mutant is semi lethal.

To test whether lethality occurred during pupal stages, I then calculated the survival index at pupal stage. The heterozygous pupae carried balancer *SM6aTM6B* which has a marker *Tb-* making the pupae look tubby compared to the wild type pupae, while the transheterozygous *Toll-2* mutant pupae did not carry the balancer, which would look like wild type pupae (Figure 2.8). Therefore, the number of tubby and non-tubby pupae were counted. It shows that the survival index of Toll-2^{pTV}/18w$^{D7\text{-}35}$ is significantly decreased compared with control (Figure 3.14b). This suggests that the transheterozygous *Toll-2* mutant flies died before pupa stage. However, when comparing the S.I at pupa and adult stage, the difference between control and *Toll-2* mutant in adult stage is more significant that the difference at pupa stage. This suggests that the defects caused by loss of *Toll-2* functions might still persist at pupal stage during metamorphosis. To conclude, loss of *Toll-2* function causes lethality before and at pupa stage.

Figure 3.14 The effect of loss of Toll-2 function on survival of pupae and adult

a.



b.

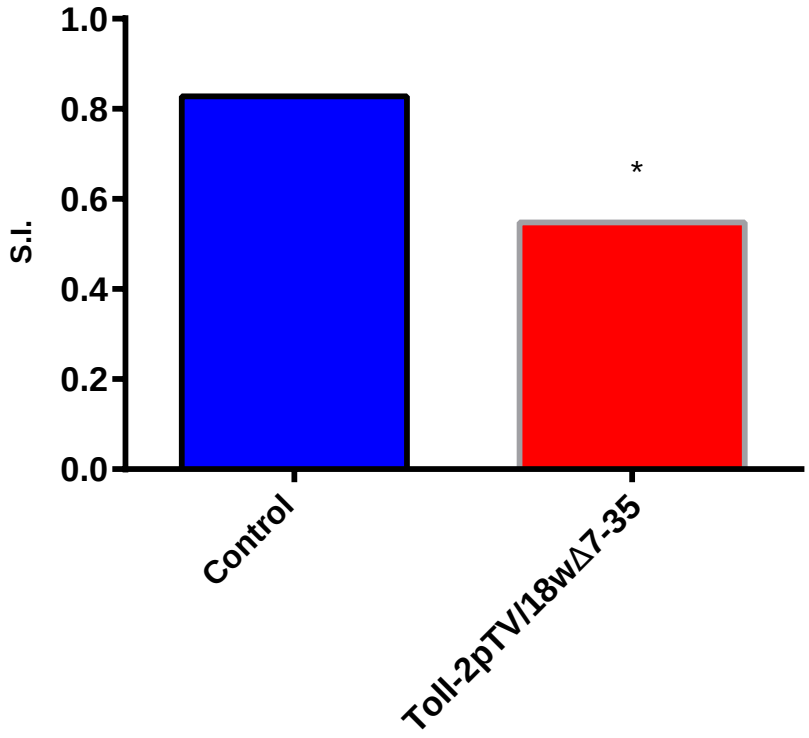


Figure 3.14 The effect of loss of *Toll-2* function on survival of pupae and adult
(a). The survival index of control and the crosses of different Toll-2 mutants in adult flies. The survival index of all three groups are significantly decreased compared with the control (Chi-square test, $p<0.0001$).
Sample size from left to right: N=341, 2399, 1984, 932.
(b). The survival index of control and the Toll-2 mutant cross in pupae. The survival index in Toll-2 mutant group is significantly decreased compared with control (Chi-Square test, $p=0.0138$). Sample size from left to right: N= 205, 1246.

3.2.7 Loss of *Toll-2* function causes defects in longevity of adult flies

I then tested whether loss of *Toll-2* function would affect the longevity of adult flies (Figure 3.15). There were 97% of the control flies surviving at Day 22 at 25°C when nearly half of the Toll-2pTV/18wD7-35 flies died at that time. Also, at the end of D30 at 25°C, 96% of the control survived while less than half (43%) of *Toll-2* mutant flies did. Therefore, loss of *Toll-2* function shortens life span of adult flies. Moreover, this results further indicates that *Toll-2* is required throughout adulthood.

3.2.8 Loss of *Toll-2* function causes defects in adult fly locomotion

When carrying out the longevity test, I noticed that the locomotion of *Toll-2* mutant flies seemed to be slower compared with the control. Therefore, I carried out climbing assay to further quantify this phenotype. I firstly tested whether loss of *Toll-2* function in the animal throughout development would have any effect on climbing. By the end of 10 seconds, nearly 70% of the flies in the control group could climb up to 2cm, however, less than 15% of the Toll-2^{pTV}/$18w^{\Delta 7\text{-}35}$ and less than 10% of the Toll-2^{pTV}/Df(2R)BSC594 flies could climb up to the same height within the same time (Figure 3.16a). This result shows that loss of *Toll-2* function leads to impaired locomotion in adult flies.

However, it is still unclear whether the defect in adult locomotion is related to the defects in central nervous system (CNS), or whether this defect is specific to adult flies. In order to answer these two questions, I carried out another two sets of climbing assays. Firstly, I tested whether the defect is related to CNS. I overexpressed *Toll-2 RNAi* (BDCS #30498) in neurons using *Elav Gal4*. However, it

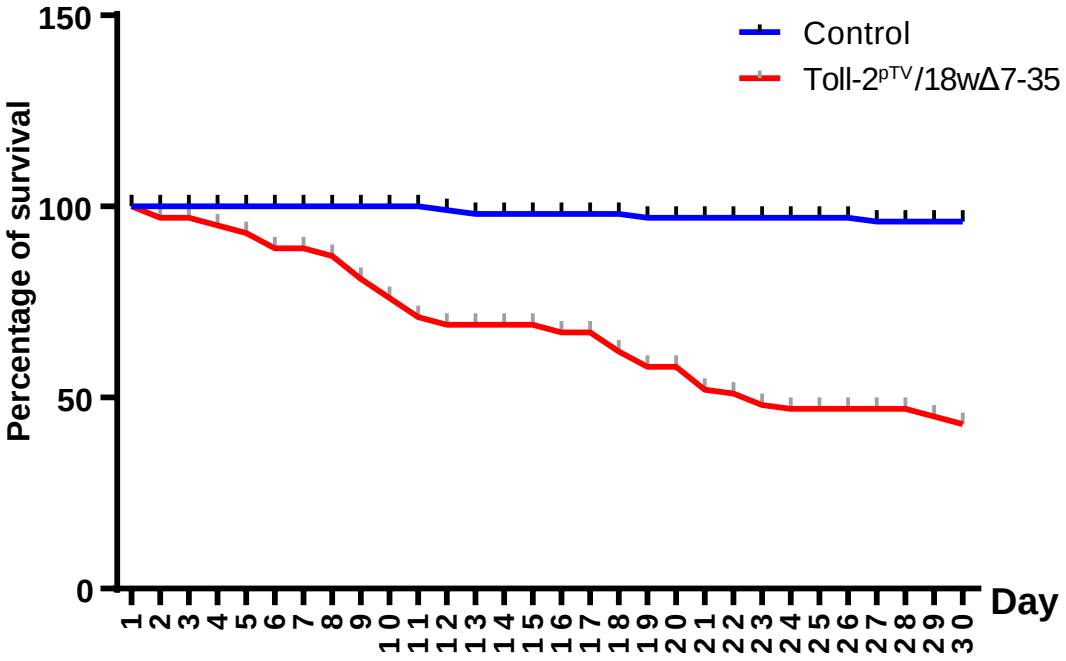
could be seen that knocking down *Toll-2* in neurons did not affect the climbing ability in adult flies (Figure 3.16b). This result suggests that the defect of climbing might not be caused by altered *Toll-2* function in neurons, or that *Elav Gal4 UAS Toll-2 RNAi* was not a strong knock out.

Secondly, I asked whether the adult locomotion defect might reflect an adult specific function of *Toll-2* or not. To answer this, I used *Toll-2 Gal4; Toll-2 RNAi/Tubulin Gal80^{ts}* which allows the inducible expression of Gal4. *Gal80^{ts}* is the inhibitor of *Gal4* but sensitive to temperature. It is switched on at 18°C and inhibits *Gal4* and is switched off at 30°C to release the inhibition. Therefore, to knock down *Toll-2* specifically at adult stage, I kept the flies at 18°C until eclosion and then switched to 30°C for two days (48 hours) (Figure 3.16c). The result shows that when knocking down *Toll-2* in *Toll-2* expressing cells specifically in adult stage, the locomotion in *Toll-2* RNAi flies is actually improved compared with the control group.

3.2.9 Loss of *Toll-2* function causes defects in visual system of adult flies

The expression of Toll-2^{pTV} Gal4 driving UAS Flybow has shown that *Toll-2* is highly expressed in the optic lobe and lamina, which suggests that Toll-2 might have functions in the visual system. Thus, I carried out Buridan Arena test to find out whether *Toll-2* is involved in flies' vision. To carry out this experiment, we collaborated with the Heisenberg lab from Würzburg, Germany. In this experiment, a single fly with the wings cut was kept in the Buridan Arena with two black stripes on both side of the arena. When a fly with normal visual capacity sees the contrast between black stripe and white wall, it will be attracted and keep walking between the

Figure 3.15 Loss of *Toll-2* function shortened life span of adult flies

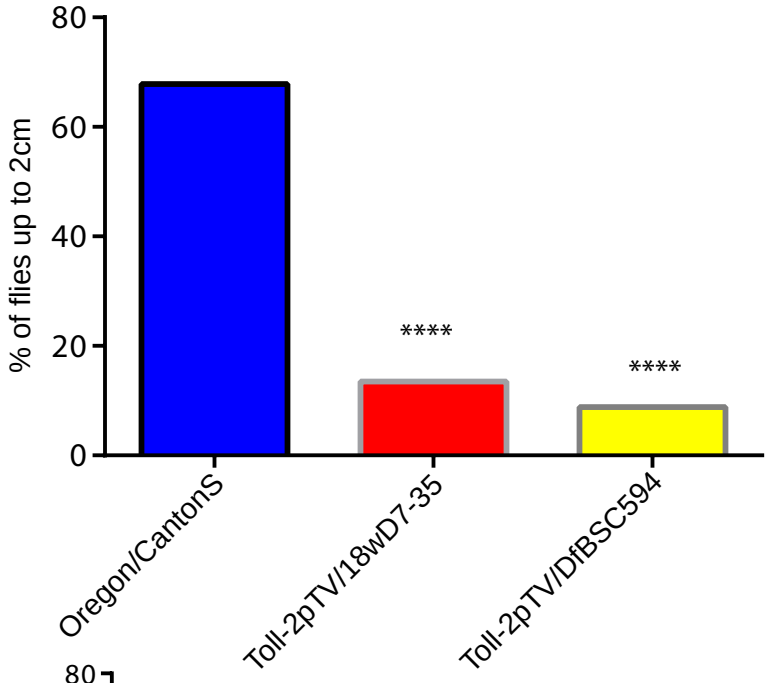


It shows that *Toll-2* is required to maintain survival of adult flies. Survival rate was calculated everyday and compared between control and *Toll-2* mutant group. Blue line indicates the survival rate of control and red line indicates survival rate of *Toll-2* mutant, each dot on the line indicates the survival rate on each day.
N= 119 (control), 91 (Toll-2 mutant).

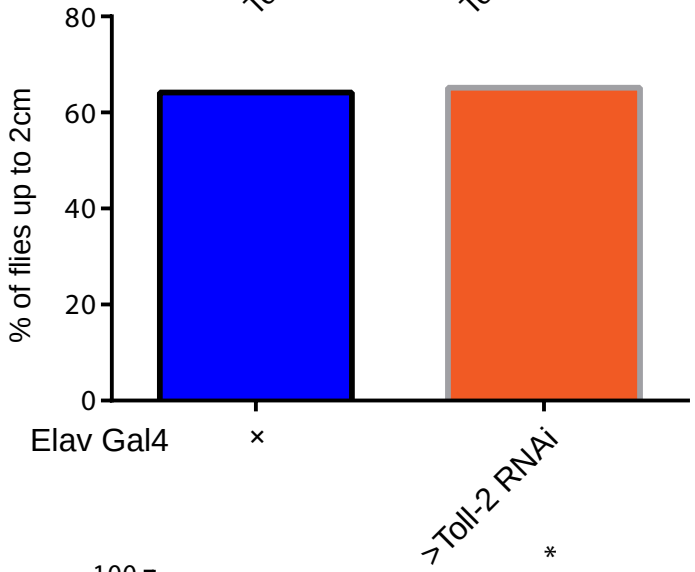
Genotype: Control: Oregon(R)/CantonS
Toll-2 mutant: Toll-2^{pTV}/18wΔ7-35.

Figure 3.16 Effect of loss of *Toll-2* function on adult climbing behavior

a.



b.



c.

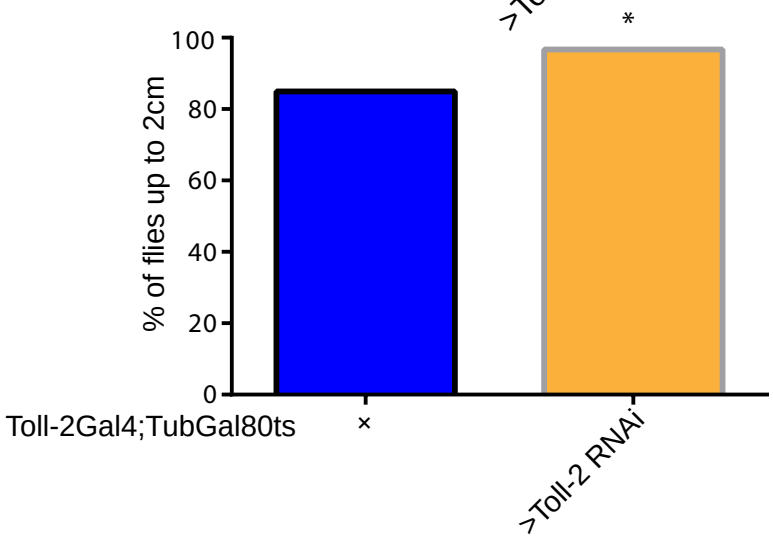


Figure 3.16 Effect of loss of *Toll-2* function on adult climbing behavior
(a). Loss of Toll-2 function throughout development causes defects on climbing in adult flies.
Genotype: Control: Oregon/CantonS, N=134
Toll-2 loss of function: Toll-2^{pTV}/$18w^{\Delta 7\text{-}35}$, N=85
Toll-2^{pTV}/DfBSC594, N=78
(b).Knocking down *Toll-2* in neurons throughout development did not affect climbing behaviour in adult.
Genotype: Control: Elav Gal4/+, N=24
Toll-2 loss of function: Elav Gal4>Toll-2 RNAi, N=22
(c). Knocking down *Toll-2* in *Toll-2* expressing cells specifically in adult improved the climbing behaviour in adult.
Genotype: Control: *Toll-*2^{pTV} Gal4; TubulinGal80ts, N=27
Toll-2 loss of function: *Toll-2pTV* Gal4>*Toll-2* RNAi;TubulinGal80ts, N=20

stripes. However, if a fly is not able to see the contrast, it will be distracted and walk randomly in the arena.

In this experiment, I used three different genotypes to test the effect of loss of Toll-2 function on the visual system including *Toll-2^{pTV}/Df(2R)BSC22*, *18w$^{\Delta 17\text{-}35}$/Df(2R)BSC22*, and *ElavGal4/+;UAS18wRNAi/TubGal80ts*. *Df(2R)*BSC22 is another deficiency line in which *Toll-2* is deleted in the genome (BDSC #6647). In the first 2 genotype, *Toll-2* was knocked out in the animal throughout development to test whether *Toll-2* had functions in the visual system during development. In the third genotype, as mentioned above, flies were kept at 18°C until eclosion and then shifted to 30°C for two days, so that *Toll-2* was knocked down in neurons only in adult stage. Each fly was put into the arena and walked for 10 minutes, the walking trajectory of each fly was recorded and presented as an image. Based on the density of the traces between two black stripes, the trajectories of all the flies from each group were divided into four categories: normal, medium, severe, and no walk (Figure 3.17a).

The number of flies in each category from each genotype was counted and listed (Figure 3.17b). The percentage of the flies in each category was also calculated and compared to the control via $\chi 2$ test. However, to test the effect of *Toll-2* in visual system, flies showed defected walking behaviour was not analysed (Figure 3.18a). The result of $\chi 2$ test showed that there is no significant difference between control to other groups with loss of *Toll-2* function. However, in the group of *18w$^{\Delta 17\text{-}35}$/Df(2R)BSC22*, there were no flies showing normal visual behaviour, which suggests that loss of *Toll-2* function might cause defects in the visual system. The reason of not showing significant difference might be that the sample size was too

small (N=11-13). Moreover, although the statistic result was not significant, there is a trend showing that when knocking down *Toll-2* in neurons in adult stage (*ElavGal4/+;UAS18wRNAi/TubGal80ts*), more flies had abnormal visual behaviour and walking behaviour compared to the control. Therefore, this suggests that *Toll-2* might have functions in neurons.

To conclude the Buridan Arena results, it suggests that loss of *Toll-2* function during disrupts the visual system in adult flies. Moreover, knocking down *Toll-2* in neurons in adult stage might also cause defects in the visual system.

3.2.10 Test *Toll-2* functions in brain circuitry by using *UAS Flybow*

To asked what the mechanisms behind the behavioural defects were, I tested whether *Toll-2* is involved in neural circuit development. I firstly tested whether loss of *Toll-2* function in *Toll-2* expressing cells caused effect on brain circuitry such as formation of axons and dendrites. Using *Toll-2^{pTV}Gal4* crossing to *UAS Flybow 18w$^{\Delta 7\text{-}35}$* which is a recombinant allele I made to combine Toll-2 mutant allele with the UAS reporter (*Toll-2^{pTV}Gal4/UAS Flybow 18w$^{\Delta 7\text{-}35}$*). As explained in Chapter 3.2.4, *Toll-2^{pTV}Gal4* is also a *Toll-2* mutant allele, therefore, by crossing these two alleles, I could visualize the Toll-2 cell membrane, including cell body, axons and dendrites, from fluorescence of *Flybow* at a *Toll-2* mutant background.

I looked at the brain circuitry of Day 3 adult. Since loss of *Toll-2* function caused defects in the visual system, I firstly looked at the circuits in the optic lobe (Figure 3.19 a and b). However, in the optic lobe including medulla and lobula, I could not see any significant difference between control and *Toll-2* mutant flies. I have also

looked into other parts of the brain such as mushroom bodies. No significant difference was noticed either (Figure 3.19 c and d). These results suggest that *Toll-2* mutant might not cause major defects in the brain circuits. However, in this experiment, the projections of *Toll-2* expressing cells were seen together, which might make it difficult to see if there had been any subtle effects. To overcome these, I carried out MARCM clone, which will be further explained in the next section.

3.2.11 *Toll-2* mutant clone causes mistargeting in neurons in pupae

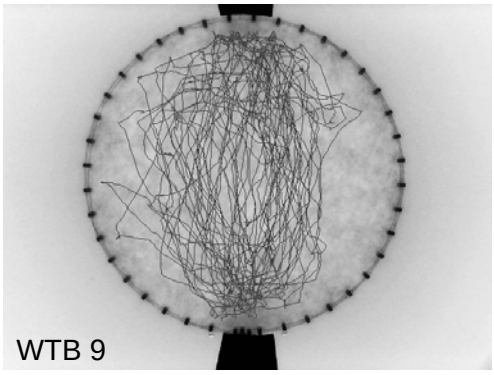
To further test whether loss of *Toll-2* function caused any effects on brain circuitry, I carried out MARCM clone (Figure 3.20). The detailed regime of MARCM clone is explained in Figure 2.5 I induced *Toll-2*^{pTV} mutant MARCM clones in dividing cells in pupa using *heat-shock Flippase* (*hs-FLP*) and visualized resulting mutant neurons in the D4 pupal brain (96 hours after puparium formation) with elav>mCD8GFP. Loss of dendrites can be clearly observed in the lamina. Axonal degeneration and misrouting can be observed in medulla and lobula. It can also be found that the neuropils of SOG and fan shaped body were massively lost in the mutant. Moreover, dramatic neuronal loss was also found throughout many brain domains, including lamina, medulla, lobula, lobula plate.

However, the effects on the mushroom bodies were less discernible. This could be due to the heat shock regime missing the peak division time of mushroom body neuroblasts, as not many mushroom body projections were observed in the control either. To conclude, loss of *Toll-2* function causes widespread neurodegeneration in the pupal brain.

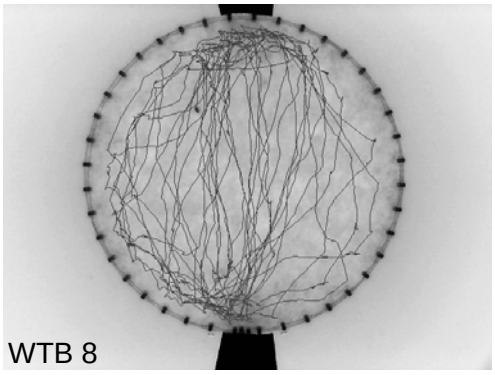
Figure 3.17 Effect of *Toll-2* loss of function on visual system using Buridan Arena test

a.

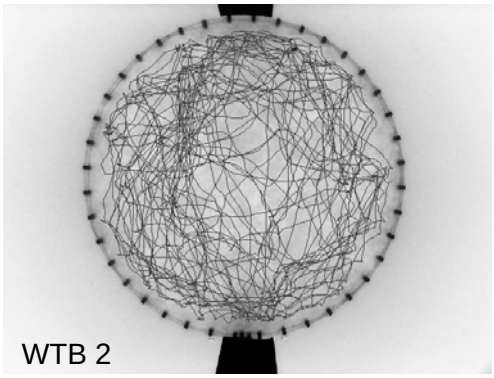
Normal



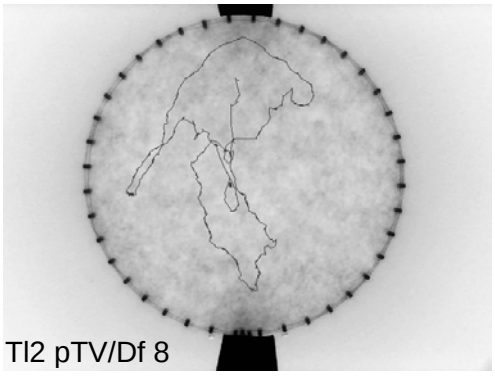
Medium



Severe



No walk



b.

Genotype / Category	WT	Toll-2pTV/Df	18wΔ7-35/Df	Elav>Toll-2RNAi TubGal80ts
Normal	5	2	0	3
Medium	5	3	6	4
Severe	3	3	5	4
No walk	0	3	2	3

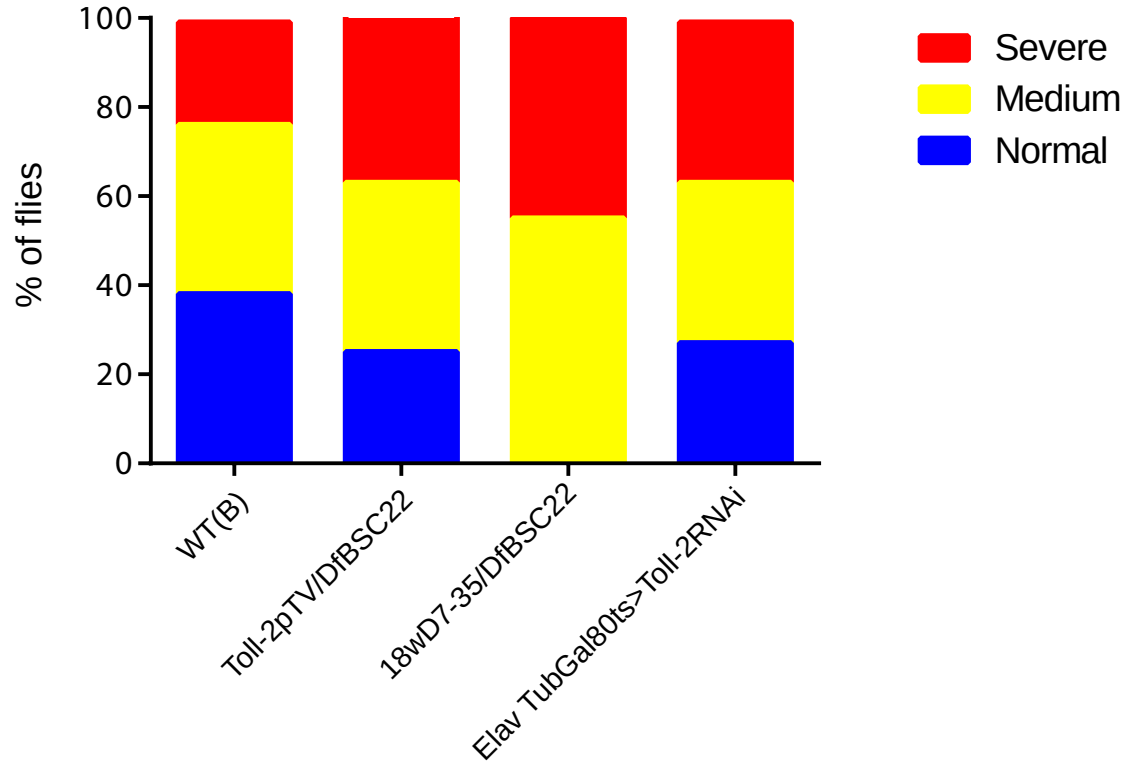
Figure 3.17 Effect of *Toll-2* loss of function on visual system using Buridan Arena test

(a). Trajectories of fly walking in Buridan Arena. Based on the sensity of tracks between two stripes, the trajectories from each fly was divided into four categories:
Normal: most of the tracks are distributed between two black stripes.
Medium: Around half of the tracks are distributed between two black stripes.
Severe: Almost all the tracks are distributed randomly in the arena,
No walk: Not many tracks in the arena because of the locomotion defects.
(b). Samples from all genotypes were allocated into different categories.

Genotype:
WTB: wild type Berlin
Toll-2pTV/Df: Toll-2pTV/ DfBSC22
18wD7-35/Df: 18wD7-35/ DfBSC22
Elav>Toll-2RNAi TubGal80ts: Elav Gal4 UAS Toll-2 RNAi; Tubulin Gal80ts

Figure 3.18 Knocking down *Toll-2* caused defects in visual system

a.



This figure shows the distribution of different phenotypes from Buridan Arena test in the control and three different Toll-2 loss of functon groups. Different color indicates different severity. Chi-square test, p=0.4929, N=13, 8,11, 11.

Genotype:
WTB: wild type Berlin
Toll-2pTV/Df: Toll-2pTV/ DfBSC22
18wD7-35/Df: 18wD7-35/ DfBSC22
Elav>Toll-2RNAi TubGal80ts: Elav Gal4 UAS Toll-2 RNAi; Tubulin Gal80ts

Figure 3.19 Comparison of brain circuitry between control and *Toll-2* loss of function using UAS Flybow

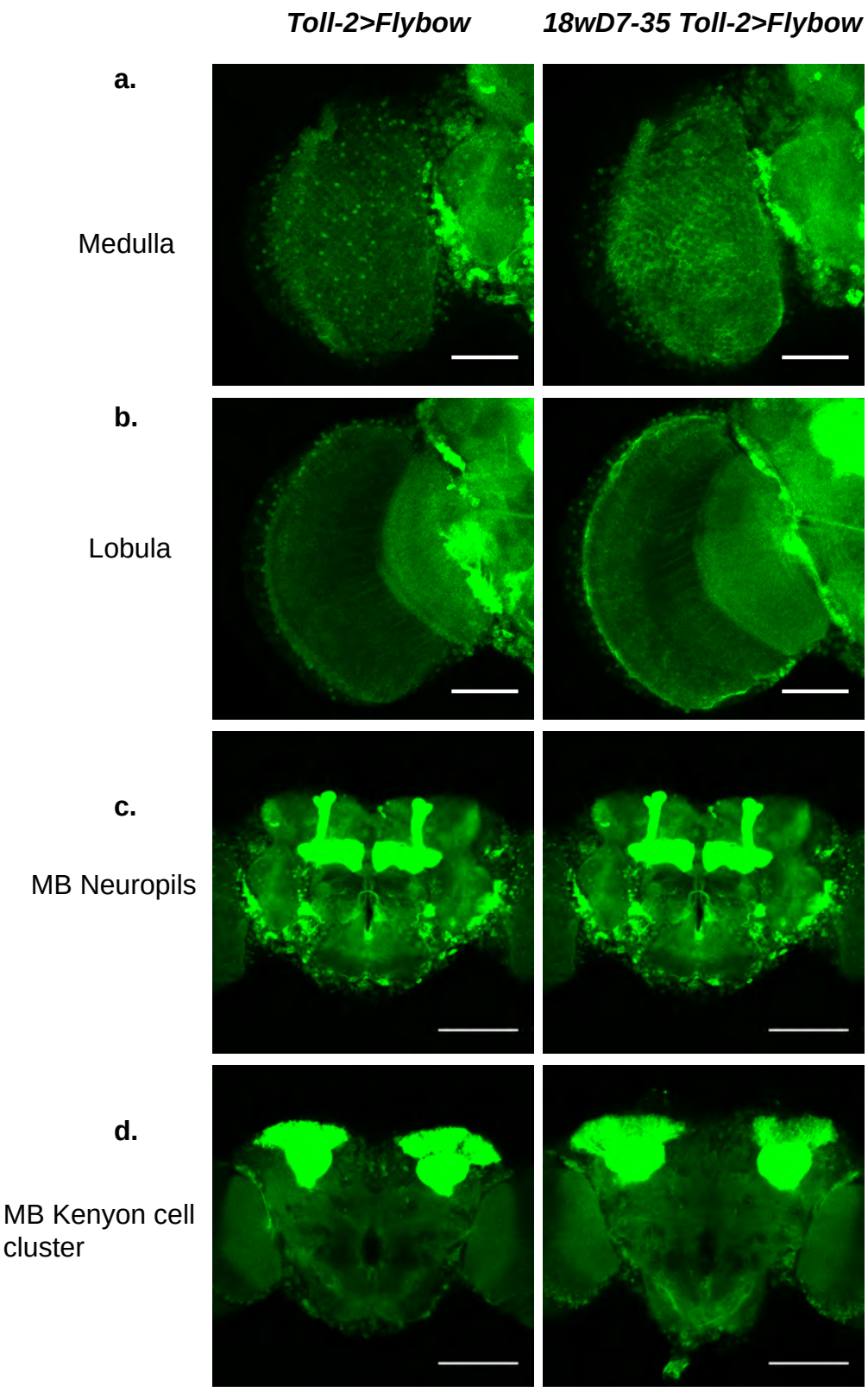


Figure 3.19 Comparison of brain circuitry between control and *Toll-2* loss of function using UAS Flybow

Cell projections in different domains of the brain were compared between control and loss of *Toll-2* function throughout development

Genotype: *Toll-2 >Flybow*

Toll-2 LOF: *18wD7-35 Toll-2>Flybow*

(a). Medulla

(b). Lobula

(c). Mushroom body neuropils

(d). Mushroom body Kenyon cells

Scale bar: a and b: 50μm; c and d: 100μm.

Figure 3.20 *Toll-2* mutant clones caused cell loss and disrupted connectivity

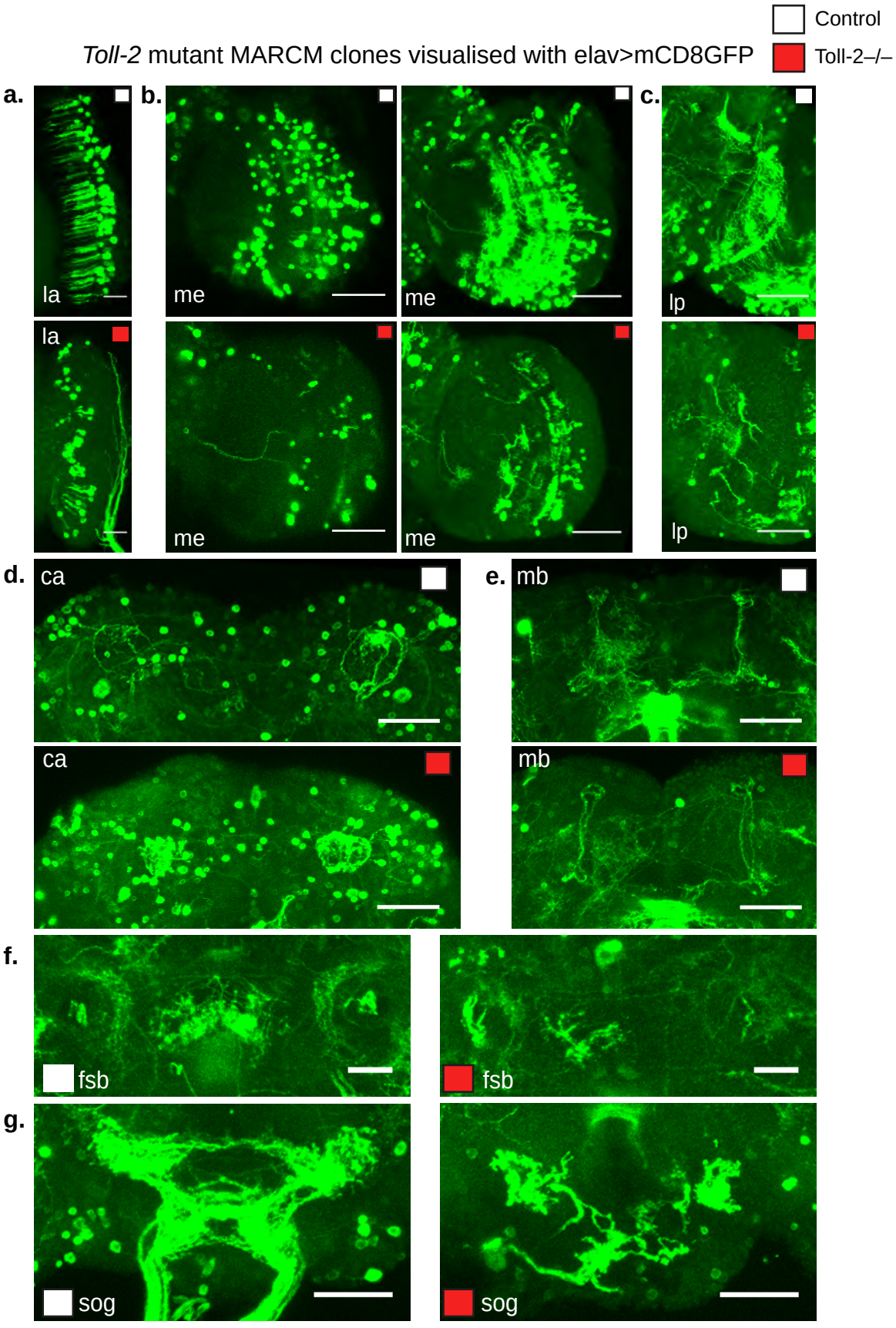


Figure 3.20 *Toll-2* mutant clones caused cell loss and disrupted connectivity

MARCM clones in control and *Toll-2*^{pTV} mutant in D4 pupal brain. Clones in control are labelled in white and clones in *Toll-2* mutant are labelled in red.

Cell loss and disrupted connectivity occured in multiple brain domains.

(a). lamina
(b). medulla
(c). lobula plate
(d). calyx
(e). mushroom body
(f). fan shapped body
(g). sub-oesophageal ganglion

Genotype:
Control: elav Gal4, UAS mCD8 GFP, hs-FLP; neoFRT^{42D}
Toll-2 mutant: elav Gal4, UAS mCD8 GFP, hs-FLP; neoFRT^{42D}, Toll-2^{pTV}

Scale bar: a and f: 25µm; b,c,d,e,g: 50µm.

3.3 Discussion

In this chapter, I showed that I had used CRISPR/Cas9 generating two knock-in alleles, *Toll-2^{pTV}* and Toll-2^{pTV}*Gal4* to visualize Toll-2 expression and study the function of *Toll-2*. Both lines consistently showed that *Toll-2* is highly expressed in the CNS, including the optic lobes and constructs in the central brain such as mushroom bodies, in all stages of flies. I also showed that loss of *Toll-2* function could induce lethality, shortened life span, and defected locomotion in adult flies. *Toll-2* mutant could also induce defects in the visual system. Moreover, I showed that *Toll-2* mutant clones caused cell loss and disrupted cell connections in the pupal brain.

After generating the *Toll-2^{pTV}* line, I have confirmed that *pTV^{mCherry}* cassette had been inserted at *Toll-2* locus using PCRs. However, from the results of PCRs detecting *Toll-2* CDS and RT-PCR, it is suggested that Toll-2 is not knocked out and it could still be transcribed. Moreover, the sequencing result of *Toll-2^{pTV}* suggests that there might be gene duplication when pTV cassette was inserted into the genome. In order to solve the molecular issue from this cloning, 5'RACE would be carried out to check the length of *Toll-2* CDS, which might further indicate whether the *Toll-2* CDS is intact and would still be functional. However, when comparing the *Toll-2* mutant defects in lethality and locomotion, *18w$^{\Delta 7\text{-}35}$* always caused stronger phenotypes than *Toll-2^{pTV}*. *18w$^{\Delta 7\text{-}35}$* has been published to be a null mutant (Eldon et al., 1994). This therefore suggests that *Toll-2^{pTV}* might not be a null allele.

The result of climbing assay has shown that knocking down *Toll-2* throughout development caused defects in adult climbing behaviour, while knocking down *Toll-2*

in neurons did not cause significant effects. It has been published that *Toll-2* has functions during epidermal development (Pare et al., 2014). Epidermis is attached to the muscle, therefore, if loss of *Toll-2* function caused defects in epidermal development, the development of muscle might also be affected, which would further affect the locomotion. Thus, the climbing defects caused by loss of *Toll-2* function might be due to developmental defects instead of neuronal functions. In contrast, it has also been shown that knocking down *Toll-2* in *Toll-2* cells in adult flies improved the locomotion of adult flies. One possibility is that *Toll-2* might be required in inhibitory neurons, like GABAergic neurons (Isaacson and Scanziani, 2011). When blocking *Toll-2* function in these neurons, other neurons will keep being excited, which leads to the increased locomotion. However, I could not further test whether this possibility is true, such as immunostaining using anti-GABA transporter 1 (GAT1), to test whether Toll-2 is expressed in GABAergic neurons.

When analysing the results of Buridan Arena test, although the percentage of flies showing abnormal visual behaviour was higher compared the control, the statistical analysis did not show significant differences. Considering that the sample size in each group was small (N=11-14), this experiment would be further repeated to increase the sample size. Moreover, we had been suggested that it would be better to use *white*+ flies when carrying out experiments related to the visual system. This is because the gene *white* is responsible for pigmental formation in the eyes, and *white*- might cause side effect on the visual behaviour. However, because of the time restriction, I did not change the eye colour background when carrying out the Buridan Arena tests. Therefore, for further experiments, I would change the eye colour background on the X chromosome to w+ first.

When studying the function of *Toll-2* in brain circuitry using MARCM, phenotypes in the mushroom body was not as significant as other brain domains. Not many cell projections had be observed even in the control. It is known that the general cell proliferation peak time is 5h APF and most of the NB would stop proliferating 24h APF. However, some of the MBNB stay mitotic active until 30h APF (Siegrist et al., 2010). Therefore, the peak time of cell proliferation might be later than 5h APF which is the time I selected to do heat shock. In order to visualize more circuits, a later time point will be selected for heat shock, such as 15h or 24h APF.

In the next chapter, I will discuss about the function of *Toll-2* in regulating cell number during development.

Chapter 4

Function of *Toll-2* in regulating cell number in the brain during development

4.1 Introduction

The pupal stage is when metamorphosis happens, in which cell mass is changed through cell death, proliferation and differentiation (Tissot and Stocker, 2000). During metamorphosis, most of the larval cells are eliminated and new cells are generated to form the adult flies. Therefore, strict regulations are required to mediate cell number changes. Toll receptors have been found to regulate cell number in the central nervous system (CNS). *Toll-1* has been found to negatively regulate neuronal number in the larval and pupal ventral nerve cords (VNCs) (Foldi et al., 2017). *Toll-6* can promote both cell survival in the embryonic and larval CNS and cell death in the pupal VNC (McIlroy et al., 2013, Foldi et al., 2017). *Toll-7* has also been found to promote cell survival in the embryonic and larval VNC (McIlroy et al., 2013, Foldi et al., 2017). I therefore asked whether *Toll* receptors are also involved in cell number regulation in the brain. The aim of this chapter is to test whether *Toll-2* is involved in cell number regulation in the pupal brain.

From results of MARCM clones in the previous chapter, I have shown that *Toll-2* mutations caused cell mis-targeting and cell loss in the pupal brain, which suggests that loss of *Toll-2* function may cause neurodegenerative phenotypes. Therefore, in this chapter, I further studied whether *Toll-2* is involved in regulating cell number by quantifying cell number changes after altering the expression of *Toll-2* throughout development or at specific time points in pupa. The plasticity of different cell types is

different during development: for instance, cell types that are essential for sensory processing are less plastic compared to central inter-neurons (Lin et al., 2013). This suggests that different brain domains might behave differently during development. Therefore, cell number in different brain domains will be counted including the central brain and mushroom bodies specifically.

4.2 Result

4.2.1 *Toll-2* and *MyD88* are expressed in overlapping sets of neurons throughout the brain

It has been previously reported that *Toll* receptors can promote cell survival via the *MyD88-NFκB* pathway (Foldi et al., 2017). Since the results of MARCM has shown that loss of *Toll-2* function caused neurodegenerative phenotypes, I then asked where MyD88 is expressed relative to *Toll-2* in the brain (Figure 4.1). In order to visualize the expression of MyD88 in the brain, I used a *MyD88* driver *MyD88 Gal4* (Kyoto #105229) driving a membrane reporter *UAS Tomato* to visualize the cell membrane of MyD88 expressing cells (Figure 4.1 a and c). It can be seen that MyD88 is expressed throughout the brain including optic lobes, central brain and mushroom bodies. Compared with the expression of *Toll-2* in the adult brain (Figure 4.1 b and d), the expression of *MyD88* and *Toll-2* seem to overlap but are distinct. *Toll-2* is expressed throughout the optic lobes including medulla, lobula plate ad lobula, whereas *MyD88* is also expressed in multiple neuropils in the optic lobes but in fewer cells. Both *Toll-2* and MyD88 are expressed in the central brain including mushroom bodies and the sub-oesophageal ganglion (SOG), but *Toll-2* is more prominently expressed in the mushroom bodies, while *MyD88* is expressed more

pronouncedly in the SOG (Figure 4.1 a and b). These results indicate that *Toll-2* and *MyD88* are expressed in overlapping but distinct patterns.

I further asked which cell types - neurons or glia - express *Toll-2* and *MyD88*. I crossed *Toll-2^{pTV} Gal4* and *MyD88 Gal4* with a nuclear reporter *UAS histone YFP* to visualize cell nuclei. Consistently with what has been shown above, it can be seen that *Toll-2* is expressed massively in Kenyon cells while *MyD88* is expressed in a subset of them (Figure 4.1 e and f). To test whether Toll-2+ and MyD88+ cells are neurons or glia, I carried out double stainings with anti-*ELAV* or anti-*REPO* in Toll-2>histone YFP and MyD88>histone YFP brains (Figure 4.1 g and h). Most of the Toll-2+ cells were Elav+, and none were Repo+, this shows that *Toll-2* is prominently neuronal. MyD88+ cells contained both Elav+ and Repo+ cells. Furthermore, amongst both Toll-2+ and MyD88+ cells, there were large cells that were Elav- and Repo-, which suggests that those cells might be previously undetected progenitor cells.

4.2.2 Loss of *Toll-2* function during development decreased cell number in the pupal central brain

I next studied the function of *Toll-2* in regulating cell number in the pupal brain. Since both *MyD88* and *Toll-2* were expressed in too many cells in the normal brain, the software I used for automatic cell counting in 3D - DeadEasy - was not able to accurately count all the cells in one go in the whole brain. Furthermore, since the Kenyon cells are many and very tightly packed, counting them required scanning at a higher resolution than the MyD88+ central brain cells. Therefore, I counted two parts of the pupal brain separately: the central brain using *MyD88 Gal4* and scanned with a

Figure 4.1 Comparison of *Toll-2* and *MyD88* expression patter in the brain

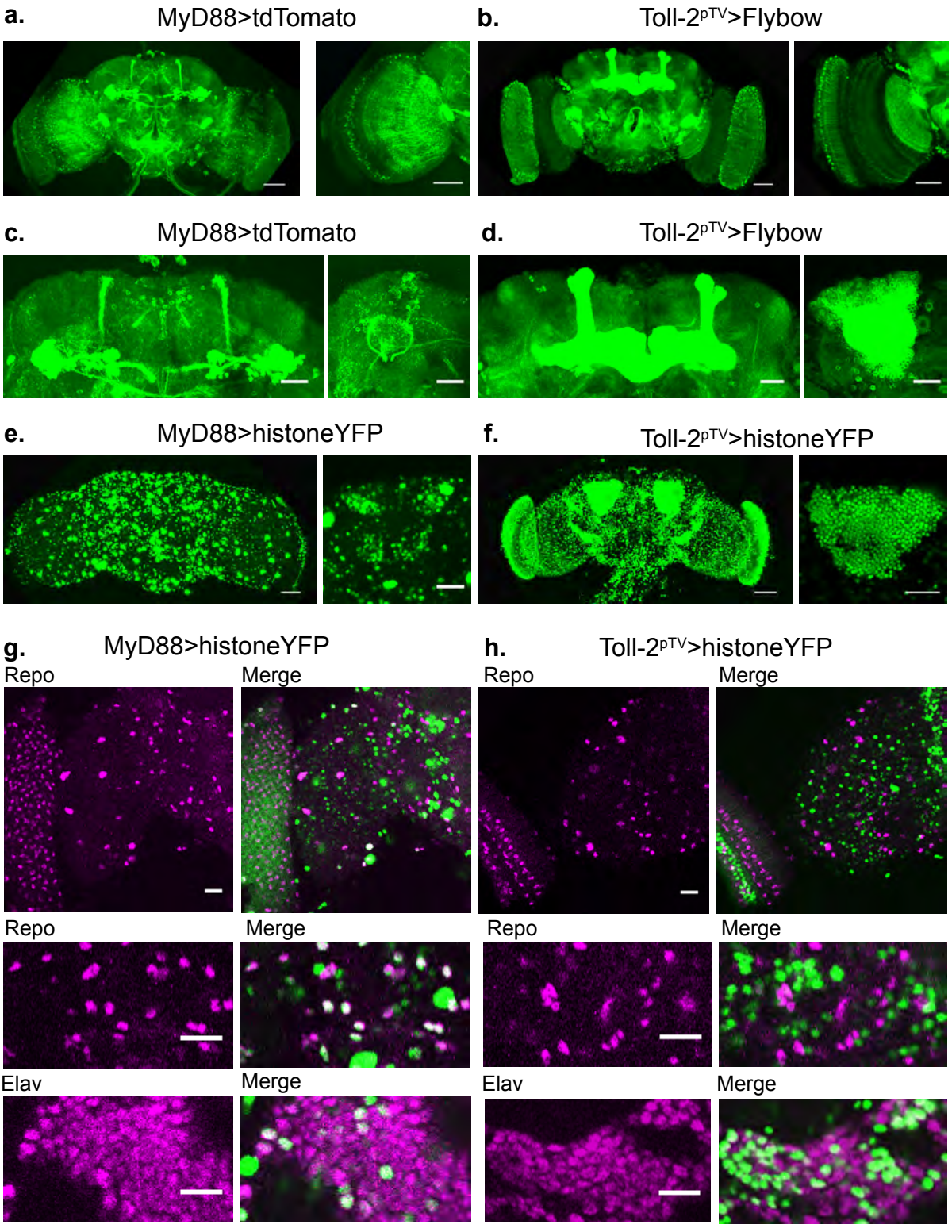


Figure 4.1 Comparison of *Toll-2* and MyD88 expression patter in the brain

a), Expression of MyD88 in adult brain and adult optic lobe.

Genotype: MyD88 Gal4>UAS tdTomato, stained with anti-DsRed, 546

b), Expression of Toll-2 in adult brain and adult optic lobe.

Genotype: Toll-2^{pTV} Gal4> UAS Flybow, endogenous GFP, 488.

c), Expression of MyD88 in adult mushroom bodies and calyx.

Genotype: MyD88 Gal4>UAS tdTomato, stained with anti-DsRed, 546

d), Expression of Toll-2 in adult mushroom bodies and calyx.

Genotype: Toll-2^{pTV} Gal4> UAS Flybow, enodogenous GFP, 488.

e), and f), MyD88 and Toll-2 expressing cells in adult brain and MB.

Genotypes: e),MyD88 Gal4>UAS histone YFP; f), Toll-2^{pTV} Gal4> UAS histone YFP, endogenous YFP, 488.

g), MyD88 expressing cells colocalized with glia and neurons in the adult brain

Genotype: MyD88 Gal4>UAS histone YFP, endogenous YFP, 488; stained with anti-REPO or anti-ELAV, 633.

h), Toll-2 expressing cells colocalized with neurons but not glia.

Genotype: MyD88 Gal4>UAS histone YFP, endogenous YFP, 488;
stained with anti-REPO or anti-ELAV, 633.

Scale bar: a,b,e (whole brain), f (whole brain): 50μm;
c,d,e (MB), f (MB): 25μm; g and h: 15μm.

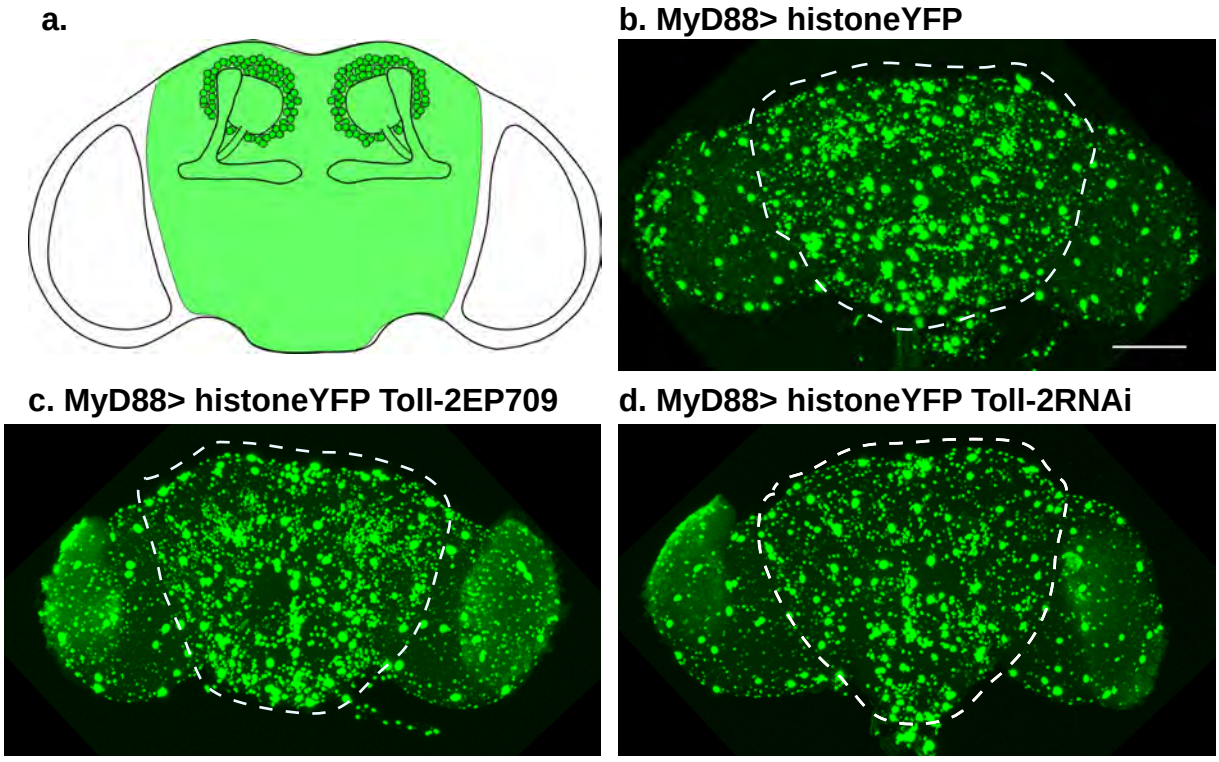
20x objective, and mushroom body Kenyon cells using *Toll-2 Gal4* scanned with a 63X lens objective. I used *UAS histone YFP* to visualize the cell nucleus.

I first studied the function of *Toll-2* on cell number control in the central brain during development (Figure 4.2a). I over-expressed or knocked down *Toll-2* in MyD88 cells using *MyD88>hisYFP,Toll-2EP709* and *MyD88>hisYFP,Toll-2 RNAi* (Figure 4.2b). Then I counted MyD88+ YFP cells in the D4 pupal central brain using the *ImageJ* plug-in *DeadEasy*. The result showed that whereas over-expressing *Toll-2* did not have a significant effect on cell number in the D4 pupal brain, knocking down Toll-2 reduced cell number significantly in the central brain of D4 pupae (Figure 4.2c). This indicates that Toll-2 is required to maintain cell survival during development.

4.2.3 A pulse of *Toll-2* function specifically in pupa stage increased cell number in pupal brain

I then asked whether the cell number decrease in the pupal brain was due to loss of *Toll-2* function during development or specifically during pupa stages. To answer this question, I then tested the function of *Toll-2* in regulating cell number in a narrow time window specifically during pupa stages. To induce gain or loss of *Toll-2* function only at pupal stages, I used *tubulin Gal80^{ts}* to control the expression of *Gal4*. GAL80 is a repressor of GAL4, and the variant GAL80^{ts} works well at 18°C but is inactivated at 30°C. Thus, I bred the flies at 18°C from embryos until D0 pupae, so that *tubulin Gal80^{ts}* would be switched on to suppress the activity of *Gal4*. When puparium formation started (0h APF), I shifted the pupae to 30°C to switch off *tubulin Gal80^{ts}* and switch on *Gal4* to induce gain and loss of Toll-2 function by UAS Toll-2 or UAS Toll-2 RNAi (*MyD88>histone YFP Toll-2^{EP709};tubulinGal80ts* and *MyD88> histone*

Figure 4.2 Loss of *Toll-2* function during development causes cell number decrease in D4 pupal central brain



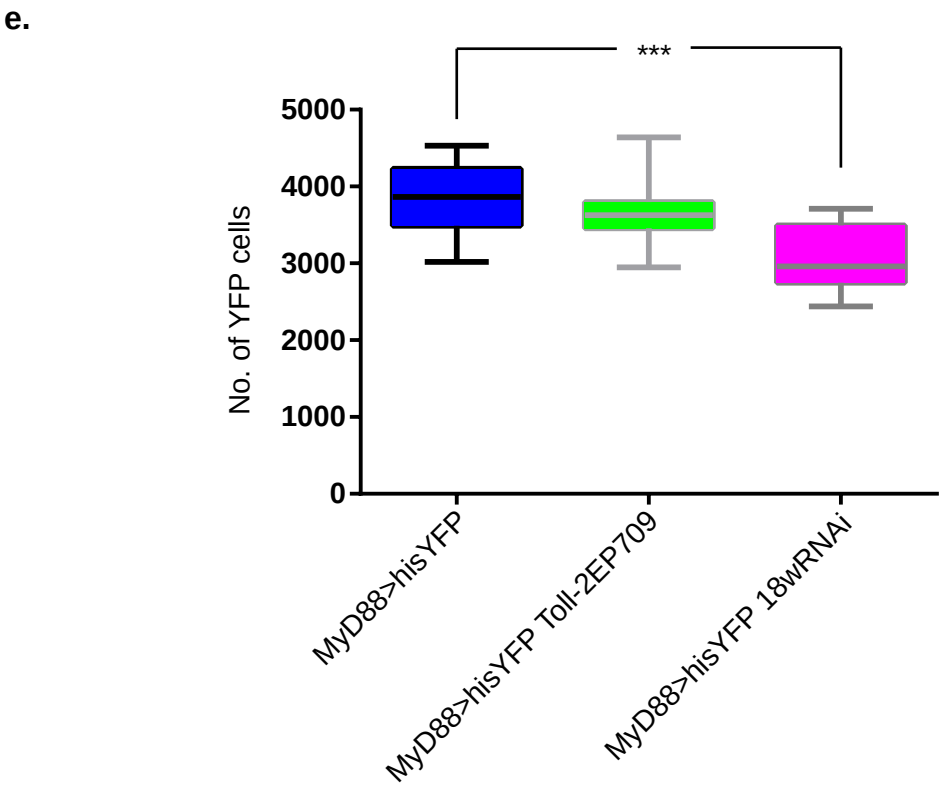


Figure 4.2 Loss of *Toll-2* function during development causes cell loss in D4 pupal central brain

(a). Structural model of the brain, the part labelled in green is central brain analysed in this experiment.

(b) to (d). Expression of MyD88 cells in D4 pupal brain. Central brains (in white circles) were selected as ROIs.

(e). MyD88 cells in central brains are quantified using Deasy. Cell change is not detected in Toll-2 GOF (green bar, N=14) compared with the control (blue bar, N=9). Meanwhile, Toll-2 LOF induced cell decrease of MyD88 cell in D4 pupal central brains (Magenta bar, N=10). One-way ANOVA with post-hoc Dunnett's correction (p=0.0011).

Genotype:
Control: MyD88 Gal4 UAS histone YFP
Toll-2 GOF: MyD88 Gal4 UAS histone YFP/UAS Toll-2
Toll-2 LOF: MyD88 Gal4 UAS histone YFP; UAS Toll-2 RNAi

Scale bar: a to c: 100μm.

YFP;Toll-2 RNAi tubulinGal80ts). After 72 hours, the pupae were dissected and cell number in the pupal central brain was counted (Figure 4.3 a and b). It is shown that gain of *Toll-2* function specifically during pupal stages caused an increase in cell number in the central brain (Figure 4.3 c and d). As in the pupal brain many cells die during metamorphosis, this cell number increase consistently suggests that *Toll-2* is required to maintain cell survival during this period.

However, I also found that loss of *Toll-2* function specifically in pupal stages also increased cell number in the central brain (Figure 4.3 c and d). Considering that neuroblasts undergo proliferation actively in the early pupal brain, the cell number increase might be due to compensatory proliferation, which could be induced by cell loss caused by *Toll-2* loss of function. Importantly, since *Toll-2* loss of function is induced in MyD88 expressing cells and *Toll-2* expression had been shown to overlap with MyD88 cells, my data, most particularly the gain of function phenotype, suggested that *Toll-2* can promote cell survival via MyD88.

4.2.4 *Toll-2* function did not change the number of MB KCs during development

As explained above, I scanned the mushroom body Kenyon cells (MBKCs) separately at higher resolution to ensure the accurate separation of each cell, and I studied whether *Toll-2* is involved in regulating cell number in the MB (Figure 4.4a). To count *Toll-2* cells in the MB, I used *Toll-2^{pTV} Gal4* driving *UAS histone YFP* to visualize the nuclei of *Toll-2* expressing cells. In order to study the function of *Toll-2* during development, I induced *Toll-2* gain and loss of function throughout development and counted *Toll-2*+ cells in MB in D4 pupae (96h APF). Similarly, I

Figure 4.3 A pulse of *Toll-2* function in pupa stage increased cell number in the pupal central brain

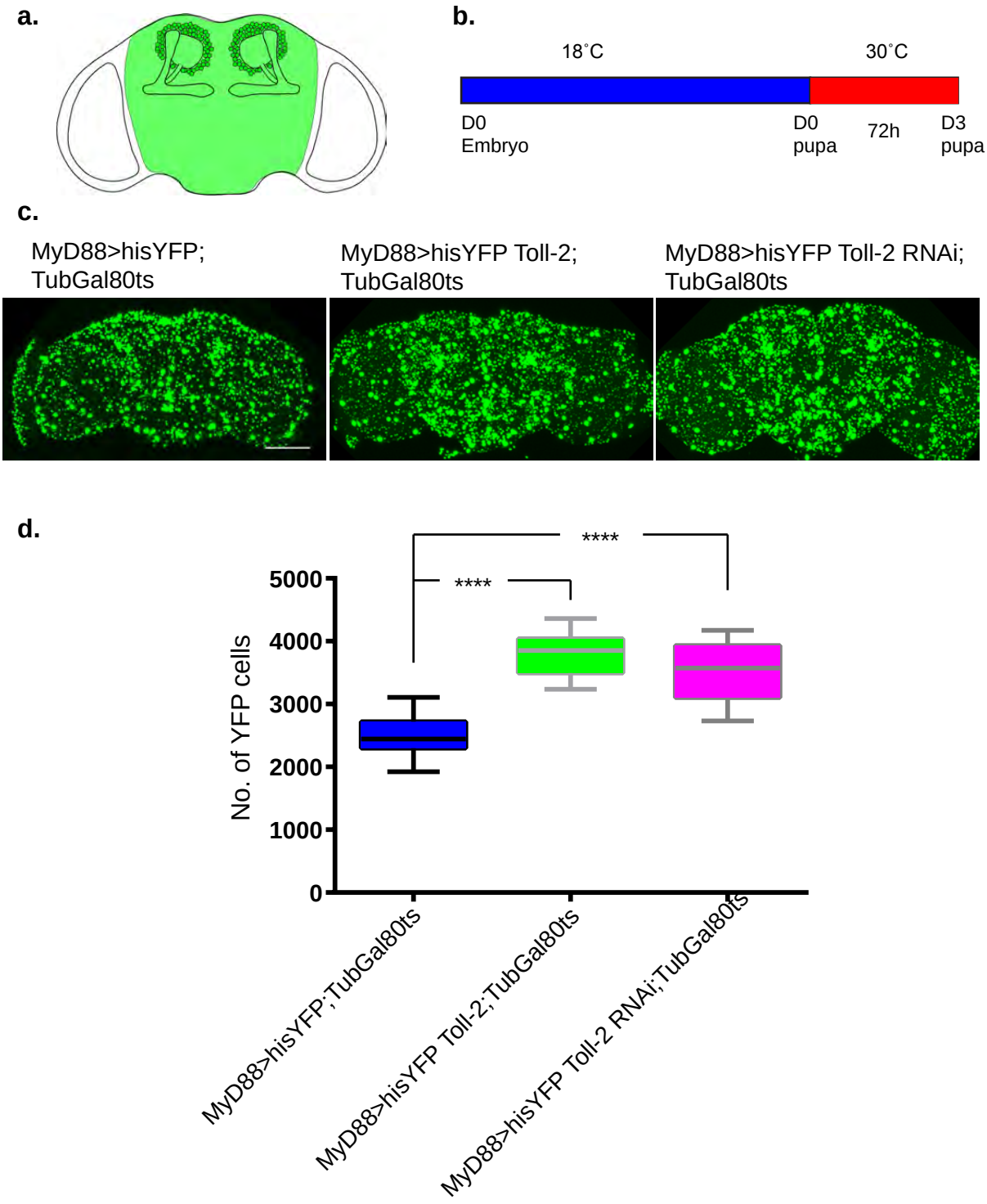


Figure 4.3 A pulse of *Toll-2* function in pupal stage increased cell number in the pupal central brain

(a). Area labelled in green indicates adult central brain analyzed in this experiment

(b). Temperature shifting regime in pupae. Flies were kept at 18˚C (blue) until puparium formation, and shifted to 30˚C (red) for 72 hours. D3 pupae were then dissected

(c). Expression of MyD88 cells in D3 pupal brain. Central brains (in white circles) were selected as ROIs.

(d). MyD88 cells in central brain were quantified. Compared with control (blue bar, N=9), both Toll-2 GOF (green bar, N=14) and LOF (magenta bar, N=13) shows significantly increased cell number. One-way ANOVA with post-hoc Dunnett's multiple comparison, $p<0.0001$.

Genotype:
Control: MyD88 Gal4 UAS histone YFP; tubulin Gal80ts
Toll-2 GOF: MyD88 Gal4 UAS histone YFP/UAS Toll-2; tubulin Gal80ts
Toll-2 LOF: MyD88 Gal4 UAS histone YFP; tubulin Gal80ts/UAS Toll-2 RNAi

Scale bar: 100μm.

Figure 4.4 Gain and loss of *Toll-2* function in regulating *Toll-2* cells in MB during development

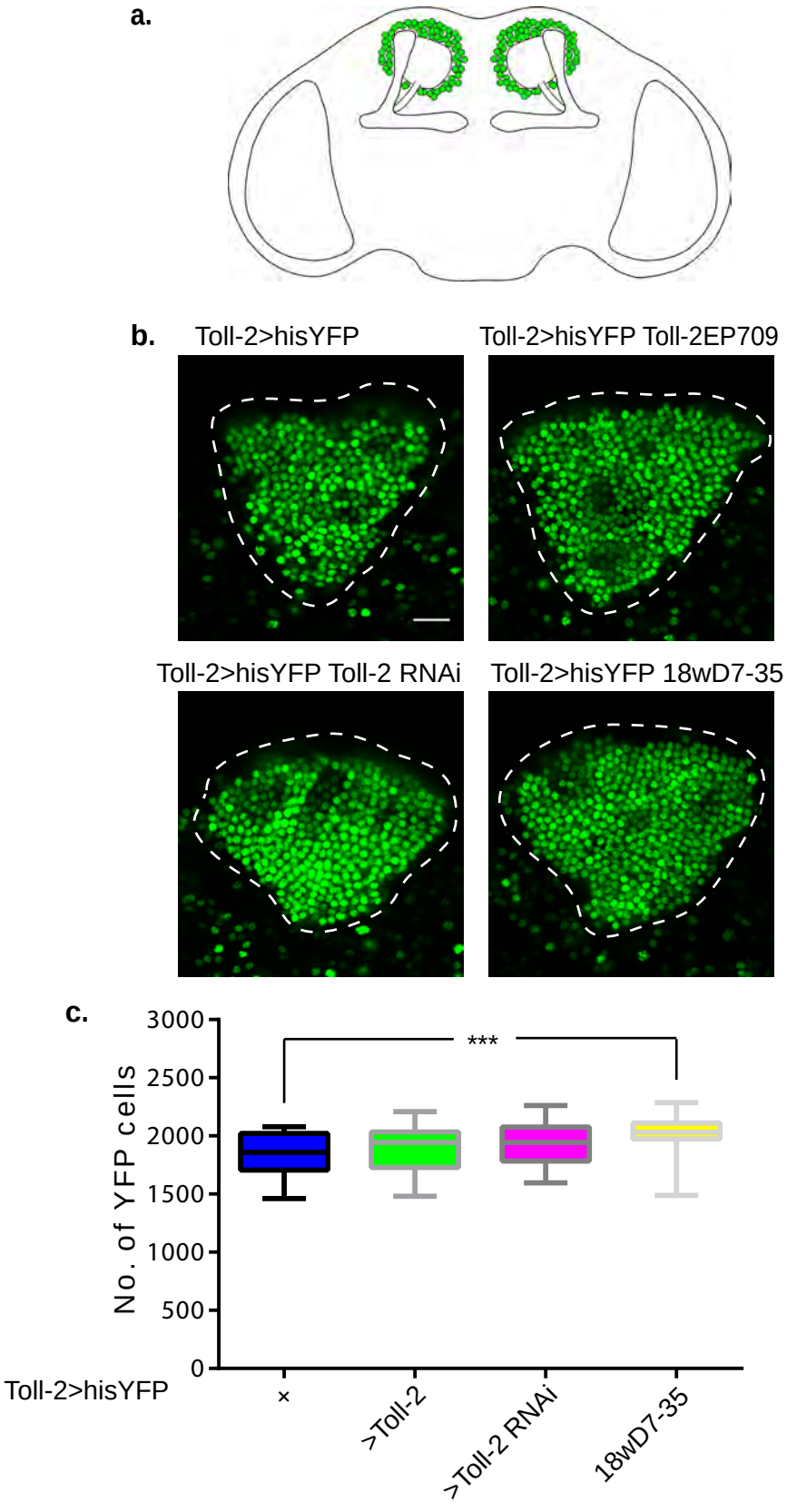


Figure 4.4 Gain and loss of *Toll-2* function in regulating *Toll-2* cells in MB during development

(a), Kenyon cells (KCs) are a cluster of neurons in MB located at the ventral side of the brain, labelled in green.

(b), MB Kenyon cells in D4 pupal brain, ROI labelled in white circles are analysed.

(c), Results of cell number counting by DeadEasy. No significant cell number change was detected in UAS Toll-2 or UAS Toll-2 RNAi, however, Toll-2 mutant 18wD7-35 increased cell number (Kruskal-Wallis test with post-hoc Dunn's correction, **p<0.01 N=15, 20, 13, 28).

Genotypes:

Control: Toll-2 pTV Gal4 UAS histone YFP;

Toll-2 GOF: Toll-2 pTV UAS histone YFP/UAS Toll-2EP709;

Toll-2 LOF: Toll-2 pTV Gal4 UAS histone YFP; UAS Toll-2 RNAi;

Toll-2 pTV Gal4 UAS histone YFP/18wD7-35

Scale bar: 15μm

used *Toll-2^{pTV} Gal4* driving *UAS Toll-2^{EP709}* and *UAS Toll-2 RNAi* for *Toll-2* gain and loss of function, respectively. Moreover, since *Toll-2^{pTV} Gal4* is also a mutant allele, I crossed it with a *Toll-2* null allele, *18w$^{\Delta 7\text{-}35}$*, to generate a *Toll-2* loss of function trans-heterozygous mutant genotypes (Figure 4.4b). The result shows that gain or loss of *Toll-2* function by UAS Toll-2 or UAS Toll-2 RNAi during development did not significantly change cell number in the MB (Figure 4.4c). However, loss of *Toll-2* function in Toll-2^{pTVGAL4} /Toll-2$^{18w\Delta 7\text{-}35}$ trans-heterozygotes increased MB cell number significantly.

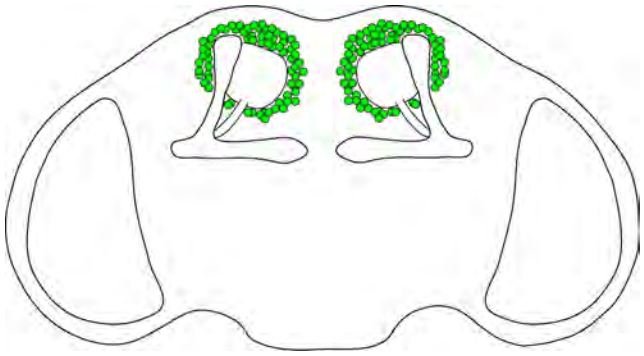
However, as mentioned above, *Toll-2^{pTV} Gal4* is a mutant allele. Thus, *Toll-2^{pTV} Gal4* driving *UAS Toll-2^{EP709}* might not be truly gain of function, but rather closer to a rescue. To further test the effect of *Toll-2* over-expression, I also tested another mushroom body driver *MB Gal4* to induce *Toll-2* gain of function throughout development (Figure 4.5 a and b). I counted the MB cell number in D4 pupae and the result shows that over-expression of *Toll-2* throughout development did not change cell number significantly in the pupal brain (Figure 4.5 c and d).

4.2.5 Pulse of *Toll-2* function specifically in pupal stages did not significantly change MB cell number

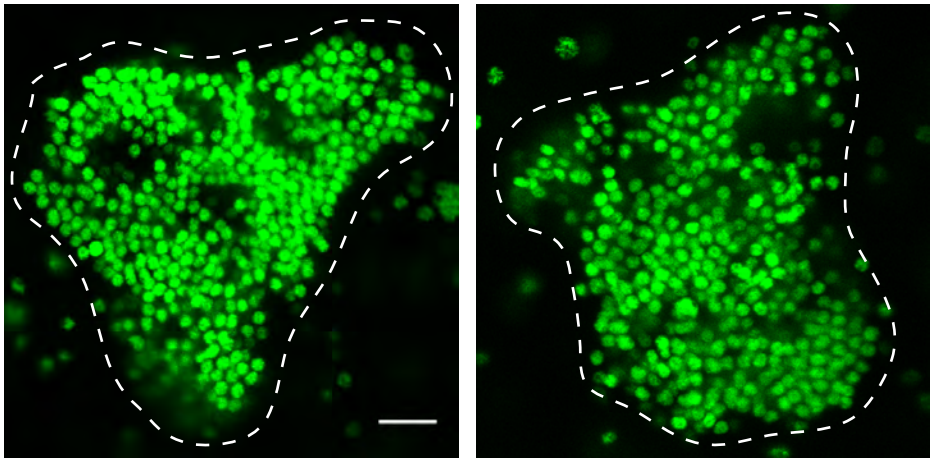
In the two previous experiments, *Toll-2* gain and loss of function was induced throughout development. The long-time window might allow mushroom bodies to compensate the potential effect caused by manipulating *Toll-2* function. In order to study the function of *Toll-2* in a narrow time window, such as during metamorphosis in pupal stages, I used *tubulin Gal80^{ts}* to induce gain and loss of *Toll-2* function specifically in pupa and counted the MB cell number in D3 pupae (72h APF) (Figure

Figure 4.5 Gain of *Toll-2* function during development did not change the MB cell number significantly in D4 pupal brain

a.



b. MB>histoneYFP MB>histoneYFP Toll-2 attP2



c.

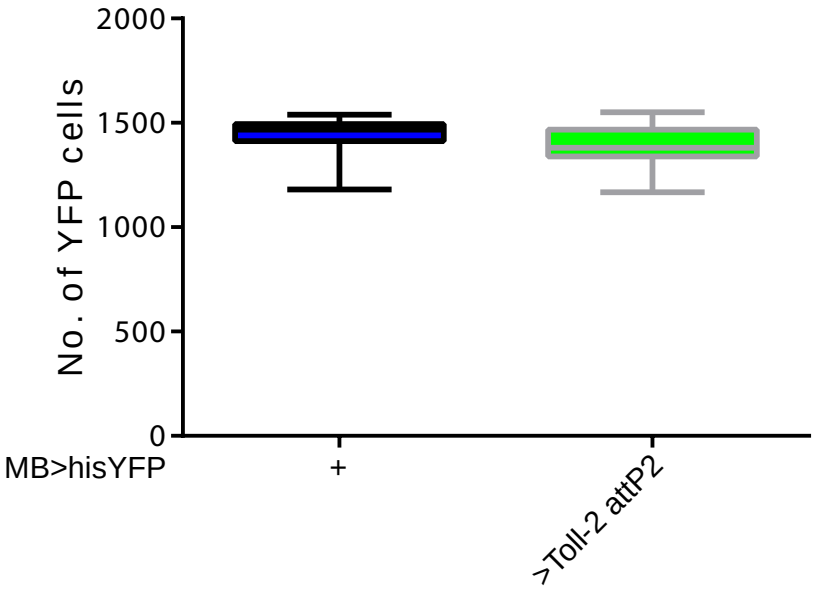


Figure 4.5 Gain of *Toll-2* function during development did not change the MB cell number significantly in D4 pupal brain

(a), Kenyon cells (KCs) in MB labelled in green.

(b), KCs expressed by UAS histone YFP driven by MB Gal4 in control and Toll-2 GOF. Regions labelled in white circles were analyzed by Deadeasy.

(c). KCs in both control and Toll-2 GOF were quantified using Deadeasy. No significant cell number change was detected. Mann-Whitney test, p= 0.11, N=13.

Genotype:

Control: MB Gal4/UAS histone YFP

Toll-2 GOF: MB Gal4 UAS/histone YFP;UAS Toll-2 attP2

Scale bar: 15μm

Figure 4.6 Gain and loss of *Toll-2* function specifically in pupae did not change Toll-2 cell number in D3 pupal MB

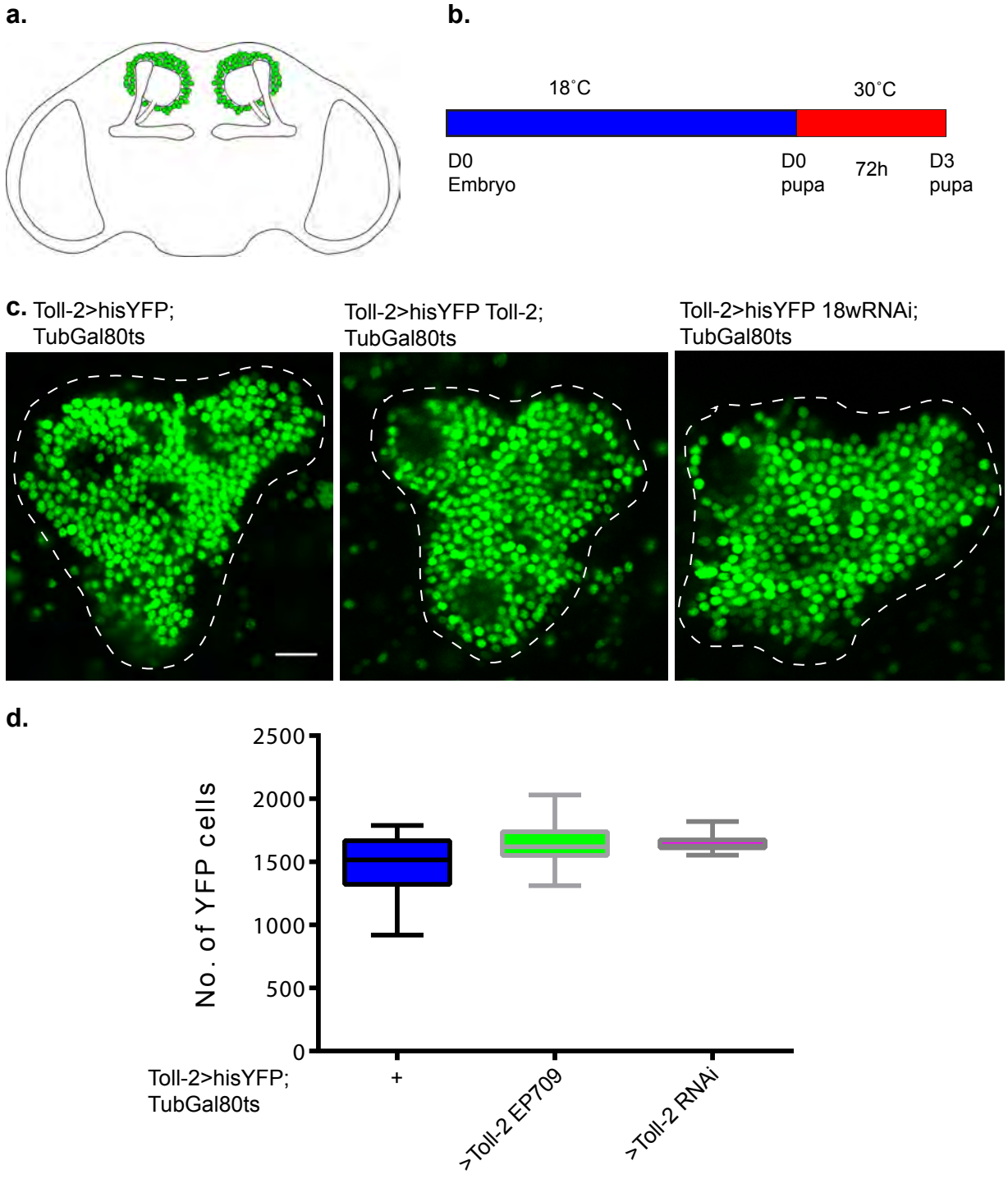


Figure 4.6 Gain and loss of *Toll-2* function specifically in pupae did not change *Toll-2* cell number in D3 pupal MB

a), Kenyon cells (KCs) in MB labelled in green.

b), Temperature shifting regime in pupae. Flies were kept at 18˚C (blue) until puparium formation, and shifted to 30˚C (red) for 72 hours. D3 pupae were then dissected.

c), MB Kenyon cells in control, *Toll-2* GOF and LOF.

d), No significant cell number change was detected when overexpressing or knocking down *Toll-2* specifically in pupae. Kruskal-Wallis test with post-Dunn's multiple comparison, p=0.0936, N=17,17,15.

Genotypes:

Control: Toll-2^{pTV} Gal4 UAS histone YFP; Tubulin Gal80ts

Toll-2 GOF: Toll-2^{pTV} UAS histone YFP/UAS Toll-2EP709; Tubulin Gal80ts

Toll-2 LOF: Toll-2^{pTV} Gal4 UAS histone YFP; UAS Toll-2 RNAi/TubulinGal80ts

Scale bar: 15μm

4.6d). Again, the result showed that gain or loss of *Toll-2* function specifically in pupa stage did not significantly change MB cell number. Altogether, my data suggest that cell number plasticity in the mushroom body during development might be more robust that in other brain domains.

4.3 Discussion

In this chapter, I have shown that *MyD88* is pronouncedly expressed in the brain and *MyD88* and *Toll-2* showed overlapping but distinct expression patterns. Moreover, both *Toll-2* and *MyD88* expressing cells contained Elav- and Repo- cells suggesting that there might be expressed in progenitor cells that had not been detected before. I also showed that *Toll-2* is required to maintain cell survival in the pupal central brain during development. Evidence was also provided that cell number plasticity in the MB is more robust during development and change of *Toll-2* function was not enough to change MB Kenyon cell number.

The expression of *Toll-2* and *MyD88* overlapped in some cells in the brain, including optic lobes, central brain and mushroom bodies. This indirectly suggests that in the cells expressing both *Toll-2* and *MyD88*, *Toll-2* might function through *MyD88* signalling pathways. There are also many cells that express either *Toll-2* or *MyD88*. For example, *Toll-2* is expressed massively in mushroom body Kenyon cells and neurons in the optic lobes, while *MyD88* is expressed only in a subset of cells in these two regions. This suggests that in cells that do not express *MyD88*, *Toll-2* might function through other signalling pathways that are independent from *MyD88*.

I have also shown that *Toll-2* is mainly neuronal and *MyD88* is expressed in both neurons and glia. Intriguingly, in both *Toll-2* and *MyD88* expressing cells, there are

large cells that show neither neuronal nor glial markers. This suggests that they could be either polyploid cells or progenitor cells in the brain.

In order to investigate cell number change, multiple brain domains were analysed separately. Firstly, it was known that plasticity of different cell types might be differ (Lin et al., 2013). Secondly, there are so many cells in the brain that I could not count all of them in single scans, therefore, I used *Toll-2 Gal4* to analyse cells in the mushroom bodies and optic lobes (See Chapter 5 and 6), and *MyD88 Gal4* to analyse cells in the central brain.

I have consistently shown that *Toll-2* is required to maintain cell survival during development and specifically in pupal stages. Moreover, since knocking down *Toll-2* RNAi reduced cell number in the MyD88+ cells, this further indicates that *Toll-2* could promote cell survival via *MyD88* signalling pathway, which is further consistent with the overlapping expression pattern of *Toll-2* and *MyD88*.

However, I also found that loss of *Toll-2* function increased cell number, which could be explained as due to a compensatory effect in response to the cell loss caused by *Toll-2* loss of function in the pupal brain. In fact, the large MyD88+ Elav- Repo- cells might be progenitor cells that are able to proliferate. However, further tests need to be carried out to verify whether there was compensatory proliferation induced by loss of *Toll-2* function and whether *MyD88* is expressed in progenitor cells.

I have also investigated cell number plasticity during development in the pupal mushroom bodies. My data indicates that cell number plasticity is more robust in the MB since neither gain nor loss of *Toll-2* function changed MB cell number significantly. It is still unclear why knocking down *Toll-2* in $Toll\text{-}2^{PTV}GAL4^{/}/18w^{\Delta 7\text{-}35}$

transheterozygotes during development increased mushroom body cell number. The sample size of this genotype was much higher than for the others (N=28 vs.13-20). Therefore, I would firstly increase the sample size of other genotypes and check whether as a result, the phenotypic differences across the genotypes (Figure 4.4) become more pronounced or disappear.

In the next chapter, I will investigate cell number plasticity in the adult brain and whether *Toll-2* is involved.

Chapter 5

Regulation of cell number by *Toll-2* in adult brain: brain structural plasticity

5.1 Introduction

Evidence has shown that structural plasticity occurs in the *Drosophila* brain. Breeding flies in constant darkness or constant light could either decrease or increase brain volume, respectively (Barth et al., 1997, Barth, 1999, Barth and Heisenberg, 1997). Moreover, fly population density and gender of flies in the vial were both found to change brain volume of adult flies (Technau, 1984, Heisenberg et al., 1995). Changes in fibre number correlated to brain volume changes (Barth and Heisenberg, 1997, Technau, 1984), but cell number changes are linked, has not been studied. Therefore, the aim of this chapter is to study whether cell number is plastic in *Drosophila* adult brains and whether *Toll-2* is involved in the regulation.

Changes of the brain are prominent during the critical period spanning from eclosion until Day 5 adult. Brain changes in this time period correlate with environmental adaption (Barth and Heisenberg, 1997). I therefore studied the function of *Toll-2* in the adult brain both during development and specifically at the critical period. To study cell number plasticity in the adult brain during development, I induced *Toll-2* gain and loss of function throughout development and tested cell number changes in the adult. Moreover, to study cell number plasticity during the critical period, I over-expressed or downregulated *Toll-2* specifically during the critical period in the adult stage.

Multiple brain domains have been found to be plastic, such as medulla, central complex and mushroom bodies (Fernandez-Hernandez et al., 2013, Barth and Heisenberg, 1997) I focused on the central brain and MB Kenyon cells to study cell number plasticity during pupal stages. During pupal stages, the lamina is tightly attached to the brain, and since *Toll-2* is expressed both in lamina and medulla, this made it difficult to count cells in the optic lobe. Therefore, cell number regulation in pupal optic lobes was not tested in the previous chapter. In the adult brain, however, the lamina is attached less tightly to the optic lobe. Therefore, I could separate the retina and lamina from the rest of the optic lobes. This made cell counting easier in adult brain optic lobes. In this chapter, apart from central brain and MB, optic lobes were also used to investigate cell number plasticity and regulation in the adult brain.

As shown in Chapter 3, I found that loss of *Toll-2* function decreased longevity in adult flies, suggesting that *Toll-2* is required to maintain survival of adult flies as they age. However, how *Toll-2* is involved in this phenotype and whether cell number changes during ageing is not known. Therefore, in this chapter, I also studied whether cell number changes during ageing and whether *Toll-2* is involved in the regulation.

5.2 Results

5.2.1 *Toll-2* is involved in regulating cell number in the central brain in adult flies

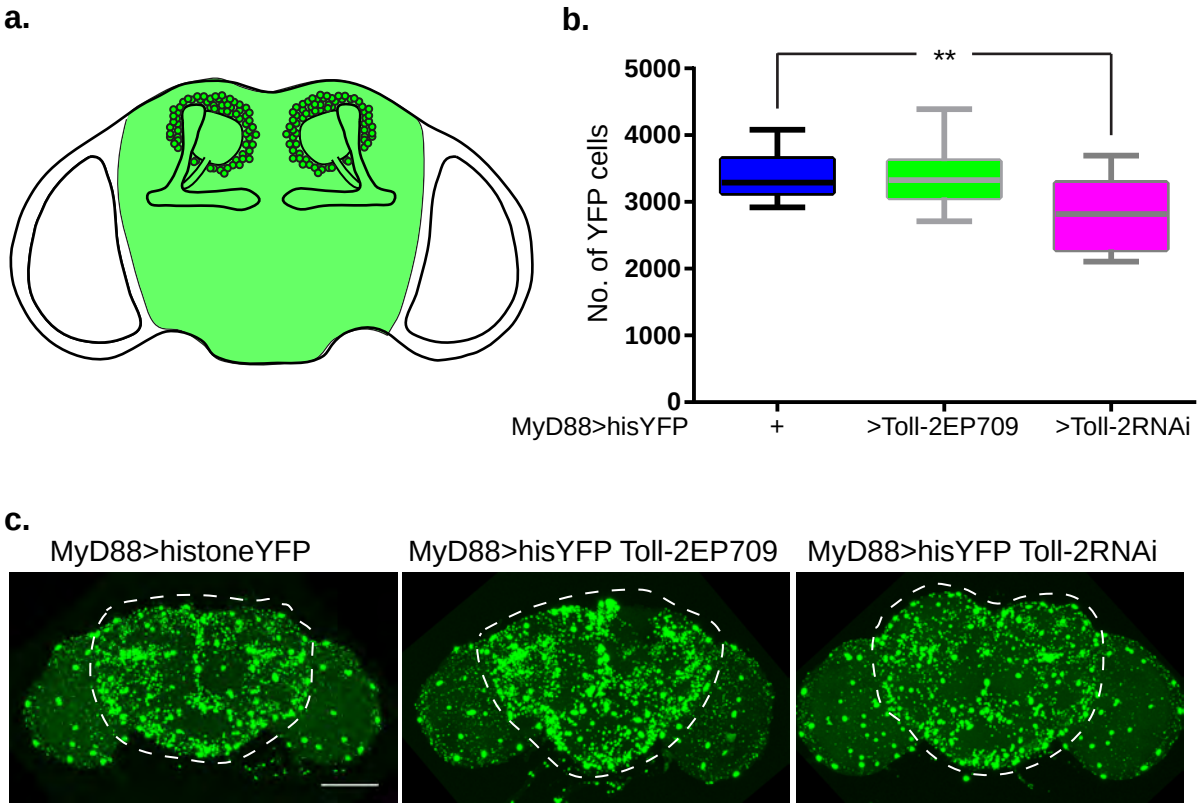
To ask whether cell number in the adult brain is plastic and whether *Toll-2* is involved in the regulation of cell number, I tested whether altering *Toll-2* function through development changed cell number by adult day 3 (Figure 5.1a). As in the previous

chapter, since *Toll-2* is widely expressed in the whole brain, and Kenyon cells are very tightly packed, it was not possible to count all cells in the brain with single scans. Therefore, multiple brain domains were studied separately: central brain, MB KCs and medulla. To count cells in central brain, I used *MyD88 Gal4* driving *UAS histone YFP* so that I could visualize all the nuclei of *MyD88*+ cells (Figure 5.1a). To alter the activity of *Toll-2*, I used *UAS Toll-2*^{EP709} for gain of function and *UAS Toll-2 RNAi* for loss of function. Cells in the central brain were counted with *DeadEasy* software, like in the previous chapter, and analysed (Figure 5.1c). I found that whereas no effect was detected in *Toll-2* gain of function flies, knocking down *Toll-2* through development decreased cell number by adult day 3. These data show that *Toll-2* is not pro-apoptotic and instead it is required to maintain cell survival in adult brain.

5.2.2 Gain or loss of *Toll-2* function during development did not affect MB Kenyon cell number in the adult brain

I next asked whether cell number in MB is plastic in the adult (Figure 5.2a). To address this question, I looked at whether altering *Toll-2* expression through development would change *Toll-2* cell number in adult MB. I used *UAS Toll-2*^{EP709} to overexpress *Toll-2*, and *Toll-2 RNAi* to knock down *Toll-2* (Figure 5.2b). Since the *Toll-2*^{pTV} *Gal4* is a Toll-2 mutant allele, I also used trans-heterozygous flies of genotype *Toll-2*^{pTV}*/18w*$^{\Delta 7\text{-}35}$ for loss of *Toll-2* function (Figure 5.2b). I then counted the KCs, whose projections form the MB (Figure 5.2a). The quantification showed that neither gain nor loss of *Toll-2* function throughout development affects MB Kenyon cells by day 3 adult (Figure 5.3c). This data suggests that cell number in the MB may not be plastic.

Figure 5.1 Loss of *Toll-2* function causes cell loss in D3 adult central brain



(a). Area labelled in green indicates central brain, which is the region of interest (ROI) indicated in (c).

(b). Quantification of cell number using Deadeasy.

Compared with control, gain of *Toll-2* function does not caused a significantly diffrent cell number count, while loss of *Toll-2* function causes significant decrease in the cell number in the central brain. One-way ANOVA , p=0.001, Dunnett's multiple comparison, **p<0.01, N=18, 20, 17.

(c). D3 adult brains from three genotypes, ROI indicated in white circles were analysed. Genotypes:

Control: MyD88 Gal4/UAS histone YFP

Toll-2 GOF: MyD88 Gal4 UAS histone YFP/UAS Toll-2EP709

Toll-2 LOF: MyD88 Gal4 UAS histone YFP; UAS Toll-2 RNAi

Scale bar: 100μm

Figure 5.2 Gain or loss of *Toll-2* function did not affect MB Kenyon cell number in D3 adult brain

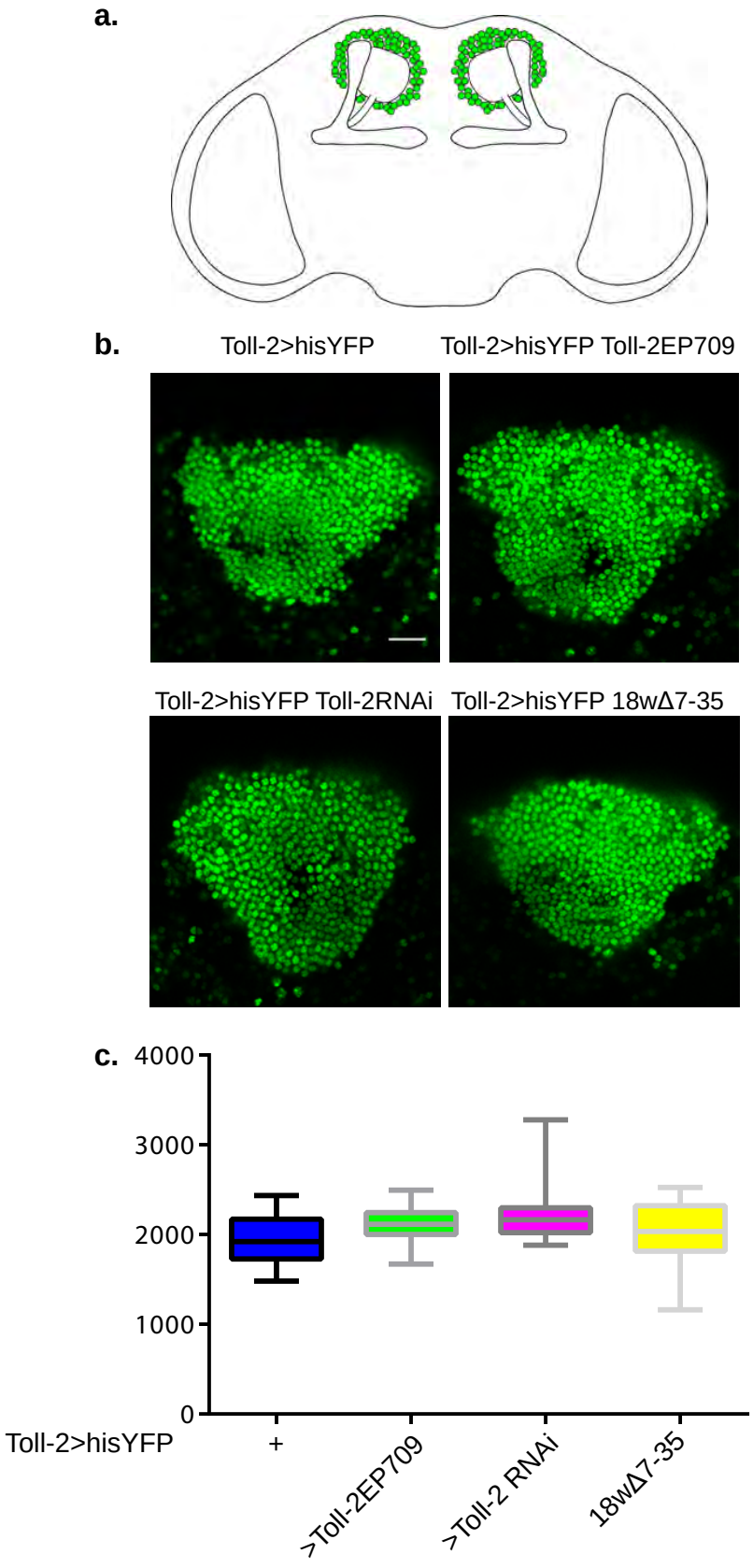


Figure 5.2 Gain or loss of *Toll-2* function did not affect MB Kenyon cell number in D3 adult brain

(a). Cells labelled in green indicate MB Kenyon cells analysed in this experiment.

(b).*Toll-2* expressing cells in MB in Day 3 adult brain.

(c). Quantificatoin using DeadEasy. Compared with the control, neither gain nor loss of *Toll-2* function caused significant cell number changes.

Kruskal-Wallis test, p=0.2161, Dunn's multiple comparrson, p>0.05, N=13, 16, 11, 12.

Genotype:

Control: Toll-2^{pTV} Gal4/UAS histone YFP

Toll-2 GOF: Toll-2^{pTV} Gal4 UAS histone YFP/UAS Toll-2EP709

Toll-2 LOF: Toll-2^{pTV} Gal4 UAS histone YFP;UAS Toll-2 RNAi

and: Toll-2^{pTV} Gal4 UAS histone YFP/18wΔ7-35

Scale bar: 15μm

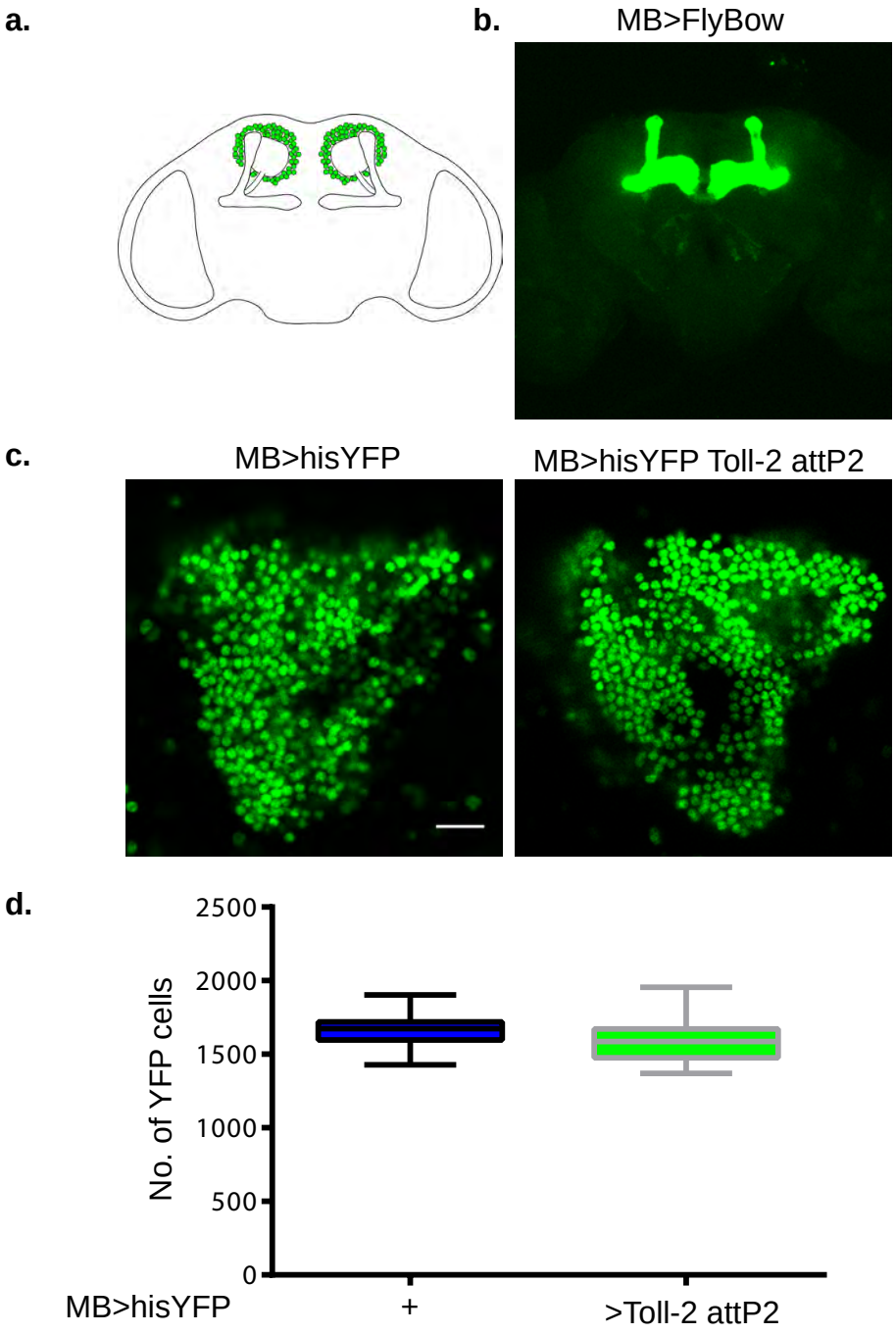
As discussed in Chapter 4.3, *Toll-2^{pTV} Gal4* is also a *Toll-2* loss of function allele. Therefore, when using this allele to overexpress *Toll-2*, it was difficult to determine whether *Toll-2^{pTV}Gal4>UAS Toll-2* was truly a gain of function for *Toll-2*. To further study the effect of *Toll-2* gain of function, I used a different *MB Gal4* line which drives expression independently of *Toll-2* (Figure 5.3 a and b). I used *UAS histone YFP* to visualize MB KCs (Figure 5.3c) and *UAS Toll-2^{attP2}* to overexpress *Toll-2*. Then the number of MB KCs in both control and *Toll-2* gain of function was quantified (Figure 5.4d). The result showed that gain of *Toll-2* through development did not affect MB KC number by day 3 adult. This result further suggests that cell number of MB KC might be more robust and less plastic than in other brain domains.

5.2.3 Conditional gain of *Toll-2* function during the adult critical period increased cell number in the medulla

Since the cell loss shown above was the result of knocking down *Toll-2* throughout development, this phenotype could correspond to the loss of *Toll-2* in earlier development stages rather than an adult specific function. Therefore, I then investigated whether *Toll-2* is required specifically in the adult brain. I focused in the adult critical period, when the brain has been shown to be particularly plastic (Barth et al., 1997). Since it is difficult to count all the cells in the brain, I studied cell number in three different brain domains respectively in medulla, central brain and MB Kenyon cells.

The medulla was found to be a plastic region in the brain (Fernandez-Hernandez et al., 2013). Therefore, I studied whether cell number in the optic lobe is plastic and whether *Toll-2* is involved in cell number regulation. To visualize cells in the medulla,

Figure 5.3 Gain of *Toll-2* function during development causes no effect on MB cell number in D3 adult brain



(a). Cells labelled in green indicate MB Kenyon cells analysed in this experiment.

(b). Expression pattern of MB Gal4 driving UAS Flybow.

(c). MB Kenyon cells in two genotypes. Control: MB Gal4/UAS histone YFP

Toll-2 GOF: MB Gal4/UAS histone YFP; UAS Toll-2 attP2.

(d). Quantification with DeadEasy, no significant difference was detected,

t-test, p=0.1708, N=15, 21. Scale bar: 15μm.

I used *Toll-2^{pTV} Gal4* driving *UAS histone YFP* to see the nuclei of *Toll-2*+ cells (Figure 5.4 a and c). To induce *Toll-2* gain and loss of function, I used *UAS Toll-2EP709* and *UAS Toll-2 RNAi*, respectively (Figure 5.4c). To alter the expression of *Toll-2* specifically at the adult critical period, I used *tubulinGal80ts* to control *Gal4* expression. *tubulinGal80ts* inhibits Gal4 at 18˚C but is inactive at 30˚C. I kept the flies at 18˚C until 96h (4 days) after eclosion and shifted them to 30˚C for 6 hours to switch off *tubGal80ts* and switch on *Gal4*, followed by a shift to 25˚C for 24 hours to give cells time to respond to the alteration in *Toll-2* level (Figure 5.4b). In this way, *Toll-2* gain and loss of function was induced specifically in a 6-hour time window at the adult critical period. This regime also enabled me to count accurately a subset of Toll-2+ cells in the medulla. In fact, since *Toll-2* is widely expressed in the adult brain, when flies were bred at the normal 25°C temperature in the absence of GAL80, I was not able to count all the Toll-2+ cells in the optic lobe. By applying the above regime, I could visualize a subset of *Toll-2*+ cells, which made cell counting possible. I then counted *Toll-2* cells in adult medulla using *DeadEasy*. While no significant change was detected in loss of *Toll-2* function, cell number in the medulla was significantly increased when over-expressing *Toll-2* (Figure 5.4d). This result firstly suggests that cell number is plastic in adult critical period. Moreover, the cell number increase suggests that *Toll-2* can promote either cell survival or cell proliferation in the medulla at the adult critical period.

5.2.4 Conditional gain and loss of *Toll-2* function during the critical period increased cell number in the adult central brain

I next studied whether *Toll-2* is involved in regulating cell number in the central brain specifically in the adult stage (Figure 5.5a). To visualize cells in the adult central

brain, I used *MyD88 Gal4* driving *UAS histone YFP.* To induce *Toll-2* gain or loss of function, I used *UAS Toll-2EP709* and *UAS Toll-2 RNAi*. Similarly, I used tubulinGal80^{ts} to induce gain or loss of *Toll-2* function specifically at the adult critical period. I bred the flies at 18˚C during development, and shifted them to 30˚C after eclosion, to switch on Gal4. Gal4 drove overexpression or RNAi-knockdown of *Toll-2* from adult day 0 for 48 hours and brains were fixed and analysed at adult day 2 (Figure 5.5b and c). The number of cells in central brains were quantified using *DeadEasy*. The result shows that when *Toll-2* function was altered, cell number increased both in gain and loss of function genotypes (Figure 5.5d). The increase in cell number caused by *Toll-2* gain of function was consistent with what has been observed in medulla suggesting that *Toll-2* may be required to maintain cell survival or promote cell proliferation in the adult central brain. On the other hand, the increased cell number in *Toll-2* loss of function flies cannot be explained by a pro-apoptotic function of *Toll-2*, as over-expression of *Toll-2* does not cause cell loss, but instead suggests that cell death due to *Toll-2* loss of function may induce compensatory proliferation.

5.2.5 Conditional alteration of *Toll-2* function during the adult critical period did not affect MB cell number

I next tested the function of *Toll-2* in the MB restricted to the adult critical period (Figure 5.6a). To do this, I used *tubulinGal80ts* to control the activity of Toll-2^{pTV} Gal4 using the same temperature shift regime as in the central brain (Figure 5.6b). I used *UAS Toll-2^{EP709}* and *UAS 18wRNAi* to induce Toll-2 gain and loss of function, respectively (Figure 5.6c). From the quantification and statistical analysis (Figure 5.6d), it can be seen that cell number in adult MB was not affected by either gain or

Figure 5.4 Gain of *Toll-2* function at the adult critical period only increased cell number in adult medulla

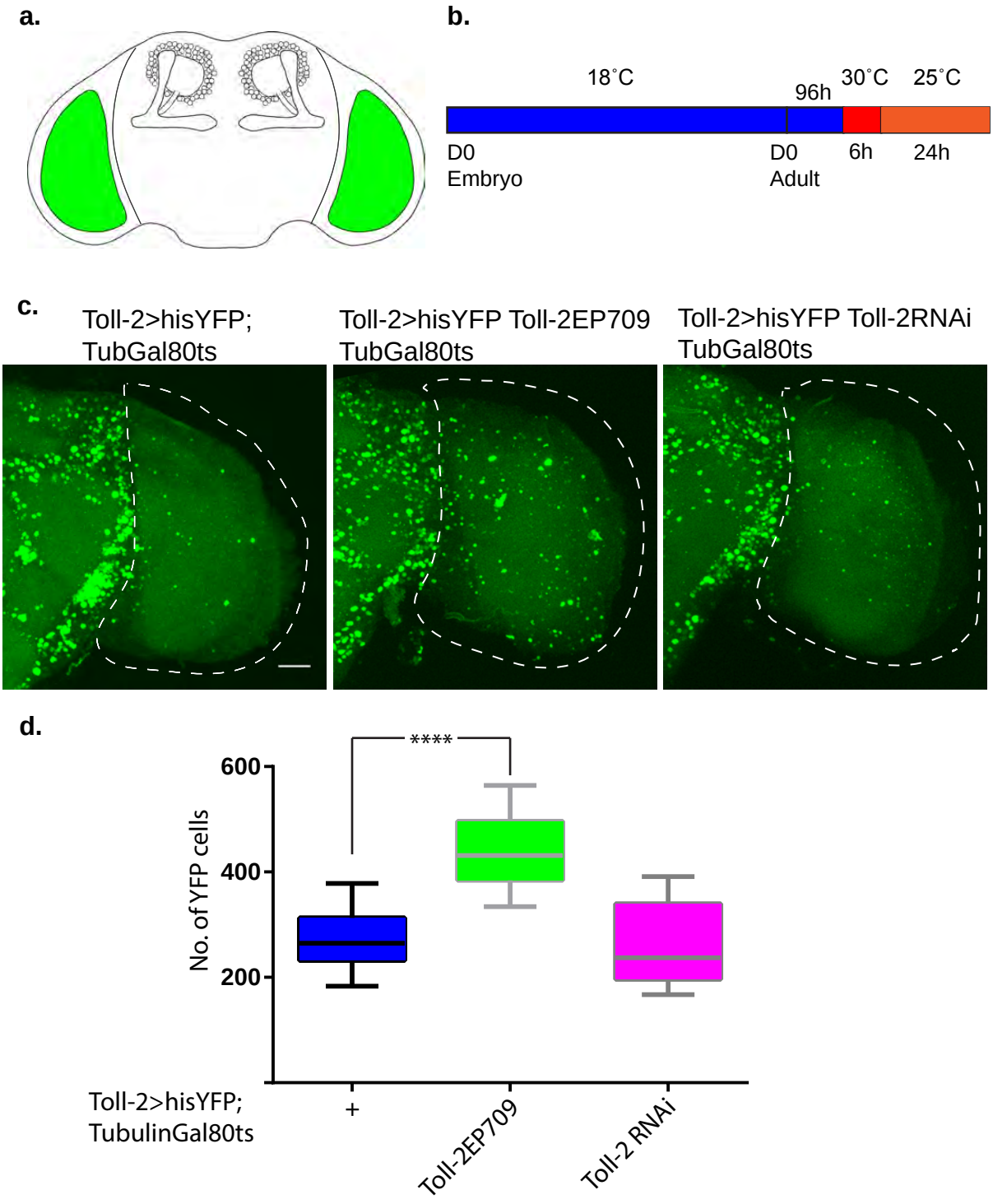


Figure 5.4 Gain of *Toll-2* function at the adult critical period only increased cell number in adult medulla

(a). Area labelled in green indicates medulla, the ROI analysed in this experiment

(b). Temperature shifting regime for medulla cell counting in adult brain. Flies were kept at 18˚C (blue) until 4 days after eclosion, and shifted to 30˚C (red) for 6 hours, then shifted to 25˚C (Orange) for 24h to recover. Adult flies were then dissected and analysed.

(c). *Toll-2* expressing cells in adult medulla in each genotype.

Control: Toll-2^{pTV} Gal4 UAS histone YFP; TubulinGa80ts

Toll-2 GOF: Toll-2^{pTV} Gal4 UAS histone YFP/ UAS Toll-2 EP709; TubulinGa80ts

Toll-2 LOF: Toll-2^{pTV} Gal4 UAS histone YFP; UAS Toll-2 RNAi/TubulinGa80ts

(d). Cell number quantification using DeadEasy.

Gain of *Toll-2* function specifically in adult stage increase the cell number in medulla

One-Way ANOVA, $p<0.0001$, Dunnett's multiple comparison, ****$p<0.0001$,

N=10, 13, 14.

Scale bar: 25μm.

Figure 5.5 Alteration of *Toll-2* function at the critical period only changes cell number in the adult central brain

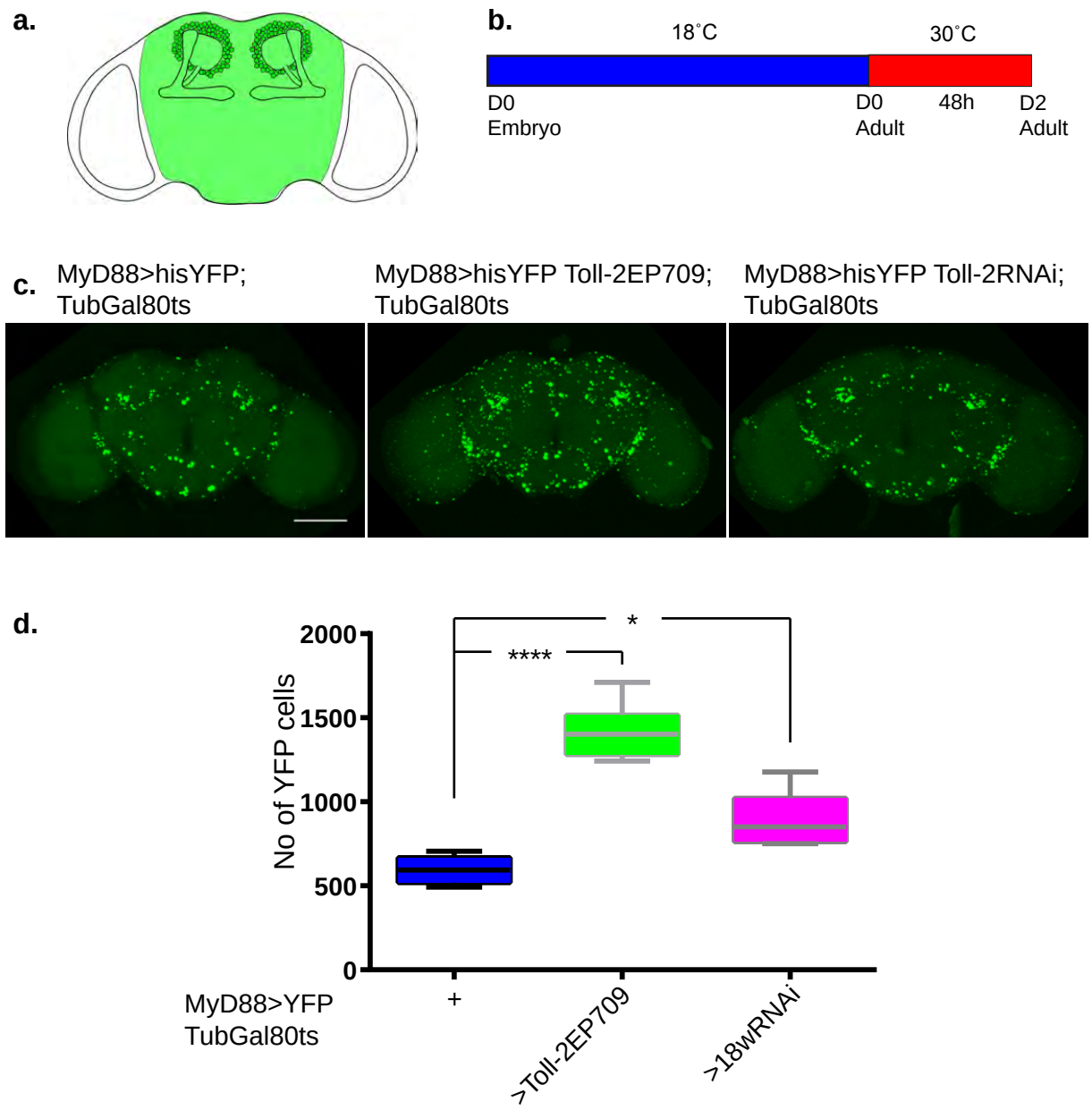


Figure 5.5 Alteration of *Toll-2* function at the critical period only changes cell number in the adult central brain

(a). Area labelled in green indicates adult central brain analysed in this experiment.

(b). Temperature shifting regime in adult. Flies were kept at 18˚C (blue) until eclosion, and shifted to 30˚C (red) for 48 hours. Brains are fixed and analysed at D2.

(c). MyD88 expressing cells in adult central brain in each genotype

Control: MyD88 Gal4 UAS histone YFP; TubulinGal80ts

Toll-2 GOF: MyD88 Gal4 UAS histone YFP/ UAS Toll-2 EP709; TubulinGal80ts

Toll-2 LOF: MyD88 Gal4 UAS histone YFP/ UAS Toll-2 RNAi; TubulinGal80ts

(d). Cell number quantification using DeadEasy. Compared with the control, both gain and loss of *Toll-2* function causes significant increase of cell number in D2 adult central brain. Kruskal-Wallis test, $p<0.0001$, Dunn's multiple comparison, *$p=0.0278$, ****$p<0.0001$, N=10, 11, 10.

Scale bar: 100μm

loss of *Toll*-2 function in the adult critical period. This result suggests that cell number plasticity in MBs is more robust and alteration of *Toll-2* function alone might not be able to affect MB cell number.

5.2.6 Cell number in the brain decreased during ageing

When studying the function of *Toll-2* in longevity, I observed that loss of *Toll-2* function shortened life span of adult flies (see chapter 3). This suggested that *Toll-2* is required throughout adulthood and is protective during ageing. So far, the correlation between ageing and cell number in the brain has not been studied. Therefore, here I ask how cell number changes in the healthy ageing brain and whether *Toll-2* is involved in regulating cell number during ageing. To answer this question, I firstly investigated how cell number changed in flies during development and ageing. Therefore, I counted cells in both central brain and MB during pupa, early adult and aged adult flies in control genotypes. To visualize cells in central brain, I used *MyD88 Gal4* driving *UAS histone YFP* to visualized nuclei of *MyD88*+ cells (Figure 5.7 a and b). Cell number in different stages including day 4 pupa, day 3 adult and day 30 adult flies was counted automatically with *DeadEasy* software and analysed. During metamorphosis from pupae to adult, cell number in the central brain was significantly decreased. Moreover, cell number also decreased from day 3 to day 30 adult during ageing (Figure 5.7c). These results show that in pupal brains, excess cells formed during metamorphosis are removed when reaching the adult stage and that neurodegeneration occurs as flies age.

To ask whether cell number also changed in other brain domains, I studied MB Kenyon cells. I used *Toll-2*^{pTV} *Gal4* driving *UAS histone YFP* to visualize nuclei of MB

Figure 5.6 Alteration of *Toll-2* function at the critical period only did not affect cell number change in adult MB

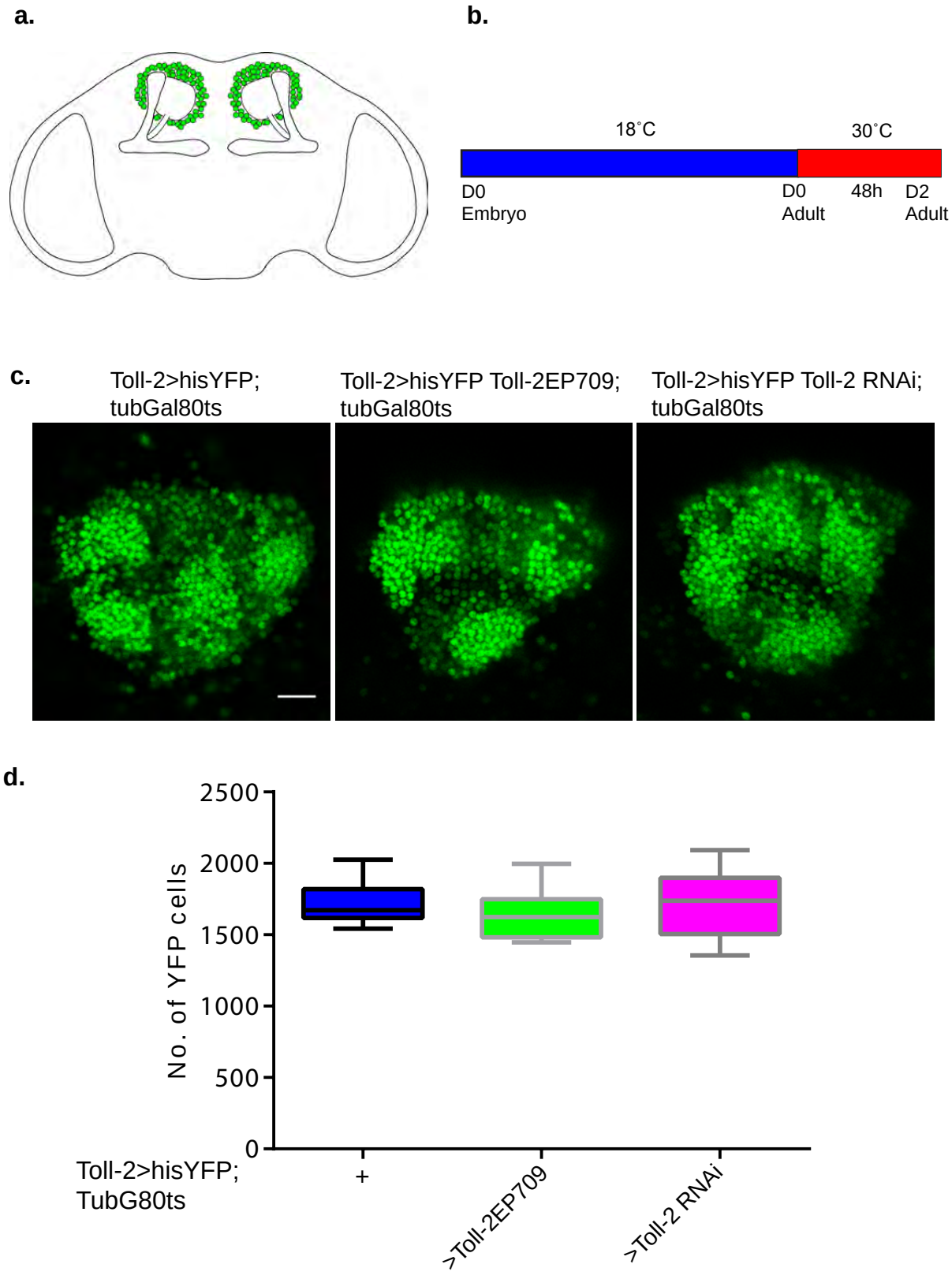


Figure 5.6 Alteration of *Toll-2* function at the critical period only did not affect cell number in adult MB

(a). Cells labelled in green indicate MB Kenyon cells analysed in this experiment.

(b). Temperature shifting regime. Flies were kept at 18˚C (blue) until eclosion, and shifted to 30˚C (red) for 48 hours. Brains are fixed and analysed at Day 2.

(c). *Toll-2* expressing cells in MB in each genotype.

Control: Toll-2^{pTV} Gal4 UAS histone YFP

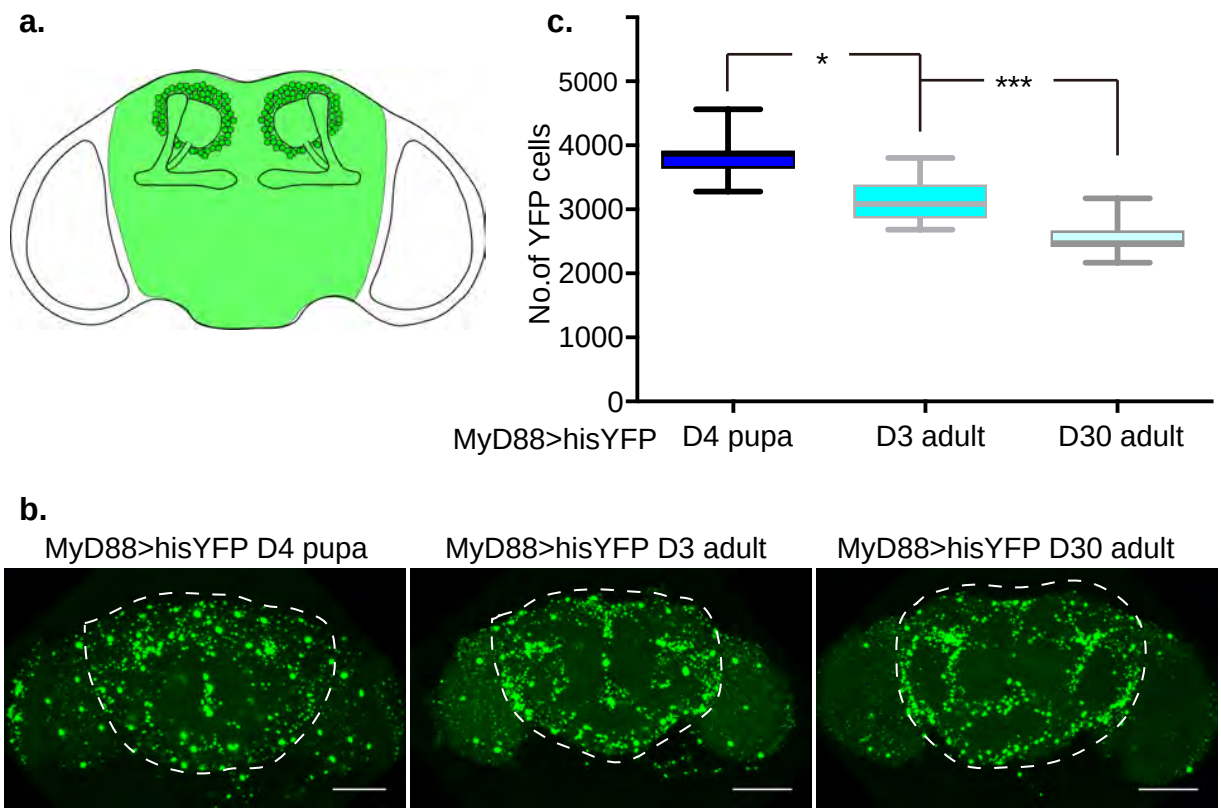
Toll-2 GOF: Toll-2^{pTV} Gal4 UAS histone YFP/UAS Toll-2EP709

Toll-2 LOF: Toll-2^{pTV} Gal4 UAS histone YFP;UAS Toll-2 RNAi

(d). Quantification of KC number using DeadEasy. Compared with the control, gain or loss of *Toll-2* function specifically in adult critical period did not cause significant change of cell number. One-way ANOVA, p=0.4886, Dunnett's multiple comparison, p>0.05, N=12, 11, 11.

Scale bar: 15μm

Figure 5.7
Cell number in the central brain decreases during development and ageing



(a). Area labelled in green indicates central brain analysed in this experiment.

(b). MyD88 cells in the brain of D4 pupa, D3 adult and D30 adult.

Genotype: MyD88 Gal4/UAS histone YFP

(c). Cell number quantification using DeadEasy. Cell number in the central brain in D3 and D30 adult brain significantly decreased compared with the cell number in pupal brain (Kruskal-Wallis test, $p<0.0001$, Dunn's multiple comparison, *$p=0.0432$, ***$p=0.0009$, N=9, 15, 15).

Scale bar: 100μm

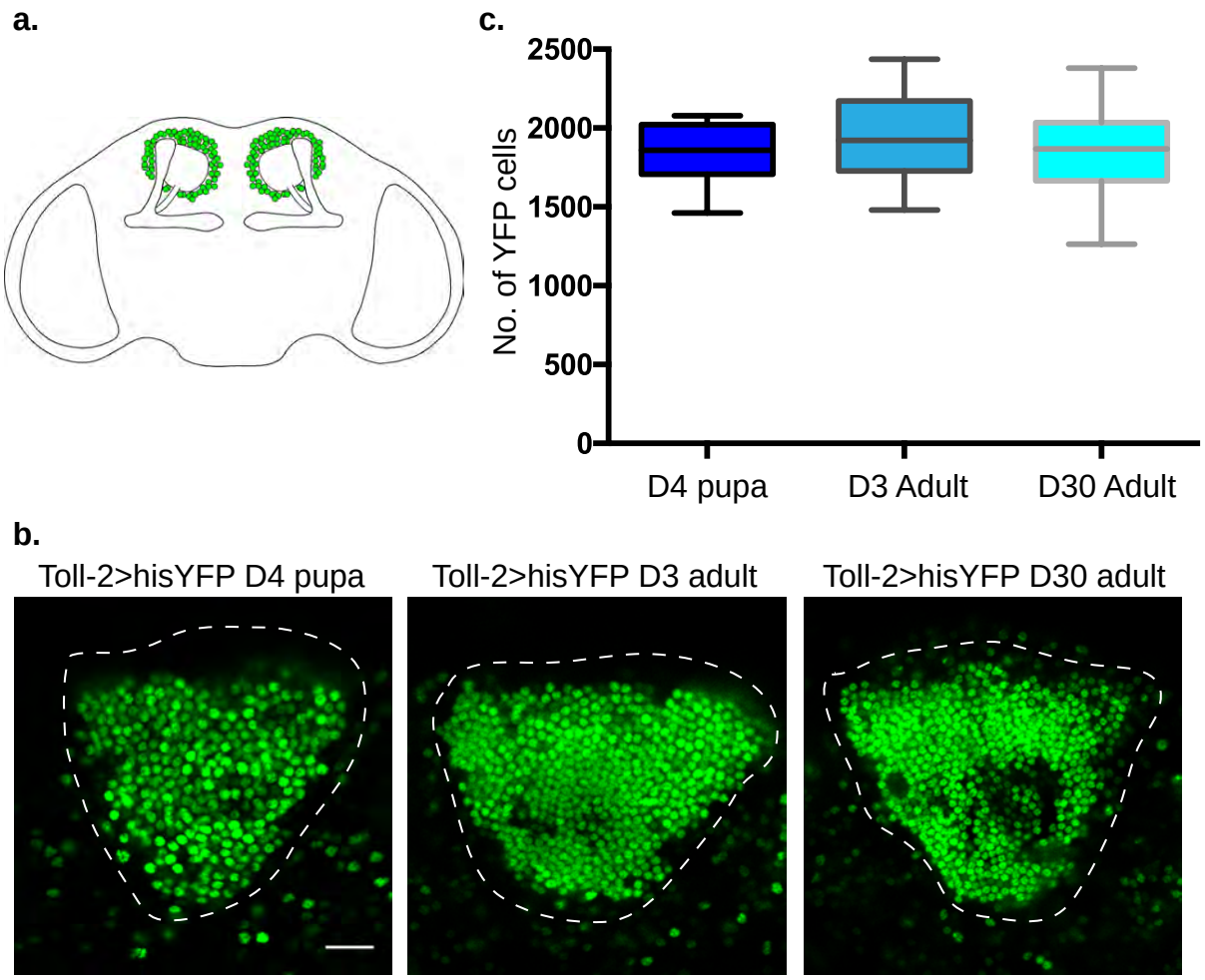
KCs. Cell number in MB at day 4 pupae, day 3 adult and day 30 adult was counted with *DeadEasy* software and analysed (Figure 5.8 a and b). Result shows that MB cell number did not significantly change from pupa to adult brain, or from day 3 adult to day 30 adult (Figure 5.8c). This result suggests that MB KCs number is steady in the brain during ageing.

5.2.7 Loss of *Toll-2* function caused neurodegeneration in ageing fly brains

The previous experiment suggested that neurodegeneration might happen during ageing resulting in cell loss. I therefore asked whether *Toll-2* is involved in cell number regulation during ageing. I used *MyD88 Gal4* to visualize cells in the central brain and studied whether *Toll-2* was involved in regulating cell number there during ageing. To this aim, I used *MyD88 Gal4* driving *Toll-2* gain and loss of function with *UAS Toll-2EP709* and *UAS Toll-2 RNAi*, respectively, through development and counted cell number in the day 30 adult central brain (Figure 5.9 a and b). The result of cell counting showed that loss of *Toll-2* function during ageing caused a significant decrease in cell number in day 30 adult central brains (Figure 5.9c). This suggests that *Toll-2* is required to maintain cell survival throughout the life course.

I also looked at cells in MBs using *Toll-2^{pTV} Gal4* driving *UAS histone YFP*. To study the function of *Toll-2*, I induced gain of function for *Toll-2* using *UAS Toll-2EP709*, and loss of function using *UAS Toll-2 RNAi* and Toll-2^{pTV}GAL4/*18w$^{\Delta 7\text{-}35}$* trans-heterozygotes, through development until day 30 adult (Figure 5.10 a and b). The result of cell counting using *DeadEasy* software showed that altering *Toll-2* levels did not significantly affect MB Kenyon cell number by adult day 30 (Figure 5.10 c). This

Figure 5.8 Kenyon cell number does not change significantly during development and ageing



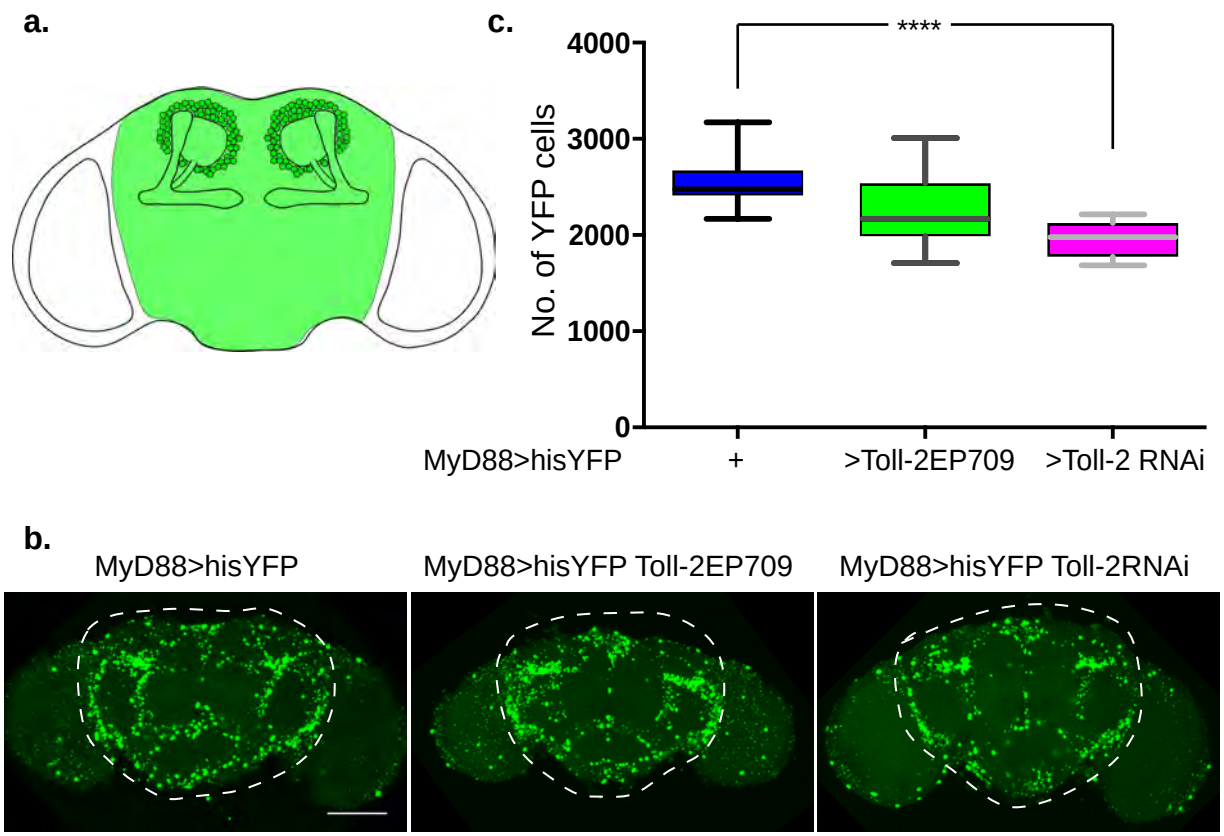
(a). Cells labelled in green indicate MB Kenyon cells analysed in this experiment.

(b). *Toll-2* expressing cells in MB in D4 pupa, D3 adult, and D30 adult brain. Genotype: Toll-2^{pTV}Gal4/UAS histone YFP

(c). Cell number quantificatin using DeadEasy. MB cell number in D4 pupa, D3 adult, and Day 30 adult brain is not significantly different. One-way ANOVA, p=0.3888, Dunnett's multiple comparison, p>0.05, N=15, 13, 12.

Scale bar: 15μm

Figure 5.9
Loss of *Toll-2* function causes cell loss in central brain in D30 old flies



(a). Area labelled in green indicates central brain analysed in this experiment

(b). MyD88 cells in D30 adult brain in 3 genotypes, area labelled in white circle is the ROI analysed in this experiment.

Genotype: Control: MyD88 Gal4/UAS histoneYFP

Toll-2 GOF: MyD88 Gal4 UAS histone YFP/UAS Toll-2EP709

Toll-2 LOF: MyD88 Gal4 UAS histone YFP; UAS Toll-2 RNAi

(d). Result of cell number quantification

Compared with the control, no significant difference was detected in gain of *Toll-2* function, while loss of *Toll-2* function causes significant decrease of cell number in D30 adult central brain. Kruskal-Wallis test, p=0.0002, Dunn's multiple comparison, ****p<0.0001, N=15, 11, 10.

Scale bar: 100μm

Figure 5.10 Alteration of Toll-2 function does not cause significant effect on cell number in D30 adult MB

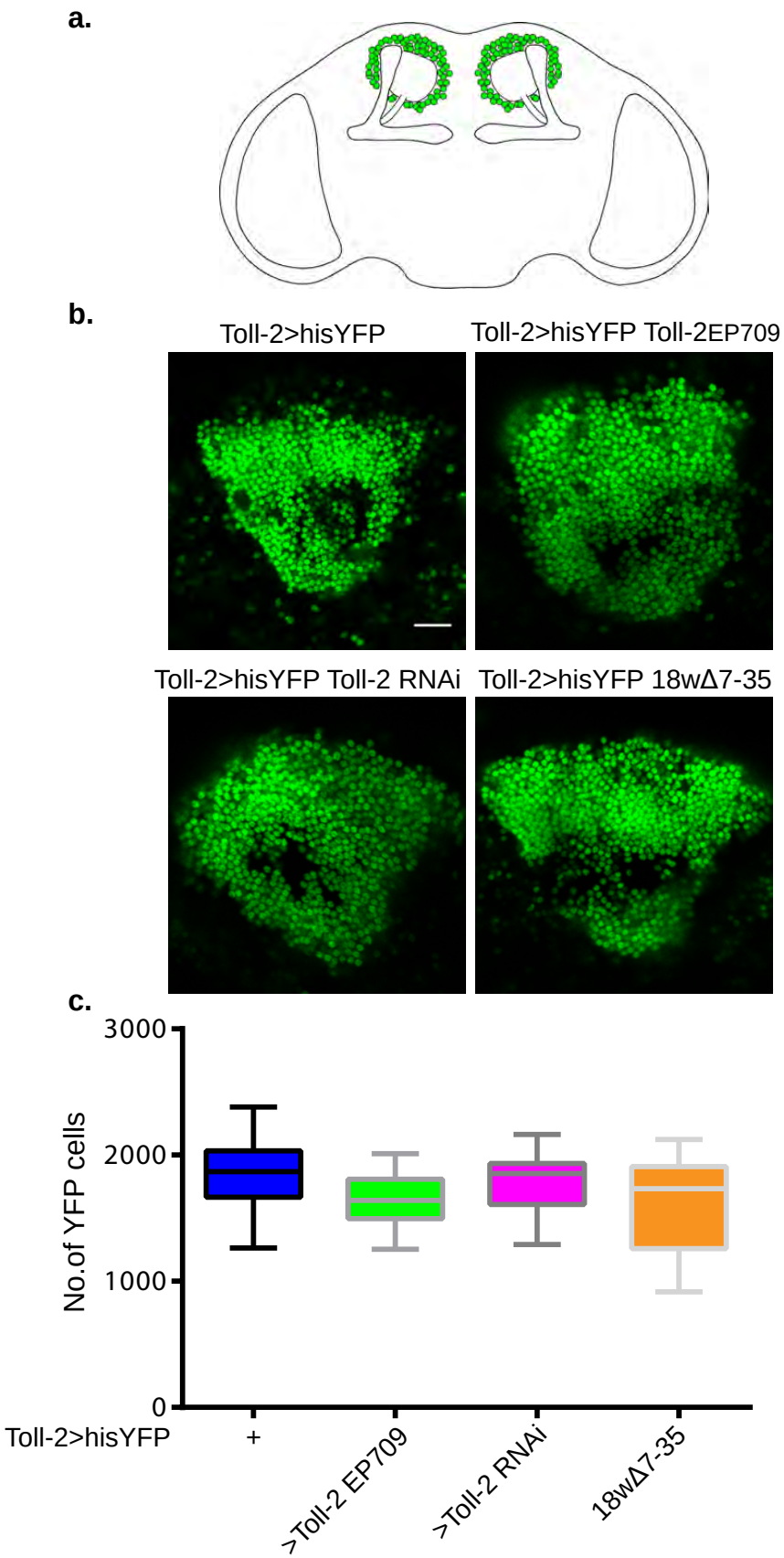


Figure 5.10 Alteration of Toll-2 function does not cause significant effect on cell number in D30 adult MB

(a). Cells labelled in green indicate MB Kenyon cells analysed in this experiment.

(b). Toll-2 expressing cells in MB in Day30 adult brain.

Control: Toll-2^{pTV} Gal4 UAS histone YFP

Toll-2 GOF: Toll-2^{pTV} Gal4 UAS histone YFP UAS Toll-2EP709

Toll-2 LOF: Toll-2^{pTV} Gal4 UAS histone YFP UAS Toll-2 RNAi

and: Toll-2^{pTV} Gal4 UAS histone YFP 18wΔ7-35

(c). Result of MB cell quantification. Compared with the control, no significant difference was detected in either gain or loss of Toll-2 function.

One-way ANOVA, p=0.1585, Dunnett's multiple comparison, p>0.05, N=12,16,7,13.

Scale bar: 15μm

result further indicates that MB Kenyon cell number is robustly maintained in the brain.

5.3 Discussion

In this chapter, I have shown that cell number can change in the adult brain, and *Toll-2* is involved in regulating cell number in multiple brain domains including the central brain and optic lobes. However, cell number did not change in the MBs, meaning that cell number is not plastic for KCs or it is more robustly maintained there than in the other two brain domains analysed. I also showed that cell number changes during ageing, as neurodegeneration takes place as flies get old. My data indicate that *Toll-2* is involved in regulating cell number throughout the life course.

I have shown that alteration of Toll-2 function specifically in the adult critical period could change cell number in the brain. This shows that cell number is plastic during the critical period. I have shown that gain of *Toll-2* function only in the adult critical period increased cell number in both the central brain and medulla. However, whether the cell increase is due to induced cell survival or cell proliferation has not been investigated. Therefore, further tests need to be carried out such as carrying out anti-phospho-Histone-H3 (anti-pH3) staining to detect dividing cells, or blocking cell proliferation to see whether this phenotype would be rescued.

Moreover, it has also been shown that loss of *Toll-2* function specifically in the adult critical period increased cell number in the central brain. Other experiments showing increased cell number due to gain of *Toll-2* function have suggested that *Toll-2* is pro-survival. This means that the increase in cell number with *Toll-2* loss of function is unlikely to be due to a pro-apoptotic function of *Toll-2*, and instead, loss of *Toll-2*

function might have caused cell loss, which further induced compensatory proliferation in the adult brain. Therefore, further experiments need to be carried out such as with anti-pH3 staining to test whether there is cell proliferation in the adult brain.

Cell number regulation in the central nervous system during ageing has not been studied before. Therefore, in this chapter I also investigated how cell number changed throughout the life-course. I have shown that cell number in the pupal brain was significantly higher compared with the adult brain. This suggests that cells are produced in excess during pupal stages and the excess cells are eliminated by apoptosis as the adult brain is made. This finding supports the neurotrophic theory (Levi-Montalcini, 1987). In this chapter, I also found that cell number in the brain decreases during ageing because of neurodegeneration, and *Toll-2* is neuroprotective during ageing. However, since the function of *Toll-2* is altered through development until adult D30, it is not known whether the phenotype observed for loss of *Toll-2* in ageing reflects a specific function in this late adult period, or not. Therefore, further tests will to be carried out to study the specific function of *Toll-2* during ageing.

In the next chapter, I will investigate whether cell number is linked to neuronal activity in the adult critical period.

Chapter 6

Neuronal activity influences neuronal number

6.1 Introduction

In mammals, there is abundant evidence showing that neuronal activity influences cell number in the brain. It has been proposed that cleavage of neurotrophin BDNF depends on neuronal activity and this will lead to either cell survival or cell death depending on whether BDNF functions in cleaved or full-length pro-form (Liu et al., 2015). It has also been found neuronal activity regulates the survival and proliferation of oligodendrocytes (Barres et al., 1996). Moreover, exercise which increases neuronal activity has also been found to trigger neurogenesis (Gage, 2004). These findings all indicate that neuronal activity is tightly linked with cell number regulation in the brain.

In *Drosophila*, there is evidence that experience (e.g. vision) promotes brain plasticity, and whilst this implies that neuronal activity is involved, whether cell number was affected remained unexplored (Barth and Heisenberg, 1997). So far, there is no direct evidence showing that cell number can be regulated by neuronal activity. I have shown in the previous two chapters that cell number is plastic in the adult critical period in optic lobes and central brain and *Toll-2* is involved in the regulation of cell number. *Toll* receptors are known to be the receptors of *Drosophila* neurotrophins, and since Tolls can bind DNTs promiscuously (Foldi et al., 2017, McIlroy et al., 2013), this suggests that *Toll-2* is also a potential receptor receiving signals from neurotrophin ligands. This therefore suggests that cell number changes induced by alteration in *Toll-2* expression might be related to neuronal activity.

Therefore, the aim of this chapter is to study whether alterations in neuronal activity could affect cell number in adult flies during the critical period. Multiple brain regions will be analysed including optic lobes and central brain.

6.2 Results

6.2.1 Blocking neuronal activity during the adult critical period reduced cell number in the optic lobe medulla

To ask whether cell number is regulated by neuronal activity, I firstly tested whether activating or blocking neurons could affect cell number in the adult brain medulla. In this experiment, I used *Toll-2^{pTV}Gal4* driving *UAS histone YFP* to visualize Toll-2+ cells in optic lobes. However, since *Toll-2* is expressed massively in the optic lobe, it was difficult to count all *Toll-2* cells. Therefore, I used *tubGal80^{ts}* to control the expression of *Gal4*. Furthermore, as blocking neuronal activity throughout development might prevent flies from reaching adulthood, in this way I could specifically block activity in the adults. Flies were kept at 18°C for 4 days (96 hours) after eclosion and then shifted to 30°C for 5 hours which allowed *tubulinGal80^{ts}* to be switched off and *Gal4* to be switched on. After that, flies were shifted between 30°C and 18°C every 10 minutes for an hour. Finally, flies were kept at 25°C for another 24 hours to enable cells to respond to the alteration of neuronal activity (Figure 6.1b). In this way, instead of all Toll-2 expressing cells, I could visualize only cells that expressed *Toll-2* at the time period when Gal4 was switched on, so that the number of cells was countable. Since the flies kept at 18°C take twice as long to develop compared to flies kept at 25°C, flies analysed using this regime would be equivalent to flies analysed on day 3 at 25°C, which is during the adult critical period.

Figure 6.1 Blocking neuronal activity decreases cell number in adult medulla

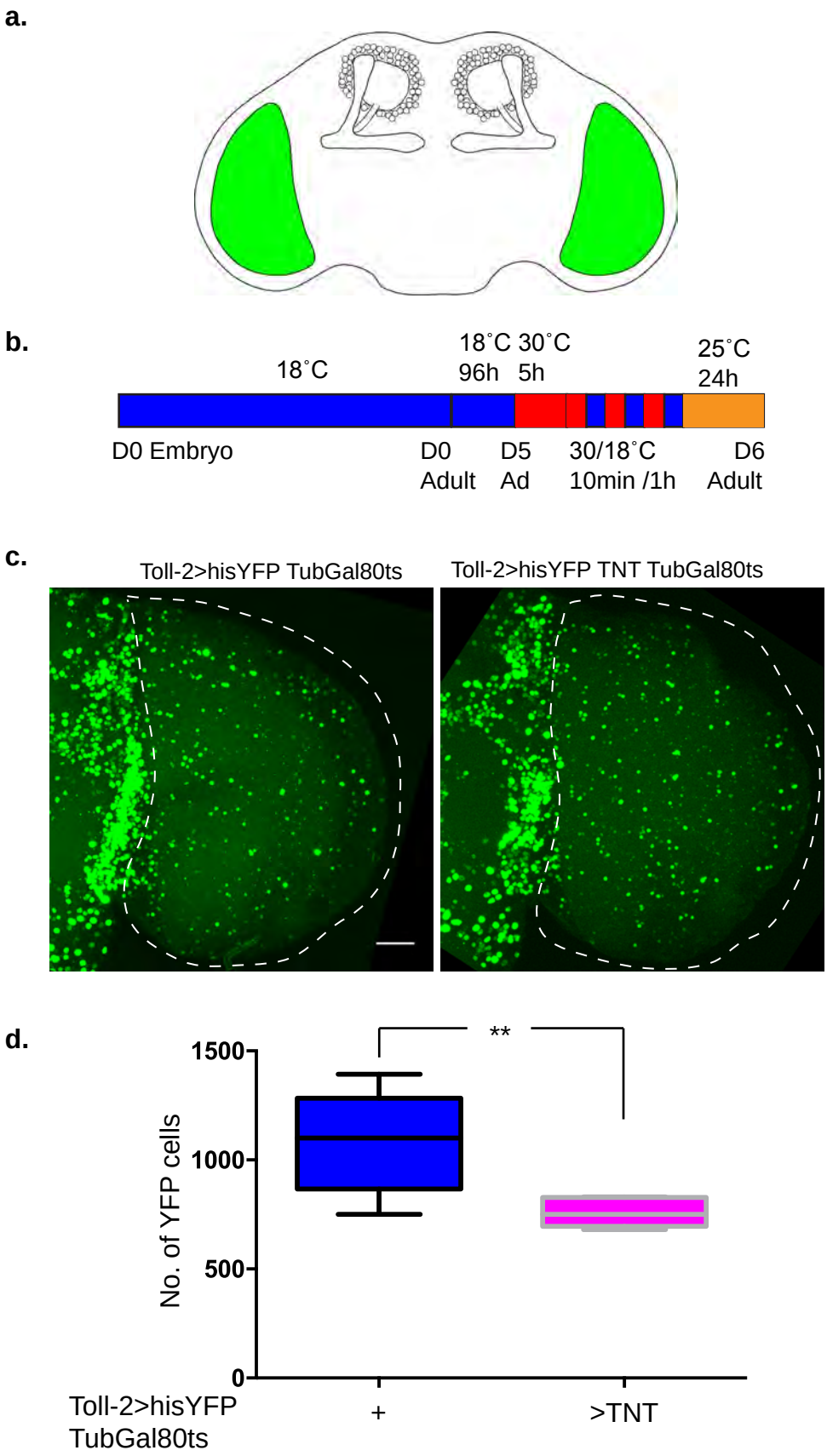


Figure 6.1 Blocking neuronal activity decreases cell number in adult medulla
(a). Structure of adult brain, area labelled in green is medulla that is studied in this experiment.
(b). Temperature shifting regime for neuronal activity tests. Flies were kept at 18°C until 96h after eclosion (blue), then flies were shifted to 30°C for 5 hours (red), they were then shifted between 18°C and 30°C every 10min for 1 hour, and finally flies were kept at 25°C for 24 hours to recove (Orange) and fixed and analysed.
(c). Medulla in two genotypes in this experiment:
Control: Toll-2^{pTV} Gal4 UAS histone YFP;Tubulin Gal80ts
TNT: Toll-2^{pTV} Gal4 UAS histone YFP/TNT ;Tubulin Gal80ts.
(d). Quantification of cell number using Deadeasy. Compared with the control, blocking neuronal activity reduced cell number. t-test, **p=0.0083.

Scale bar: 25μm

To block neuronal activity, I used UAS Tetanus neurotoxin light chain (UAS TNT), which blocks synaptic transmission (Figure 6.1 c). After applying the temperature shifting regime mentioned above, the number of cells in the medulla was quantified using *DeadEasy* software. The results of cell counting show that blocking neuronal activity caused a significant decrease in cell number in D6 adult medulla. This result indicated that altering neuronal activity could induce cell number changes.

6.2.2 Activating neurons caused cell number increase in adult optic lobe medulla

I then tested whether activating neurons affected cell number in adult medulla during the critical period (Figure 6.2a). To carry out this experiment, I used *UAS TrpA1* to activate neurons by activating TRPA1 cation channels. TRPA1 is a temperature sensitive protein that is functional at or above 25°C. However, switching on TrpA1 for too long might induce cytotoxicity and cell loss. To avoid this side effect of TrpA1, I applied similar temperature shifting regime to the one mentioned above but changed the recovery temperature from 25°C to 23°C, so that the TrpA1 would not cause side effects. Moreover, the temperature shifting between 30°C and 18°C for every 10 minutes could also prevent TrpA1 causing cytotoxicity (Figure 6.2 b). After treating the flies under this temperature shifting regime, I then quantified cell number in medulla using *DeadEasy*. The result shows that compared with the control, activating neurons caused a significant increase in Toll-2 cell number in D6 adult medulla (6.2 c and d). This result further suggests that altering neuronal activity induced changes in cell number in adult flies.

Figure 6.2 Activating neurons increases cell number in adult medulla

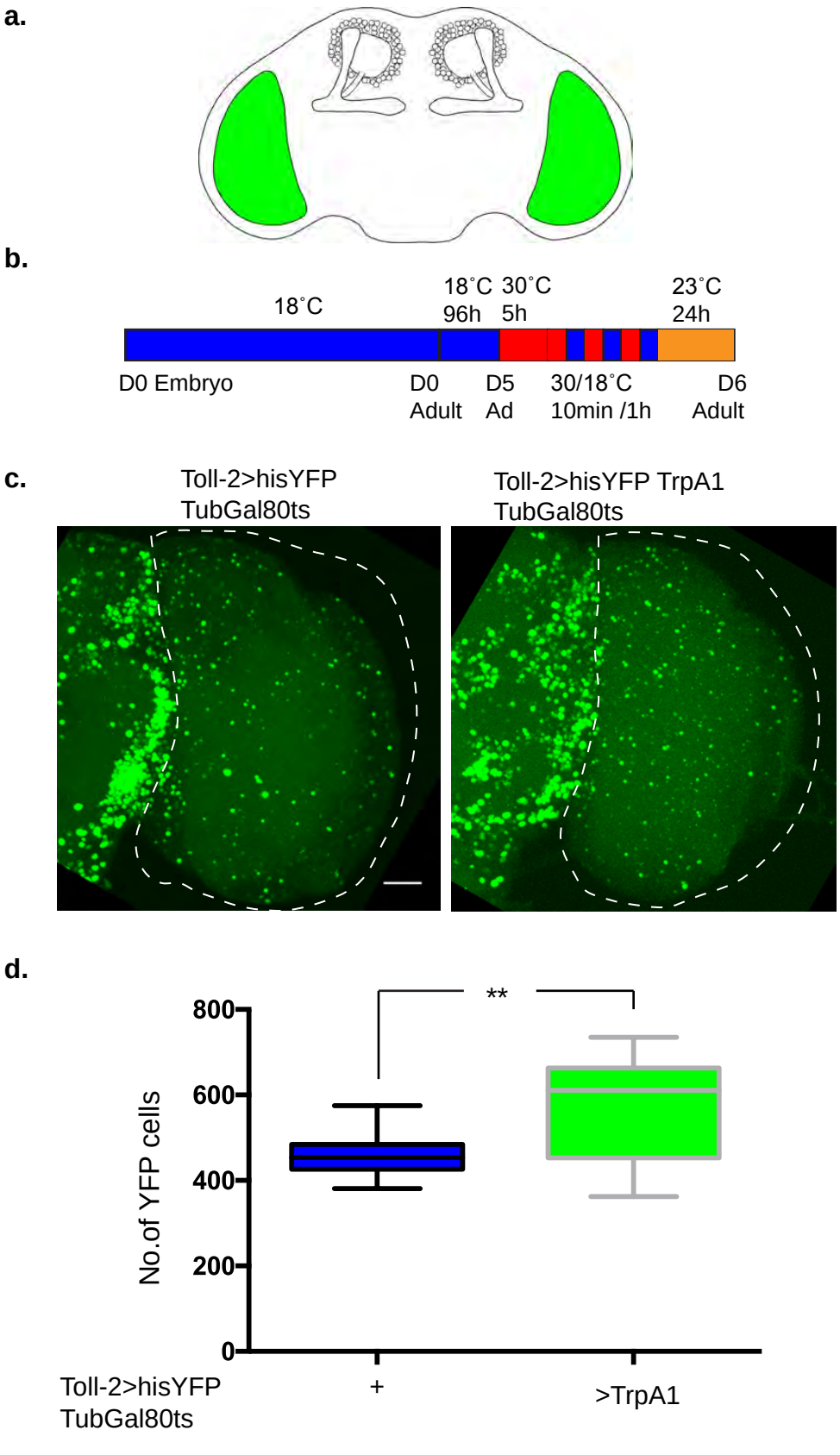


Figure 6.2 Activating neurons increases cell number in adult medulla

(a). Structure of adult brain, area labelled in green is medulla that is studied in this experiment.

(b). Temperature shifting regime for neuronal activity tests. Flies were kept at 18°C until 96h after eclosion (blue), then flies were shifted to 30°C for 5 hours (red), they were then shifted between 18°C and 30°C every 10min for 1 hour, and finally flies were kept at 23°C for 24 hours to recover (Orange) and fixed and analysed.

(c). Medulla in two genotypes analysed in this experiment:

Control: Toll-2^{pTV}>histone YFP;Tubulin Gal80ts

Activating neurons: Toll-2^{pTV}>histone YFP/TrpA1;Tubulin Gal80ts.

(d). Quantification of cell number using Deadeasy. Compared with the control, activating neurons increases cell number in adult medulla. t-test, **p=0.0058.

Scale bar: 25μm

6.2.3 Blocking neuronal activity causes two different phenotypes in cell number in the adult central brain

I then tested the effect of neuronal activity on cell number in the central brain (Figure 6.3a). To visualize cells in the central brain, I used *MyD88 Gal4*. Similarly, I used the temperature shifting regime described above to alter neuronal activity by using TrpA1 and TNT. To avoid the side effect caused by TrpA1, flies were kept at 23°C for 24h for recovery instead of 25°C (Figure 6.3b). Cell number in the central brain in both TrpA1 and TNT flies was then quantified using *DeadEasy*. However, when counting the cell number in TrpA1 flies, it was noticed that the expression level of histone YFP was too low to count correctly. Therefore, I was not able to study the effect of TrpA1 in the central brain in this experiment. I therefore only tested the effect of blocking neuronal activity in the central brain (Figure 6.3 c). In flies expressing TNT, two phenotypes were observed with different penetrance: 67% of brains showed no significant change in cell number, whereas 33% of brains had an increase in cell number (Figure 6.3 c-e). This suggested that blocking neuronal activity might induce cell death, which might further cause compensatory cell proliferation.

6.3 Discussion

In this chapter, I have shown that neuronal activity can alter cell number in the adult brain. Both activating and blocking neurons could induce changes in cell number in the adult medulla. In the central brain, blocking neuronal activity also caused a change in cell number, which might further induce compensatory cell proliferation.

In this chapter, I have presented two different temperature shifting regimes, the difference between these two was the temperature at the final recovery step, one of

Figure 6.3
Blocking neuronal activity increased cell number in D6 adult central brain

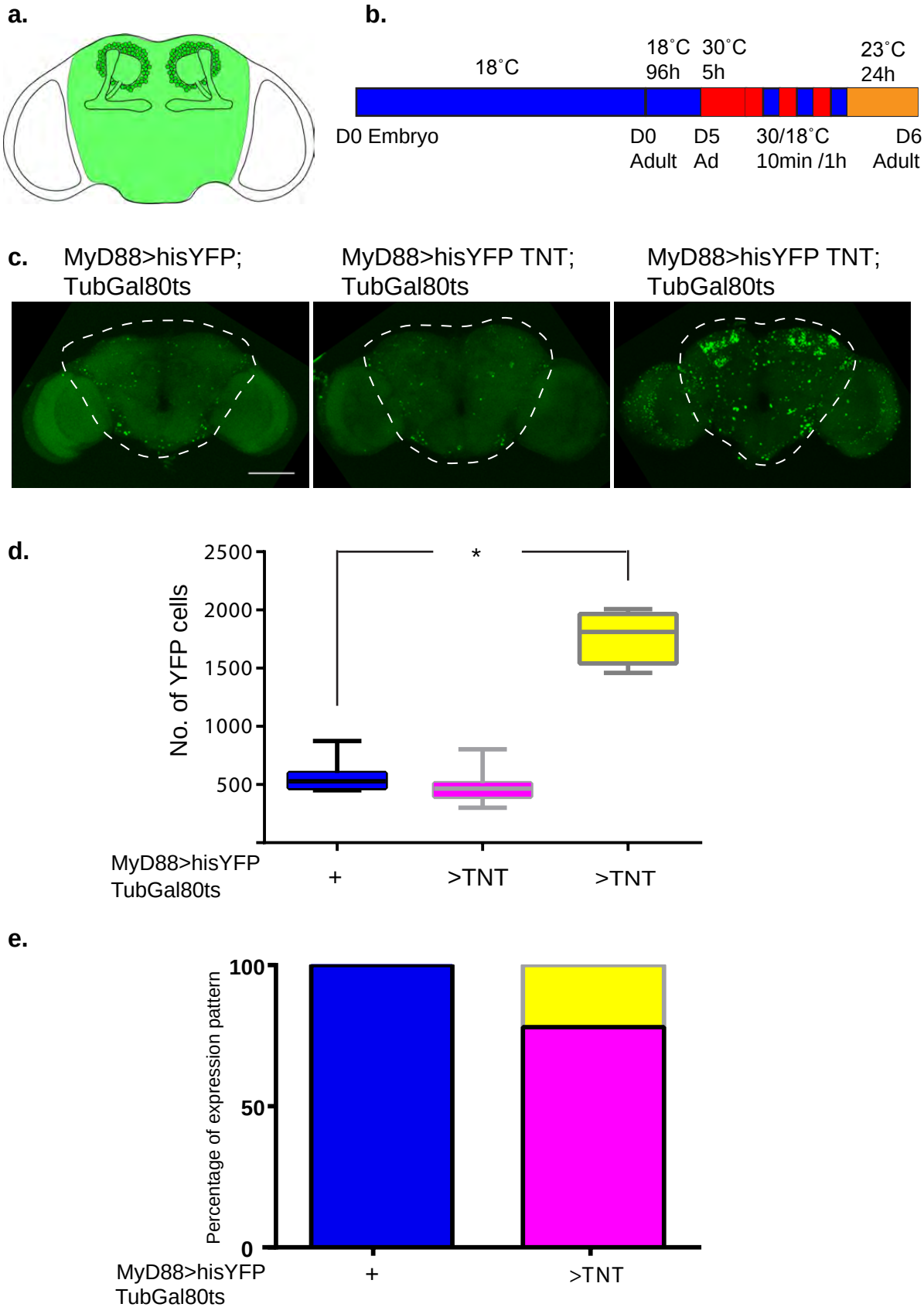


Figure 6.3

Blocking neuronal activity increased cell number in D6 adult central brain

(a). Structure of adult brain, area labelled in green indicates central brain analysed in this experiment.

(b). Temperature shifting regime for neuronal activity tests. Flies were kept at 18°C until 96h after eclosion (blue), then flies were shifted to 30°C for 5 hours (red), they were then shifted between 18°C and 30°C every 10min for 1 hour, and finally flies were kept at 23°C for 24 hours to recove (Orange) and fixed and analysed.

(c). Central brain in two genotypes analysed in this experiment.

Control: MyD88>histone YFP; Tubulin Gal80ts

Blocking neuronal activity: MyD88>histone YFP/TNT; Tubulin Gal80ts.

(d). Quantification of cell number using DeadEasy. Based on the cell number, samples from TNT group were divided into two groups. In the first group, blocking neuronal activity did not cause significant cell number change whereas the other group, blocking neuronal activity significantly increased cell number.

(Kruskal-Wallis test, p=0.0017, Dunn's multiple comparison, *p= 0.038 N= 12,14,4.

(e). Percentage of two types of YFP cells expression pattern in both control and TNT group. In the control, all of the 12 samples are with similar expression pattern. However, when blocking neuronal activity, 14 out of 18 shows similar expression pattern to the control, while 4 out of 18 shows significantly higher YFP cells level.

Scale bar: 100μm

which was 25°C while the other one was 23°C. This was because TrpA1 is a cation channel that can be activated at 25°C, and leaving TrpA1 on for 24 hours might induce cytotoxicity through excess calcium entry into the cell, causing cell loss. Therefore, I set the recovery temperature at 23°C for testing the effect of TrpA1 while 25°C was used in tests for the effect of TNT in adult medulla.

Although decreasing the temperature for recovery would solve the issue of TrpA1 induced toxicity, it also has the disadvantage that lower temperature would also reduce the expression level of Gal4. When the temperature decreases, the efficiency of Gal4 would also be reduced. Therefore, when keeping the flies at 23°C for recovery, the expression level of TNT would be decreased as a result of decreased Gal4 level. This could be the reason why blocking neuronal activity with TNT decreased cell number when flies recovered at 25°C, while no effect was detected when they recovered at 23°C.

When studying the effect of neuronal activity on cell number in central brain, it was noticed that YFP cells in *MyD88>TrpA1* flies were too faint to count. So far, I have not figured out the precise reason causing this phenotype. However, I would next test the effect of activating neurons in the central brain using another regime. Although here I wanted to compare the results of inhibiting with TNT and activating with TrpA1 side by side, TRPA1 is a temperature sensitive channel that is opened by temperature at or above 25°C even without *Gal4*. Therefore, I will use MyD88 Gal4 to drive UAS TrpA1 and control the activity of *TrpA1* only by temperature without *tubulinGal80ts*. In this way, the activity of TrpA1 could be regulated directly by temperature instead of other factors, which might resolve the issue.

When testing the effect of blocking neuronal activity in the central brain, two phenotypes were observed in MyD88>TNT flies. In one of the phenotypes, no significant difference was detected comparing with the control, however, considering the sample size was N=8, I would increase the sample size to answer whether blocking neuronal activity would truly decrease cell number in the adult central brain. Moreover, based on the temperature shifting regime applied for this experiment, flies were kept at 23°C for recovery, which might reduce TNT expression. Therefore, in a further experiment, I would change the recovery temperature to 25°C for testing MyD88>TNT in the central brain.

In another group however, cell number was significantly increased compared with the control, which is opposite from what has been observed in the medulla. Perhaps blocking neuronal activity might cause cell death which would further induce compensatory proliferation. Therefore, further experiments such as carrying out an anti-PH3 staining could test whether cell proliferation was induced.

In the next chapter, I will explain the roles of *Toll* receptor signalling pathways in regulating cell number in the adult brain and whether other *Toll* receptors are involved in regulating brain plasticity.

Chapter 7

Function of *Toll* signalling pathways and other *Toll* receptors in regulating cell number in the adult brain

7.1 Introduction

In Chapters 4 and 5, I have shown that *Toll-2* is involved in regulating cell number in the brain during pupa and adult stages. However, the intracellular molecular mechanisms downstream of *Toll-2* are still unknown. It has been shown that *Toll-6* can either promote cell survival through *MyD88-NFκB* pathway or promote cell death through *wek-Sarm-JNK* in the larval and early pupal CNS (Foldi et al., 2017, Figure 7.1a). It has also been shown that *Toll-1* can induce cell apoptosis via *JNK* signalling pathway in embryos (Liu et al., 2015). However, whether the downstream signalling pathways of *Toll* receptors are active or not in late pupal or adult central nervous system has not been investigated. Moreover, whether the downstream signalling pathways are involved in regulating cell number in the brain is also unknown.

There are 9 *Toll* paralogues in *Drosophila* (Tauszig et al., 2000, Ooi et al., 2002, Luo and Zheng, 2000). As mentioned above, different *Toll* receptors could regulate different cellular events, such as *Toll-1* could promote cell apoptosis, *Toll-6* could promote both cell survival and cell death, and *Toll-7* could also promote cell survival (Foldi et al., 2017). Preliminary data using antibody stainings and GAL4 drivers and reporters, have shown that *Toll-1, 6, 7* and *Toll-8* are expressed in the adult brain (Jill Wentzell and Niki Anthoney, Hidalgo lab, unpublished data) (McIlroy et al., 2013). However, whether other *Toll* receptors are expressed in the adult brain and whether they are involved in regulating cell number plasticity have not been explored.

Moreover, *Tolls* might have redundant functions. It has been shown that *Toll-6* or *Toll-7* single mutants had weak effects on crawling behaviour of larvae, while *Toll-6 Toll-7* double mutant caused significant locomotion deficits (McIlroy et al, 2013). However, whether different *Tolls* could have redundant functions or play antagonistic roles have not been studied either.

The aim of this chapter is firstly to investigate whether known *Toll* downstream signalling molecules are active in the brain, and whether they are involved in regulating cell number plasticity. Secondly, I also aim to test whether other *Toll* receptors are active in adult brain and whether they have redundant functions to regulate cell number plasticity.

7.2 Results

7.2.1 Both cell pro-survival and pro-apoptotic pathways are active in the pupal brain

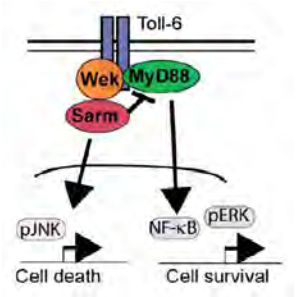
Since I have shown in previous chapters that *Toll-2* is involved in cell number change during pupal stages, here I asked whether this occurs via the known *Toll* downstream signalling pathways. To answer this question, I tested whether downstream signalling molecules of *Toll* receptors are expressed in the pupal brain including both the *MyD88-NFκB* pathway and the *JNK* signalling pathway. I firstly visualized the expression of *MyD88* using *MyD88 Gal4* driving UAS histone YFP (Figure 7.1 b and c). In D4 pupal brain, *MyD88* drives expression pronouncedly in different domains including the central brain and optic lobes. I also studied the expression of the transcription factors downstream of *MyD88*, *NF-κB* factors, *Dorsal* and *Dorsal-related immunity factor* (*Dif*). Literature has shown that nuclear and cytoplasmic isoforms of

Dorsal and *Dif* function differently. Nuclear isoforms of *Dorsal* and *Dif* function as transcription factors to regulate dorsal/ventral establishment, cell survival and anti-microbial responses. By contrast, the cytoplasmic isoform of *Dorsal* is expressed in NMJs post-synaptically and it regulates clustering of Glutamate receptors (Heckscher et al., 2007). Moreover, the cytoplasmic isoform of *Dif* is found in the larval mushroom bodies, and thus might be involved in regulating learning and memory (Zhou et al., 2015). Here, I focused on nuclear isoforms of *Dorsal* and *Dif* which have been known to function downstream of *Tolls*. To visualize the nuclear isoform of *Dorsal*, I used the fly in which the nuclear isoform of *Dorsal* is tagged with enhanced *GFP* (w;;PBac{dl-GFP.FPTB}VK00033, BDSC #42677) and stained GFP in D2 pupal brain. *Dorsal* is expressed mainly in the central brain in the cytoplasm around the nuclei (Figure 7.1 e). Similarly, I also studied the expression of *Dif* in the pupal brain using Dif-GFP tagged flies (w;;PBac{Dif-GFP.FPTB}VK00033, BDSC#42673). The staining of GFP shows that the nuclear isoform of *Dif* is expressed mainly in cells also in the cytoplasm around the nuclei in the central brain (Figure 7.1f). These results suggest that the *MyD88- NF-κB* pathway is active in the pupa brain.

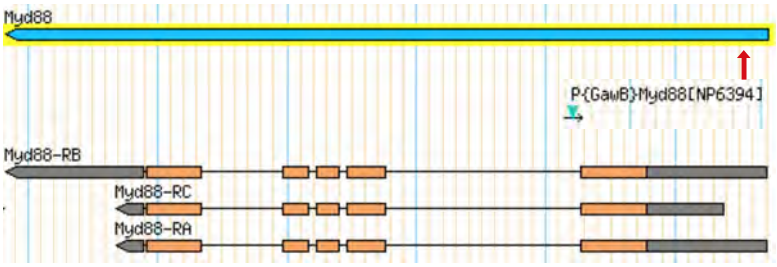
Since many cells die during pupal stages during metamorphosis, I studied whether the *JNK* signalling pathway that regulates cell death downstream of Toll receptors is also active in pupal brain. To study this, I stained *wek-GFP*-tagged flies (w;;PBac{wek-GFP.FPTB}VK00033/TM3, BDSC #67719) with anti-GFP in D1 pupa brain and showed that *wek* is expressed in relatively low levels and few cells in the pupal brain, but it can be detected in some cells in the central brain (7.1b). The result suggests that the signalling pathway that *wek* is involved in is also active in the pupa brain.

Figure 7.1 Signalling pathways for both cell survival and cell death are active in pupa brain

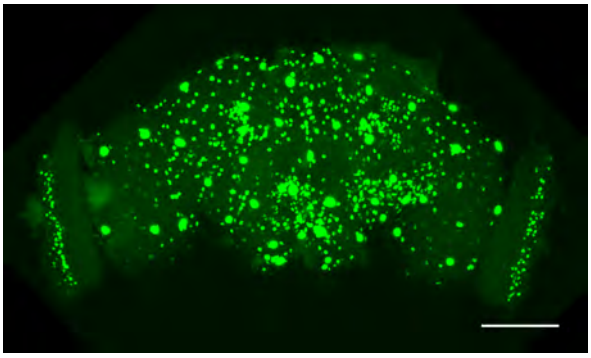
a.



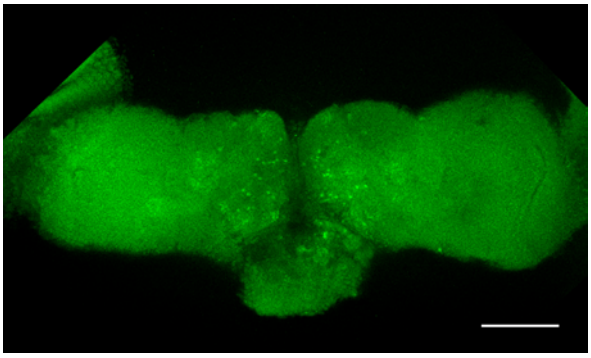
b.



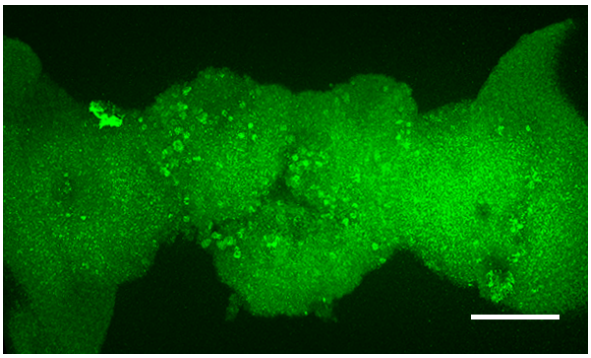
c. MyD88> histoneYFP D3 pupa brain



d. wek-GFP GFP 488 D1 pupa brain



e. Dorsal-GFP GFP 488 D2 pupa brain



f. Dif-GFP GFP 488 D2 pupa brain

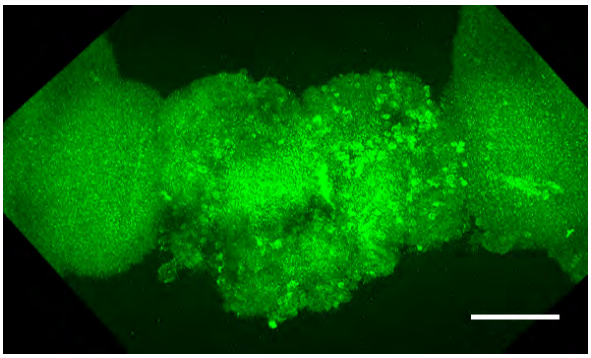


Figure 7.1 Signalling pathways for both cell survival and cell death are active in pupa brain

a). The known signalling pathway downstream of Toll-6 receptor. Toll-6 activates JNK signalling pathway to promote cell death via wek and Sarm. Toll-6 also promotes cell survival via MyD88-NFκB pathway.

b). The MyD88 locus. The red arrow indicates the site where Gal4 is inserted in the opposite orientation to transcription of MyD88.

c). Expression of MyD88 in D3 pupal brain (MyD88 Gal4/UAS histone YFP).

d). Expression of wek in D1 pupa brain by staining wek-GFP tagged flies with anti-GFP antibodies (w;;PBac{wek-GFP.FPTB}VK00033/TM3).

e) and f). Expression of Dorsal and Dif in D2 pupa brain by staining GFP tagged flies with anti-GFP.
(w;;PBac{dl-GFP.FPTB}VK00033 and w;;PBac{Dif-GFP.FPTB}VK00033)

Scale bar: 100μm

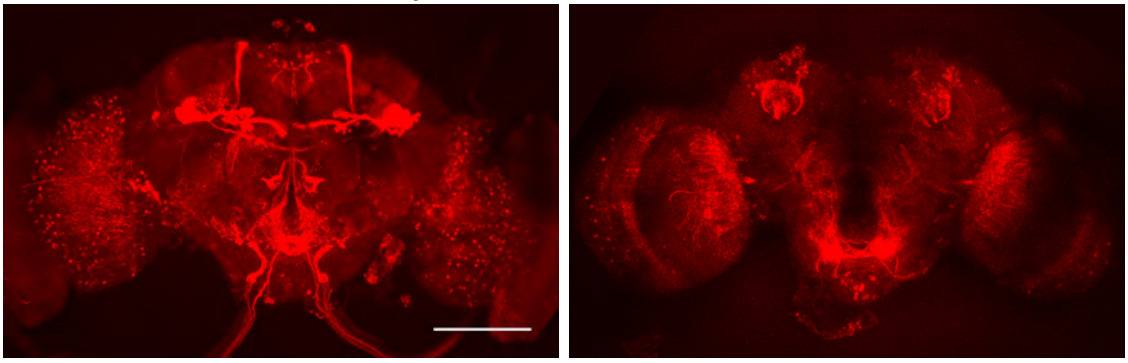
7.2.2 Both cell pro-survival and pro-apoptotic pathways are present in adult brain

I then tested whether the known downstream signalling molecules of *Toll* receptors are expressed in the adult brain including the *MyD88-NFκB* pathway and the *JNK* signalling pathway. In Chapter 4, I showed that *MyD88* is expressed in the adult brain (Figure 4.1 a,c,e,g). *MyD88>tdTomato* has revealed that *MyD88* is expressed in the mushroom bodies, optic lobes and sub-oesophageal ganglion (SOG) (Figure 7.2 a). To test the expression of *MyD88-NF-κB* pathway, I also visualized the expression of *Dif* by staining *Dif-GFP*-tagged flies with anti-*GFP* antibodies (Figure 7.2b). This shows that the nuclear isoform of *Dif* is localized around the antennal lobes. These results show that the MyD88 signalling pathway is active in the adult brain.

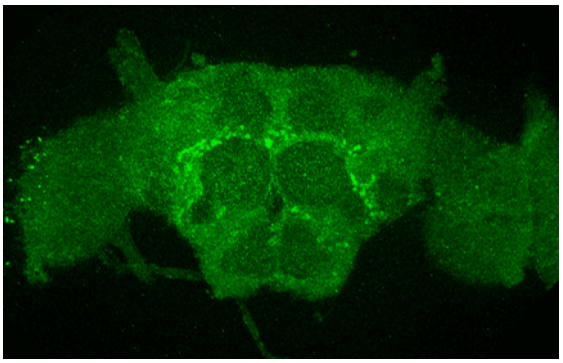
I also tested whether the *wek-Sarm-JNK* signalling pathway is active in adult brain. To test this, I visualized the expression pattern of *Sarm* which is the downstream adaptor of *Tolls* to promote cell death upstream of *JNK*. I used two *Sarm Gal4* lines driving *UAS Flybow* to visualize the expression of different isoforms of *Sarm* (Figure 7.2e). The results show that *Sarm* is expressed in the adult brain including in the SOG, antennal lobes, MB and OLs. However, there are eight different *Sarm* isoforms, which might be expressed in different brain domains (Figure 7.2 c and d). These results suggest that *Sarm* signalling pathway that promotes cell death is active in adult brains.

Figure 7.2 Downstream Toll-signalling effectors are present in the adult brain

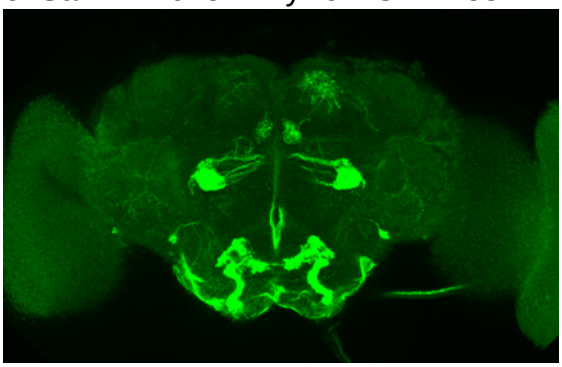
a. MyD88>Tomato DsRed 546



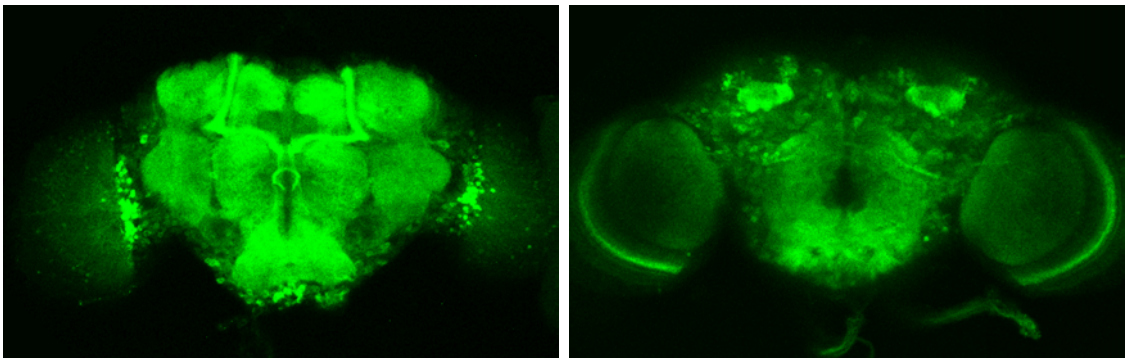
b. Dif-GFP GFP 488



c. Sarm NP0257>FlyBow GFP 488



d. Sarm NP7460>FlyBow GFP 488



e.

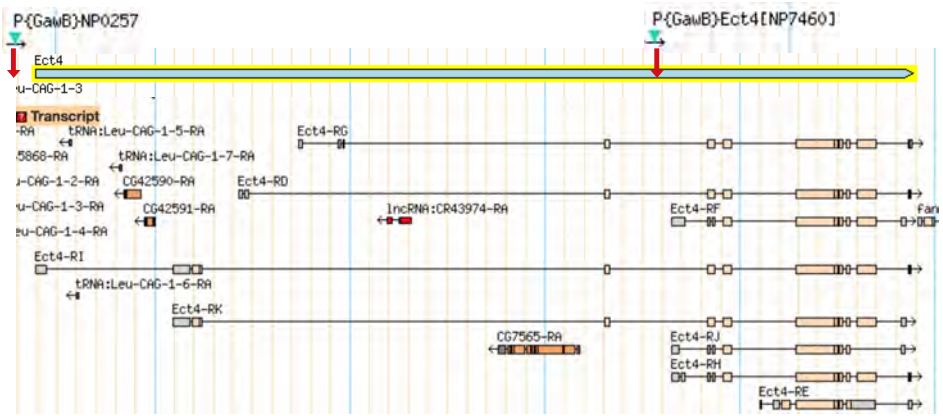


Figure 7.2 Downstream Toll-signalling effectors are present in the adult brain

(a). Expression of MyD88 in adult brain stained with anti-DsRed, 546.
Genotype: MyD88 Gal4NP6394/UAS tdTomato.
(b). Expression of Dif in adult brain staining Dif-GFP tagged flies with anti-GFP
Genotype: w;;PBac{Dif-GFP.FPTB}VK00033.
(c). Expression of Sarm in adult brain stained with anti-GFP, 488.
Genotype: Sarm Gal4NP0257/UAS Flybow.
(d). Expression of Sarm in adult brain stained with anti-GFP, 488.
Genotype: Sarm Gal4NP7460/UAS Flybow.
(e). Sarm locus. The two red arrows indicate where Gal4 is inserted into the genome generating Sarm Gal4NP0257 and Sarm Gal4NP7460.

Scale bar: 100μm

7.2.3 Changing the activity of downstream molecules changed cell number in the adult brain.

Since the molecules downstream of *Toll* receptors are expressed in pupal and adult brains, I then tested whether the downstream signalling pathways are involved in regulating cell number in the adult brain. I firstly altered the activity of the downstream signalling molecules of both pro-survival and pro-apoptotic pathways specifically in adult brain to test whether cell number in the central brain would be affected (Figure 7.3 a and b). To promote cell survival and block cell death, I activated *Dp110* that is activated *PI3 Kinase* and blocked *JNK* and *Cactus* to block cell death (*MyD88>hisYFP Dp110 JNKRNAi CactusRNAi*). *Dp110* provokes the nuclear export of *Foxo* as nuclear *Foxo* is known to promote cell apoptosis. Knocking down *Cactus* induced the nuclear translocation of *NFκB*. On the contrary, to promote cell death and inhibit cell survival, I overexpressed *wek* and knocked down *MyD88* (*MyD88>hisYFP MyD88RNAi; WekHA*). To alter the activity specifically in adult, I used *TubulinGal80^{ts}* to control the expression of *Gal4* (Figure 7.3b). The result of cell counting shows that when blocking cell death and promoting cell survival, cell number in the central brain seemed to be increased, which however was not significant. However, when blocking cell survival and promoting cell death, cell number was significantly increased, which is opposite to what was expected. These results suggest that changing the activity of downstream signalling molecules of *Toll* receptors could induce cell number changes in the adult brain. Moreover, it is also suggested that induced cell death might provoke compensatory proliferation in the adult central brain or *wek* might function via *MyD88* independent pathways to promote cell proliferation.

Figure 7.3 Altering *Toll*-receptor signalling in the adult central brain increases cell number

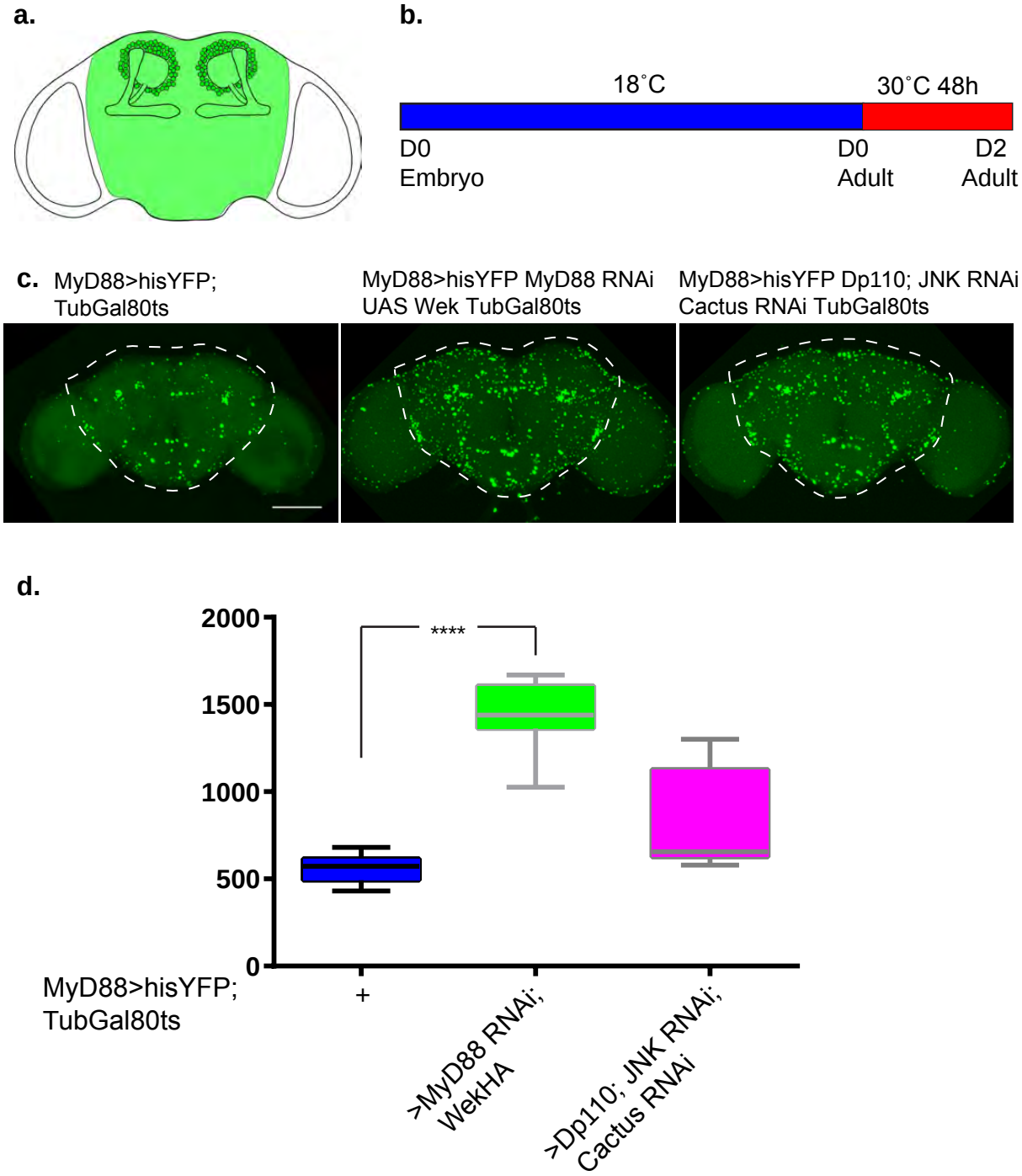


Figure 7.3 Altering *Toll*-receptor signalling in the adult central brain increases cell number

(a). The green area indicates the area of central brain that is analysed in this experiment.

(b). Temperature shifting regime used for testing the function of downstream signalling pathways on cell number regulation. The region in blue shows the period when the flies were kept at 18˚C and the red shows when the flies were kept at 30˚C.

(c). Example of the brain in three genotypes for cell counting in the central brain.

Genotype:

Control: MyD88 Gal4 UAS histone YFP; Tubulin Gal80ts

Blocking cell survival and promoting cell death:

MyD88 Gal4 UAS histone YFP / UAS MyD88RNAi; UAS Wek /TubGal80ts

Blocking cell death and promoting cell survival:

Dp110; MyD88 Gal4 UAS histone YFP /UAS JNKRNAi; UAS CactusRNAi/TubGal80ts

(d). Cell number counted with Deadeasy. Blocking cell death and promoting cell survival did not cause significant cell number change, whereas promoting cell death and blocking cell survival induced significant cell number increase in the central brain. Kruskal-Wallis test, $p<0.0001$, DUNN's multiple comparison, ****$p<0.0001$, N=10,10,11.

Scale bar: 100μm

Apart from the central brain, I then asked the same question in adult mushroom bodies to test whether altering the activity of downstream signalling molecules could change Kenyon cell number (Figure 7.4a). To visualize Kenyon cells in MB, I used *Toll-2^{pTV} Gal4* driving *UAS histone YFP*. Similarly, I used *TubulinGal80ts* to switch on *Gal4* specifically in the adult (Figure 7.4b). I used the same genotypes mentioned above to promote or block the cell pro-survival and pro-death signalling pathways (Figure 7.4c). The result shows that neither blocking cell survival, promoting cell death nor the other way around changed cell number significantly (Figure 7.4d). However, when blocking cell survival and promoting cell death, cell number seemed to be slightly, albeit not significantly, increased. This result is consistent with what had been shown in the adult central brain that induced cell death might provoke compensatory proliferation or *wek* might promote cell proliferation via a pathway that is independent from *MyD88*. Either way, this result suggests that there might be cells that are able to proliferate in the adult brain.

7.2.4 *Toll-2* expressing cells in the mushroom body are able to proliferate

To test whether *Toll-2* expressing cells might undergo proliferation, I asked whether *Toll-2*+ cells can divide in normal brain development. To carry out this experiment, I over-expressed *UAS Retinoblastoma-family protein 280* (*Rbf280*) to block cell proliferation and *UAS p35* to block cell death (Figure 7.5). I used *Toll-2^{pTV} Gal4* driving *UAS histone YFP* to visualize Toll-2+ cells (Figure 7.5 b and c). However, over-expression of *Rbf* or *p35* in *Toll-2* cells caused lethality and flies died at Day 1 pupae. Thus, I was not able to study the effect in adult flies. Instead, I looked at *Toll-2* cell number in D1 pupal MBs. The result shows that whereas blocking cell death

Figure 7.4 Altering *Toll*-receptor signalling in the adult brain does not affect Kenyon cell number significantly

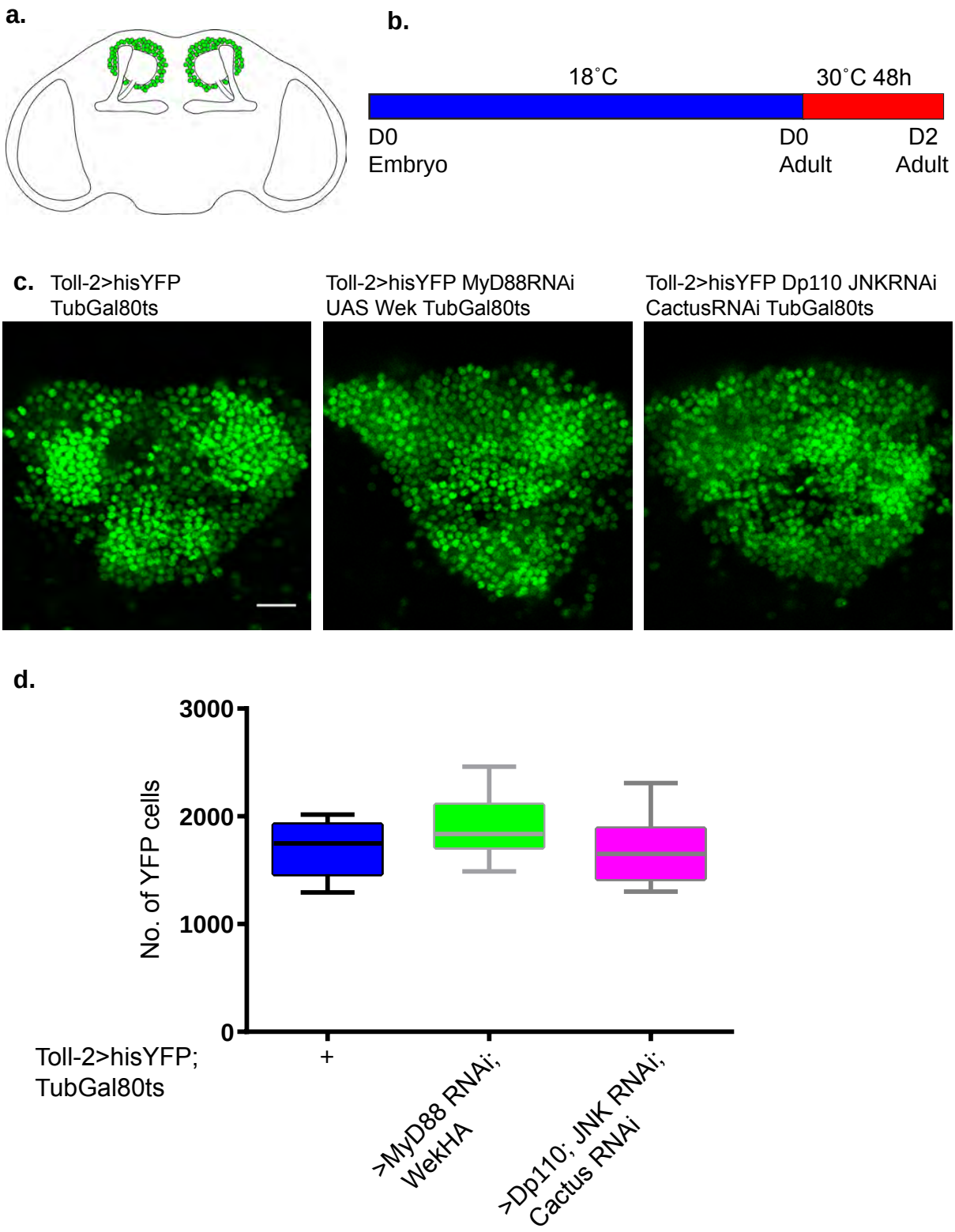


Figure 7.4 Altering *Toll*-receptor signalling in the adult brain does not affect Kenyon cell number significantly.

(a). The green brain area indicates the area of MB Kenyon cells that are analysed in this experiment.

(b). Temperature shifting regime used for testing the function of downstream signalling pathways on cell number regulation. The region in blue shows the period when the flies were kept at 18˚C and the red shows when the flies were kept at 30˚C.

(c). Examples of the brain in three genotypes for cell counting in the MB.

Control: MyD88 Gal4 UAS histone YFP; Tubulin Gal80ts

Blocking cell survival and promoting cell death:

MyD88 Gal4 UAS histone YFP/ UAS MyD88 RNAi; UAS WekHA/TubGal80ts

Blocking cell death and promoting cell survival:

Dp110; MyD88 Gal4 UAS histone YFP /UAS JNK RNAi; UAS Cactus RNAi/TubGal80ts

(d). Cell number counted with DeadEasy.

One-Way ANOVA, $p=0.979$, Dunnett's multiple comparison, $p>0.05$, N=12,17, 20.

Scale bar: 15μm

Figure 7.5 *Toll-2* cells undergo proliferation during development

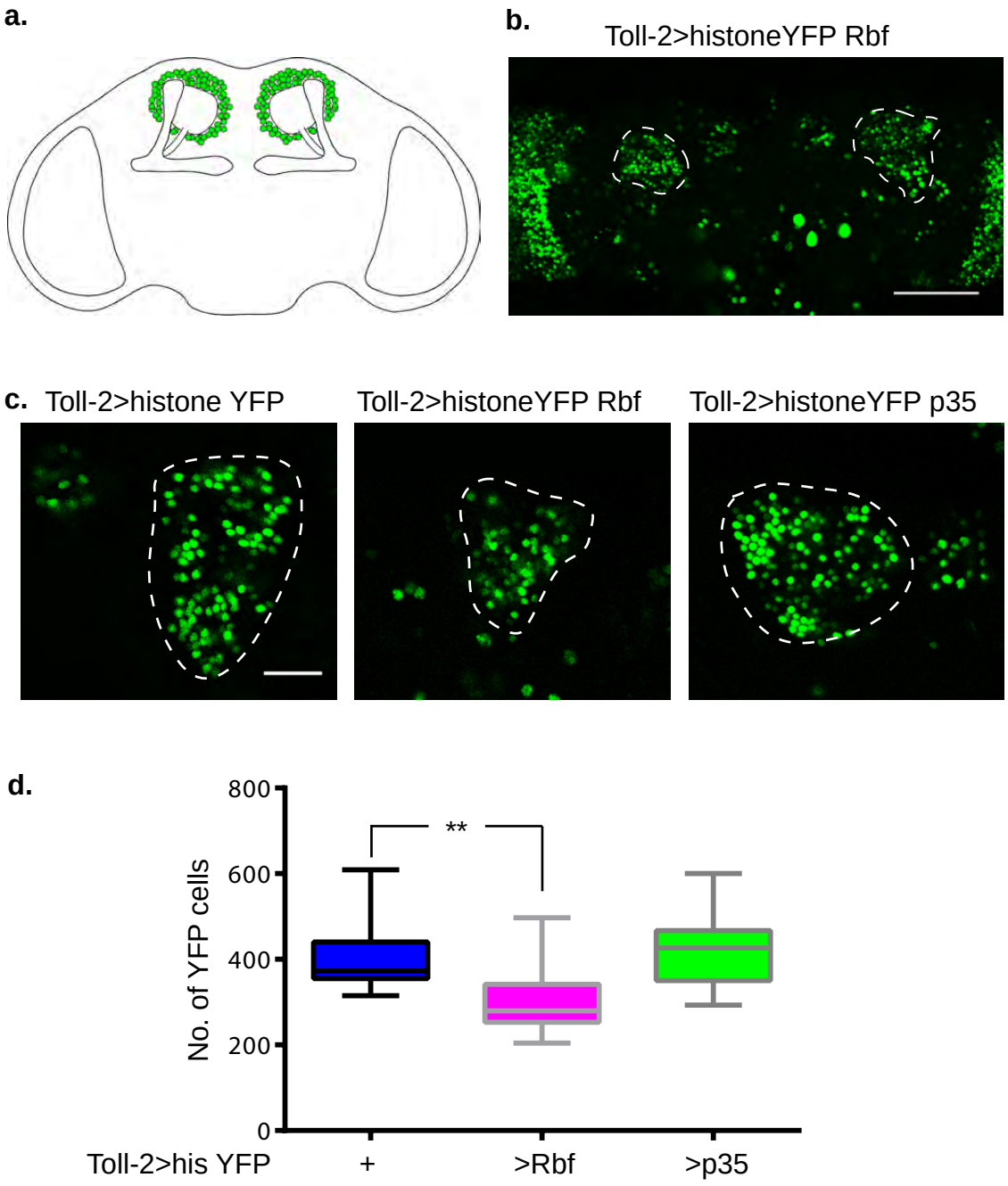


Figure 7.5 *Toll-2* cells undergo proliferation during development

a), Brain structure with MB labelled in green.

b), Toll-2 expression in D1 pupal brain, MBs are labelled in white circles.

c), Toll-2 cells in MB in three different genotypes. ROIs are labelled in white circles.

Genotypes:

Control: Toll-2^{pTV} Gal4 UAS histone YFP

Rbf: Toll-2^{pTV} Gal4 UAS histone YFP; UAS Rbf

p35: Toll-2^{pTV} Gal4 UAS histone YFP/ UAS p35

d), Cell number change is not detected by blocking cell death using p35 (green bar) compared with the control (blue bar, N=15). However, cell number is significantly decreased when blocking cell proliferation using UAS Rbf (magenta bar). Kruskal-Wallis test, p=0.0002, Dunn's multiple comparison, p=0.0021, N=15,18,17.

Scale bar: b: 100μm; c: 25μm

using *p35* did not cause cell number changes, blocking cell proliferation using *Rbf280* deceased cell number in pupal MB significantly (Figure 7.5d). This indicates that *Toll-2+* cells are able to proliferate in normal development.

7.2.5 Other *Toll* receptors are expressed in the adult brain

As published before, *Toll-1*, *6*, and *7* are involved in regulating cell number in embryonic and larval CNS (Foldi at al., 2017). Therefore, here I asked whether they and other *Tolls* are involved in regulating cell number in adult brain as well. To answer these questions, I firstly studied whether other *Toll* receptors are expressed in the adult brain. To study the expression of *Toll-3, 6,* and *7*, I used lines bearing *Minos*-mediated integration cassette insertions (MiMIC, Toll-3^{MI02994}, BDSC #35889; Toll-6^{MI02127}, BDSC #34467; Toll-7^{MI13963}, BDSC #59468). The *MiMIC* cassette is flanked by *attP* sites, which could be swapped by any sequence flanked with *attB* sequence through recombinase-mediated cassette exchange (RMCE). I therefore swapped the cassette with p*Gal4-attB*, after which *Gal4* would be expressed under the regulation of the endogenous gene. To do this, *pGal4-attB* was amplified and sent to *BestGene Inc.* to be injected. The transgenic flies were then sent back to be screened and balanced. In this way, I screened and balanced *Toll-3^{MI02994} Gal4* (Figure 2.3), and technician Marta Moreira in the lab screened *Toll-6^{MI02127} Gal4* and *Toll-7^{MI13963} Gal4*, and Alicia Hidalgo balanced them. I then used these *Gal4* lines driving UAS reporters to visualize the expression of the genes. The *Toll-8 Gal4* flies were bought from Bloomington centre (BDSC #36548).

To visualize *Toll-3, 6* and *8*, I used *Toll-3^{MI02994} Gal4*, *Toll-6^{MI02127} Gal4*, and *Toll-8 Gal4^{MD806}* driving *UAS tdTomato*. To visualize *Toll-7*, I used *Toll-7^{MI13963} Gal4* driving

UAS FlyBow. It can be seen that *Toll-3* is expressed in lamina and in a thin layer of fan shaped body (Figure 7.6 a and b). Compared with *Toll-3*, *Toll-6* is expressed more pronouncedly in the adult brain. *Toll-6* is highly expressed in MBs, lamina, medulla and fan shaped body (Figure 7.6 a to d). *Toll-8* is also expressed in multiple domains in the adult brain. It is highly expressed in the MB, lamina, optic lobe including medulla, lobula and lobula plate, a few layers of fan shaped body, and also in the antennal lobe (Figure 7.6 a to e). *Toll-7* is mainly expressed in the central brain in MB, ellipsoid body, and antennal lobes (Figure 7.6 a, c, d, e). These results indicate that different *Toll* receptors are expressed in distinct patterns in the adult brain.

7.2.6 Knocking down multiple *Toll* receptors causes lethality and affects brain structure in late pupae

Since *Toll* receptors 6, 7, 8 are all highly expressed in adult brain, I asked whether these receptors have functions in the brain. To do this, I combined UAS RNAi lines of different *Toll* receptors to generate multiple *Tolls* RNAi lines including UAS *Toll-1, 2, 7* RNAi, UAS *Toll-2, 6, 7* RNAi, and UAS *Toll-2, 7, 8* RNAi. I then used *Toll-2^{pTV} Gal4* driving *UAS histone YFP* to investigate the effect of knocking down multiple *Toll* receptors on brain structure. However, when collecting the Toll-2^{pTV}Gal4 Tolls RNAi flies, I noticed that the flies with RNAi against Tolls died at a late pupal stage. Based on the appearance of the body and wings, the pupae seemed to reach Day 4, however, the heads of the pupae looked much smaller than wild type Day 4 pupae and the eyes seemed either smaller or were not formed at all. Therefore, this phenotype suggests that knocking down multiple *Toll* receptors at the same time caused lethality of flies at late pupal stage.

Figure 7.6 *Toll-3, 6, 7, 8* are expressed in the adult brain

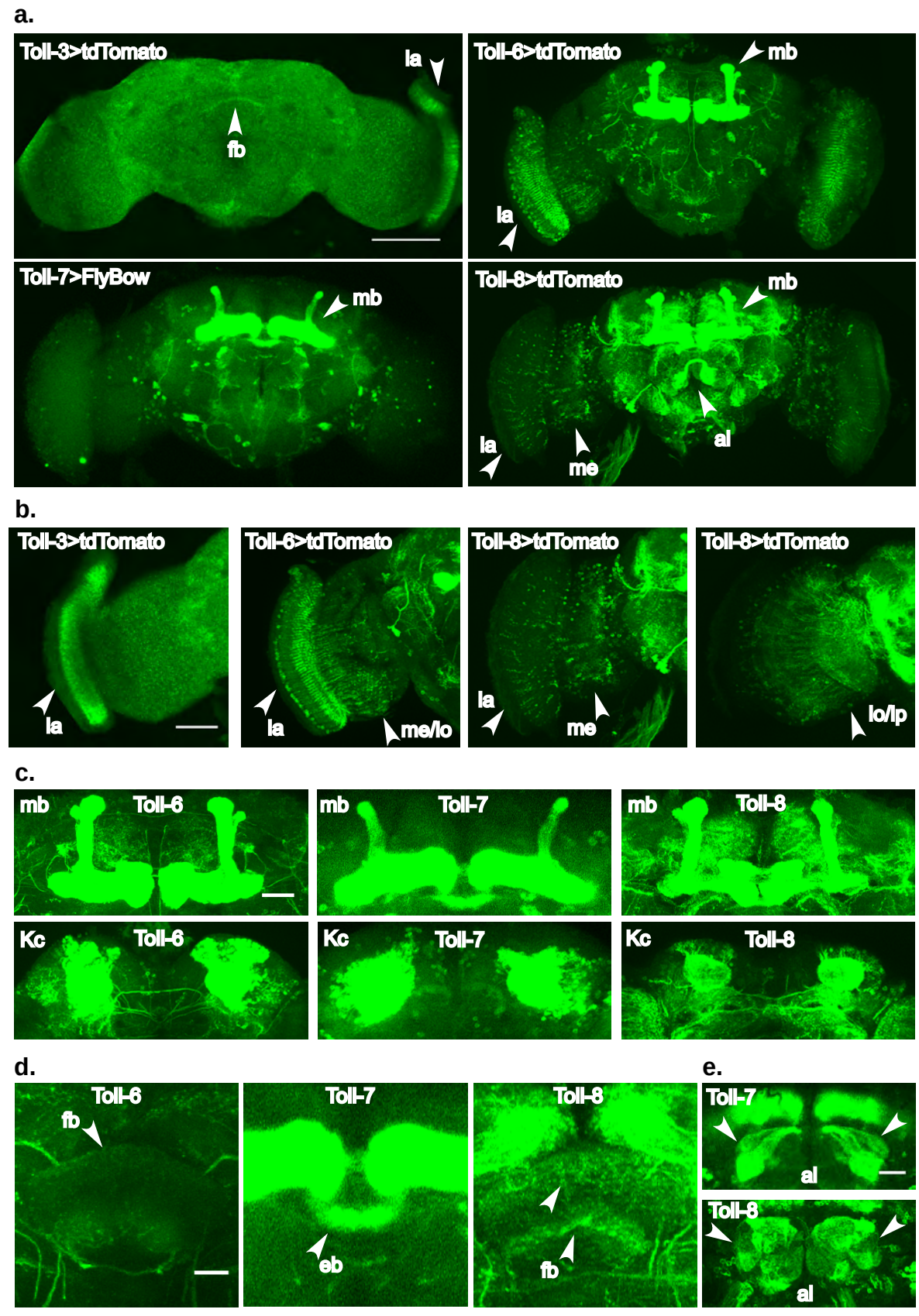


Figure 7.6 *Toll-3, 6, 7, 8* are expressed in the adult brain

(a). Expression pattern of *Toll-3, 6, 7, and 8* in adult brain. The white arrow and annotation indicates the brain region where the gene is highly expressed.

(b). *Toll-3, 6* and *8* are expressed in the optic lobe.

(c). *Toll-6, 7*, and *8* are expressed in the MB.

(d). *Toll-6* and *Toll-8* are expressed in the fan-shaped body, and *Toll-7* is highly expressed in the ellipsoid body.

(e). *Toll-7* and *Toll-8* are highly expressed in the antennal lobe.

Genotype:

Toll-3: Toll-3 $Gal4^{MI02994}$ UAS myr-Td-tomato

Toll-6: Toll-6 $Gal4^{MI02127}$ UAS myr-Td-tomato

Toll-7: Toll-7 $Gal4^{MI13963}$ UAS FlyBow

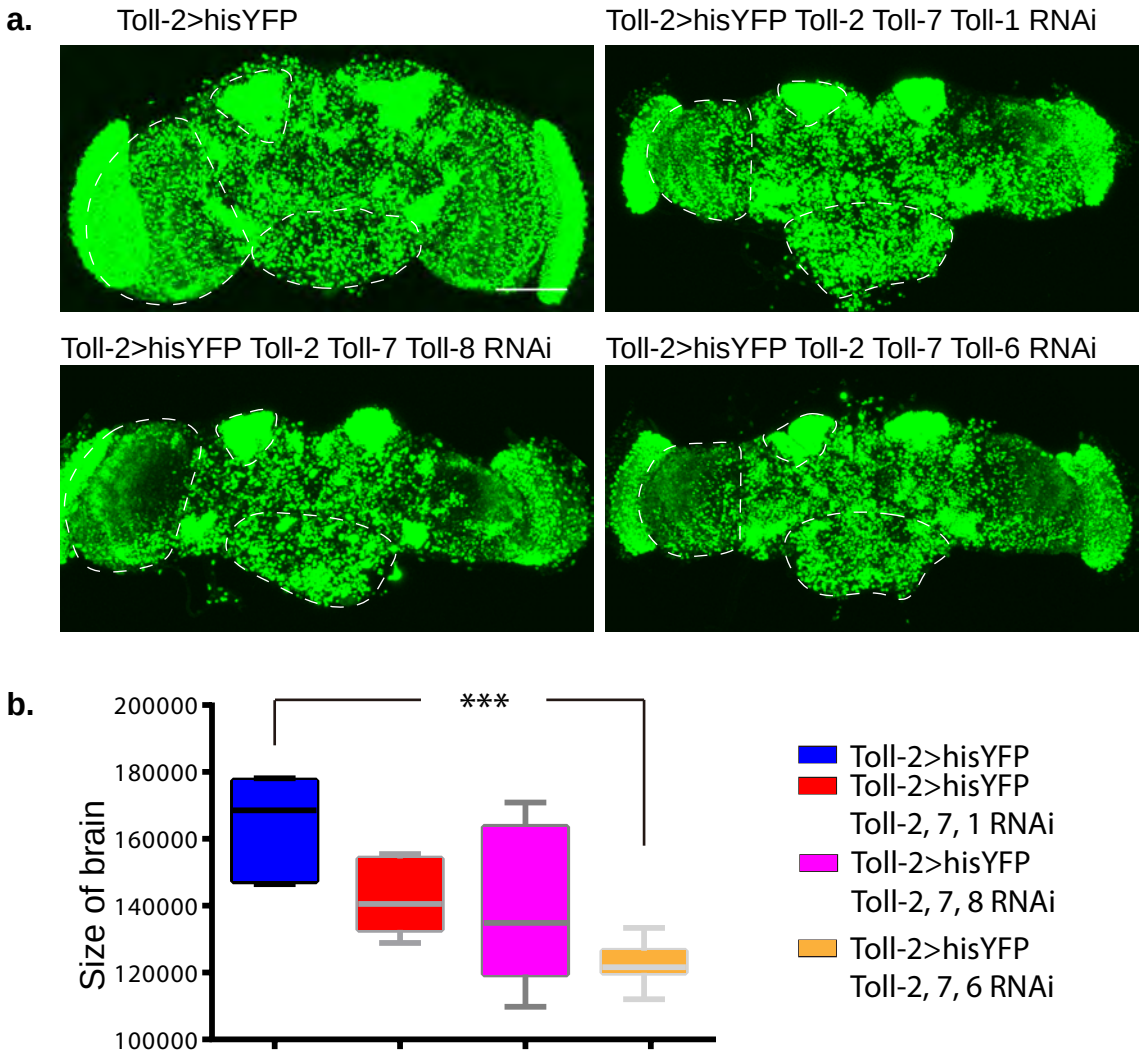
Toll-8: Toll-8 $Gal4^{MD806}$ UAS myr-Td-tomato

Scale bar: a: 100μm; b: 50μm; c and e: 25μm; d: 15μm

Although this meant I could not study the effect of simultaneous knock-down for multiple *Tolls* in the adult brain, I dissected D4 pupal brains and studied how multiple *Tolls* RNAi affected brain structure in the late pupa. It was noticed that the head of the pupa seemed smaller than the control, I therefore firstly measured the size of the whole brain. Results show that among different combination of *Tolls* RNAi, when knocking down *Toll-1*, *2*, *7* or *Toll-2*, *7*, *8* brain size was not significantly changed, although there was a trend showing that the size of the brain in these two genotypes decreased (*Toll-2^{pTV}Gal4/UAS histone YFP Toll-1 RNAi;Toll-2 RNAi/Toll-7 RNAi* and *Toll-2^{pTV}Gal4/UAS histone YFP Toll-8 RNAi;Toll-2 RNAi/Toll-7 RNAi*). By contrast, knocking down Toll-2, 6, and 7 significantly decreased brain size (*Toll-2^{pTV}Gal4/UAS histone YFP Toll-6 RNAi;Toll-2 RNAi/Toll-7 RNAi*) (Figure 7.7 a and b). This result therefore suggests that knocking down multiple Toll receptors decreased brain size.

When measuring brain size, it was noticed that the shape of the brain was different when knocking down *Toll* receptors compared to the control. I therefore measured the size of different brain area. I first studied the effect of knocking down multiple *Tolls* in the MB. MB Kenyon cells were more spread out and less compacted than in controls. As a result, the depth of the cluster of the Kenyon cells was higher than the capacity of *DeadEasy* to handle images, and I was not able to count the number of cells in the MB. As an alternative approach, I measured the depth of the MB KC clusters (Figure 7.8 a and d). I showed that knocking down multiple *Tolls* increased the depth of the KC cluster, though only knocking down *Toll-1*, *2*, *7* showed a significant depth increase, meaning that KCs were less compacted together than in controls. I then measured the area of the MB KC cluster and normalized with the area of the whole brain (Figure 7.8 b and c). Knocking down multiple *Tolls* decreased

Figure 7.7 Simultaneous RNAi knock-down for multiple Tolls reduces brain size



a), D4 pupa brain of the four genotypes including control (Toll-2^{pTV}>histoneYFP), Toll-2, 6, 7 RNAi (Toll-2^{pTV} Gal4>histone YFP, Toll-7 RNAi; Toll-1 RNAi/Toll-2 RNAi), Toll-2, 7, 8 RNAi (Toll-2^{pTV} Gal4>histone YFP, Toll-7 RNAi; Toll-8 RNAi/Toll-2 RNAi), Toll-2, 6, 7 RNAi (Toll-2^{pTV} Gal4>histone YFP, Toll-7 RNAi; Toll-6 RNAi/Toll-2 RNAi). b), Results of measuring the brain size in the control and knocking down multiple Tolls. N=5, 5, 5, 7, One-Way ANOVA, p=0.0018, Dunnett's correction, ***p<0.001. Scale bar: 100μm

Figure 7.8 Simultaneous RNAi knock-down for multiple *Tolls* alters brain structure

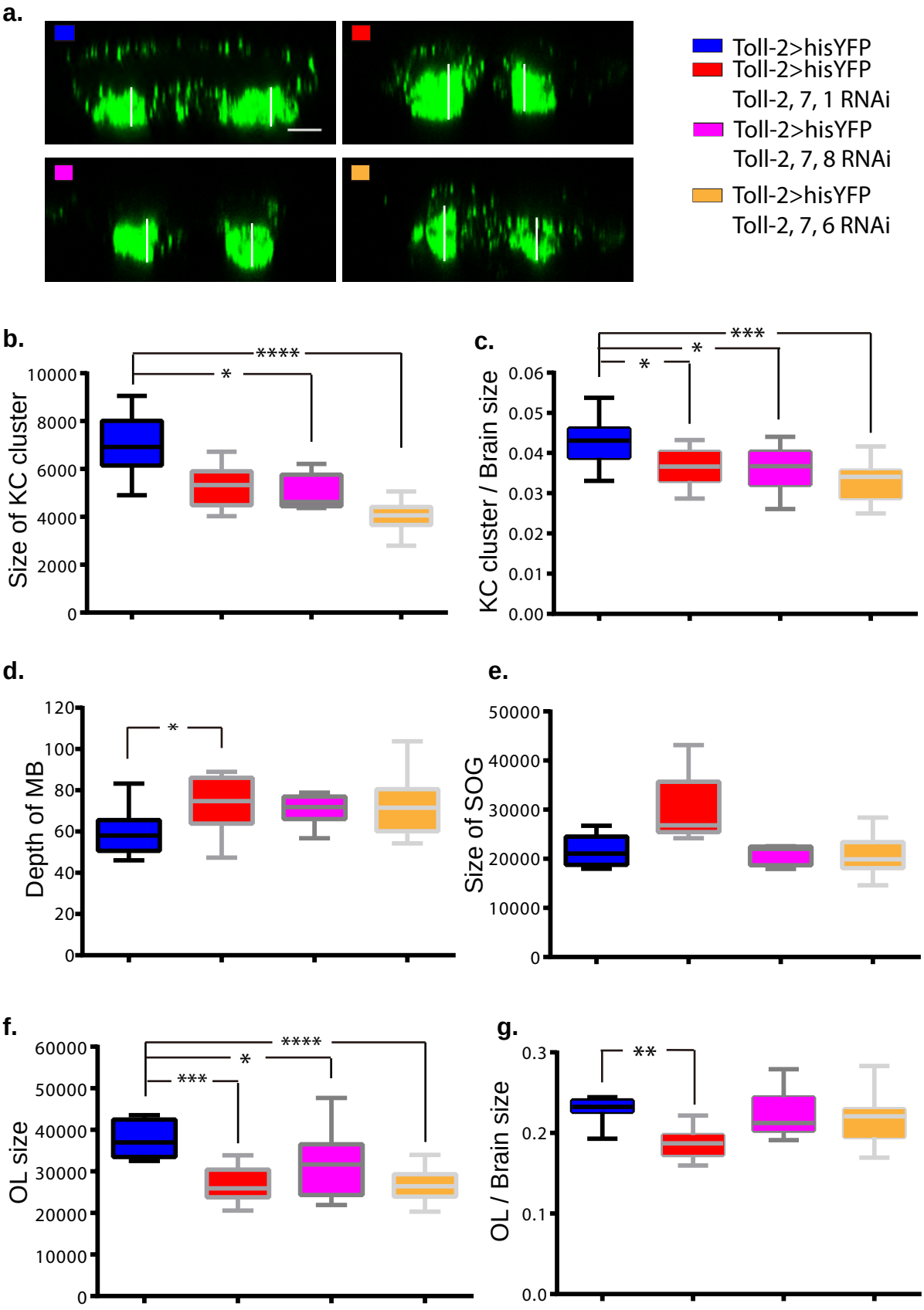


Figure 7.8 Simultaneous RNAi knock-down for multiple *Tolls* alters brain structure

(a). Sagital view of D4 pupal brain, the white lines indicate how depth of MB was measured.

Genotypes: control (Toll-2^{pTV}>histoneYFP),

Toll-2, 7, 1 RNAi (Toll-2^{pTV}Gal4 UAS hisYFP, Toll-7 RNAi; Toll-1 RNAi/Toll-2 RNAi),

Toll-2, 7, 8 RNAi (Toll-2^{pTV}Gal4 UAS hisYFP, Toll-7 RNAi; Toll-8 RNAi/Toll-2 RNAi),

Toll-2, 6, 7 RNAi (Toll-2^{pTV}Gal4 UAS hisYFP, Toll-7 RNAi; Toll-6 RNAi/Toll-2 RNAi).

(b). Result of MB size measurements in the control and knocking down multiple *Tolls.*

Kruskal-Wallis test, $p<0.0001$, Dunn's multiple comparison, *$p<0.05$, ****$p<0.0001$

N=10, 10, 10, 14.

(c). Ratio of size between MB and the whole brain. One-Way ANOVA, $p=0.0005$,

Dunnet's multiple comparison, *$p<0.05$, ***$p<0.001$, N=10, 10, 10, 14.

(d). Result of MB depth measurements. Kruskal-Wallis test, $p=0.06$,

Dunn's multiple comparison, *$p<0.05$, N=10, 10, 10, 14.

(e). Result of SOG size measurements. Kruskal-Wallis test, $p=0.041$,

Dunn's multiple comparison, $p>0.09$, N=5, 5, 5, 7.

(f). Result of OL size measurements. One-way ANOVA, $p<0.0001$,

Dunnet's multiple comparison, *$p<0.05$, ***$p<0.001$, ****$p<0.0001$, N=10, 10, 10, 14.

(g). Ratio of size between OL and the whole brain. One-Way ANOVA, $p=0.002$,

Dunnet's multiple comparison, **$p<0.01$, N=10, 10, 10, 14.

Scale bar: 50μm

the area of MB KC clusters. I also showed that the ratio of MB-KC area to whole brain area significantly decreased in all three combinations of multiple Tolls RNAi genotypes compared with the control (Figure 7.8c). This suggests that knocking down multiple Tolls might have stronger effects on the size of MBs than on the whole brain, suggesting that there might be redundancy between the *Tolls.*

I noticed that when knocking down multiple *Tolls*, some of the brains showed a protruding sub-oesophageal ganglion (SOG). I therefore measured the size of SOG (Figure 7.8e). Here I showed that knocking down *Toll-1, 2*, and *7* increased the size of SOG while other combinations of *Tolls* RNAis did not have a significant effect. Although the increase in *Toll-1*, *2*, *7* RNAi flies was not statistically significant, the trend of increase still suggests that knocking down *Toll-1, 2*, and *7* might cause overgrowth of the SOG.

I also measured the area of optic lobes and normalized it by total brain area (Figure 7.8 f and g). The result shows that knocking down multiple *Tolls* caused significant decrease of size of the optic lobes (Figure 7.8f). The ratio between optic lobes and the whole brain showed that knocking down *Toll-1, 2, 7* caused significant decrease of the OL/brain area ratio, whereas the other *Tolls* RNAi combinations did not have significant effect (Figure 7.8g).

Therefore, knocking down *Toll-1* together with *Toll-2* and *Toll-7* might cause stronger phenotypes than other combinations of *Tolls* in OL.

7.3 Discussion

In this chapter, I have shown that the downstream signalling molecules involved in the *MyD88-NFκB* pathway and the *wek-Sarm-JNK* signalling pathway are active in both pupal and adult brains. Also, altering the activity of downstream signalling molecules specifically in the adult brain could change cell number in the central brain and MB. I also showed that *Toll-3, 6, 7, 8* are expressed in the adult brain. Moreover, knocking down multiple *Tolls* could cause lethality in adult flies and affect the structure of the brain in late pupal stage.

When studying the expression of downstream signalling molecules of the *JNK* pathway, because of the restriction of time and tools, I only studied the expression of *wek* in pupa and *Sarm* in adult. However, as more tools were generated, Mieszyslaw Parker (master student in our lab) investigated more molecules in the pupal and adult brains. For instance, he found that *JNK* signalling is functional in both pupal and adult brains (Mieszyslaw Parker and Alicia Hidalgo, unpublished data). This further confirmed that the *JNK* signalling pathway is active in the pupal and adult brain.

When studying the function of downstream signalling molecules in cell number regulation, activating the cell survival pathways and blocking the cell apoptotic pathways had no significant effect on cell number in either central brain or MB Kenyon cells in the adult. Considering there is not much cell apoptosis during adult stage, blocking cell apoptosis therefore might not cause significant effects on brain cell number. However, there was a trend of increase, albeit not significant, and it is possible that had the sample size been bigger, that increase might have been significant.

It was also noticed that when blocking cell survival and promoting cell death in the adult central brain, cell number was increased, which is opposite to what was expected. This could be explained in two ways. First, promoting cell death might induce secondary proliferation. Second, it has been found that the *Hippo* pathway also functions downstream of *Toll* receptor (Liu et al., 2016). Moreover, activation of *Yorkie*, one of the downstream molecules in the *Hippo* pathway, induces cell proliferation and tissue overgrowth (Zhang et al., 2008). These studies indicate that there might be another *MyD88* independent signalling pathway functioning via *wek*, which promotes cell proliferation downstream of *Toll* receptors.

Cell number in adult MB seems to be less affected when promoting cell death and blocking cell survival or the other way around. A trend shows that promoting cell death and blocking cell survival might increase the cell number in adult MB. This phenotype further suggests that there might be compensatory proliferation or another *Toll* signalling pathway that promotes cell proliferation which is independent from *MyD88*. However, the cell increase was not significant compared with the control. There are two possibilities causing this phenotype. Firstly, it is possible that the sample size was not big enough. To solve this, I could increase the sample size at first and then test whether the increase was significant or not. Secondly, the cell proliferation could be subtle, which might not induce a massive cell number change. In order to test this, I could stain the brain with anti-PH3 antibody or BrdU labelling method to visualize proliferating cells. This could help answer why the cell number increase was not significant.

When studying the interaction between *Toll* receptors in regulating cell number, it was noticed that when knocking down multiple *Tolls*, the size of the whole brain and the MB were reduced. It was shown that the ratio between MB size and the brain size was also reduced. This suggests that decrease of size of the whole brain and MB was not proportional indicating that knocking down multiple *Toll* receptors might cause stronger phenotypes in the MB. Moreover, it was noticed that knocking down multiple *Toll* receptors might cause an increase of MB thickness, meaning that Kenyon cells are not as compactly packed as in wild-type, or that there are more KCs in these genotypes. The statistical analysis showed that only the increase in *Toll-1, 2, 7* RNAi flies was significant, considering that the sample size was not large (N=10-14 MBs, 5-7 brains). However, collectively, these data suggest that combination of multiple *Toll* receptors might be involved to controlling the structure of the MB.

Evidence also showed that knocking down multiple *Toll* receptors decreased the size of the optic lobes. Moreover, knocking down *Toll-1, 2* and *7* also decreased the size ratio between OL and the whole brain while the other two *Toll* RNAi combinations did not (Toll-2, 6, 7 RNAis and Toll-2, 7, 8 RNAis). This suggests that *Toll-1*, *Toll-2* and *Toll-7* might function together to regulate the development of the optic lobes. It also shows that knocking down *Toll-1, 2*, and *7* leads to protruding SOG. I had shown that *Sarm* is pronouncedly expressed in SOG. *Sarm* has been found to promote cell death downstream of *Tolls*. Knocking down *Tolls* might block the function of Sarm, which blocked the cell death caused by Sarm and induced the overgrowth in SOG. Collectively, these data show that *Toll* receptors might have redundant functions to control the structure of the brain. Moreover, different combinations of *Tolls* might regulate different parts of the brain.

Chapter 8 Discussion

8.1 Summary of findings

The aim of this project was to investigate whether Toll receptors regulate cell number plasticity in the brain.

Focusing on *Toll-2*, I first visualised the expression of *Toll-2* by generating *Toll-2* knock-in alleles using the CRISPR-Cas9 system. Firstly, I generated a knock-in allele in which an RFP reporter *mCherry* was inserted into the *Toll-2* locus. Secondly, I generated a *Gal4* knock-in allele in which Gal4 is expressed under the regulation of the *Toll-2* promoter. By staining *Toll-2^{pTV} mCherry* and *Toll-2^{pTV} Gal4* driving *UAS Flybow*, I showed that *Toll-2* is expressed in the larval CNS, pupal brain and adult brain, prominently in optic lobe, central brain and mushroom bodies.

I then studied the effect of *Toll-2* mutants on behaviour. I showed that loss of *Toll-2* function during development reduced longevity and viability, and altered locomotion and vision in adult flies. In order to test whether these defects correlated with cellular phenotypes, I carried out MARCM clones in pupae and showed that *Toll-2* mutant clones caused cell loss and disrupted connectivity in the pupal brain. These phenotypes could be seen in multiple brain domains including the optic lobes, central brain, and mushroom bodies.

I then investigated the effect of *Toll-2* in regulating cell number plasticity in the brain. Here I firstly showed that loss of *Toll-2* function using Toll-2 RNAi during development decreased MyD88+ cell number in the pupal and adult central brain. I then showed that upregulating *Toll-2* expression specifically in the pupal or adult

brain increased MyD88+ cell number in the central brain and medulla in adult optic lobes. These results suggest that *Toll-2* maintains neuronal survival. However, I found that when *Toll-2* was knocked down specifically during pupal stages, cell number in the central brain increased. This might suggest that compensatory proliferation may happen in response to cell death due to loss of *Toll-2* function. Alternatively, *Toll-2* may normally induced cell death, which would explain the increase in cell number upon knock-down. Either way, these results indicate that cell number is plastic in the brain during development, and *Toll-2* is involved in the cell number regulation.

Evidence was also presented that cell number is plastic during the critical period in the adult brain. Knocking down *Toll-2* specifically during adult stages was found to increase MyD88+ cell number in the adult central brain and overexpression of *Toll-2* increases both MyD88+ cell number in the central brain and Toll-2+ cell number in the optic lobes. As in development, the MyD88+ cell number increase caused by loss of Toll-2 function could reveal a pro-apoptotic function of *Toll-2*, or be due to compensatory proliferation after cell loss caused by loss of *Toll-2* function. The cell number increase caused by gain of *Toll-2* function is consistent with *Toll-2* being required to maintain cell survival, although induction of proliferation cannot be ruled out.

I also examined the effect of *Toll-2* on cell number in the MB and found that alteration of *Toll-2* function during development or in a narrowed time window did not change Kenyon cell number significantly. This indicates that cell number regulation in the MB is more robust than in other brain domains.

Investigation of the effect of neuronal activity on cell number also revealed cell number plasticity in the adult brain. Here I showed that activating neurons increased cell number while blocking neuronal activity decreased the cell number in medulla of the adult brain. This result suggests that neuronal activity is linked to cell number regulation.

To examine whether the *Toll* pathway is involved in regulating cell number in the brain, I altered the expression of the signalling molecules functioning downstream of *Toll* and tested the effect on cell number in the central brain and MB Kenyon cells. Firstly, I showed that overexpressing *PI3K* and inhibiting *Cactus* and *JNK* specifically in the adult increased Kenyon cell number, albeit not significantly. Intriguingly, overexpressing *wek* and inhibiting *MyD88* specifically in adult, increased cell number in both the central brain and MB KCs. This suggests that cells may proliferate - either directly triggered by *wek*, or indirectly through compensatory proliferation – via a *MyD88* independent pathway.

Finally, I investigated the function of multiple *Toll* receptors in the brain. Here I showed that *Toll-3*, *6*, *7*, *8* are expressed in the adult brain. I also showed that knocking down multiple *Toll* receptors caused lethality at day 4 pupa. It also altered brain structure and decreased brain size. Optic lobes were smaller compared with the control and the sub-oesophageal ganglion was enlarged.

8.2 *Toll-2* is required throughout development and in the adult *Drosophila*

Toll-2 is expressed from larval CNS to pupal and adult brain. A previous study had shown that *Toll-2* is expressed in high levels in embryos and is involved in planar cell

polarity and cell intercalation during embryogenesis (Pare et al., 2014). Therefore, *Toll-2* is expressed throughout the life of flies. *Toll-2* null mutations cause lethality at embryogenesis, and the survived Toll-2^{pTV}/$18w^{\Delta 7\text{-}35}$ transheterozygous mutant adult flies have shorter life span. These all suggest that *Toll-2* is required throughout development and adult life.

However, different *Toll-2* mutant lines showed different levels of viability. Transheterozygous mutant $18w^{\Delta 7\text{-}35}$/DfBSC594 had a much lower survival rate compared with Toll-2^{pTV}/Toll-$2^{\Delta 7\text{-}35}$ or Toll-2^{pTV}/DfBSC594, while a previously reported transheterozygous mutant $18w^{\Delta 1\text{-}82}$/$18w^{\Delta 7\text{-}35}$ showed an even lower survival rate (1%-3%) (Eldon et al., 1994). Moreover, most of the eclosed $18w^{\Delta 1\text{-}82}$/$18w^{\Delta 7\text{-}35}$ adult flies also showed morphological defects in legs and wings, which has not been observed in this project (Eldon et al., 1994). This may be explained in two ways: firstly, the genetic background of each mutant generated could be different and contribute to the phenotypes. Therefore, the genetic background from different alleles may cause different lethality to different extents in the homozygotes. Secondly, the efficiency of gene knocking down in each mutant line could be different. *Toll-2^{pTV}* was shown to be a knock-in allele in which the coding region is still in the genome while the 5' of the coding region was damaged. Moreover, I showed that parts of the *Toll-2* transcripts could still be detected in the flies. This suggests that *Toll-2^{pTV}* might not be a null allele. However, a previous report has shown that both $18w^{\Delta 1\text{-}82}$ and $18w^{\Delta 7\text{-}35}$ carry deletions, whereby the transcription start site or the first 1.7kb of the Toll-2 coding region were deleted in $18w^{\Delta 1\text{-}82}$ allele and $18w^{\Delta 7\text{-}35}$ allele respectively (Eldon et al., 1994). Moreover, severely reduced or no *Toll-2* mRNA could be detected in these

two alleles. Therefore, the different levels of *Toll-2* expression might explain the variable expressivity of viability and other adult phenotypes.

Toll-2 mutations also cause defects in adult climbing behaviour, seen in Toll-2^{pTV}/$18w^{\Delta 7\text{-}35}$ and Toll-2^{pTV}/DfBSC594 flies. However, this phenotype was not reproduced when inducing loss of *Toll-2* function specifically in neurons or in adult flies only. This indicates that the locomotion phenotype is not due to defective neuronal function or adult specific loss of *Toll-2* function. It has been reported that *Toll-2* plays important roles in the epidermis during embryogenesis involved in cell-cell interaction, cell planar polarity and cell migration during embryogenesis (Eldon et al., 1994, Kleve et al., 2006, Pare et al., 2014). *Toll-2* mutations might cause defects in the epidermis, which might also affect the muscle function as the muscle attaches to the epidermis. This suggests that the defects in locomotion might be due to the loss of *Toll-2* function during development instead of neuronal functions.

8.3 *Toll-2* functions in the brain of *Drosophila*

Apart from developmental function, evidence also shows that *Toll-2* is involved in the nervous system. Results from the Buridan arena test has showed that loss of *Toll-2* function caused defects in vision, and it has been shown that knocking down *Toll-2* through development or specifically in neurons during adult stage both altered visual behaviour. This phenotype matches the finding that *Toll-2* is expressed prominently in optic lobe neurons. Other *Toll* family receptors have been found to have neuronal functions. It has been reported previously that *Toll* has functions on regulating synaptic formation and neuronal survival in embryo CNS (Rose et al., 1997, Zhu et al., 2008). It was also found that *Toll-6* and *Toll-7* functions in CNS regulating

neuronal survival in embryos and neuronal wiring in the embryo and adult (McIlroy et al., 2013; Ward et al., 2015). However, the neuronal functions of *Toll-2* had not been well explored. Therefore, the visual defects caused by loss of *Toll-2* functions in neurons is the first finding showing that *Toll-2* has neuronal functions in the adult brain.

Moreover, results from MARCM clones showed that *Toll-2* mutation in neurons caused neuronal loss and disrupted connectivity. This further indicates that *Toll-2* has neuronal functions and is required for the formation of the brain including the regulation of both cell number and connectivity patterns. It had been previously found that *Toll-6* and *Toll-7* can function as partner matching factors to regulate axonal and dendritic wiring in the adult olfactory system, in a cell-to-cell manner via a cytoplasmic-signalling independent pathway (Ward et al., 2015). Since *Toll-2* is a receptor, the cell loss and disrupted connectivity imply that both cell number and connectivity patterns are regulated by cell interactions in development. However, whether the interaction with *Toll-2* is via cell-cell contact, such as with adhesion molecules, or whether it involves activation by ligands, needs to be further studied. Collectively, these phenotypes indicate that the cell number and circuits in the brain is not hard wired.

8.4 *Toll-2* is required to maintain cell survival via *MyD88-NFκB* pathway during development

Based on the cell loss phenotype from MARCM, I then aimed to verify whether *Toll-2* is truly involved in regulating cell number during development. The *Toll-MyD88-NFκB* pathway is best known for its function in anti-microbial response and dorsal-ventral

patterning (Lemaitre et al., 1996). However, evidence also showed that *Toll* signalling could regulate cell number. It has been found that *Spz* functions via *Toll* and *Toll-8* promoting cell death in cell competition. Downstream molecules *Sarm*, *Tube*, and *NFκB* factor *Relish* (*Rel*) were also involved in this function, although the direct molecular interactions are unknown (Alpar et al., 2018, Meyer et al., 2014). *Relish*, as the downstream factor of the IMD pathway in innate immunity, was also found to cause neurodegeneration upon microbial infection (Kounatidis et al., 2017). These findings suggest that *NFκB* factors can promote cell death. However, in contrast, *Toll-6* has been shown to promote neuronal survival via the *MyD88-NFκB* pathway in the larval CNS (Foldi et al., 2017). I showed that loss of *Toll-2* function during development decreased the MyD88+ cell number in the pupal central brain. This result indicates that *Toll-2* is required to maintain cell survival during development. And Since the Toll-2 RNAi knock-down in this experiment was expressed in *MyD88* cells, the pro-survival function of *Toll-2* is most likely via *MyD88*. Moreover, in order to define which pathway *Toll-2* might function through to regulate cell number, I showed that *MyD88*, and NFκB factors *Dorsal* and *Dif* are all expressed in the brain, suggesting that the NFκB pathway is active in the brain. Therefore, these results indicate that *Toll-2* could promote cell survival possibly via the *MyD88-NFκB* pathway in the developing brain.

I also showed that gain of *Toll-2* function specifically in the pupa stage could increase cell number in the pupal central brain. This is consistent with the pro-survival function of *Toll-2* during development. Pupal stage is when metamorphosis happens and most of the cells die in the CNS to make place for the new cells that will form the adult brain (Tissot and Stocker, 2000). Therefore, the pulse of *Toll-2* could prevent

MyD88+ cells from dying during metamorphosis, thus resulting in the cell number change.

Interestingly, when *Toll-2* function was knocked down specifically at pupal stage, the cell number increased in the pupal central brain. During metamorphosis, neuroblasts are highly active and proliferate and generate new cells. It has been found that the activity of neuroblasts is the highest in the first 48 hours after puparium formation (APF). It is therefore conceivable that loss of *Toll-2* function in the pupae causes cell death, which induces neuroblasts to proliferate more to compensate the cell loss, ultimately leads to a cell number increase.

8.5 Cell number is plastic in the adult brain during critical period

There has been literature, but limited, showing that cell number in the adult brain is plastic. However, I showed that knocking down *Toll-2* during development decreased the MyD88+ cell number, also when cells were counted in the adult central brain. This suggests that *Toll-2* may also be required to maintain cell survival not just in the pupal brain, but in the adult. It has been previously reported that in the normal brain there is not much cell death in adult (Kato et al., 2009). However, when I manipulate *Toll-2* function, the normal mechanisms that maintain tissue integrity break down, and cells die. Therefore, the pro-survival function of *Toll-2* means that the adult brain is not static and cell survival is actively maintained.

In order to study whether cell number is plastic in the adult brain during the critical period, I altered *Toll-2* function specifically in the adult stage. Here I showed that overexpression of *Toll-2* specifically in adult increased cell number in the central brain and medulla. Since it has been found that cell apoptosis is very rare in the adult

brain, the significant cell increase caused by *Toll-2* overexpression is unlikely to be due to the neurons being rescued from cell death in the adult. In this case, it is more likely that overexpression of *Toll-2* induced the cell proliferation in the adult brain.

Cell proliferation in the adult brain has been controversial, but there is evidence showing that there is cell proliferation in the adult brain. It has been shown that glial cells are able to proliferate after injury (Kato et al., 2009). Subtle neurogenesis was observed through MARCM clones in the adult medulla suggesting that there are slow cycling progenitors in the adult brain, at least in the optic lobe medulla (Fernandez-Hernandez et al., 2013). Moreover, evidence has also been provided that glial loss in the adult by caused by mutant miR31 could be compensated in the later adult stage, also suggesting that there are neural progenitor cells in the adult brain (Foo et al., 2017). Furthermore, mushroom body neuroblasts have also been found to persist in the adult brain when knocking down gene *Foxo* or *reaper* (Siegrist et al., 2010). These findings suggest that there might be undiscovered progenitors or reactivated neuroblasts in the adult brain and the cell increase caused by overexpression of *Toll-2* might be due to the cell proliferation in adult brain.

In the adult brain, I found that knocking down *Toll-2* specifically in adult could increase cell number, suggesting that there might be compensatory proliferation stimulated by cell loss caused by loss of *Toll-2* function. This is similar to what have been observed in the pupal brain. And it is also reminiscent of the previous report that apoptosis in the normal adult brain induces proliferation in glial cells (Kato et al., 2009). However, differently, no neuroblasts have been detected in the adult brain. When visualizing *MyD88* expression in the adult brain, some large cells were noticed

that were Elav- and Repo- suggesting that these cells might be polyploid cells that cannot divide or previously uncharacterized progenitor cells other than neurons or glia. However, I could not detect *Dpn*+ cells in the adult brain. This suggests that if there are progenitor cells in the adult brain, they do not express *Deadpan*. Perhaps there are cells in a pre-progenitor state, that do not yet express Dpn. Altogether, my data suggest that there might be progenitor cells in the adult brain that can proliferate under specific conditions, like cell loss. However, new markers need to be generated to detect these progenitor cells in the adult brain.

8.6 Neuronal activity is linked with the cell number plasticity in the adult brain

Neuronal activity was found to be another factor affecting cell number in the adult brain. Heisenberg's lab had shown that stimuli from the environment in early adulthood could change the volume of the size of multiple brain domains (Barth et al., 1997; Barth and Heisenberg, 1997; Heisenberg et al., 1995). They noticed a significant change of the circuitry in calyx (Heisenberg et al., 1995). They also mentioned that cell number might also be involved in the brain volume change, although they did not study this any further. Therefore, I studied how neuronal number responds to the stimuli in adult. Here I showed that activating or blocking neurons in the adult changes cell number in the medulla, whereby activating neurons increase the cell number and blocking neurons decrease the cell number. These results further indicate that neuronal number is plastic in the adult brain. They also suggest that neuronal activity can maintain the survival. Furthermore, since activating neurons is important for behaviours like learning and memory, the link between

neuronal activity and cell number might suggest that cell number plasticity could be influence how the brain elicits or modifies behaviour.

8.7 Multiple *Tolls* play redundant roles in mushroom body

According to the previous findings, mushroom bodies seemed to be highly plastic responding to the environmental change (Barth and Heisenberg, 1997; Barth et al., 1997). However, those reported changes in MBs were interpreted as changes in synaptogenesis and axonal and dendritic structure. Although cell number is plastic in the central brain and medulla, in my experiments, Kenyon cells number was more robust compared to other brain domains as no dramatic change was observed here. Evidence shows that alterations in *Toll-2* function during development did not change the KC number neither in the pupal or adult brain. A pulse of *Toll-2* function specifically in the adult did not cause significant Kenyon cell number change either. This might suggest that MBs are more plastic in cell size and shape, as reported by Heisenberg and Barth, whereas cell number may be more stable and robust.

Robustness of the MB Kenyon cells might be conferred by the expression of multiple *Toll* receptors. It has been previously found that although loss of either *Toll-6* or *Toll-7* caused cell death in the embryonic central nervous system and locomotion defects in larvae, *Toll-6 Toll-7* double mutants showed much stronger phenotypes that the single mutants alone (McIlroy et al., 2013). This suggests that there is redundancy between *Toll-6* and *Toll-7*. I have shown that at least 4 *Toll* receptors are expressed prominently in the MB including *Toll-2*, *6*, *7*, and *8*, and data from other lab members also showed that *Toll-5* is expressed in the mushroom bodies (Jacob Hasenauer, Hidalgo lab). Among these Toll receptors, *Toll-1*, *Toll-6* and *Toll-7* can promote cell

survival (Zhu et al., 2008, McIlroy et al., 2013) ad it has been shown that at least Toll-6 does so via the *MyD88-NFkB* pathway, and promotes cell death via *wek-sarm-JNK*, in larval and pupal CNS (Foldi et al., 2017). Therefore, perhaps knocking down *Toll-2* alone did not affect the Kenyon cell number because other *Tolls* might have redundant functions, and thus compensate for the loss of *Toll-2*, to maintain cell number stability. I have provided evidence that knocking down multiple *Tolls* caused lethality in late pupae and altered brain structure. Overall brain size was found smaller compared with that of controls with a significant decrease in optic lobe size and MB Kenyon cell cluster area. By contrast, the size of the sub-oesophageal ganglion (SOG) was enlarged particularly when knocking down *Toll-1, 2,* and *7*. I have shown that *Sarm* is expressed in the brain prominently in the SOG. *Sarm* is a well-known downstream factor of *Toll-1* promoting apoptosis in innate immunity (Valanne et al., 2011), and it also functions downstream of *Toll-1* and *Toll-6* promoting cell death in the CNS (Foldi et al., 2017). Therefore, when knocking down *Toll-1* and *Toll-6*, cell apoptosis might be blocked in SOG inducing the increase in size in this region. To conclude, MB Kenyon cell number shows higher robustness than that of other brain domains, which might be due to the redundancy of multiple Toll receptors.

8.8 Cell proliferation via non-canonical signalling pathways downstream of *Toll-2* in adult brain

I have shown that *Toll-2* could promote cell survival via the *MyD88-NFkB* pathway in both pupal and adult brain. *FOXO* is also known to be involved in maintaining cell survival downstream of PI3K signalling, and *FOXO* is also a known downstream target of *Toll-6* (McLaughlin et al., 2016). When activating the downstream signalling

pathways of *Toll*, including the *NFkB* pathway and the *PI3K* pathway, and blocking the *JNK* signalling pathway, cell number increase was observed in adult central brain. This indicates that *Toll*-receptors downstream signalling pathways can influence and maintain neuronal survival in the adult brain. However, when blocking *MyD88* and overexpressing *wek*, cell number increase was also detected in the adult central brain and potentially in MB. There are two possible mechanisms causing this cell increase: firstly, cell apoptosis induced by this genotype might cause non-autonomous compensatory proliferation; secondly, *wek* could induce cell-autonomous cell proliferation via a *MyD88*-independ pathway. In fact, I have shown that *Toll-2* cells are able to proliferate as overexpression of the cell cycle inhibitor *Retinoblastoma* (*Rbf*) induced decreased cell number in the pupal brain. As mentioned before, there are large MyD88+ cells that are neither Repo+ nor Elav+ in the brain, and instead might be polyploid cells or uncharacterized neuroblasts. Therefore, there are Toll-2+ and MyD88+ cells that might be able to proliferate in the adult brain but are inhibited under normal conditions.

It has been shown that *MyD88* inhibits *Yorkie* indirectly via *Pelle*-*Cka*-*Hippo* pathway (Liu et al., 2016). *Yorkie* is known to promote cell proliferation. Therefore, blocking *MyD88* might release the inhibition of *yorkie*, which induces cell proliferation. Moreover, overexpression of *wek* might also trigger the recruitment of wek to promote cell proliferation via *yorkie* or other factors, which is *MyD88* independent.

8.9 Future work

I have shown that cell number is plastic in the adult brain, but whether the cell number change is via apoptosis, survival or proliferation has not been demonstrated.

In the future, I would test whether cell loss caused by loss of *Toll-2* function is via cell apoptosis and whether it could be rescued by the cell death inhibitor *p35*. Moreover, I would test whether cell increase caused by gain of *Toll-2* function, increase of neuronal activity, and alteration of downstream signalling molecules is caused by neuronal survival or / and cell proliferation. To test this, I would carry out immunostaining like anti-PH3 staining to detect proliferating cells and also test whether the cell number increase could be rescued by cell cycle inhibitor *Rbf*. I would also test whether I can visualise newly generated neurons with activity or *Toll-2* gain of function with MARCM clones. Moreover, I would test whether *yorkie* is involved, for example, whether the cell increase caused by over-expression of *Toll-2* can be rescued with *yorkie* knock-down.

Moreover, I have shown that both a pulse of *Toll-2* expression or alteration in neuronal activity can change cell number specifically in the adult brain. However, whether *Toll-2* is involved in neuronal activity has not been studied. In the next step, I would study whether *Toll-2* is involved in cell number changes by neuronal activity.

8.10 Conclusion and implications

To conclude, my PhD research has shown that *Tolls* are expressed and functional in the adult brain. My data show that *Toll* receptors are required for brain formation and to maintain brain integrity throughout life and into ageing. *Tolls* were best known for their functions in immunity. My findings have revealed non-immune functions in the adult brain, regulating brain plasticity via downstream, nuclear signalling pathway.

My work makes a tight link between *Toll* receptors and neuronal functions in the brain. It will be important to test whether similar mechanisms would operate in the human

brain. For example, this would promote the investigation of the neuronal functions of *TLRs*, the homologues of *Tolls* in mammals. The discoveries on cell number plasticity would shed more light on studies of cancer and brain tumours, ageing, and neurodegeneration related brain diseases like Alzheimer's disease and Parkinson's disease.

References

ADAMS, M. D., CELNIKER, S. E., HOLT, R. A., EVANS, C. A., GOCAYNE, J. D., AMANATIDES, P. G., SCHERER, S. E., LI, P. W., HOSKINS, R. A., GALLE, R. F., GEORGE, R. A., LEWIS, S. E., RICHARDS, S., ASHBURNER, M., HENDERSON, S. N., SUTTON, G. G., WORTMAN, J. R., YANDELL, M. D., ZHANG, Q., CHEN, L. X., BRANDON, R. C., ROGERS, Y. H., BLAZEJ, R. G., CHAMPE, M., PFEIFFER, B. D., WAN, K. H., DOYLE, C., BAXTER, E. G., HELT, G., NELSON, C. R., GABOR, G. L., ABRIL, J. F., AGBAYANI, A., AN, H. J., ANDREWS-PFANNKOCH, C., BALDWIN, D., BALLEW, R. M., BASU, A., BAXENDALE, J., BAYRAKTAROGLU, L., BEASLEY, E. M., BEESON, K. Y., BENOS, P. V., BERMAN, B. P., BHANDARI, D., BOLSHAKOV, S., BORKOVA, D., BOTCHAN, M. R., BOUCK, J., BROKSTEIN, P., BROTTIER, P., BURTIS, K. C., BUSAM, D. A., BUTLER, H., CADIEU, E., CENTER, A., CHANDRA, I., CHERRY, J. M., CAWLEY, S., DAHLKE, C., DAVENPORT, L. B., DAVIES, P., DE PABLOS, B., DELCHER, A., DENG, Z., MAYS, A. D., DEW, I., DIETZ, S. M., DODSON, K., DOUP, L. E., DOWNES, M., DUGAN-ROCHA, S., DUNKOV, B. C., DUNN, P., DURBIN, K. J., EVANGELISTA, C. C., FERRAZ, C., FERRIERA, S., FLEISCHMANN, W., FOSLER, C., GABRIELIAN, A. E., GARG, N. S., GELBART, W. M., GLASSER, K., GLODEK, A., GONG, F., GORRELL, J. H., GU, Z., GUAN, P., HARRIS, M., HARRIS, N. L., HARVEY, D., HEIMAN, T. J., HERNANDEZ, J. R., HOUCK, J., HOSTIN, D., HOUSTON, K. A., HOWLAND, T. J., WEI, M. H., IBEGWAM, C., et al. 2000. The genome sequence of Drosophila melanogaster. *Science,* 287**,** 2185-95.

AKIRA, S. 2006. TLR signaling. *Curr Top Microbiol Immunol,* 311**,** 1-16.

AKIRA, S. & TAKEDA, K. 2004a. Functions of toll-like receptors: lessons from KO mice. *C R Biol,* 327**,** 581-9.

AKIRA, S. & TAKEDA, K. 2004b. Toll-like receptor signalling. *Nat Rev Immunol,* 4**,** 499-511.

ALEXOPOULOU, L., HOLT, A. C., MEDZHITOV, R. & FLAVELL, R. A. 2001. Recognition of double-stranded RNA and activation of NF-kappaB by Toll-like receptor 3. *Nature,* 413**,** 732-8.

ANDERSON, K. V. 2000. Toll signaling pathways in the innate immune response. *Curr Opin Immunol,* 12**,** 13-9.

APITZ, H. & SALECKER, I. 2015. A region-specific neurogenesis mode requires migratory progenitors in the Drosophila visual system. *Nat Neurosci,* 18**,** 46-55.

BAENA-LOPEZ, L. A., ALEXANDRE, C., MITCHELL, A., PASAKARNIS, L. & VINCENT, J. P. 2013. Accelerated homologous recombination and subsequent genome modification in Drosophila. *Development,* 140**,** 4818-25.

BALLARD, S. L., MILLER, D. L. & GANETZKY, B. 2014. Retrograde neurotrophin signaling through Tollo regulates synaptic growth in Drosophila. *J Cell Biol,* 204**,** 1157-72.

BARRES, B. A., BURNE, J. F., HOLTMANN, B., THOENEN, H., SENDTNER, M. & RAFF, M. C. 1996. Ciliary neurotrophic factor enhances the rate of oligodendrocyte generation. *Mol Cell Neurosci,* 8**,** 146-56.

BARTH, M. 1999. Experience-dependent development of the adult optic lobe and central brain in Drosophila melanogaster. *Ross Fiziol Zh Im I M Sechenova,* 85**,** 184-94.

BARTH, M. & HEISENBERG, M. 1997. Vision affects mushroom bodies and central complex in Drosophila melanogaster. *Learn Mem,* 4**,** 219-29.

BARTH, M., HIRSCH, H. V., MEINERTZHAGEN, I. A. & HEISENBERG, M. 1997. Experience-dependent developmental plasticity in the optic lobe of Drosophila melanogaster. *J Neurosci,* 17**,** 1493-504.

BAZELLIERES, E., ASSEMAT, E., ARSANTO, J. P., LE BIVIC, A. & MASSEY-HARROCHE, D. 2009. Crumbs proteins in epithelial morphogenesis. *Front Biosci (Landmark Ed),* 14**,** 2149-69.

BELVIN, M. P. & ANDERSON, K. V. 1996. A conserved signaling pathway: the Drosophila toll-dorsal pathway. *Annu Rev Cell Dev Biol,* 12**,** 393-416.

BIBEL, M. & BARDE, Y. A. 2000. Neurotrophins: key regulators of cell fate and cell shape in the vertebrate nervous system. *Genes Dev,* 14**,** 2919-37.

BLOCHL, A., BLUMENSTEIN, L. & AHMADIAN, M. R. 2004. Inactivation and activation of Ras by the neurotrophin receptor p75. *Eur J Neurosci,* 20**,** 2321-35.

BUCHON, N., POIDEVIN, M., KWON, H. M., GUILLOU, A., SOTTAS, V., LEE, B. L. & LEMAITRE, B. 2009. A single modular serine protease integrates signals from pattern-recognition receptors upstream of the Drosophila Toll pathway. *Proc Natl Acad Sci U S A,* 106**,** 12442-7.

CARPENTIER, P. A., DUNCAN, D. S. & MILLER, S. D. 2008. Glial toll-like receptor signaling in central nervous system infection and autoimmunity. *Brain Behav Immun,* 22**,** 140-7.

CHAO, M. V. 2003. Neurotrophins and their receptors: a convergence point for many signalling pathways. *Nat Rev Neurosci,* 4**,** 299-309.

CHEN, Z. Y., IERACI, A., TENG, H., DALL, H., MENG, C. X., HERRERA, D. G., NYKJAER, A., HEMPSTEAD, B. L. & LEE, F. S. 2005. Sortilin controls intracellular sorting of brain-derived neurotrophic factor to the regulated secretory pathway. *J Neurosci,* 25**,** 6156-66.

COUTINHO-BUDD, J. C., SHEEHAN, A. E. & FREEMAN, M. R. 2017. The secreted neurotrophin Spatzle 3 promotes glial morphogenesis and supports neuronal survival and function. *Genes Dev,* 31**,** 2023-2038.

CROWDER, R. J. & FREEMAN, R. S. 1998. Phosphatidylinositol 3-kinase and Akt protein kinase are necessary and sufficient for the survival of nerve growth factor-dependent sympathetic neurons. *J Neurosci,* 18**,** 2933-43.

DAVIS, G. W. & GOODMAN, C. S. 1998. Genetic analysis of synaptic development and plasticity: homeostatic regulation of synaptic efficacy. *Curr Opin Neurobiol,* 8**,** 149-56.

DELOTTO, Y. & DELOTTO, R. 1998. Proteolytic processing of the Drosophila Spatzle protein by easter generates a dimeric NGF-like molecule with ventralising activity. *Mech Dev,* 72**,** 141-8.

DENG, W., AIMONE, J. B. & GAGE, F. H. 2010. New neurons and new memories: how does adult hippocampal neurogenesis affect learning and memory? *Nat Rev Neurosci,* 11**,** 339-50.

DOBROWSKY, R. T., WERNER, M. H., CASTELLINO, A. M., CHAO, M. V. & HANNUN, Y. A. 1994. Activation of the sphingomyelin cycle through the low-affinity neurotrophin receptor. *Science,* 265**,** 1596-9.

DUPRET, D., FABRE, A., DOBROSSY, M. D., PANATIER, A., RODRIGUEZ, J. J., LAMARQUE, S., LEMAIRE, V., OLIET, S. H., PIAZZA, P. V. & ABROUS, D. N. 2007.

Spatial learning depends on both the addition and removal of new hippocampal neurons. *PLoS Biol,* 5**,** e214.

EL CHAMY, L., LECLERC, V., CALDELARI, I. & REICHHART, J. M. 2008. Sensing of 'danger signals' and pathogen-associated molecular patterns defines binary signaling pathways 'upstream' of Toll. *Nat Immunol,* 9**,** 1165-70.

ELDON, E., KOOYER, S., D'EVELYN, D., DUMAN, M., LAWINGER, P., BOTAS, J. & BELLEN, H. 1994. The Drosophila 18 wheeler is required for morphogenesis and has striking similarities to Toll. *Development,* 120**,** 885-99.

ERIKSSON, P. S., PERFILIEVA, E., BJORK-ERIKSSON, T., ALBORN, A. M., NORDBORG, C., PETERSON, D. A. & GAGE, F. H. 1998. Neurogenesis in the adult human hippocampus. *Nat Med,* 4**,** 1313-7.

FEHLBAUM, P., BULET, P., MICHAUT, L., LAGUEUX, M., BROEKAERT, W. F., HETRU, C. & HOFFMANN, J. A. 1994. Insect immunity. Septic injury of Drosophila induces the synthesis of a potent antifungal peptide with sequence homology to plant antifungal peptides. *J Biol Chem,* 269**,** 33159-63.

FERNANDEZ-HERNANDEZ, I., RHINER, C. & MORENO, E. 2013. Adult neurogenesis in Drosophila. *Cell Rep,* 3**,** 1857-65.

FOLDI, I., ANTHONEY, N., HARRISON, N., GANGLOFF, M., VERSTAK, B., NALLASIVAN, M. P., ALAHMED, S., ZHU, B., PHIZACKLEA, M., LOSADA-PEREZ, M., MOREIRA, M., GAY, N. J. & HIDALGO, A. 2017. Three-tier regulation of cell number plasticity by neurotrophins and Tolls in Drosophila. *J Cell Biol,* 216**,** 1421-1438.

FOO, L. C., SONG, S. & COHEN, S. M. 2017. miR-31 mutants reveal continuous glial homeostasis in the adult Drosophila brain. *EMBO J,* 36**,** 1215-1226.

FRANKE, T. F., KAPLAN, D. R. & CANTLEY, L. C. 1997. PI3K: downstream AKTion blocks apoptosis. *Cell,* 88**,** 435-7.

GAGE, F. H. 2004. Structural plasticity of the adult brain. *Dialogues Clin Neurosci,* 6**,** 135-41.

GALLAUD, E., PHAM, T. & CABERNARD, C. 2017. Drosophila melanogaster Neuroblasts: A Model for Asymmetric Stem Cell Divisions. *Results Probl Cell Differ,* 61**,** 183-210.

GARTNER, A., POLNAU, D. G., STAIGER, V., SCIARRETTA, C., MINICHIELLO, L., THOENEN, H., BONHOEFFER, T. & KORTE, M. 2006. Hippocampal long-term potentiation is supported by presynaptic and postsynaptic tyrosine receptor kinase B-mediated phospholipase Cgamma signaling. *J Neurosci,* 26**,** 3496-504.

GAY, N. J. & GANGLOFF, M. 2008. Structure of toll-like receptors. *Handb Exp Pharmacol***,** 181-200.

GENEVET, A., POLESELLO, C., BLIGHT, K., ROBERTSON, F., COLLINSON, L. M., PICHAUD, F. & TAPON, N. 2009. The Hippo pathway regulates apical-domain size independently of its growth-control function. *J Cell Sci,* 122**,** 2360-70.

GORSKA-ANDRZEJAK, J., KELLER, A., RAABE, T., KILIANEK, L. & PYZA, E. 2005. Structural daily rhythms in GFP-labelled neurons in the visual system of Drosophila melanogaster. *Photochem Photobiol Sci,* 4**,** 721-6.

GOTTAR, M., GOBERT, V., MATSKEVICH, A. A., REICHHART, J. M., WANG, C., BUTT, T. M., BELVIN, M., HOFFMANN, J. A. & FERRANDON, D. 2006. Dual detection of fungal infections in Drosophila via recognition of glucans and sensing of virulence factors. *Cell,* 127**,** 1425-37.

HAGHAYEGHI, A., SARAC, A., CZERNIECKI, S., GROSSHANS, J. & SCHOCK, F. 2010. Pellino enhances innate immunity in Drosophila. *Mech Dev,* 127**,** 301-7.

HALFON, M. S., HASHIMOTO, C. & KESHISHIAN, H. 1995. The Drosophila toll gene functions zygotically and is necessary for proper motoneuron and muscle development. *Dev Biol,* 169**,** 151-67.

HEIL, F., HEMMI, H., HOCHREIN, H., AMPENBERGER, F., KIRSCHNING, C., AKIRA, S., LIPFORD, G., WAGNER, H. & BAUER, S. 2004. Species-specific recognition of single-stranded RNA via toll-like receptor 7 and 8. *Science,* 303**,** 1526-9.

HEISENBERG, M. 1998. What do the mushroom bodies do for the insect brain? an introduction. *Learn Mem,* 5**,** 1-10.

HEISENBERG, M., HEUSIPP, M. & WANKE, C. 1995. Structural plasticity in the Drosophila brain. *J Neurosci,* 15**,** 1951-60.

HEMMI, H., KAISHO, T., TAKEUCHI, O., SATO, S., SANJO, H., HOSHINO, K., HORIUCHI, T., TOMIZAWA, H., TAKEDA, K. & AKIRA, S. 2002. Small anti-viral compounds activate immune cells via the TLR7 MyD88-dependent signaling pathway. *Nat Immunol,* 3**,** 196-200.

HETRU, C., TROXLER, L. & HOFFMANN, J. A. 2003. Drosophila melanogaster antimicrobial defense. *J Infect Dis,* 187 Suppl 2**,** S327-34.

HOFER, S. B., MRSIC-FLOGEL, T. D., BONHOEFFER, T. & HUBENER, M. 2009. Experience leaves a lasting structural trace in cortical circuits. *Nature,* 457**,** 313-7.

HOLGADO-MADRUGA, M., MOSCATELLO, D. K., EMLET, D. R., DIETERICH, R. & WONG, A. J. 1997. Grb2-associated binder-1 mediates phosphatidylinositol 3-kinase

activation and the promotion of cell survival by nerve growth factor. *Proc Natl Acad Sci U S A,* 94**,** 12419-24.

HOLTMAAT, A. & SVOBODA, K. 2009. Experience-dependent structural synaptic plasticity in the mammalian brain. *Nat Rev Neurosci,* 10**,** 647-58.

HOMEM, C. C. & KNOBLICH, J. A. 2012. Drosophila neuroblasts: a model for stem cell biology. *Development,* 139**,** 4297-310.

HUANG, E. J. & REICHARDT, L. F. 2003. Trk receptors: roles in neuronal signal transduction. *Annu Rev Biochem,* 72**,** 609-42.

IMLER, J. L. & ZHENG, L. 2004. Biology of Toll receptors: lessons from insects and mammals. *J Leukoc Biol,* 75**,** 18-26.

IP, Y. T., REACH, M., ENGSTROM, Y., KADALAYIL, L., CAI, H., GONZALEZ-CRESPO, S., TATEI, K. & LEVINE, M. 1993. Dif, a dorsal-related gene that mediates an immune response in Drosophila. *Cell,* 75**,** 753-63.

JOHNSON, R. & HALDER, G. 2014. The two faces of Hippo: targeting the Hippo pathway for regenerative medicine and cancer treatment. *Nat Rev Drug Discov,* 13**,** 63-79.

KAPLAN, D. R. & MILLER, F. D. 2000. Neurotrophin signal transduction in the nervous system. *Curr Opin Neurobiol,* 10**,** 381-91.

KATO, K., AWASAKI, T. & ITO, K. 2009. Neuronal programmed cell death induces glial cell division in the adult Drosophila brain. *Development,* 136**,** 51-9.

KEITH, F. J. & GAY, N. J. 1990. The Drosophila membrane receptor Toll can function to promote cellular adhesion. *EMBO J,* 9**,** 4299-306.

KOUHARA, H., HADARI, Y. R., SPIVAK-KROIZMAN, T., SCHILLING, J., BAR-SAGI, D., LAX, I. & SCHLESSINGER, J. 1997. A lipid-anchored Grb2-binding protein that links FGF-receptor activation to the Ras/MAPK signaling pathway. *Cell,* 89**,** 693-702.

KRAFT, K. F., MASSEY, E. M., KOLB, D., WALLDORF, U. & URBACH, R. 2016. Retinal homeobox promotes cell growth, proliferation and survival of mushroom body neuroblasts in the Drosophila brain. *Mech Dev,* 142**,** 50-61.

KREMER, M. C., CHRISTIANSEN, F., LEISS, F., PAEHLER, M., KNAPEK, S., ANDLAUER, T. F., FORSTNER, F., KLOPPENBURG, P., SIGRIST, S. J. & TAVOSANIS, G. 2010. Structural long-term changes at mushroom body input synapses. *Curr Biol,* 20**,** 1938-44.

KURUSU, M., AWASAKI, T., MASUDA-NAKAGAWA, L. M., KAWAUCHI, H., ITO, K. & FURUKUBO-TOKUNAGA, K. 2002. Embryonic and larval development of the Drosophila mushroom bodies: concentric layer subdivisions and the role of fasciclin II. *Development,* 129**,** 409-19.

LANET, E., GOULD, A. P. & MAURANGE, C. 2013. Protection of neuronal diversity at the expense of neuronal numbers during nutrient restriction in the Drosophila visual system. *Cell Rep,* 3**,** 587-94.

LEE, R., KERMANI, P., TENG, K. K. & HEMPSTEAD, B. L. 2001. Regulation of cell survival by secreted proneurotrophins. *Science,* 294**,** 1945-8.

LEHNARDT, S., HENNEKE, P., LIEN, E., KASPER, D. L., VOLPE, J. J., BECHMANN, I., NITSCH, R., WEBER, J. R., GOLENBOCK, D. T. & VARTANIAN, T. 2006. A mechanism for neurodegeneration induced by group B streptococci through activation of the TLR2/MyD88 pathway in microglia. *J Immunol,* 177**,** 583-92.

LEHNARDT, S., LACHANCE, C., PATRIZI, S., LEFEBVRE, S., FOLLETT, P. L., JENSEN, F. E., ROSENBERG, P. A., VOLPE, J. J. & VARTANIAN, T. 2002. The toll-like receptor TLR4 is necessary for lipopolysaccharide-induced oligodendrocyte injury in the CNS. *J Neurosci,* 22**,** 2478-86.

LEHNARDT, S., MASSILLON, L., FOLLETT, P., JENSEN, F. E., RATAN, R., ROSENBERG, P. A., VOLPE, J. J. & VARTANIAN, T. 2003. Activation of innate immunity in the CNS triggers neurodegeneration through a Toll-like receptor 4-dependent pathway. *Proc Natl Acad Sci U S A,* 100**,** 8514-9.

LEMAITRE, B., NICOLAS, E., MICHAUT, L., REICHHART, J. M. & HOFFMANN, J. A. 1996. The dorsoventral regulatory gene cassette spatzle/Toll/cactus controls the potent antifungal response in Drosophila adults. *Cell,* 86**,** 973-83.

LEULIER, F. & LEMAITRE, B. 2008. Toll-like receptors--taking an evolutionary approach. *Nat Rev Genet,* 9**,** 165-78.

LEVI-MONTALCINI, R. 1987. The nerve growth factor 35 years later. *Science,* 237**,** 1154-62.

LEWIS, M., ARNOT, C. J., BEESTON, H., MCCOY, A., ASHCROFT, A. E., GAY, N. J. & GANGLOFF, M. 2013. Cytokine Spatzle binds to the Drosophila immunoreceptor Toll with a neurotrophin-like specificity and couples receptor activation. *Proc Natl Acad Sci U S A,* 110**,** 20461-6.

LIN, S., MARIN, E. C., YANG, C. P., KAO, C. F., APENTENG, B. A., HUANG, Y., O'CONNOR, M. B., TRUMAN, J. W. & LEE, T. 2013. Extremes of lineage plasticity in the Drosophila brain. *Curr Biol,* 23**,** 1908-13.

LIU, M., KAY, J. C., SHEN, S. & QIAO, L. Y. 2015. Endogenous BDNF augments NMDA receptor phosphorylation in the spinal cord via PLCgamma, PKC, and PI3K/Akt pathways during colitis. *J Neuroinflammation,* 12**,** 151.

LU, B., PANG, P. T. & WOO, N. H. 2005. The yin and yang of neurotrophin action. *Nat Rev Neurosci,* 6**,** 603-14.

LUO, C., SHEN, B., MANLEY, J. L. & ZHENG, L. 2001. Tehao functions in the Toll pathway in Drosophila melanogaster: possible roles in development and innate immunity. *Insect Mol Biol,* 10**,** 457-64.

LUO, C. & ZHENG, L. 2000. Independent evolution of Toll and related genes in insects and mammals. *Immunogenetics,* 51**,** 92-8.

MA, Y., LI, J., CHIU, I., WANG, Y., SLOANE, J. A., LU, J., KOSARAS, B., SIDMAN, R. L., VOLPE, J. J. & VARTANIAN, T. 2006. Toll-like receptor 8 functions as a negative regulator of neurite outgrowth and inducer of neuronal apoptosis. *J Cell Biol,* 175**,** 209-15.

MANFRUELLI, P., REICHHART, J. M., STEWARD, R., HOFFMANN, J. A. & LEMAITRE, B. 1999. A mosaic analysis in Drosophila fat body cells of the control of antimicrobial peptide genes by the Rel proteins Dorsal and DIF. *EMBO J,* 18**,** 3380-91.

MARTIN-ZANCA, D., OSKAM, R., MITRA, G., COPELAND, T. & BARBACID, M. 1989. Molecular and biochemical characterization of the human trk proto-oncogene. *Mol Cell Biol,* 9**,** 24-33.

MCILROY, G., FOLDI, I., AURIKKO, J., WENTZELL, J. S., LIM, M. A., FENTON, J. C., GAY, N. J. & HIDALGO, A. 2013. Toll-6 and Toll-7 function as neurotrophin receptors in the Drosophila melanogaster CNS. *Nat Neurosci,* 16**,** 1248-56.

MEDZHITOV, R. & JANEWAY, C. A., JR. 2002. Decoding the patterns of self and nonself by the innate immune system. *Science,* 296**,** 298-300.

MEYER, S. N., AMOYEL, M., BERGANTINOS, C., DE LA COVA, C., SCHERTEL, C., BASLER, K. & JOHNSTON, L. A. 2014. An ancient defense system eliminates unfit cells from developing tissues during cell competition. *Science,* 346**,** 1258236.

MINICHIELLO, L. 2009. TrkB signalling pathways in LTP and learning. *Nat Rev Neurosci,* 10**,** 850-60.

MIZUGUCHI, K., PARKER, J. S., BLUNDELL, T. L. & GAY, N. J. 1998. Getting knotted: a model for the structure and activation of Spatzle. *Trends Biochem Sci,* 23**,** 239-42.

MORISATO, D. & ANDERSON, K. V. 1994. The spatzle gene encodes a component of the extracellular signaling pathway establishing the dorsal-ventral pattern of the Drosophila embryo. *Cell,* 76**,** 677-88.

MOUSSIAN, B. & ROTH, S. 2005. Dorsoventral axis formation in the Drosophila embryo--shaping and transducing a morphogen gradient. *Curr Biol,* 15**,** R887-99.

MOWLA, S. J., PAREEK, S., FARHADI, H. F., PETRECCA, K., FAWCETT, J. P., SEIDAH, N. G., MORRIS, S. J., SOSSIN, W. S. & MURPHY, R. A. 1999. Differential sorting of nerve growth factor and brain-derived neurotrophic factor in hippocampal neurons. *J Neurosci,* 19**,** 2069-80.

MULLER, G., STORZ, P., BOURTEELE, S., DOPPLER, H., PFIZENMAIER, K., MISCHAK, H., PHILIPP, A., KAISER, C. & KOLCH, W. 1998. Regulation of Raf-1 kinase by TNF via its second messenger ceramide and cross-talk with mitogenic signalling. *EMBO J,* 17**,** 732-42.

MUZIO, M. & MANTOVANI, A. 2001. The Toll receptor family. *Allergy,* 56**,** 103-8.

NARBONNE-REVEAU, K., CHARROUX, B. & ROYET, J. 2011. Lack of an antibacterial response defect in Drosophila Toll-9 mutant. *PLoS One,* 6**,** e17470.

NERIEC, N. & DESPLAN, C. 2016. From the Eye to the Brain: Development of the Drosophila Visual System. *Curr Top Dev Biol,* 116**,** 247-71.

NYKJAER, A., LEE, R., TENG, K. K., JANSEN, P., MADSEN, P., NIELSEN, M. S., JACOBSEN, C., KLIEMANNEL, M., SCHWARZ, E., WILLNOW, T. E., HEMPSTEAD, B. L. & PETERSEN, C. M. 2004. Sortilin is essential for proNGF-induced neuronal cell death. *Nature,* 427**,** 843-8.

OKUN, E., GRIFFIOEN, K. J., LATHIA, J. D., TANG, S. C., MATTSON, M. P. & ARUMUGAM, T. V. 2009. Toll-like receptors in neurodegeneration. *Brain Res Rev,* 59**,** 278-92.

OOI, J. Y., YAGI, Y., HU, X. & IP, Y. T. 2002. The Drosophila Toll-9 activates a constitutive antimicrobial defense. *EMBO Rep,* 3**,** 82-7.

PAN, D. 2010. The hippo signaling pathway in development and cancer. *Dev Cell,* 19**,** 491-505.

PAN, Y., ZHOU, Y., GUO, C., GONG, H., GONG, Z. & LIU, L. 2009. Differential roles of the fan-shaped body and the ellipsoid body in Drosophila visual pattern memory. *Learn Mem,* 16**,** 289-95.

PARE, A. C., VICHAS, A., FINCHER, C. T., MIRMAN, Z., FARRELL, D. L., MAINIERI, A. & ZALLEN, J. A. 2014. A positional Toll receptor code directs convergent extension in Drosophila. *Nature,* 515**,** 523-7.

PASARE, C. & MEDZHITOV, R. 2003. Toll pathway-dependent blockade of CD4+CD25+ T cell-mediated suppression by dendritic cells. *Science,* 299**,** 1033-6.

PICCININI, A. M. & MIDWOOD, K. S. 2010. DAMPening inflammation by modulating TLR signalling. *Mediators Inflamm,* 2010.

PROKOP, A. & TECHNAU, G. M. 1991. The origin of postembryonic neuroblasts in the ventral nerve cord of Drosophila melanogaster. *Development,* 111**,** 79-88.

PYZA, E. & GORSKA-ANDRZEJAK, J. 2004. Involvement of glial cells in rhythmic size changes in neurons of the housefly's visual system. *J Neurobiol,* 59**,** 205-15.

REICHARDT, L. F. 2006. Neurotrophin-regulated signalling pathways. *Philos Trans R Soc Lond B Biol Sci,* 361**,** 1545-64.

ROLLS, A., SHECHTER, R., LONDON, A., ZIV, Y., RONEN, A., LEVY, R. & SCHWARTZ, M. 2007. Toll-like receptors modulate adult hippocampal neurogenesis. *Nat Cell Biol,* 9**,** 1081-8.

ROSE, D., ZHU, X., KOSE, H., HOANG, B., CHO, J. & CHIBA, A. 1997. Toll, a muscle cell surface molecule, locally inhibits synaptic initiation of the RP3 motoneuron growth cone in Drosophila. *Development,* 124**,** 1561-71.

ROUX, P. P. & BARKER, P. A. 2002. Neurotrophin signaling through the p75 neurotrophin receptor. *Prog Neurobiol,* 67**,** 203-33.

SEIDAH, N. G., BENJANNET, S., PAREEK, S., SAVARIA, D., HAMELIN, J., GOULET, B., LALIBERTE, J., LAZURE, C., CHRETIEN, M. & MURPHY, R. A. 1996. Cellular processing of the nerve growth factor precursor by the mammalian pro-protein convertases. *Biochem J,* 314 (Pt 3)**,** 951-60.

SHIA, A. K., GLITTENBERG, M., THOMPSON, G., WEBER, A. N., REICHHART, J. M. & LIGOXYGAKIS, P. 2009. Toll-dependent antimicrobial responses in Drosophila larval fat body require Spatzle secreted by haemocytes. *J Cell Sci,* 122**,** 4505-15.

SILBERING, A. F., OKADA, R., ITO, K. & GALIZIA, C. G. 2008. Olfactory information processing in the Drosophila antennal lobe: anything goes? *J Neurosci,* 28**,** 13075-87.

SORRELLS, S. F., PAREDES, M. F., CEBRIAN-SILLA, A., SANDOVAL, K., QI, D., KELLEY, K. W., JAMES, D., MAYER, S., CHANG, J., AUGUSTE, K. I., CHANG, E. F., GUTIERREZ, A. J., KRIEGSTEIN, A. R., MATHERN, G. W., OLDHAM, M. C., HUANG, E. J., GARCIA-VERDUGO, J. M., YANG, Z. & ALVAREZ-BUYLLA, A. 2018. Human hippocampal neurogenesis drops sharply in children to undetectable levels in adults. *Nature,* 555**,** 377-381.

SPALDING, K. L., BERGMANN, O., ALKASS, K., BERNARD, S., SALEHPOUR, M., HUTTNER, H. B., BOSTROM, E., WESTERLUND, I., VIAL, C., BUCHHOLZ, B. A., POSSNERT, G., MASH, D. C., DRUID, H. & FRISEN, J. 2013. Dynamics of hippocampal neurogenesis in adult humans. *Cell,* 153**,** 1219-1227.

STATHOPOULOS, A. & LEVINE, M. 2002. Dorsal gradient networks in the Drosophila embryo. *Dev Biol,* 246**,** 57-67.

SUTCLIFFE, B., FORERO, M. G., ZHU, B., ROBINSON, I. M. & HIDALGO, A. 2013. Neuron-type specific functions of DNT1, DNT2 and Spz at the Drosophila neuromuscular junction. *PLoS One,* 8**,** e75902.

TASHIRO, A., SANDLER, V. M., TONI, N., ZHAO, C. & GAGE, F. H. 2006. NMDA-receptor-mediated, cell-specific integration of new neurons in adult dentate gyrus. *Nature,* 442**,** 929-33.

TAUSZIG, S., JOUANGUY, E., HOFFMANN, J. A. & IMLER, J. L. 2000. Toll-related receptors and the control of antimicrobial peptide expression in Drosophila. *Proc Natl Acad Sci U S A,* 97**,** 10520-5.

TECHNAU, G. M. 1984. Fiber number in the mushroom bodies of adult Drosophila melanogaster depends on age, sex and experience. *J Neurogenet,* 1**,** 113-26.

TREANOR, J. J., SCHMELZER, C., KNUSEL, B., WINSLOW, J. W., SHELTON, D. L., HEFTI, F., NIKOLICS, K. & BURTON, L. E. 1995. Heterodimeric neurotrophins induce phosphorylation of Trk receptors and promote neuronal differentiation in PC12 cells. *J Biol Chem,* 270**,** 23104-10.

TRUMAN, J. W. 1990. Metamorphosis of the central nervous system of Drosophila. *J Neurobiol,* 21**,** 1072-84.

ULIAN-BENITEZ, S., BISHOP, S., FOLDI, I., WENTZELL, J., OKENWA, C., FORERO, M. G., ZHU, B., MOREIRA, M., PHIZACKLEA, M., MCILROY, G., LI, G., GAY, N. J. & HIDALGO, A. 2017. Kek-6: A truncated-Trk-like receptor for Drosophila neurotrophin 2 regulates structural synaptic plasticity. *PLoS Genet,* 13**,** e1006968.

VAN SWINDEREN, B. 2009. Fly memory: a mushroom body story in parts. *Curr Biol,* 19**,** R855-7.

VANDENPLAS, M. L., MAMIDIPUDI, V., LAMAR SEIBENHENER, M. & WOOTEN, M. W. 2002. Nerve growth factor activates kinases that phosphorylate atypical protein kinase C. *Cell Signal,* 14**,** 359-63.

WARD, A., HONG, W., FAVALORO, V. & LUO, L. 2015. Toll receptors instruct axon and dendrite targeting and participate in synaptic partner matching in a Drosophila olfactory circuit. *Neuron,* 85**,** 1013-28.

WEBER, P., KULA-EVERSOLE, E. & PYZA, E. 2009. Circadian control of dendrite morphology in the visual system of Drosophila melanogaster. *PLoS One,* 4**,** e4290.

WIESEL, T. N. & HUBEL, D. H. 1965. Comparison of the effects of unilateral and bilateral eye closure on cortical unit responses in kittens. *J Neurophysiol,* 28**,** 1029-40.

WOHLEB, E. S., FRANKLIN, T., IWATA, M. & DUMAN, R. S. 2016. Integrating neuroimmune systems in the neurobiology of depression. *Nat Rev Neurosci,* 17**,** 497-511.

WOOTEN, M. W., VANDENPLAS, M. L., SEIBENHENER, M. L., GEETHA, T. & DIAZ-MECO, M. T. 2001. Nerve growth factor stimulates multisite tyrosine phosphorylation and activation of the atypical protein kinase C's via a src kinase pathway. *Mol Cell Biol,* 21**,** 8414-27.

XIE, X., TABUCHI, M., BROWN, M. P., MITCHELL, S. P., WU, M. N. & KOLODKIN, A. L. 2017. The laminar organization of the Drosophila ellipsoid body is semaphorin-dependent and prevents the formation of ectopic synaptic connections. *Elife,* 6.

YAGITA, Y., KITAGAWA, K., OHTSUKI, T., TAKASAWA, K., MIYATA, T., OKANO, H., HORI, M. & MATSUMOTO, M. 2001. Neurogenesis by progenitor cells in the ischemic adult rat hippocampus. *Stroke,* 32**,** 1890-6.

YAMADA, M., OHNISHI, H., SANO, S., NAKATANI, A., IKEUCHI, T. & HATANAKA, H. 1997. Insulin receptor substrate (IRS)-1 and IRS-2 are tyrosine-phosphorylated and associated with phosphatidylinositol 3-kinase in response to brain-derived neurotrophic factor in cultured cerebral cortical neurons. *J Biol Chem,* 272**,** 30334-9.

YAMASHITA, T., TUCKER, K. L. & BARDE, Y. A. 1999. Neurotrophin binding to the p75 receptor modulates Rho activity and axonal outgrowth. *Neuron,* 24**,** 585-93.

ZAREMBER, K. A. & GODOWSKI, P. J. 2002. Tissue expression of human Toll-like receptors and differential regulation of Toll-like receptor mRNAs in leukocytes in response to microbes, their products, and cytokines. *J Immunol,* 168**,** 554-61.

ZHU, B., PENNACK, J. A., MCQUILTON, P., FORERO, M. G., MIZUGUCHI, K., SUTCLIFFE, B., GU, C. J., FENTON, J. C. & HIDALGO, A. 2008. Drosophila neurotrophins reveal a common mechanism for nervous system formation. *PLoS Biol,* 6**,** e284.

ZHU, Y. 2013. The Drosophila visual system: From neural circuits to behavior. *Cell Adh Migr,* 7**,** 333-44.